UNIVERSIDAD COMPLUTENSE DE MADRID

FACULTAD DE CIENCIAS QUÍMICAS

Departamento de Ingeniería Química

CAPTURA DE GASES SOBRE LÍQUIDOS IÓNICOS : APLICACIÓN A LOS CASOS DEL CO2 Y NH3

MEMORIA PARA OPTAR AL GRADO DE DOCTOR
PRESENTADA POR

María González Miquel

Bajo la dirección de los doctores

Francisco Rodríguez Somolinos
José Palomar Herrero

Madrid, 2013

UNIVERSIDAD COMPLUTENSE DE MADRID

Facultad de Ciencias Químicas

Departamento de Ingeniería Química

"Captura de gases sobre líquidos iónicos. Aplicación a los casos del CO_2 y NH_3."

MEMORIA

que para optar al Título de Doctor
por la Universidad Complutense de Madrid
en el Programa de Doctorado de Ingeniería Química
presenta

María González Miquel

Madrid, 2013

D. FRANCISCO RODRÍGUEZ SOMOLINOS, Catedrático del Departamento de Ingeniería Química de la Facultad de Ciencias Químicas de la Universidad Complutense de Madrid, y D. JOSÉ PALOMAR HERRERO, Profesor del Departamento de Química Física Aplicada (Sección de Ingeniería Química) de la Facultad de Ciencias de la Universidad Autónoma de Madrid,

CERTIFICAN: que el presente trabajo de investigación titulado "Captura de gases sobre líquidos iónicos. Aplicación a los casos del CO_2 y NH_3" constituye la memoria que presenta María González Miquel para optar al grado de doctor, y que ha sido realizada en las instalaciones del Departamento de Ingeniería Química de la Universidad Complutense de Madrid y del Departamento de Química Física Aplicada (Sección de Ingeniería Química) de la Universidad Autónoma de Madrid bajo su dirección.

Dr. D. Francisco Rodríguez Somolinos Dr. D. José Palomar Herrero

En primer lugar, me gustaría expresar mi más sincero agradecimiento a mis directores de tesis, D. Francisco Rodríguez Somolinos, Catedrático del Departamento de Ingeniería Química de la Universidad Complutense de Madrid, y D. José Palomar Herrero, Profesor del Departamento de Química Física Aplicada (Sección de Ingeniería Química) de la Facultad de Ciencias de la Universidad Autónoma de Madrid, por su inestimable confianza, dedicación y apoyo a lo largo de estos años; por sus conocimientos y experiencia, que me han guiado durante todo este tiempo; y por haberme ofrecido esta oportunidad única de formación y aprendizaje.

Asimismo, expresar mi gratitud a la Conserjería de Educación de la Comunidad Autónoma de Madrid por su financiación para desarrollar el proyecto de investigación LIQUORGAS S2009/PPQ-1545 en el que estoy contratada, así como a las empresas CEPSA y COSMOlogic por su participación en el mencionado proyecto.

Me gustaría mostrar mi agradecimiento a los profesores Dr. Charles A. Eckert y Dr. Charles L. Liotta del Departamento de Ingeniería Química del Instituto Tecnológico de Georgia (Georgia Institute of Technology, Atlanta, E.E.U.U.) por haberme brindado la oportunidad de realizar una estancia de investigación en su grupo.

Por otro lado, me gustaría agradecer a Dña. Virginia Alonso Rubio, Profesora del Departamento de Ingeniería Química de la Universidad Complutense de Madrid, por su apoyo, interés y confianza desde el principio, así como por haberme ayudado a descubrir el mundo de la investigación y animarme a continuar a en él.

Expresar mi gratitud a mis compañeros de la Universidad Complutense de Madrid. A Ana por su amistad a lo largo de estos años y por su apoyo desde el primer momento en el que empezamos a dar los primeros pasos en el laboratorio. A Tamara por su afecto y su ayuda durante estos últimos meses que hemos tenido la oportunidad de compartir. A Marcos, Ester, Belén, Pablo, Silvia y Juan Carlos por fomentar un buen ambiente de trabajo en el departamento. Asimismo, expresar mi gratitud a mis compañeros de la Universidad Autónoma de Madrid. A Elia por su amistad y por los buenos momentos compartidos tanto dentro como fuera de la universidad. A Salama por su gran ayuda con Gaussian. A Jorge por su ayuda en la parte experimental. A Jesús por su compañerismo. Y a Juan y Cristian por su colaboración.

Mi más especial agradecimiento a Jesús por su cariño, confianza, apoyo y lealtad a lo largo de todos estos años juntos. Soy afortunada por haber podido crecer contigo todo este tiempo y deseo que nuestro camino no haya hecho más que comenzar.

Finalmente, deseo expresar mi más profundo agradecimiento a mi familia por su cariño, esfuerzo, paciencia, confianza, comprensión y apoyo incondicional a lo largo de toda mi vida. Sin vosotros nada de esto hubiera sido posible. Gracias de todo corazón.

ÍNDICE

ÍNDICE

ABSTRACT **1**

1. ALCANCE Y OBJETIVOS **7**

2. LÍQUIDOS IÓNICOS **13**

2.1. Características generales de los líquidos iónicos **15**

2.2. Aplicaciones de los líquidos iónicos **19**

2.2.1. Aplicaciones de los líquidos iónicos en procesos de separación 19

2.2.2. Otras aplicaciones de los líquidos iónicos 21

2.2.3. Aplicaciones de los líquidos iónicos a nivel industrial 22

3. ABSORCIÓN DE GASES CON LÍQUIDOS IÓNICOS **25**

3.1. Dióxido de carbono **28**

3.1.1. Emisiones de dióxido de carbono 28

3.1.2. Procesos de captura de dióxido de carbono 31

3.1.3. Tecnologías disponibles para la captura de dióxido de carbono en post-combustión 35

3.1.3.1. Sistemas basados en absorción con aminas *35*

3.1.3.2. Tecnologías emergentes para captura de dióxido de carbono *39*

3.1.4. Captura de dióxido de carbono mediante sistemas basados en líquidos iónicos 41

Absorción física de CO_2 con LIs *41*

Membranas soportadas en LIs (SILMs) *43*

Absorción química de CO_2 con LIs *44*

3.2. Amoniaco **48**

3.2.1. El amoniaco como contaminante 48

3.2.2. Técnicas disponibles para el tratamiento de amoniaco..... 52

3.2.3. Absorción de amoniaco con líquidos iónicos 55

3.3. Compuestos orgánicos volátiles..... **57**

3.3.1. Técnicas disponibles para el tratamiento de compuestos orgánicos volátiles 59

3.3.2. Tratamiento de compuestos orgánicos volátiles con líquidos iónicos 60

4. TÉCNICAS DE MEDIDA DE SOLUBILIDAD DE GASES EN LÍQUIDOS IÓNICOS..... **63**

4.1. Termogravimetría a presión atmosférica..... **65**

4.2. Termogravimetría de alta presión..... **66**

4.3. Célula de presión **67**

4.4. Otras técnicas..... **68**

5. SIMULACIÓN MOLECULAR COSMO-RS PARA LA SELECCIÓN Y DISEÑO DE LÍQUIDOS IÓNICOS **69**

5.1. Características generales del método COSMO-RS..... **71**

5.2. Aplicación de COSMO-RS en sistemas basados en líquidos iónicos..... **76**

6. RESULTADOS **79**

6.1. Absorción de dióxido de carbono con líquidos iónicos **82**

6.2. Absorción de amoniaco con líquidos iónicos **90**

6.3. Selección de líquidos iónicos para absorción de compuestos orgánicos volátiles mediante simulación molecular COSMO-RS **92**

7. CONCLUSIONES **97**

BIBLIOGRAFÍA **105**

ANEXO I. Publicaciones **137**

Publicación 1: "Understanding the physical absorption of CO_2 in ionic liquids using COSMO-RS method" 139

Publicación 2: "CO_2/N_2 selectivity prediction in supported ionic liquid membranes (SILMs) by COSMO-RS" 153

Publicación 3: "COSMO-RS studies: structure-property relationships for CO_2 capture by reversible ionic liquids" 165

Publicación 4: "Anion effects on kinetics and thermodynamics of CO_2 absorption in ionic liquids" 175

Publicación 5: "Solubility and diffusivity of CO_2 in [hxmim][NTf_2], [omim][NTf_2] and [dcmim][NTf_2] at T=(298.15, 308.15 and 323.15) K and pressures up to 20 bar" 187

Publicación 6: "Task-specific ionic liquids for efficient ammonia absorption" 207

Publicación 7: "Screening ionic liquids as suitable NH_3 absorbents on the basis on thermodynamic and kinetic analysis" 219

Publicación 8: "Selection of ionic liquids for enhancing the gas solubility of volatile organic compounds" 229

ANEXO II. Nomenclatura **243**

ABSTRACT

ABSTRACT

1. Introduction

In the present days there is a growing concern about greenhouse gas emissions and other atmospheric pollutants causing devastating effects on the environment and human health[1]. Carbon dioxide (CO_2) is the most important greenhouse gas, whose emissions from fossil fuel-fired power plants are the main contributor to global climate change. Conventional technologies for CO_2 capture are based on amines solutions, which involve several disadvantages including their corrosive and volatile nature that leads to high operational costs and environmental impact. Moreover, increasing ammonia (NH_3) emissions from industrial refrigeration systems or amine-based solvents significantly contributes to acid deposition, eutrophication and atmospheric pollution. In addition, the intensive use of volatile organic compounds (VOCs) as common solvents in the chemical industry causes indoor air pollution and contributes to climate change through atmospheric photochemical reactions. Under this scenario, one of the main challenges for industry today is to develop sustainable technologies based on novel solvents capable of efficiently reducing the atmospheric emissions of harmful pollutants, such as CO_2, NH_3 or VOCs.

In recent years, ionic liquids (ILs) –organic salts with melting points below 100 ^{o}C- have received increasing attention as alternative solvents in gas absorption processes due to their unique properties, such as negligible vapor pressure, high thermal and chemical stability, and high solvent capacity[2]. Moreover, ILs are considered "designer solvents" since their physicochemical properties can be tuned by selecting the counterions of their structure. In this regard, the application of molecular simulation tools, such as the quantum chemistry COSMO-RS method, to estimate the thermodynamic properties of the solvents is of great help to select/design appropriate ILs for specific applications[3].

The main goal of this work is to develop a research methodology which combines molecular simulation methods with experimental techniques in order to propose novel solvents to be used in the development of CO_2 capture and NH_3 absorption technologies based on ILs.

2. Contents

First, the capability of the COSMO-RS method to predict the solubility behavior of a wide range of gaseous solutes in ILs was validated. In order to accomplish such goal, different molecular models to define the structure of the solvents and optimize the geometry of the compounds were implemented in quantum-chemical calculations. The computational COSMO-RS results were compared with the available experimental data so as to select the molecular model which best describes the behavior of the gas-IL systems under study.

Once the molecular model was selected, different molecular simulation analyses based on COSMO-RS were performed to evaluate the thermodynamic and energetic aspects of the absorption process. This helped to understand the kind of the intermolecular interactions which enhance the capacity of the ILs to absorb CO_2 and NH_3. Consequently, appropriate ILs structures were suggested for each specific application and computational screenings were completed to select ILs with favorable characteristics to enhance the absorption of the solutes.

After selecting the prospective IL through molecular simulation analyses, experimental assays were performed to evaluate the effect of the structure of the ILs and the operating conditions on the thermodynamics and kinetics of the absorption process of CO_2 and NH_3 in ILs. The absorption-desorption isotherms and the kinetic curves of the solutes in the ILs were determined by thermogravimetric measurements. The experiments of CO_2 absorption in [bmim][PF_6], [bmim][FAP], [bmim][NTf_2], [hxmim][NTf_2], [omim][NTf_2] and [dcmim][NTf_2] were performed in a magnetic suspension balance operating in dynamic mode at temperatures ranging from 25 to 50 ^oC and pressures up to 20 bar. The experiments of NH_3 absorption in [EtOHmim][BF_4], [choline][NTf_2],

[MTEOA][$MeSO_4$], [EtOHmim][DCN] and [bmim][BF_4] were conducted in a thermogravimetric balance at temperatures ranging from 20 to 40 ^oC and pressures up to 1 bar. From the collected thermogravimetric data, the solubilities and the Henry´s law constants of the solutes in the ILs were determined. In addition, the experimental diffusion coefficients of the solutes in the ILs were calculated by applying a one-dimensional mass-diffusion model. The experimental values of the diffusion coefficients were compared to those estimated by applying the empirical equation of Wilke-Chang.

Finally, in order to evaluate the capacity of the ILs to absorb other pollutants of interest, the molecular simulation analyses were extended to a broad group of VOCs of different chemical nature, in order to obtain valuable information for designing future experimental research in our laboratory.

3. Conclusions

- CO_2 capture in ILs: COSMO-RS method has been shown to be a valuable tool to predict and understand the thermodynamic behavior of gas-IL systems. COSMO-RS has been successfully applied a) to design novel brominated ILs for CO_2 capture; b) to propose commercially available $[SCN]^-$-based ILs for CO_2/N_2 separation in SILMs; and c) to develop structure-property relationships to design reversible ILs for CO_2 capture. Experimental results confirmed that CO_2 solubility in ILs increases with pressure and decreases with temperature, following the subsequent trend with the anion: [bmim][FAP] > [bmim][NTf_2] > [bmim][PF_6]; and slightly increasing with the length of the alkyl chain of the cation as follows: [dcmim][NTf_2] > [omim][NTf_2] > [hxmim][NTf_2]. Maximum molar fraction of absorbed CO_2 (0.47) was obtained with [bmim][FAP] at 25 ^oC (lowest temperature) and 20 bar (highest pressure). The diffusion coefficients of CO_2 in the ILs are in the order of magnitude ranging from 10^{-10} to 10^{-11} m^2/s, increasing with temperature and pressure, and following the subsequent trends with the anion: [bmim][NTf_2] > [bmim][FAP] > [bmim][PF_6], and the cation: [hxmim][NTf_2] > [omim][NTf_2] > [dcmim][NTf_2].

- NH_3 absorption in ILs: COSMO-RS was successfully applied to propose task-specific ILs functionalized with acidic groups for NH_3 absorption. Experimental results confirmed that NH_3 solubility in ILs increases with pressure and decreases with temperature. At ambient pressure [MTEOA][$MeSO_4$] provided the maximum molar fraction of absorbed NH_3 (0.7) at 20 ^oC (lowest temperature), while [choline][NTf_2] provided the maximum molar fraction of absorbed NH_3 (0.6) at 40 ^oC (highest temperature). The diffusion coefficients of NH_3 en ILs are in the order of magnitude of 10^{-10} m^2/s, increasing with the temperature and showing the following trend: [choline][NTf_2] > [EtOHmim][DCN] > [bmim][BF_4] > [EtOHmim][BF_4] > [MTEOA][$MeSO_4$]. [Choline][NTf_2] is the most suitable IL for NH_3 absorption based on an efficiency parameter accounting both for thermodynamic and kinetic performances.

- VOCs absorption in ILs: COSMO-RS screenings and energetic analysis on a wide sample of ILs were used to establish a roadmap of IL structures with favorable characteristics to absorb VOCs containing different functional groups, which might be helpful to guide the selection of suitable solvents for treatment technologies of such pollutants.

4. References

(1) IPCC. "In Climate Change 2007: The Physical Science Basis. Contribution of Working Group I to the Fourth Assessment Report of the Intergovernmental Panel on Climate Change". *Cambridge University Press* (Cambridge, United Kingdom), **2007**.

(2) Ramdin, M.; de Loos, T.W.; Vlugt, T.H.J. "State-of-the-Art of CO_2 Capture with Ionic Liquids". *Ind. Eng. Chem. Res*. **2012**, *51*, 8149− 8177.

(3) Palomar, J.; Torrecilla, J.S.; Ferro, V.R; Rodríguez, F. "Development of an a priori ionic liquid design tool 2: ionic liquid selection through the prediction of COSMO-RS molecular descriptor by inverse neural network". *Ind. Eng. Chem. Res*. **2009**, *48*, 2257–2265.

1. ALCANCE Y OBJETIVOS

1. ALCANCE Y OBJETIVOS

En la actualidad, existe una creciente preocupación sobre la contribución de las emisiones de gases de efecto invernadero sobre el calentamiento climático global. De hecho, el Panel Intergubernamental sobre Cambio Climático (IPCC) ha informado de la necesidad de reducir considerablemente las emisiones atmosféricas de tales gases para el año 2050 con el objetivo de mitigar sus efectos devastadores sobre el medio ambiente. El dióxido de carbono (CO_2) es el gas de efecto invernadero más importante, siendo las centrales termoeléctricas de combustibles fósiles su principal foco antropogénico de emisión. Los actuales sistemas de captura de CO_2 asociados a tales plantas termoeléctricas se basan en absorción con disoluciones amínicas. Estos disolventes presentan una elevada volatilidad, degradabilidad y reactividad, y por tanto generan un importante impacto ambiental por pérdidas de disolvente y problemas operacionales, además de presentar un elevado requerimiento energético para su regeneración. Por tanto, resulta crítico el desarrollo de nuevos disolventes para la captura de CO_2 que sean capaces de solventar los inconvenientes asociados a las tecnologías actuales y cuya implantación resulte viable a corto plazo.

Asimismo, las emisiones atmosféricas de amoniaco (NH_3) contribuyen significativamente a la deposición ácida, eutrofización y polución atmosférica, generando problemas medioambientales y en la salud. Aunque la mayoría de estas emisiones provienen de sectores agrícolas, están incrementando notablemente las emisiones de NH_3 provenientes de focos industriales, como por ejemplo las causadas por los sistemas de refrigeración basados en amoniaco o por los disolventes basados en aminas. De hecho, con el objetivo de tratar de controlar la calidad del aire, se han establecido acuerdos como el Protocolo de Gotemburgo (UNECE, 1999) que fija los límites nacionales de emisión de NH_3 y otros contaminantes para 2020 a nivel europeo. Por tanto, es necesario el desarrollo de nuevos disolventes con elevada capacidad de absorción de NH_3 y

baja volatilidad que puedan ser empleados en sistemas dirigidos a la reducción de las emisiones de los principales focos contaminantes y en ciclos de absorción.

En este sentido, los líquidos iónicos (LIs) -sales orgánicas habitualmente líquidas a temperatura ambiente- están recibiendo gran atención como disolventes para la captura y separación de gases mediante procesos de absorción debido a sus particulares características: presión de vapor despreciable, que evita las emisiones; elevada estabilidad térmica y química, que minimiza los problemas de degradación y corrosión; y alta capacidad disolvente de solutos orgánicos e inorgánicos. Además, una importante ventaja de estos novedosos compuestos es que sus propiedades físico-químicas pueden seleccionarse variando los iones constituyentes del LI, resultando disolventes de diseño con un gran potencial para aplicaciones prácticas específicas.

Sin embargo, considerando que el número de combinaciones de contraiones posibles es del orden de 10^6 y teniendo en cuenta la escasez de datos experimentales disponibles, resulta de gran interés la aplicación de modelos predictivos para la estimación de las propiedades de los LIs. En este aspecto, la metodología químico cuántica COSMO-RS se presenta como una práctica herramienta que permite la predicción de propiedades termodinámicas de fluidos puros y mezclas utilizando únicamente información estructural de las moléculas. Por ello, dicho método es de gran utilidad en la etapa inicial del desarrollo de procesos basados en LIs, con el objetivo de determinar datos termodinámicos de los sistemas que ayuden a seleccionar LIs potencialmente adecuados para las aplicaciones de interés.

El principal objetivo del presente trabajo de investigación es desarrollar una metodología de estudio en la que se integran técnicas tanto de simulación molecular como experimentales para proponer LIs con características adecuadas para ser potencialmente empleados como disolventes en sistemas de absorción de solutos gaseosos contaminantes, como el CO_2 y el NH_3.

En primer lugar, se valida la capacidad del método COSMO-RS para predecir la solubilidad de una amplia variedad de solutos gaseosos en LIs. Para ello, se implementan distintos modelos moleculares para definir la estructura del disolvente y optimizar la geometría de los compuestos. Los resultados computacionales obtenidos mediante los distintos modelos se comparan con los datos experimentales disponibles, para así seleccionar el modelo que mejor describe el comportamiento de los sistemas gas-LI.

Una vez seleccionado el modelo de cálculo más apropiado, se realizan distintos análisis computacionales según la metodología COSMO-RS para evaluar los aspectos termodinámicos y energéticos del proceso de absorción, y así comprender el origen las interacciones intermoleculares que favorecen la capacidad de absorción del CO_2 y del NH_3 en los LIs y poder diseñar/seleccionar LIs que favorezcan la disolución de los solutos en estudio.

Una vez seleccionados los LIs potencialmente adecuados mediante simulación molecular, se procede a evaluar experimentalmente el comportamiento de tales disolventes en la absorción de CO_2 y NH_3 mediante ensayos termogravimétricos. En concreto, se realizan estudios tanto termodinámicos como cinéticos para analizar el efecto de la estructura del disolvente y de las condiciones de presión y temperatura de trabajo en el proceso de absorción de los solutos.

Por último, con el objetivo de evaluar la capacidad de los LIs para absorber otros contaminantes de interés, el estudio de simulación molecular se extiende a un amplio conjunto de compuestos orgánicos volátiles (COVs) de distinta naturaleza química. De este modo, se establecen criterios para seleccionar aniones y cationes que originen interacciones intermoleculares soluto-disolvente favorables para el posible desarrollo de sistemas de tratamiento de contaminantes COVs basados en LIs.

2. LÍQUIDOS IÓNICOS

2. LÍQUIDOS IÓNICOS

Durante los últimos años, los líquidos iónicos (LIs) están recibiendo una creciente atención por parte de la comunidad científica debido a sus singulares propiedades, entre las que destacan una extremadamente baja volatilidad, alta estabilidad térmica y química, baja inflamabilidad y alta capacidad disolvente (Wasserscheid y Welton, 2003). Por ello, los líquidos iónicos están siendo investigados como alternativa de bajo impacto ambiental a los disolventes orgánicos tradiciones en multitud de campos, incluyendo procesos de separación, síntesis orgánica, catálisis o electroquímica. A continuación, se exponen las principales características de esta nueva clase de disolventes y se presentan sus principales aplicaciones, tanto en el campo de la investigación académica como en el industrial (Plechkova y Seddon, 2008).

2.1. Características generales de los líquidos iónicos

Los líquidos iónicos se definen como sales orgánicas con puntos de fusión inferiores a los 100 ^{o}C, cuyas propiedades termodinámicas características les hacen ser considerados como nuevos disolventes en la industria química (Rogers y Seddon, 2002 y 2003). Además, las propiedades físicas y químicas de estos compuestos pueden seleccionarse variando los iones que lo constituyen, por lo que resultan disolventes de diseño con un gran potencial para aplicaciones prácticas específicas.

En cuanto a su **estructura**, los líquidos iónicos habitualmente se componen de cationes orgánicos voluminosos como imidazolios, piridinios o fosfonios, acompañados de una gran variedad de aniones orgánicos o inorgánicos como $[BF_4]^-$, $[PF_6]^-$, $[CF_3SO_3]^-$, $[CH_3SO_4]^-$, ó $[AlCl_4]^-$ (Wasserscheid y Welton, 2003). En general, los LIs se forman porque la carga en los iones se encuentra deslocalizada, lo que reduce la fuerza de la energía de enlace en el compuesto iónico, disminuyendo así la energía reticular del sistema (Endres y

col., 2008). En la siguiente figura se recogen las estructuras de algunos de los cationes y aniones más comunes.

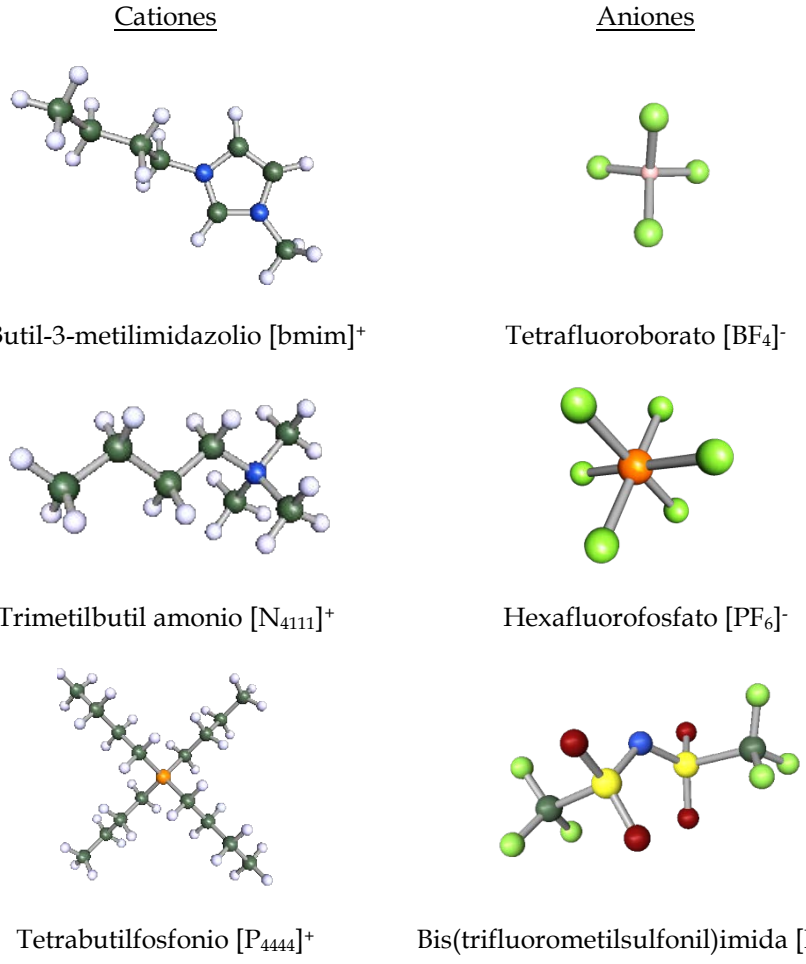

Figura 2.1.1. Estructura de algunos líquidos iónicos.

En cuanto a la **clasificación** de los líquidos iónicos, se suele distinguir entre disolventes de primera y segunda generación, incluyéndose en la primera generación a aquellos basados en mezclas eutécticas con aniones como haloaluminatos, y en la segunda generación a aquellos basados en aniones discretos como $[BF_4]^-$ ó $[PF_6]^-$ (Holbrey y Seddon, 1999a; Welton, 1999). La

principal diferencia es que los primeros presentan la característica de actuar como ácidos y bases de Lewis, pero reaccionan más fácilmente con el agua formando complejos que desestabilizan el compuesto, mientras que los segundos son más estables frente al aire y al agua. Recientemente, se hace referencia a una tercera generación denominada "task-specific ionc liquids" (TSILs), en la que se incluyen a aquellos líquidos iónicos con distintos grupos funcionales diseñados para una aplicación específica (Bates y col., 2002; Davis, 2004; Giernoth, 2010).

Una de las principales propiedades de los líquidos iónicos es su **presión de vapor prácticamente nula**, lo que unido a su **elevada estabilidad química y térmica**, y a su **baja inflamabilidad y corrosividad**, les confiere características únicas para ser empleados como alternativa a los disolventes orgánicos volátiles en procesos de separación y reacción (Welton, 1999; Plechkova y Seddon, 2008).

Aunque por definición se establece que el **punto de fusión** máximo de los líquidos iónicos es de 100 ^{o} C, la mayoría de ellos son líquidos a temperatura ambiente; a estos últimos se les conoce como "room-temperature ionic liquids" o RTILs (Wasserscheid y Keim, 2000). Tanto los cationes como los aniones contribuyen al bajo punto de fusión de los líquidos iónicos, de modo que al aumentar el tamaño del anión, o el tamaño y la asimetría del catión, disminuye el punto de fusión (Holbrey y Seddon, 1999b; Endres y El Abedin, 2006).

En general, los líquidos iónicos son más densos que el agua, presentando valores de **densidad** comprendidos entre 1 y 1.6 g/cm^3 (Marsh y col., 2004). Para series homólogas de líquidos iónicos basados en el mismo anión, la densidad disminuye a medida que aumenta la longitud de la cadena alquílica del catión (Seddon y col., 2002).

En general, la **viscosidad** de los líquidos iónicos es elevada, presentando valores de entre 10 y 500 mPa·s a temperatura ambiente, y viene determinada por las fuerzas de van der Waals y los enlaces de hidrógeno

(Endres y El Abedin, 2006). De este modo, la viscosidad aumenta con la longitud de la cadena alquílica del catión, puesto que también aumenta la posibilidad de que se establezcan interacciones tipo van der Waals entre los cationes.

Los líquidos iónicos presentan valores de **tensión superficial** en torno a 30-60 N/m a temperatura ambiente, aumentando a medida que disminuye la longitud de la cadena alquílica del catión (Huddleston y col., 2001; Law y Watson, 2001).

La **miscibilidad con agua** de los líquidos iónicos está fuertemente determinada por la naturaleza del anión, de modo que aquellos LIs que contienen $[PF_6]^-$ son inmiscibles en agua, los que contienen haluros, $[NO_3]^-$, $[CH_3CO_2]^-$ o $[CF_3CO_2]^-$ son miscibles con agua, y los basados en $[BF_4]^-$ y $[CF_3SO_3]^-$ se encuentran en una situación intermedia. Además, la solubilidad del agua en el líquido iónico disminuye al aumentar la longitud de la cadena alquílica del catión (Seddon y col., 2000). Nótese que los LIs hidrofóbicos, como es el caso del $[PF_6]^-$, son higroscópicos, de modo que, aunque en menor medida que los líquidos iónicos hidrofílicos, también absorben gradualmente agua de la atmósfera.

El riesgo de polución atmosférica por empleo de líquidos iónicos es mínimo debido a su extremadamente baja volatilidad. Sin embargo, en aplicaciones a nivel industrial y teniendo en cuenta su alta estabilidad, la bioacumulación de los líquidos iónicos a través del medio acuático debido a fugas o efluentes podría contribuir a problemas medioambientales debido a su potencial **toxicidad** (Petkovic y col., 2011). Sin embargo, recientemente se han planteado estudios que sugieren métodos capaces de **biodegradar** eficazmente los líquidos iónicos (Abrusci y col., 2011).

2.2. Aplicaciones de los líquidos iónicos

Como se ha indicado, los líquidos iónicos están siendo considerados como nuevos disolventes en química, y por sus peculiares características resultan potencialmente adecuados como alternativas de bajo impacto ambiental a los disolventes orgánicos tradicionales en procesos de separación, medios de reacción o sistemas electroquímicos (Han y Armstrong, 2007; Plechkova y Seddon, 2008; Han y Row, 2010; Patel y Lee, 2012).

A continuación, se presenta una revisión de las aplicaciones generales de los líquidos iónicos, en la que se incluyen tanto las principales propuestas procedentes del ámbito académico como sus primeras aplicaciones a nivel industrial.

2.2.1. Aplicaciones de los líquidos iónicos en procesos de separación

Líquidos iónicos como disolventes en absorción de gases

Existe un creciente interés en el estudio de los líquidos iónicos como disolventes de absorción en procesos de separación de gases y captura de compuestos contaminantes. De este modo, está siendo ampliamente estudiada la absorción de solutos gaseosos como CO_2, H_2, N_2, O_2, SO_2, H_2S, N_2, etc. (Jacquemin y col., 2006a y 2006b; Anderson y col., 2007). Una peculiar característica de los líquidos iónicos es su elevada capacidad para absorber grandes cantidades de CO_2 y SO_2, por lo que numerosos estudios se centran en la aplicación de estos disolventes en la captura de los gases ácidos generados en los procesos de combustión (Anthony y col., 2004; Figueroa y col., 2008; Bara y col., 2009; Huang y Rüther, 2009). Resulta especialmente prometedor el desarrollo de procesos basados en líquidos iónicos para la captura en post-combustión de CO_2 de centrales térmicas de combustibles fósiles (Bara y col., 2010; Karadas y col., 2010; Ramdin y col., 2012).

Líquidos iónicos como disolventes de extracción

Los LIs se proponen como alternativa a los disolventes orgánicos en el desarrollo de nuevos procesos de extracción menos perjudiciales para el medio ambiente. Debido a su elevada capacidad disolvente de moléculas orgánicas e iones metálicos, están siendo investigados para extraer contaminantes de muestras de agua y suelo (Pei y col., 2008; Abulhassani y col., 2009; Chen y col., 2010). También están siendo empleados como entrainers en destilación extractiva y separaciones azeotrópicas (Orchillés y col., 2007; Roughton y col., 2012). Asimismo, están siendo estudiados para su aplicación en la desulfuración de gasolinas (Alonso y col., 2007). Otra aplicación en auge es su empleo como disolventes de extracción de compuestos bioactivos de fuentes naturales para disminuir el impacto ambiental y mejorar la selectividad y el rendimiento de los procesos tradicionales basados en compuestos orgánicos volátiles (Tang y col., 2012). Resulta prometedor su empleo para extracción de celulosa en procesos de biorrefinería (Casas y col., 2012; Vancov y col., 2012). La extracción líquido-líquido iónico también se está estudiando para separar hidrocarburos aromáticos de otros hidrocarburos no aromáticos en el aprovechamiento de gasolina de pirólisis (Meindersma y col., 2010; García y col., 2013).

Membranas soportadas en líquidos

Las membranas líquidas soportadas (SLMs) en disolventes orgánicos no resultan estables debido a la pérdida del compuesto orgánico inmovilizado, bien por evaporación, o bien por disolución en el alimento o en la solución absorbente. Sin embargo, debido a la volatilidad despreciable de los líquidos iónicos y su inmiscibilidad con algunos disolventes orgánicos, resulta posible solventar los problemas asociados a las SLMs tradicionales empleando membranas soportadas en líquidos iónicos (SILMs). Una importante aplicación de las SILMs es su empleo en sistemas de separación de gases, especialmente de CO_2/N_2 y CO_2/CH_4 (Scovazzo, 2009; Bara y col., 2010; Han y Row, 2010).

Líquidos iónicos en cromatografía

Los líquidos iónicos pueden emplearse como aditivos de fase móvil en cromatografía líquida para reducir el ensanchamiento de banda y aumentar la resolución; por ejemplo, al añadir [bmim][BF_4] como modificador de la fase móvil metanol/agua en la separación de ácidos nucleicos y aminoácidos, se consigue mejor resolución, se registran cromatogramas más simétricos y se requiere menor tiempo de análisis (Polyakova y col., 2006). Además, los líquidos iónicos se están empleando en el desarrollo de nuevos materiales absorbentes que reemplacen las fases estacionarias convencionales de los sistemas cromatográficos con el objetivo de aumentar la eficiencia de la columna de tales sistemas; de este modo, se han empleado absorbentes de sílice modificada con imidazoles como fase estacionaria en cromatografía de intercambio iónico para la separación de una gran variedad de iones orgánicos, inorgánicos y muestras biológicas, observándose una elevada eficiencia de columna y buena resolución (Van Meter y col., 2008).

2.2.2. Otras aplicaciones de los líquidos iónicos

Recientemente, se están desarrollando diversas aplicaciones de los líquidos iónicos como electrolitos en **sistemas electroquímicos** (Pandey, 2006; Endres y col., 2008). En concreto, se pueden emplear en pilas electrolíticas por su baja volatilidad, puesto que proporcionan baterías más seguras, y por su elevada conductividad a temperatura ambiente, que aumenta la potencia de las pilas basadas en litio. Además, otras aplicaciones hacen referencia a su utilización en células de combustible con membranas electrolíticas poliméricas (PEMFC), células solares, disolvente en electrodeposición de metales o supercondensadores (Ohno, 2011; Patel y Lee, 2012).

Actualmente, los LIs se emplean en procesos bioquímicos como extracción de proteínas, producción de biocombustibles, biotransformación y polimerización, estabilización y activación enzimática (Lozano, 2010;

Moniruzzaman y col., 2010; Zhao, 2010; Patel y Lee, 2012). Asimismo, la aplicación de LIs como medios de reacción proporciona ventajas, como un mayor control de la distribución de productos, mayor rapidez de la reacción, la inmobilización de catalizadores o el reciclado (Wasserscheid y Welton, 2003; Chowdhury y col., 2007; Patel y Lee, 2012).

Por otro lado, también se ha propuesto el empleo de los LIs como **plastificantes** por su alta estabilidad térmica y baja volatilidad. Además, por su capacidad de disminuir la fricción en contacto con materiales metálicos y cerámicos, pueden ser utilizados como **lubricantes**. Asimismo, se ha informado de su aplicación como **dispersantes** secundarios en pinturas. Algunos LIs, como los basados en amonios, también actúan como **tensoactivos** (Baker y Pandey, 2005; Weyershausen y Lehmann, 2005).

2.2.3. Aplicaciones de los líquidos iónicos a nivel industrial

El proceso **BASIL** ("Biphasic Acid Scavenging utilising Ionic Liquids") desarrollado por la compañía **BASF** e implementado en su planta de Ludwigshafen (Alemania) desde 2002, es el ejemplo más significativo de proceso industrial operando con líquidos iónicos. Este proceso se emplea para la obtención de alcoxifenilfosfinas, precursores utilizados en la producción de fotoiniciadores. En el proceso original se empleaba trietilamina para secuestrar el ácido que se formaba en el transcurso de la reacción, originándose un subproducto, cloruro de etilamonio, que formaba una pasta insoluble que dificultaba la reacción. En el nuevo proceso se sustituye la trietilamina por el 1-metil-imidazol, originándose como subproducto un líquido iónico, cloruro de 1-metilimidazolio, que se separa fácilmente de la mezcla de reacción como una fase discreta. El rendimiento del proceso es del 98% y actualmente opera en continuo en una planta con una capacidad superior a las 1000 t/año. Otros procesos desarrollados por la compañía BASF incluyen el empleo de líquidos iónicos para la separación de mezclas azeotrópicas (agua-etanol o agua-

tetrahidrofurano) o como agentes de cloración reemplazando al fosgeno por ácido clorhídrico disuelto en líquido iónico en reacciones de cloración de alcoholes. Además, la compañía trabaja en el desarrollo de distintos procesos basados en líquidos iónicos, como el de la disolución de celulosa o el del galvanizado de aluminio (Plechkova y Seddon, 2008; BASF, 2013).

Eastman Chemical Company lleva a cabo la isomerización del 3,4-epoxibut-1-eno al 2,5-dihidrofurano empleando catalizadores de ácidos de Lewis en líquidos iónicos básicos de Lewis como fosfonios. Este proceso se llevó a cabo, desde 1996 hasta 2004, por Texas Eastman Divison en Longview (Texas) en una planta con una capacidad de producción de 1400 t/año de capacidad. La planta quedó inactiva como consecuencia de la disminución de la demanda del producto en el mercado (Plechkova y Seddon, 2008).

Mientras que BASF y Eastman Chemical Company fueron los primeros en comercializar procesos basados en líquidos iónicos, el Instituto Francés del Petróleo (IFP) fue el primero en poner a punto una planta piloto con estos disolventes. En concreto, el IFP desarrolló el proceso **DIFASOL** para la dimerización de alquenos (generalmente propeno y buteno, a hexeno y octeto) utilizando un catalizador de níquel disuelto en un líquido iónico basado en cloroaluminato. La reacción se lleva a cabo mediante un sistema bifásico en el que el catalizador queda disuelto en la fase líquido iónico mientras que los productos constituyen una segunda fase que se puede separan fácilmente. En comparación con el sistema tradicional DIMERSOL, en el que se operaba en fase homogénea sin utilizar liquido iónico como disolvente para el catalizador, el sistema bifásico DIFASOL proporciona ventajas significativas, como un mejor aprovechamiento del catalizador, una mayor selectividad y un mayor rendimiento de productos (Olivier-Bourbigou y col., 2010).

La empresa **Degussa** también está desarrollando procesos basados en líquidos iónicos en distintos frentes, incluyendo procesos de hidrosilación

catalítica para la producción de compuestos orgánicos de silicio, como aditivos en pintura para proporcionar un mejor acabado y más rápido secado, y en baterías de litio como sustituto de los disolventes orgánicos volátiles e inflamables (Weyershausen y Lehmann, 2005).

La compañía **Air Products** ha comercializado un producto para el almacenamiento de gases tóxicos como PH_3 y BF_3 basado en la absorción química con líquidos iónicos. Una de las principales ventajas de este método es que los gases tóxicos pueden ser almacenados en tanques de gases estándar, aumentando la seguridad de la planta al no resultar necesario trabajar con tanques de almacenamiento de gases a elevada presión (Giernoth, 2010).

Otras compañías desarrollando procesos basados en líquidos iónicos son las siguientes (Plechkova y Seddon, 2008): en cuanto a petroquímicas, **PetroChina** está poniendo en marcha el proceso Ionikylation para la alquilación de gasolinas con ácido sulfúrico, que ya ha sido probado en planta piloto; asimismo, **BP**, **ExxonMobil** y **Chevron** poseen numerosas patentes con posibles aplicaciones de los líquidos iónicos en procesos de refinería; por otro lado, **Central Gass Company** está estudiando procesos basados en líquidos iónicos para la producción de intermedios farmacéuticos; **Eli Lilly** estudia el desarrollo de procesos industriales basados en líquidos iónicos para la producción de productos farmacéuticos; **Scionix** desarrolla aplicaciones de líquidos iónicos en la industria galvanoplástica; y **Linde** estudia la fabricación de compresores de gases utilizando líquidos iónicos a modo de pistones. Por último, y en cuanto al mercado de líquidos iónicos, **IoLiTec** (Ionic Liquid Technologies) está especializada en la síntesis y comercialización de estos compuestos y en el estudio de posibles aplicaciones (IoLiTec, 2013).

3. ABSORCIÓN DE GASES CON LÍQUIDOS IÓNICOS

3. ABSORCIÓN DE GASES CON LÍQUIDOS IÓNICOS

Debido a las novedosas propiedades de los líquidos iónicos, entre las que destacan su baja volatilidad y su capacidad para comportarse como disolvente de diseño, estos compuestos resultan potencialmente adecuados para ser empleados como absorbentes en sistemas de captura y separación de gases. En concreto, están siendo investigados como absorbentes de una amplia variedad de solutos gaseosos, incluyendo CO_2 (Camper y col., 2005, 2006a, 2006b y 2008; Kumelan y col., 2006a y 2006b; Anderson y col., 2007; Jacquemin y col., 2008; Condemarin y Scovazzo, 2009; Raeissi y Peters, 2009a y 2009b; Almantariotis y col., 2010), H_2S (Jalili y col., 2009), H_2 (Jacquemin y col., 2006a y 2006b; Costa-Gomes, 2007; Kumelan y col., 2007; Jacquemin y col., 2008; Raeissi y Peters, 2009b), gases inertes (Jacquemin y col., 2006a y 2006b; Kumelan y col., 2007), N_2 (Camper y col., 2006b; Jacquemin y col., 2006a y 2006b; Condemarin y Scovazzo, 2009), O_2 (Jacquemin y col., 2006b; Anderson y col., 2007; Condemarin y Scovazzo, 2009), SO_2 (Anderson y col., 2006 y 2007), NH_3 (Yokozeki y Shiflett, 2007a y 2007b; Huang y col., 2008; Li y col., 2010) y compuestos orgánicos volátiles (COVs) como alcanos y alquenos (Camper y col., 2005 y 2006a; Jacquemin y col., 2006a y 2006b; Lee y Outcalt, 2006; Anderson y col., 2007; Kumelan y col., 2007; Condemarin y Scovazzo, 2009), HFCs (Shiflett y Yokozeki, 2006; Kumelan y col., 2008), de dimetilsulfato, dimetil disulfuro y tolueno (Quijano y col., 2011; Bedia y col., 2012).

Cabe destacar que resulta especialmente prometedora la aplicación de los LIs como absorbentes en procesos de captura de CO_2 de centrales termoeléctricas de combustibles fósiles. Asimismo, estos disolventes presentan características adecuadas para ser utilizados como absorbentes de NH_3 y ciertos COVs. A continuación, se presenta la problemática asociada a las emisiones atmosféricas de CO_2, NH_3 y COVs; se describen las tecnologías disponibles para el tratamiento de sus emisiones y se revisan las investigaciones realizadas sobre empleo de LIs como absorbentes de tales solutos gaseosos.

3.1. Dióxido de carbono

En este apartado se expone la problemática de las emisiones de gases de efecto invernadero asociadas a las centrales térmicas de combustibles fósiles y, en particular, a las plantas de generación eléctrica por combustión de carbón, principal foco de emisiones antropogénicas de dióxido de carbono (CO_2). A continuación, se revisa el estado del arte de las tecnologías de captura de CO_2 empleadas en este tipo de centrales (mayoritariamente sistemas de absorción en post-combustión basados en aminas) y se realiza una revisión de las técnicas emergentes, entre las que los líquidos iónicos se presentan como una prometedora alternativa.

3.1.1. Emisiones de dióxido de carbono

De acuerdo con el Panel Intergubernamental sobre Cambio Climático (IPCC, 2007a), la principal causa del calentamiento climático global es el aumento de la concentración atmosférica de gases de efecto invernadero provocado por las actividades antropogénicas realizadas desde la Revolución Industrial. El dióxido de carbono (CO_2) es el gas de efecto invernadero más importante, suponiendo el 81% de las emisiones de gases de efecto invernadero que se liberan a la atmósfera a nivel mundial (EPA, 2012a).

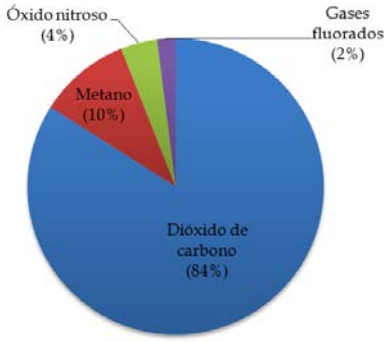

Figura 3.1.1.1. Contribución de los distintos compuestos a las emisiones mundiales de gases de efecto invernadero, 2010 (Fuente: EPA, 2012a)

Las emisiones de CO_2 han aumentado desde la Revolución Industrial. En consecuencia, la concentración atmosférica de CO_2 ha aumentado desde 280 ppm antes de la Revolución Industrial hasta 390 ppm actualmente, lo que supone un incremento superior al 39% (IEA, 2012). De hecho, las emisiones globales mundiales de CO_2 sobrepasaron las 30,2 Gt en el año 2010, lo que supone un incremento superior al 44% con respecto a las 20,9 Gt emitidas en 1990. Además, las proyecciones indican que para el año 2035 las emisiones de CO_2 sobrepasarán las 37 Gt, tal y como se ilustra en la siguiente figura.

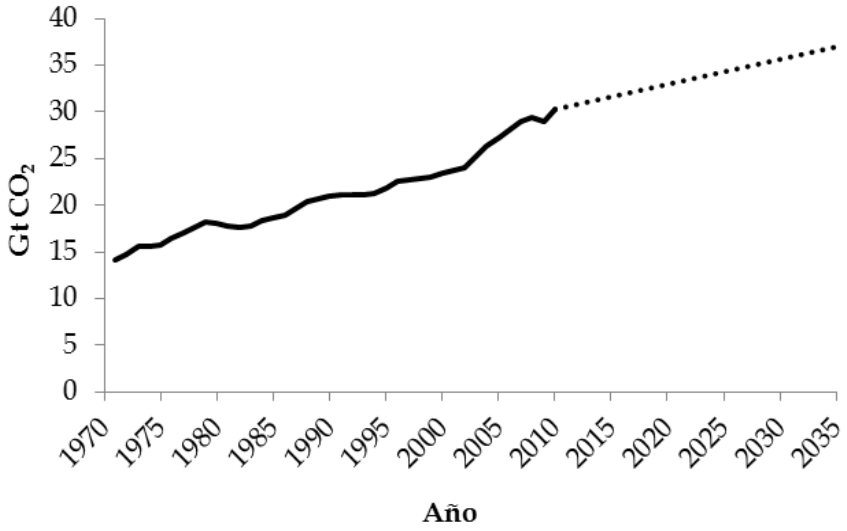

Figura 3.1.1.2. Evolución de las emisiones globales mundiales de CO_2.

(Fuente: IEA, 2012)

El sector energético es el foco mayoritario de las emisiones globales de CO_2, principalmente debido a las centrales termoeléctricas que emplean combustibles fósiles para la producción de electricidad y generación de calor. De hecho, más del 80% del suministro eléctrico mundial se obtiene por combustión de combustibles fósiles, generando la combustión de carbón más de las dos terceras partes de las emisiones atmosféricas antropogénicas globales de CO_2.

En la siguiente figura se representan las emisiones mundiales de CO_2 por sectores y por tipo de fuente energética:

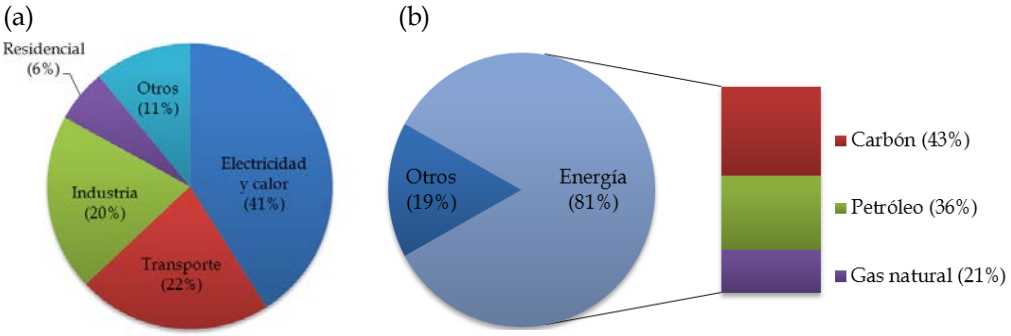

Figura 3.1.1.3. Emisiones mundiales de CO_2 (a) por sectores y (b) por tipo de fuente energética, 2010. (Fuente: EPA, 2012a)

Las proyecciones indican que la demanda energética mundial continuará aumentando alrededor del 1,2% por año, de modo que las necesidades energéticas previstas para el año 2035 serán un 30% superiores a las del año 2010 (IEA, 2010). Consecuentemente, las emisiones de CO_2 continuarán incrementando durante los próximos años, como se ilustra a continuación.

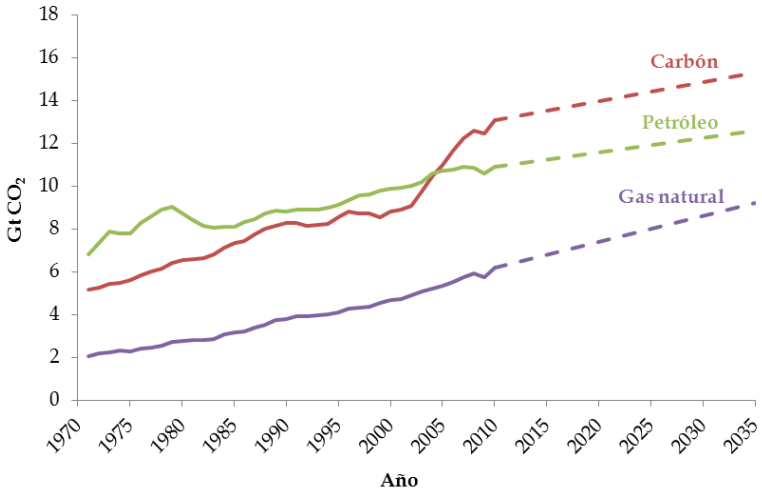

Figura 3.1.1.4. Evolución de las emisiones de CO_2 por tipo de combustible fósil (Fuente: IEA, 2010).

Aunque en las últimas décadas se esté promoviendo el uso de fuentes energéticas no emisoras de CO_2, como la energía nuclear y las renovables, el empleo de combustibles fósiles como fuente energética primaria es superior al 80%, dato que permanece prácticamente inalterable desde hace 39 años (en 1971 los combustibles fósiles constituían el 86% de las fuente energéticas primarias, mientras que en 2010 constituyeron el 81%) (IEA, 2012). Por tanto, resulta previsible que la generación de electricidad en los próximos años continúe basándose en la combustión de combustibles fósiles, y sobre todo de carbón, con el consecuente aumento de emisiones atmosférica de CO_2.

El IPCC ha indicado que para mitigar los efectos devastadores del cambio climático es necesario disminuir las emisiones de gases efecto invernadero a la atmósfera alrededor del 55-80% para el año 2050 (IPCC, 2007b). Una de las vías prioritarias para conseguir esta mitigación es reducir las emisiones en las principales fuentes de origen, como en las centrales de combustión de carbón responsables de las dos terceras partes de las emisiones que provienen del sector de generación eléctrica. En este sentido, resulta de creciente interés el desarrollo de nuevas tecnologías de captura de CO_2 asociadas a los principales focos de emisión, esto es, las plantas termoeléctricas de combustión de carbón, que sean capaces de maximizar la eficiencia del proceso y minimizar el impacto generado sobre el medio ambiente.

3.1.2. Procesos de captura de dióxido de carbono

Existen tres configuraciones para capturar el CO_2 generado en las centrales termoeléctricas de producción de energía: captura en post-combustión, captura en pre-combustión y captura en oxi-combustión. La Figura 3.1.2.1. muestra un esquema de estas tres configuraciones principales, las cuales se describen a continuación (Figueroa y col., 2008; Vega, 2010; Ramdin y col., 2012).

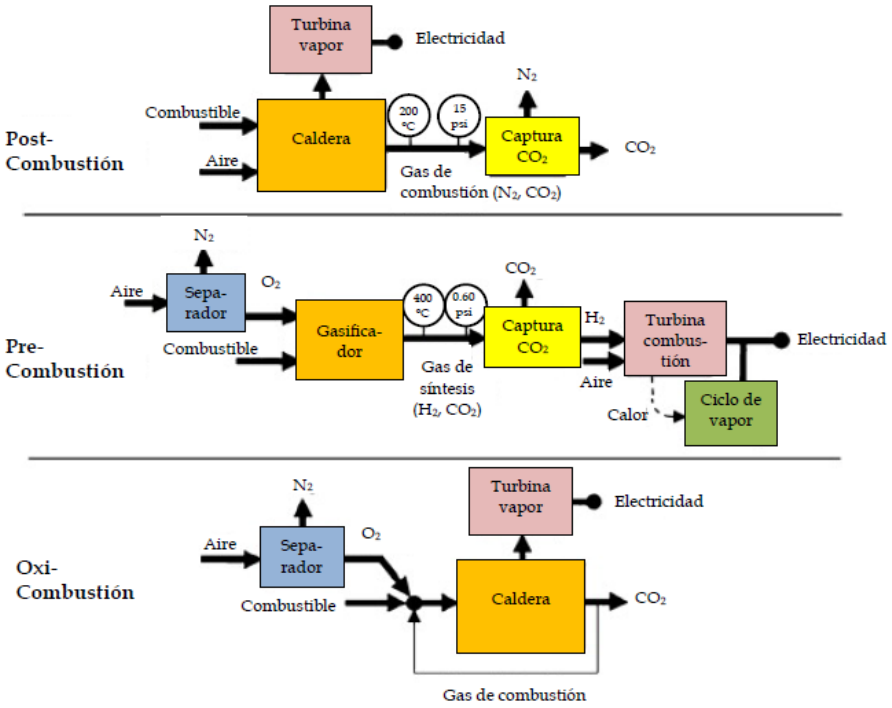

Figura 3.1.2.1. Esquema ilustrando los procesos de post-combustión, pre-combustión y oxi-combustión para captura de CO_2 en centrales termoeléctricas de combustibles fósiles. (Fuente: Adaptado de Figueroa y col., 2008)

Post-combustión: Esta tecnología se refiere al proceso de separación de CO_2 de la corriente de gases de salida del proceso de combustión. Esta configuración de combustión es la empleada tradicionalmente en las centrales termoeléctricas para la generación de energía a partir de combustibles fósiles. En condiciones de post-combustión el combustible se quema completamente en un único paso con aire. El calor desprendido se emplea para producir vapor de alta presión, que se expande en una turbina para generar electricidad. El gas de combustión, una vez limpio de partículas en suspensión y compuestos de azufre, está constituido en su mayor parte por N_2 (70-75%), CO_2 (10-15%), H_2O (5-10%) y O_2 (3-4%), y abandona el proceso a presión atmosférica y 40-70 ^oC de

temperatura. Teniendo en cuenta las condiciones de la corriente de salida, cualquier proceso de captura de CO_2 que actúe en post-combustión ha de ser selectivo para el CO_2 con respecto al N_2, y además ha de ser capaz de trabajar con elevados volúmenes de gas de combustión que presentan bajas presiones parciales de CO_2. La principal ventaja de este proceso es que puede ser implantado en cualquier planta termoeléctrica existente sin grandes modificaciones en su configuración.

Pre-combustión: Esta tecnología de captura está relacionada con el sistema de Gasificación Integrada en Ciclo Combinado (GICC) que se emplea en plantas de producción de energía a partir de gas de síntesis. En este proceso, el combustible es gasificado (en lugar de quemado completamente como en el proceso de post-combustión) en presencia de oxígeno puro (en defecto) y vapor para producir gas de síntesis. El gas de síntesis, que es una mezcla de CO y H_2, es purificado y alimentado al reactor "water-gas-shift". En el reactor se añade vapor para convertir el CO en CO_2 y H_2. Después, el CO_2 es capturado y el H_2 es quemado en una turbina de gas para producir calor y electricidad. El calor producido durante la combustión puede ser recuperado por un sistema de transferencia de calor para pasar el agua al vapor, el cual se lleva a una turbina de vapor, donde se complementa la producción de electricidad de la turbina de gas. Las condiciones típicas de pre-combustión implican un gas de síntesis que contiene aproximadamente un 40% de CO_2 y más de un 55% de H_2, a 40 ^{o}C de temperatura y 30 bar de presión. Por tanto, la separación de gases relevante en este caso es CO_2/H_2. La principal ventaja de esta configuración es que la presión de vapor de CO_2 es elevada, lo que favorece la captura de CO_2. La principal desventaja de este proceso es que solamente es aplicable a plantas de nueva construcción, por lo que su implementación a nivel industrial se encuentra muy limitada actualmente.

Oxi-combustión: Esta tecnología se encuentra en fase de desarrollo. En este proceso, se introduce oxígeno puro en el sistema para la combustión, en

lugar de introducir aire como en el proceso de post-combustión. El calor generado es empleado para producir vapor de alta presión que mueve una turbina de vapor para generar electricidad. El gas de combustión, que mayoritariamente consiste en H_2O y CO_2, se limpia de partículas en suspensión y en parte se recicla a la caldera como medida de eficiencia energética. La fracción restante se desulfura y se enfría para condensar el agua, obteniéndose como resultado una corriente concentrada de CO_2. La diferencia fundamental entre este proceso con respecto a los anteriores es que no necesita captura de CO_2, ya que la separación de gases relevante es N_2/O_2. La elevada concentración de CO_2 en la corriente es el resultado de excluir el empleo de N_2 desde un principio.

Evaluaciones económicas detalladas de los tres procesos concluyen que la captura de CO_2 en pre-combustión es la menos costosa de las opciones en cuanto a funcionamiento, pero la inversión inicial resulta más elevada que en post-combustión y oxi-combustión (Ramdin y col., 2012). La pre-combustión se beneficia de las mayores presiones de operación, las cuales permiten reducción de gastos por compresión de CO_2 y en las tecnologías de separación, pero el proceso es más complejo, requiere una mayor inversión inicial, como se ha dicho, y sólo es aplicable a plantas nuevas. La oxi-combustión no necesita captura de CO_2, pero requiere una unidad más compleja para la separación de gases y materiales especiales de construcción por las elevadas temperaturas con las que se trabaja como consecuencia de la combustión con oxígeno puro, así como por la elevada concentración de SO_2 en el gas de combustión, que puede generar problemas de funcionamiento. Además, los procesos de captura de CO_2 en pre-combustion y oxi-combustión sólo pueden ser implementados en centrales de nueva construcción, puesto que las plantas termoeléctricas existentes actualmente operan en su gran mayoría en post-combustión. La etapa más costosa en el proceso de captura de CO_2 en post-combustión es la desorción de CO_2 para la regeneración del disolvente (*stripper* con vapor). Sin embargo, la

mayor ventaja de la captura de CO_2 en post-combustión es que puede ser implantada en centrales ya existentes.

Considerando la urgencia en desarrollar procesos de captura de CO_2 para tratar de reducir las emisiones a corto plazo, la mayor parte de los esfuerzos actuales se centran en desarrollar sistemas de captura de CO_2 en post-combustión que se puedan implementar en las centrales que se encuentran actualmente en funcionamiento, sin requerir modificaciones esenciales en la configuración de la planta.

3.1.3. Tecnologías disponibles para la captura de dióxido de carbono en post-combustión

El principal problema en el desarrollo de las tecnologías de captura en postcombustión es lograr sistemas económicamente rentables y sostenibles capaces de separar eficazmente el CO_2 que se encuentra a tan bajas concentraciones en el efluente gaseoso de salida. Sin embargo, considerando que se presenta como la alternativa más efectiva a corto plazo para reducir las emisiones de gases de efecto invernadero, son muchos los esfuerzos que se están llevando a cabo para desarrollar nuevos sistemas de captura que se puedan implementar en las centrales termoeléctricas de combustión de carbón existentes. A continuación, se exponen los sistemas de absorción con aminas, tecnología más estudiada para la captura de CO_2 en postcombustión, y se revisan las tecnologías emergentes.

3.1.3.1. Sistemas basados en absorción con aminas

La tecnología más estudiada para la captura de CO_2 en post-combustión es el proceso de absorción química con disoluciones de aminas primarias, como la monoetanolamina (MEA) en solución acuosa al 30%. De hecho, esta tecnología se puede considerar madura, toda vez que se emplea desde hace años para tratar el gas del reformado del gas natural y de otros hidrocarburos (naftas sobre todo) destinado a la obtención del gas de síntesis del amoniaco.

El mecanismo mediante el cual se lleva a cabo la absorción de CO_2 por parte de este tipo de aminas se puede explicar a través del mecanismo Zwitterion de la formación de sales de carbamato según el siguiente esquema de reacción:

$$2\ R\text{-}NH_2 + CO_2 \leftrightarrow R\text{-}NH_3^+ + R\text{-}NH\text{-}COO^-$$

El proceso de depuración basado en aminas para la captura de CO_2 ha sido desarrollado por varias compañías, como ABB Lummus y Mitsubishi Heavy Industries (Llamas y Romero, 2006). En la siguiente figura se presenta un diagrama convencional de absorción de CO_2 con aminas.

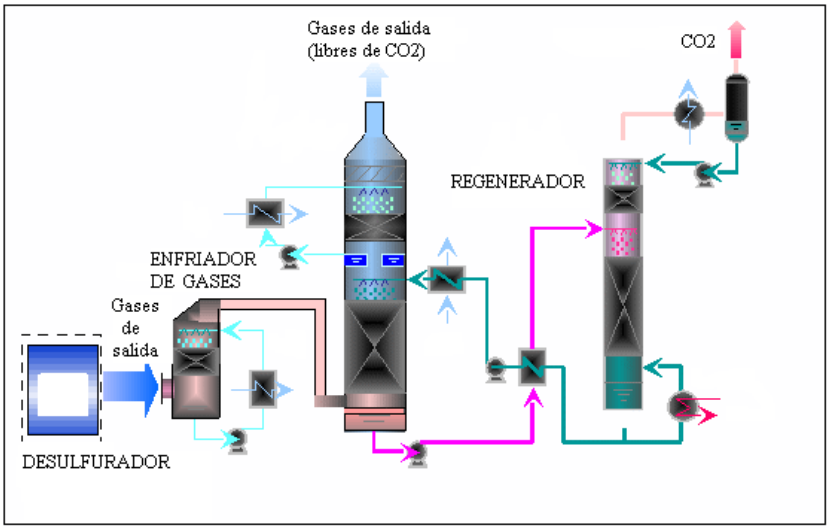

Figura 3.1.3.1.1. Esquema del proceso de captura de CO_2 basado en absorción con aminas. (Fuente: Adaptado de Mitsubishi Heavy Industries, 2012)

El proceso típico de captura de CO_2 de los gases de postcombustión de una central térmica presenta tres secciones principales: el enfriador de gases, el absorbedor (para la recuperación del CO_2) y el *stripper* (para la regeneración del disolvente). Además, si el combustible es carbón se añade una unidad de desulfuración previa al sistema de captura de CO_2 (Georgiadis y col., 2008).

El objetivo principal del enfriador de gases es disminuir la temperatura de la corriente gaseosa hasta 35-40º C antes de ser introducida al absorbedor, para aumentar la eficiencia de la reacción exotérmica de absorción y minimizar las pérdidas de disolvente. Además, el enfriador de gases está diseñado para eliminar impurezas como óxidos de azufre (SO_X), óxidos de nitrógeno (NO_X) y materia particulada suspendida.

En el absorbedor de CO_2 la corriente gaseosa se pone en contacto directo con la solución de aminas. Por cabeza de columna se obtiene una corriente de gases limpia de CO_2 que se liberan a la atmósfera después de ser lavados con agua para minimizar las pérdidas de amina en el ciclo. Por cola de columna se obtiene una corriente de disolvente rica en CO_2 que se precalienta antes de ser enviada al *stripper*, intercambiándola con la corriente del disolvente recuperado que proviene del *stripper*.

En la columna de desorción del *stripper* la corriente de disolvente precalentada se pone en contacto con vapor de agua a 120 ºC para desorber el CO_2 absorbido y regenerar así el disolvente, el cual se recicla a la columna de absorción previo enfriamiento en el referido intercambio de calor.

La mayor ventaja del proceso de absorción con MEA, además de la mencionada capacidad de regeneración, consiste en que resulta posible tratar corrientes gaseosas con baja presión parcial de CO_2 (0,15-0,3 bar). Sin embargo, su gran desventaja es la elevada demanda energética de la etapa de recuperación del disolvente, como consecuencia de la alta reactividad de las aminas primarias, con una alta entalpía de formación, asociada a la generación de los carbamatos. Este proceso presenta otras desventajas operacionales que suponen un problema para su implementación a gran escala, como la elevada volatilidad de las soluciones amínicas, que provoca pérdidas del disolvente por evaporación, generando un importante impacto ambiental en el entorno. Además, el oxígeno que contienen los gases provoca la oxidación de las aminas,

convirtiéndolas en ácidos carboxílicos que acentúan los problemas de corrosión. Asimismo, la combustión del carbón produce altas cantidades de óxidos de azufre y nitrógeno que reaccionan con las aminas dando sales estables altamente corrosivas y que favorecen las pérdidas del disolvente. Los gases a alta temperatura también causan la degradación de la amina, reduciendo la eficiencia del proceso de absorción, por lo que es necesario enfriarlos antes de introducirlos en el absorbedor. Estos inconvenientes provocan que aumente la inversión y los costes de operación de las plantas de captura basadas en aminas (Rao y Rubin, 2002; Aaron y Tsouris, 2005; Llamas, B. y Romero, 2006).

Para tratar de solucionar los inconvenientes asociados a las aminas primarias, se han estudiado como alternativas el empleo de aminas secundarias como dietanolamina (DEA) o terciarias como metildietanolamina (MDEA). La reacción del CO_2 con las aminas secundarias también se describe por el mecanismo del Zwitterion, aunque la entalpia de reacción es menor porque el carbamato formado es más inestable. Las aminas terciarias no presentan ningún protón unido al átomo de nitrógeno, por lo que tras el proceso de captura de CO_2 se forma bicarbonato en lugar de carbamato. La entalpía de formación del bicarbonato es menor que la de formación de carbamato, disminuyendo así los requerimientos energéticos en la etapa de regeneración del disolvente. Sin embargo, la reactividad de las aminas terciarias es menor que la de las primarias y secundarias porque la termodinámica de la reacción se encuentra menos favorecida (Ramdin y col., 2012).

Debido a las desventajas asociadas a los procesos de absorción de CO_2 con aminas, resulta necesario desarrollar disolventes que presenten menores requerimientos energéticos en su regeneración, así como menor volatilidad y corrosividad y mayor estabilidad térmica y química.

3.1.3.2. Tecnologías emergentes para captura de dióxido de carbono

A continuación, se exponen las tecnologías que están siendo evaluadas para la captura de CO_2 en postcombustión, que incluyen desde variaciones de los procesos existentes hasta alternativas completamente novedosas.

Sistemas basados en carbonatos

Los sistemas basados en carbonatos aprovechan la capacidad del carbonato soluble para reaccionar con CO_2 para formar bicarbonato, que al ser calentado libera el CO_2 permitiendo la regeneración del carbonato. La mayor ventaja del sistema basado en carbonatos frente al sistema convencional basado en aminas es su menor requerimiento energético para llevar a cabo la regeneración y su mayor velocidad de absorción. Sin embargo, no resuelven los problemas de degradación del disolvente y corrosión (Rochelle, 2005).

Sistemas basados en amoniaco

Los sistemas basados en amoniaco operan de forma similar a los sistemas basados en aminas. Las principales ventajas que ofrece trabajar con disoluciones de amoniaco en lugar de con disoluciones amínicas son su mayor capacidad de absorción, menor requerimiento energético y menor capacidad de degradación. Sin embargo, como desventajas cabe citar la mayor volatilidad del amoniaco frente a los compuestos amínicos y la necesidad de enfriar la corriente de gases antes de introducirla en el absorbedor hasta temperaturas inferiores a las requeridas en el sistema con aminas (Vega, 2010).

Membranas

Actualmente, se evalúan distintas alternativas para el empleo de membranas en captura de CO_2. Una opción es emplear membranas de separación de gases basadas en nuevos materiales, como polímeros, zeolitas o sílice funcionalizada con aminas. Otra posibilidad es emplear membranas de absorción de gases basadas en soluciones amínicas; sin embargo, este tipo de

membranas no resulta estable por la evaporación del disolvente y la alta capacidad de degradación del mismo (Llamas y Romero, 2006). Además, cabe destacar una novedosa aplicación de los líquidos iónicos para el desarrollo de membranas soportadas, con un gran potencial para ser aplicada en sistemas de captura de CO_2, por su elevada permeabilidad y selectividad entre otras prometedoras características (Scovazzo, 2009).

Adsorción en sólidos

Algunos sólidos pueden reaccionar con el CO_2 formando compuestos estables y posteriormente, variando las condiciones de operación, ser regenerados liberando el CO_2 capturado. Ejemplos de estos sólidos son adsorbentes con aminas inmovilizadas en la superficie, carbonato sódico soportado o estructuras monolíticas metálicas revestidas con zeolitas amínicas nanoestructuradas. Estos sistemas presentan una mayor eficiencia energética que aquellos basados en aminas, aunque su manejo resulta más complicado y aún no han sido comercializados a gran escala (Figueroa y col., 2008).

Estructuras reticulares metal-orgánico

Esta nueva clase de materiales híbridos consisten en compuestos cristalinos constituidos por iones metálicos coordinados con moléculas orgánicas, que forman estructuras porosas en las que puede ser almacenado el CO_2. Estas estructuras reticulares metal-orgánico (MOFs) presentan una elevada capacidad de almacenamiento y requieren poca energía para su regeneración, pero todavía es necesario evaluar su estabilidad después de varios ciclos y el efecto de las impurezas contenidas en el efluente gaseoso operación (D'Alessandro y col., 2010).

3.1.4. Captura de dióxido de carbono mediante sistemas basados en líquidos iónicos

El empleo de líquidos iónicos para la captura de CO_2 de efluentes gaseosos de centrales termoeléctricas de combustibles fósiles presenta un futuro prometedor. Debido a propiedades de estos compuestos, como volatilidad despreciable, elevada estabilidad química y térmica, bajo poder corrosivo y elevada capacidad para disolver selectivamente el CO_2, estos nuevos disolventes se han propuesto como alternativa a los sistemas convencionales de captura de CO_2 basados en absorción con aminas (Huang y Rüther, 2009; Bara y col., 2010; Karadas y col., 2010; Ramdin y col., 2012). Como consecuencia del reconocido potencial de los LIs para ser empleados en el desarrollo de nuevas tecnologías para la captura de CO_2, muchos grupos de investigación están centrando sus esfuerzos en explicar el comportamiento de estos sistemas. A continuación se presenta una revisión bibliográfica de las investigaciones realizadas a este respecto, que abarcan tanto la absorción física como la captura química de CO_2.

Absorción física de CO_2 con LIs

Distintos estudios sobre el efecto de las condiciones del proceso de absorción en la solubilidad del CO_2 en LIs han mostrado que la temperatura es uno de los factores predominantes; la solubilidad disminuye con la temperatura en el intervalo de ensayo comprendido entre 25 y 230 ºC (Finotello y col., 2008; Kerlé y col., 2009). También se ha estudiado el efecto de la presión, encontrándose que la solubilidad del gas aumenta con la presión desde condiciones atmosféricas hasta 8-10 Mpa, para después permanecer constante a partir de 30 MPa (Lim y col., 2009). Además de las condiciones de operación, se ha observado que la naturaleza del anión es un factor determinante en la disolución del CO_2 en LIs, mientras que los cationes parecen jugar un papel secundario (Anthony y col., 2005). El efecto del anión en la solubilidad del gas se ha estudiado para LIs de catión imidazolio combinado con diferentes aniones

como tetrafluoroborato $[BF_4]^-$ (Blanchard y col., 2001; Anthony y col., 2005; Kim y col., 2005; Soriano y col., 2008 y 2009a; Lim y col., 2009), hexafluorofosfato $[PF_6]^-$ (Blanchard y col., 2001; Kim y col., 2004 y 2005; Anthony y col., 2005; Kumelan y col., 2006a; Soriano y col., 2008; Lim y col., 2009), bis(trifluorometilsulfonil)imida $[NTf_2]^-$ (Anthony y col., 2005; Kim y col., 2005; Kumelan y col., 2006b; Hong y col., 2007; Jacquemin y col., 2007; Schilderman y col., 2007; Shiflett y Yokozeki, 2007; Raeissi y col., 2009a), dicianamida $[DCN]^-$ (Soriano y col., 2008), nitrato $[NO_3]^-$ (Soriano y col., 2009a), trifluorometanesulfonato $[CF_3SO_3]^-$ (Soriano y col., 2009a y 2009b) y series de sulfatos (Blanchard y col., 2001; Kumelan y col., 2006a) y fosfatos (Palgunadi y col., 2009). Los resultados obtenidos ponen de manifiesto que los aniones que contienen cadenas alquílicas con grupos fluorados presentan mayor capacidad para disolver el CO_2. De hecho, posteriores *screening* computacionales y ensayos experimentales corroboran que los LIs que presentan un mayor número de cadenas fluoradas, como aquellos que contienen aniones fluoroalquilfosfato $[FEP]^-$, mejoran la solubilidad del CO_2 en relación a sus análogos sin fluorar (Muldoon y col., 2007; Zhang y col., 2008 y 2009). En lo que se refiere al efecto del catión en la solubilidad del CO_2, parece que una mayor longitud de la cadena alquílica asociada al anillo imidazolio se encuentra generalmente relacionada con una ligero aumento de su solubilidad (Baltus y col., 2005; Jacquemin y col., 2007; Raeisse y col., 2009). Aunque la mayoría de los estudios se centran en sales imidazolio, también existen algunos estudios sobre otros cationes como amonio (Yuang y col., 2007), fosfonio (Bates y col., 2002), pirrolidinio (Anthony y col., 2005) o tiouronio (Zhang y col., 2008), observándose que el cambio de catión apenas afecta a la solubilidad.

Los LIs convencionales presentan una capacidad de captura de CO_2 similar a la de otros absorbentes físicos convencionales como el Selexol (en torno a 3 m^3 CO_2/m^3 disolvente a 25º C y 1 atm) empleados para absorción física de CO_2 en corrientes gaseosas que contengan elevadas concentraciones de

CO_2. Además, proporcionan una selectividad del CO_2 con respecto a otros gases muy superior (a 25 ^oC y 1 atm, el Selexol proporciona selectividades de CO_2/CH_4=15, CO_2/H_2=77, CO_2/N_2=50, mientras que los LIs convencionales presentan selectividades de CO_2/CH_4=8-35, CO_2/H_2=50-150, CO_2/N_2=30-100). Por ello, presentan un gran potencial para ser empleados en sistemas de separación de gases en los que el CO_2 se presente en bajas concentraciones. Sin embargo, los LIs convencionales no proporcionan resultados comparables a los sistemas basados en aminas para captura de CO_2 en postcombustión, en los que la presión parcial de CO_2 en la corriente gaseosa es baja (a 25 ^oC y 1 bar, las soluciones amínicas presentan una capacidad de absorción de 50-85 m^3 CO_2/m^3 disolvente). Por ello, las investigaciones actuales proponen el empleo de LIs que se comporten como absorbentes químicos de CO_2 y que puedan proporcionar capacidades de captura similares a los disolventes amínicos, presentando otras ventajas como menor volatilidad y menores requerimientos energéticos para su regeneración (Ramdin y col., 2012).

Membranas soportadas en LIs (SILMs)

En la práctica, el proceso de captura de CO_2 de los efluentes de las centrales termoeléctricas requiere su separación de la mezcla de gases de salida del proceso de combustión. La aplicación de los LIs en membranas soportadas (SILMs) pretende proporcionar la permeabilidad y selectividad adecuadas para la separación de CO_2 del efluente gaseoso de salida (Shiflett y Yokozeki, 2005; Han y Armstrong, 2007; Bara y col., 2009 y 2010; Scovazzo, 2009; Han y Row, 2010). Tras la evaluación de distintos LIs, incluyendo diferentes familias de cationes y una amplia variedad de aniones, se ha llegado a la conclusión de que las SILMs proporcionan una mayor permeabilidad y selectividad en la separación de mezclas de CO_2/N_2 y CO_2/CH_4 que la de las membranas poliméricas convencionales (Georgiadis y col., 2008; Scovazzo, 2009). En particular, las membranas soportadas en [emim][NTf_2] muestran la mayor permeabilidad (superior a 1.700 barrers) y las membranas soportadas en

[emim][DCN] proporcionan la mayor selectividad (CO_2/N_2=56.7, CO_2/CH_4=44.5) (Scovazzo, 2009). Por ello, estos sistemas se consideran prometedores para llevar a cabo la separación del CO_2 proveniente de los efluentes gaseosos de las centrales termoeléctricas de combustibles fósiles.

Absorción química de CO_2 con LIs

LIs funcionalizados con aminas: Se ha estudiado la posibilidad de capturar químicamente el gas introduciendo grupos funcionales en los iones para aumentar la capacidad de absorción de los solutos en el disolvente. El primer líquido iónico funcionalizado o "task-specific ionic liquid" (TSIL) diseñado para la captura de CO_2 fue el [Am-im][BF_4], compuesto por una sal imidazolio con una amina primaria unida covalentemente al catión, logrando una absorción molar de CO_2 comparable a la de las soluciones amínicas estándar empleadas en los sistemas de convencionales de absorción (Bates y col., 2002). Trabajos posteriores estudiaron una serie de LIs basados en cationes imidazolio funcionalizados con aminas primarias, aminas terciarias o grupos hidroxilo, [Am-im][BF_4], [Am-im][DCN], [3-Am-im][BF_4] y [OH-im][BF_4] (Galán y col., 2007). Estos compuestos fueron capaces incluso de triplicar la carga volumétrica de gas absorbido en relación a sus homólogos sin funcionalizar, encontrándose que los LIs funcionalizados con aminas primarias proporcionaban los mejores resultados. Además, tales líquidos iónicos mostraban capacidades de absorción de CO_2 similares a las de las soluciones amínicas convencionales. Asimismo, distintos trabajos estudiaron la relación entre la posición del grupo funcional y la estequiometria de reacción, sintetizando nuevos LIs basados en aminoácidos y demostrando que mientras los LIs basados en cationes funcionalizados con aminas favorecen la formación de carbamatos mediante estequiometria de reacción 1:2, los LIs basados en aniones funcionalizados como aminoácidos se aproximan a una estequiometría de reacción 1:1 (Gurkan y col., 2010). En este caso, aunque la mayor parte de la absorción se debe a mecanismos químicos, también se observa absorción física. Sin embargo, como en el caso de los LIs

basados en cationes funcionalizados con aminas, la viscosidad aumenta notablemente a medida que el LI reacciona con el CO_2, limitando su aplicación como disolventes en configuraciones industriales de absorción de CO_2 (Goodrich y col., 2011).

LIs funcionalizados con acetatos: Diversos estudios se han centrado en estudiar LIs funcionalizados con grupos acetato con resultados prometedores (Chinn y col., 2009; Shiflett y col., 2008 y 2010; Carvalho y col., 2009a; Shiflett y Yokozeki, 2009; Gurau y col., 2011). Por ejemplo, se ha patentado el empleo de [bmim][acetato] diluído al 14% en agua para la captura de CO_2 (Chinn y col., 2009). Este disolvente proporciona capacidades volumétricas de absorción 25 m^3/m^3 (intermedia entre la proporcionada por las disoluciones amínicas,~65 m^3/m^3, y los LIs para absorción física, ~3 m^3/m^3), y con entalpías de reacción de −40 kJ/mol (también intermedias entre las correspondientes a las disoluciones amínicas, −85 kJ/mol, y a los LIs para absorción física, -15 kj/mol). De este modo, se consigue una capacidad de absorción mayor que con disolventes físicos pero con necesidades energéticas inferiores a las requeridas para la regeneración de MEA. Asimismo, estudios económicos detallados del proceso indican que se podrían reducir los requerimientos energéticos en un 16% con respecto al proceso con MEA (Shiflett y Yokozeki, 2009).

LIs funcionalizados con otros grupos: Aparte de las sales de imidazolio funcionalizadas con aminas y con acetato, también se ha evaluado la capacidad de otros grupos funcionales y distintos cationes funcionalizados para aumentar la capacidad de absorción química de CO_2 en LIs. En concreto, los LIs basados en cationes imidazolio funcionalizados con grupos carbonilo no parecen aumentar la solubilidad del CO_2 en el disolvente, mientras que las cadenas alquílicas largas unidas con éteres lograron proporcionar mejores resultados (Muldoon y col., 2007). Además, algún estudio ha propuesto LIs basados en cationes fosfonio doblemente funcionalizados con aminas (Palgunadi y col., 2009). El principal inconveniente de estos últimos es su elevada viscosidad, que

puede provocar errores de medida a bajas presiones y problemas en aplicaciones prácticas al limitar la difusión del CO_2 en el disolvente (Zhang y col., 2009).

Mezclas de LIs con aminas: Para tratar de solventar los problemas de elevada viscosidad relacionados con los LIs funcionalizados, se ha estudiado la posibilidad de disolver los LIs directamente en aminas como MEA o DEA sin necesidad de introducir el grupo funcional en el catión. Al trabajar con disoluciones equimolares de [Rmim][NTf_2] y monoetanolamina (MEA) a modo de disolvente, se ha logrado capturar 1 mol de CO_2 por 2 moles de MEA mediante formación de complejos carbamato (Camper y col., 2008; Bara y col., 2010). Además, se observó que al funcionalizar el catión imidazolio del [Rmim][NTf_2] con un alcohol primario, resultaba posible capturar CO_2 con disoluciones equimolares del líquido iónico en dietanolamina (DEA). Se encontró que las soluciones de LIs y alcanolaminas comerciales resultaban tan efectivas como las soluciones amínicas convencionales empleadas para la captura de CO_2. Además, tales mezclas mostraron una absorción rápida y reversible, evitando la formación de los compuestos de alquitrán que habitualmente se forman al trabajar con LIs funcionalizados con aminas. Además, las soluciones de LIs en aminas presentan una menor volatilidad de la mezcla en relación con las disoluciones amínicas convencionales. Aun así, la viscosidad de estas disoluciones se encuentra en torno a 20 cP, unas diez veces más elevada que la de las soluciones acuosas de aminas tradicionales (Shiflett y Yokozeki, 2005).

Mezclas de LIs con superbases/superbases derivadas de LIs: Recientemente, se han estudiado mezclas de LIs y superbases para la captura equimolar de CO_2 (Wang y col., 2010 a, 2010b, 2010c y 2011). Las superbases son bases orgánicas que juegan un importante papel como aceptores de protones, y por tanto presentan una elevada capacidad para capturar CO_2. Como ejemplo, el sistema LI-superbase 1-(2-hidroxietil)-3-metilimidazolio bis(trifluorometilsulfonil)imida

[ImOH][NTf_2] y 1,8-diazabiciclo-[5.4.0]undec-7-ene (DBU), presenta un ratio molar de CO_2/LI ligeramente superior a 1. Además, el disolvente puede ser regenerado por aplicación de calor y sin observarse pérdida notable de actividad en subsecuentes ciclos de absorción-desorción (Wang y col., 2010b). También se ha estudiado la posibilidad de sintetizar superbases derivadas de LIs próticos, como el sistema [MTBDH][TFE] (9-metil-2,3,4,6,7,8-hexahidropirimido[1,2-a]pirimidina trifluoroetanol), que presenta una absorción de CO_2 de 1,13 mol de CO_2 por mol de LI, relativamente baja viscosidad (8.63 cP a 23 °C) y una rápida absorción de CO_2 y regeneración del disolvente (Wang y col., 2010 a).

LIs reversibles (RevILs): Una novedosa modalidad de captura de CO_2 que merece especial atención es la proporcionada por los denominados LIs reversibles. Estos disolventes están formados por compuestos no iónicos capaces de reaccionar químicamente con CO_2 para formar un líquido iónico, y que pueden ser revertidos a su forma no iónica original mediante exposición a un gas inerte o aplicación de calor (Jessop y col., 2005; Hart y col., 2005; Liu y col., 2006). Las primeras aproximaciones a este nuevo tipo de disolvente para captura de CO_2 sugerían el empleo de una base amínica y un alcohol, que reaccionaban con CO_2 formando la sal líquido iónico (Phan y col., 2008). Recientemente, se han estudiado LIs reversibles derivados de sililaminas, que son capaces de reaccionar químicamente con CO_2 para formar LIs que a su vez continúan absorbiendo CO_2 mediante mecanismos físicos. Estos disolventes son estables y poseen una capacidad de absorción de CO_2 comparable a las soluciones amínicas convencionales, presentando menores requerimientos energéticos para su regeneración (Blasucci y col., 2010a, 2010b; Rohan y col., 2012). En suma, se trata de un medio singular, que al absorber químicamente el CO_2 da lugar a un LI, capaz de complementar la absorción química por vía física. La desorción del CO_2 permite recuperar la estructura molecular original del medio, no iónica.

3.2. Amoniaco

A continuación se presenta la problemática asociada a las emisiones de amoniaco (NH_3), soluto gaseoso que actúa como contaminante provocando distintos problemas medioambientales y generando un efecto negativo en la salud. Asimismo, se revisan las tecnologías disponibles para mitigar las emisiones de este soluto y se presentan los prometedores avances relacionados con la absorción de amoniaco en líquidos iónicos.

3.2.1. El amoniaco como contaminante

Las emisiones de NH_3 contribuyen notablemente a la deposición ácida, eutrofización y polución atmosférica, generando diferentes problemas medioambientales y en la salud. El impacto de la deposición ácida incluye afectos adversos en los ecosistemas acuáticos de ríos y lagos y daños a los bosques, cosechas y vegetación. La eutrofización, crecimiento incontrolado de la flora acuática por la presencia de un exceso de nutrientes, en este caso nitrógeno, puede dar lugar al empeoramiento de la calidad del agua, reduciendo la biodiversidad, produciendo cambios en la composición de las especies y originando efectos tóxicos. El NH_3 también contribuye a la formación de partículas en suspensión, importantes contaminantes atmosféricos que producen efectos negativos en la salud, afectando especialmente al aparato respiratorio y al sistema cardiovascular (Sutton y Fowler, 2002; Erisman y col., 2007; Sutton y col., 2008).

En la Figura 3.2.1.1. se muestran las emisiones por sectores de los países miembros del Área Económica Europea (AEE) en 2010. Se observa que el sector agrícola se presenta como el foco mayoritario de emisiones de NH_3, sobre todo como consecuencia de la descomposición de la urea y ácido úrico de los desechos del ganado y el empleo de fertilizantes nitrogenados (Faulkner y Shaw, 2008; Ndegwa y col., 2008).

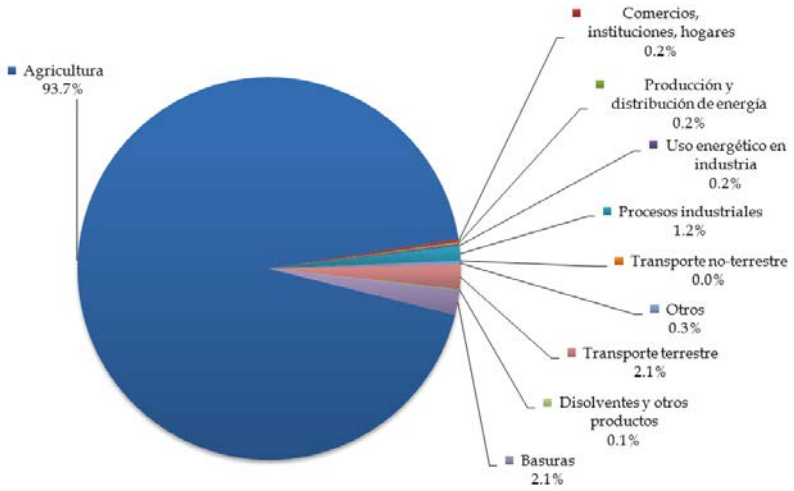

Figura 3.2.1.1. Emisiones de NH_3 por sectores en Europa, 2010.
(Fuente: EEA, 2013a)

Cabe destacar que se está prestando una especial atención a las emisiones de amoniaco de fuentes antropogénicas no agrícolas, debido a las pérdidas por evaporación de los sistemas de refrigeración basados en NH_3 (Roe y col., 2004; Melse y col., 2009). Además, la implementación de tecnologías de captura de CO_2 en post-combustión también puede provocar mayores emisiones de NH_3 como consecuencia de la degradación oxidativa de los disolventes basados en aminas, aumentando las emisiones de NH_3 provenientes del sector energético hasta un 13% (Koornneef y col., 2010).

Con el objetivo de controlar la calidad del aire a nivel europeo, se han instaurado distintas normativas para limitar las emisiones de amoniaco y otros compuestos contaminantes como dióxido de azufre (SO_2), óxidos de nitrógeno (NO_x) y compuestos orgánicos volátiles (COVs). En concreto, la Directiva 2001/81/CE de Techos Nacionales de Emisión fijó los límites para tales contaminantes hasta 2010. Actualmente se encuentra vigente el Protocolo de Gotemburgo (UNECE, 1999), creado para reducir la acidificación, eutrofización y el ozono troposférico de los países participantes, fijando los límites de emisión para 2020.

En la siguiente figura se muestra la evolución de las emisiones de NH_3 en Europa y se comparan con los objetivos propuestos por las mencionadas normativas.

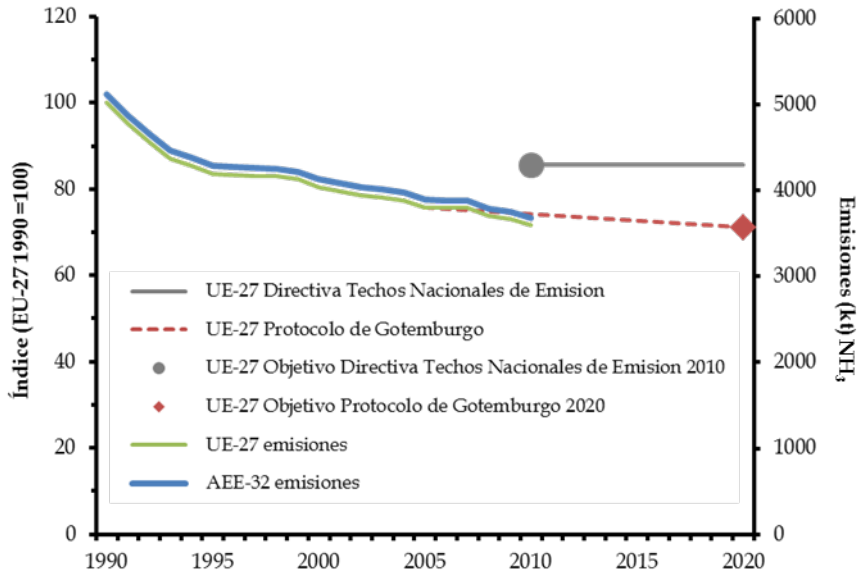

Figura 3.2.1.2. Evolución de las emisiones de NH_3 en el Área Económica Europea (AEE) y de la Unión Europea (UE). (Fuente: EEA, 2013b)

En general, las emisiones de NH_3 se han reducido aproximadamente un 25% en el periodo comprendido entre 1990 y 2010. Esta reducción ha sido principalmente debida al descenso de las emisiones agrícolas, como consecuencia de la disminución de ganado y de la limitación en el empleo de fertilizantes nitrogenados. Sin embargo, se ha producido un aumento en las emisiones provenientes del sector transportes, así como de las industrias de disolventes y de otros productos químicos.

En la Figura 3.2.1.3. se muestra la evolución de las emisiones de NH_3 en los países miembros del Área Económica Europea y se comparan con los límites nacionales de emisión establecidos en cada caso.

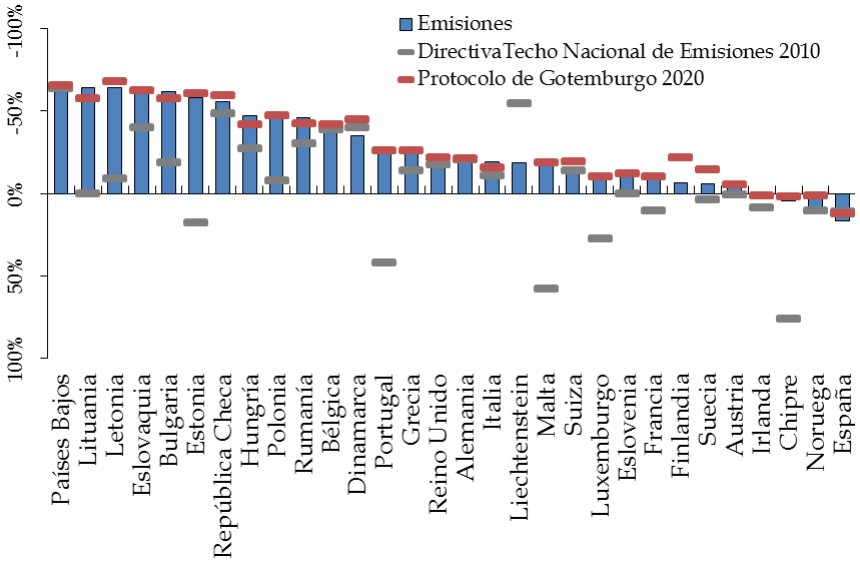

Figura 3.2.1.3. Evolución de las emisiones de NH_3 en el periodo 1990-2010 comparada con los objetivos de la Directiva 2001/81/CE de Techos Nacionales de Emisiones para 2010 y del Protocolo de Gotemburgo para 2020 en los países del Área Económica Europea (AEE). (Fuente: EEA, 2013c)

En general, los países miembros han hecho excelentes progresos en la reducción de las emisiones de amoniaco conforme a los límites nacionales de emisión establecidos en la directiva 2001/81/CE para 2010. Sin embargo, aún se requieren esfuerzos adicionales para conseguir los objetivos propuestos por el Protocolo de Gotemburgo (UNECE, 1999) para 2020. Por ello, resulta de interés el desarrollo de técnicas capaces de capturar las emisiones de amoniaco y nitrógeno reactivo de la atmósfera, así como de nuevos disolventes capaces de reducir la volatilidad de los sistemas que contienen amoniaco, como es el caso de los ciclos de refrigeración industrial.

3.2.2. Técnicas disponibles para el tratamiento de amoniaco

A continuación se revisan las distintas tecnologías disponibles para la reducción de las emisiones atmosféricas de amoniaco y se exponen sus principales ventajas e inconvenientes.

Incineración térmica

La incineración térmica se aplica a corrientes gaseosas muy concentradas en vapores de combustible. También se puede emplear si la corriente gaseosa de salida presenta compuestos orgánicos volátiles dañinos o que presentan mal olor, aunque en baja concentración. Una de las principales desventajas de esta tecnología es la formación de los denominados NO_x térmicos en el gas de cola, producidos como consecuencia de la reacción entre el nitrógeno y el oxígeno del aire a alta temperatura. Estos compuestos son muy estables, y no pueden ser revertidos a N_2 sin agentes reductores, menos en atmósfera oxidante. Además, la incineración térmica de compuestos orgánicos también puede generar cantidades importantes de CO. El amoniaco y las aminas son moléculas combustibles, cuya forma termodinámica más favorecida tras la combustión es CO_2 y NO_x. Sin embargo, también se produce NO, N_2O y CO, $COCl_2$ y dioxinas y furanos si la alimentación contiene compuestos clorados. Como estos compuestos no son olorosos, la incineración térmica resulta adecuada para el control de olores. Sin embargo, el CO y el NO son compuestos contaminantes y el N_2O es un gas de efecto invernadero, y por tanto sus emisiones han de ser reguladas (Busca y Pistarino, 2003). La alimentación no debe contener compuestos clorados por la razones ya apuntadas.

Combustión catalítica

La combustión catalítica representa una alternativa a la incineración térmica cuando los compuestos orgánicos volátiles en la corriente de salida se encuentran muy concentrados, permitiendo la recuperación del calor

producido. Las principales ventajas son una menor emisión de NO_x térmico y la menor cantidad de combustible adicional necesario, asociadas a las temperaturas de combustión más bajas requeridas por la presencia del catalizador. Las desventajas son un diseño más complejo de reactor, el coste de los catalizadores (generalmente basados en metales nobles) y la corta vida del catalizador, que se desactiva fácilmente si la alimentación presenta sulfuros, compuestos de nitrógeno y cloruros (Linz y Wittstock, 2001). Sin embargo, en el caso particular de las corrientes gaseosas con amoniaco y aminas, la producción de NO_x es habitual. La oxidación de amoniaco a NO se realiza a nivel industrial en el proceso de síntesis de ácido nítrico, posible sólo a muy bajos tiempos de contacto con el catalizador de Pt y a bajas temperaturas. Esto también ocurre en el caso de la biomasa con contenido de nitrógeno en presencia de catalizador de Pd/Al_2O_3. En el intervalo de temperatura comprendido entre 200 y 400 ºC, cuando la mayor parte de los compuestos orgánicos, hidrógeno y CO se queman, la conversión del amoniaco es prácticamente total y el resultado son grandes concentraciones de NO. Asimismo, empleando catalizadores basados en metales de transición como Mn-Ba hexa-aluminato, que son mucho menos activos, se encontró que la producción de NO y N_2O era predominante entre 500 y 700 ºC cuando el gas de biomasa se quema (Lietti y col., 1999).

Descomposición catalítica de amoniaco

El amoniaco pude descomponerse en nitrógeno e hidrógeno catalíticamente a presión atmosférica y temperaturas de entre 327 y 527 ºC. Este proceso permite disminuir el amoniaco en corrientes gaseosas a elevada temperatura sin necesidad de enfriar, como en el caso de los efluentes derivados de la combustión del carbón (Dou y col., 2002). Sin embargo, no parece ser aplicable a corrientes gaseosas que contengan oxígeno.

Condensación

El amoniaco puede ser recuperado por condensación. Debido al bajo punto de ebullición del amoniaco (-33 ºC a 1 atm) este procedimiento resulta adecuado cuando el gas se encuentra a elevadas concentraciones, presiones y cuando el enfriamiento se puede realizar mediante fluidos criogénicos (Busca y Pistarino, 2003). De hecho, este procedimiento se aplica al gas de síntesis generado en el proceso de producción de amoniaco para recuperar tal compuesto. Sin embargo, no se puede utilizar en el caso de las plantas de tratamiento de gases, puesto que habitualmente contienen grandes cantidades de vapor de agua, por lo que se produciría la condensación del agua con el amoniaco y las aminas disueltas.

Absorción

El amoniaco es altamente soluble en agua, y más aún en soluciones ácidas. Las soluciones de fosfato amónico se emplean en el proceso conocido como Phosam-W para recuperar el amoniaco de corrientes gaseosas que contienen dióxido de carbono y ácido sulfhídrico. La absorción en agua o soluciones acusas se lleva a cabo en torres de absorción, y la regeneración del disolvente es posible por *stripping* a elevadas temperaturas o sobrecalentamiento. En los procesos de tratamiento de gases el amoniaco no es destruido, de modo que si la disolución de amoniaco no se puede reutilizar en el proceso, es necesario llevar a cabo procesos de tratamiento adicionales o gestionar el residuo resultante (Busca y Pistarino, 2003; Ndegwa y col., 2008).

Adsorción

Se pueden emplear diferentes zeolitas como Linde A4 y 5A o 10X para llevar a cabo la adsorción del amoniaco, y regenerar posteriormente el material adsorbente a elevada temperatura. También pueden emplearse zeolitas naturales como la clinoptilolita, que puede mezclarse con los desechos producidos en la granjas para reducir las emisiones de amoniaco (Kelleher y

col., 2002). Asimismo, se ha propuesto el empleo de carbón activo como material adsorbente en ciclos de refrigeración, adsorbiéndose el amoniaco a temperatura ambiente y desorbiéndose a 200 ºC (Critoph, 2002).

Filtración y biofiltración

La filtración se basa en un proceso físico, mientras que la biofiltración no sólo separa el compuesto de interés sino que la película de microorganismos que recubre el relleno degrada biológicamente estos compuestos en otras formas menos nocivas (Ndegwa y col., 2008). La reducción de amoniaco mediantes filtros se puede llevar a cabo en granjas y graneros, aunque el empleo de estos equipos en la práctica está limitado por sus elevados costes y problemas técnicos (Sommer y Hutchings, 1995). Se han descrito distintos materiales con los que fabricar biofiltros para la captura de amoniaco de aires de ventilación de granjas, como mezclas de compostaje, astillas de madera y cáscaras de coco (Sun y col., 2000; Hong y Park, 2005). En planta piloto se ha evaluado un biofiltro de 500 mm de profundidad compuesto por astillas de madera de 20 mm consiguiendo una reducción del 54% al 93% del amoniaco presente en los aire de ventilación de una granja (Sheridan y col., 2002).

3.2.3. Absorción de amoniaco con líquidos iónicos

Los estudios relacionados con el comportamiento de sistemas compuestos por amoniaco y líquidos iónicos son todavía muy escasos, aunque los resultados obtenidos hasta el momento ponen de manifiesto el gran potencial de estos novedosos disolventes para ser utilizados como disolventes de absorción de dicho soluto.

La solubilidad del amoniaco en LIs se estudió por primera vez en imidazolios emparejados con distintos aniones, como hexafluorofosfato $[PF_6]^-$, cloruro $[Cl]^-$, bis(trifluorometilsulfonil)imida $[NTf_2]^-$ y tetrafluoroborato $[BF_4]^-$ en celdas de equilibrio isotérmico construidas para tal efecto. Se encontró que la solubilidad del amoniaco en LIs era muy elevada incluso en condiciones de

operación suaves, pudiéndose absorber más de 0,35 moles de amoniaco en [bmim][PF_6] a temperatura ambiente y presión de 0,174 MPa. Los resultados obtenidos mostraron que la solubilidad de estos sistemas era similar a la del amoniaco en agua. Además, se sugiere la posibilidad de emplear LIs como refrigerantes en ciclos de absorción, realizándose un estudio teórico comparativo con el simulador de procesos ASPEN, que proporciona una eficiencia energética de los ciclos NH_3/LI superior a la de los ciclos tradicionales NH_3/H_2O (Yokozeki y Shiflett, 2007a). Un estudio posterior completó los datos de solubilidad de NH_3 en una serie de LIs con catión común imidazolio y distintos aniones, entre los que se incluían acetato $[CH_3CO_2]^-$, tiocianato $[SCN]^-$, etilsulfato $[CH_3SO_4]^-$, así como un líquido iónico basado en el catión amonio emparejado con anión acetato (Yokozeki y Shiflett, 2007b). Publicaciones más recientes evaluaron el efecto del catión en la solubilidad del NH_3 en LIs. En concreto, los resultados indicaron que la absorción de amoniaco en LIs basados en el catión guanidio resultaba incluso más favorecida que con los imidazolios, superando 0,5 moles de soluto absorbido por mol de LI a temperatura ambiente y presión atmosférica, lo que pone de manifiesto que el catión juega un papel importante en la absorción de este soluto (Huang y col., 2008). Asimismo, se observó que el aumento de la longitud de la cadena alquílica asociada a los cationes imidazolio favorecía ligeramente la solubilidad del amoniaco en el líquido iónico (Li y col., 2010).

El carácter polar del amoniaco sugiere la oportunidad de diseñar LIs funcionalizados con propiedades optimizadas para la absorción de este soluto, con aplicaciones potenciales en sistemas de refrigeración industrial (Yokozeki y Shiflett, 2007c y 2007d), torres de absorción para mitigar emisiones de la industria agrícola (Melse y col., 2009) o como disolventes en tratamientos adicionales para reducir las emisiones de amoniaco provenientes de los sistemas de captura de CO_2 basados en aminas asociados a las centrales termoeléctricas de combustibles fósiles (Koornneef y col., 2010).

3.3. Compuestos orgánicos volátiles

La Organización Mundial de la Salud define los Compuestos Orgánicos Volátiles (COVs) como cualquier compuesto cuyo punto de ebullición se encuentre entre (50-100°C) o (240-260°C) con presiones de vapor saturado superiores a 102 kPa a 25°C (ISO16000-6, 1989). Estos compuestos son hidrocarburos altamente reactivos de origen natural o antropogénico, generalmente de carácter tóxico y que causan importantes daños medioambientales, pues se comportan como aerosoles orgánicos y participan en reacciones fotoquímicas que aumentan la concentración de ozono troposférico contribuyendo así al cambio climático (IPCC, 2007a).

Los principales focos naturales de emisión de COVs incluyen humedales, bosques, océanos y volcanes, mientras que los antropogénicos consisten mayoritariamente en industrias manufactureras de productos químicos, combustión de biomasa y emisiones de vehículos (Berenjian y col., 2012; EPA, 2012b).

Las emisiones naturales de COVs predominan en los trópicos, mientras que las antropogénicas se concentran en regiones industrializadas y pobladas (el 95% se producen en el hemisferio norte). La mayoría de COVs presentan tiempos cortos de vida, generando problemas de salud e impacto ambiental a nivel regional. Sin embargo, ciertos COVs, como el etano y la acetona, presentan tiempos de vida más largos, contribuyendo así a efectos dañinos de mayor alcance en la química troposférica a nivel global (IPCC, 2007a).

En la Figura 3.3.1. se presentan las contribuciones individuales de COVs emitidos desde las principales fuentes estacionarias antropogénicas, esto es, a nivel industrial y en las plantas de combustión de biomasa.

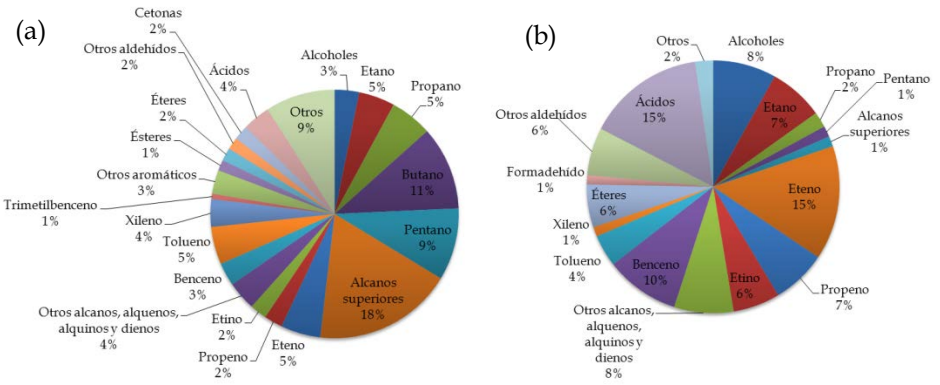

Figura 3.3.1. Contribuciones individuales de COVs (% en peso) en emisiones antropogénicas: a) Industriales (total de emisiones 210 Tg COVs/año, correspondiente a 161 Tg C/año; b) Combustión de biomasa (total de emisiones 42 Tg COVs/año, correspondiente a 33 Tg C/año). (Fuente: IPCC, 2007a)

Los COVs no son únicamente contaminantes atmosféricos, sino que también se consideran importantes contaminantes domésticos como consecuencia del empleo cotidiano de disolventes químicos, pinturas o plásticos, además de su utilización habitual en las operaciones de mantenimiento de edificios y equipos (Berenjian y col., 2012).

Como consecuencia de los expuesto anteriormente, en las grandes urbes y países industrializados existe una creciente preocupación por el control de las emisiones de estos contaminantes tanto a nivel doméstico como atmosférico, y distintas organizaciones establecen guías para limitar sus niveles máximos de exposición y emisión, como la del Protocolo de Gotemburgo, las propuestas por El Consejo Nacional de Sanidad e Investigación Médica de Australia (NHMRC, 2002) o las de la Agencia de Protección medioambiental de los Estados Unidos de América (EPA, 2012b).

3.3.1. Técnicas disponibles para el tratamiento de compuestos orgánicos volátiles

Uno de los métodos tradicionalmente más empleados para el tratamiento de COVs es la adsorción en compuestos porosos como carbón activado o zeolitas (Chiang y col., 2001; Jarraya y col., 2010). Sin embargo, su aplicación se encuentra limitada porque la humedad del gas y la deposición de otros compuestos pueden bloquear o envenenar los centros activos del sorbente disminuyendo la efectividad y dificultando la regeneración del material. Además, estos métodos presentan problemas económicos y logísticos por los desechos que se generan, por lo que en la práctica se aplican como post-tramiento de corrientes con baja concentración de COVs (Berenjian y col., 2012). En cualquier caso, la adsorción es más una técnica de concentración del contaminante que de eliminación del mismo.

Existen otros métodos para el tratamiento de los COVs, como oxidación térmica, catalítica y tratamiento UV, que implican la degradación del contaminante en otros compuestos como CO_2, H_2O y HCl (Rao, 2007). Sin embargo, estas técnicas resultan costosas, ya que presentan elevados requerimientos energéticos y en la mayoría de los casos es necesario el acondicionado previo de la corriente a tratar o métodos adicionales de post-tratamiento.

Actualmente, uno los métodos más prometedores para la eliminación de COVs son los tratamientos biológicos como bio-filtros, bio-absorbedores, bio-reactores de crecimiento suspendido y bio-reactores de membrana, puesto que ofrecen ventajas significativas como menores requerimientos energéticos de operación (Berenjian y col., 2012). Sin embargo, aunque tales métodos presentan una solución eficaz y de bajo coste para el tratamiento de los COVs, no son adecuados cuando la actividad microbiana se encuentra limitada por la lenta transferencia de materia de los COVs desde la fase gas a la fase líquida,

que es donde realmente se da el proceso de biodegradación (Arriaga y col., 2006). Una estrategia para mejorar esta difusión de los COVs es añadir una fase no acuosa con una alta afinidad por los contaminantes a tratar (Dauguis, 2011). Estos sistemas multifásicos, también conocidos como bio-reactores de partición de dos fases, han sido ampliamente investigados para el tratamiento de COVs hidrofóbicos, habiéndose empleado aceites de silicona, alcanos, perfluorocarbonados y polímeros solidos como fases no acuosas (Quijano y col., 2009).

La absorción es una de las técnicas más eficaces. Sin embargo, para compuestos hidrofóbicos, su baja solubilidad en agua reduce la capacidad de absorción (Wang y col., 2001; Heyems y col., 2006). Además, los compuestos orgánicos (por ejemplo, hexadecano para la absorción de tolueno) presentan la desventaja de su elevada volatilidad (Quijano y col., 2011).

3.3.2. Tratamiento de compuestos orgánicos volátiles con líquidos iónicos

La solubilidad de compuestos hidrocarbonados de cadena corta ha sido ampliamente investigada en bibliografía. Se ha estudiado la solubilidad del etano, eteno, propano, propeno, isobutano, butano, 1-buteno y 1,3-butadieno en [bmim][PF_6], [bmim][BF_4], [emim][NTf_2], [emim][CF_3SO_3] y [emim][DCN] a 40 ^oC y presión atmosférica empleando métodos volumétricos (Camper y col., 2006). Se encontró que la solubilidad aumentaba con el número de carbonos presentes en el compuesto, así como con el número de dobles enlaces en compuestos con el mismo número de carbonos. Posteriormente, estos autores estudiaron la difusividad del etano, eteno, propano y propeno en [emim][NTf_2] a 30 ^oC y presión atmosférica (Camper y col., 2006a).

Distintos autores han evaluado la solubilidad de alcanos y alquenos de cadena corta en [bmim][PF_6], [bmim][BF_4] y [bmim][NTf_2] (Jacquemin y col., 2006a y 2006b; Lee y Outcalt, 2006), así como la solubilidad de etano en LIs basados en pirrolidinio y choline emparejados con aniones $[NTf_2]^-$ (Hong y col.,

2007) a temperaturas comprendidas entre 10 y 70 ºC y presiones cercanas a la atmosférica mediante métodos basados en la saturación isocórica. Además, la solubilidad del metano en [hmim][NTf_2] también fue medida a temperaturas comprendidas entre 20 y 140 ºC y presiones cercanas a los 10 MPa mediante técnicas volumétricas en células de alta presión (Kumelan y col., 2007). Asimismo, se determinó la solubilidad del metano, etano y eteno a la temperatura de 25 ºC y presiones de hasta 10 bar mediante técnicas termogravimétricas en [mpy][NTf_2], y se comparó con la solubilidad de otros compuestos (como SO_2 y CO_2) y otros líquidos iónicos (Anderson y col., 2007). Los resultados pusieron de manifiesto que la tendencia en la solubilidad de estos compuestos es la siguiente, SO_2>CO_2> C_2H_4>C_2H_6>CH_4, aumentando con la presión y disminuyendo con la temperatura. Además, como en el caso del CO_2, estos gases interaccionan principalmente con el anión mientras que el catión y los sustituyentes juegan un papel secundario, aunque la fluoración y la longitud de las cadenas alquílicas pueden favorecer la solubilidad. Un estudio posterior analizó la solubilidad, difusividad y permeabilidad de distintos compuestos hidrocarbonados de cadena corta en LIs basados en imidazolio, amonio y fosfonio sugiriendo el empleo de membranas soportadas en LIs para su aplicación en separación de gases (Condemarin y Scovazzo, 2009).

Aparte de estudios de absorción de compuestos hidrocarbonados de cadena corta, existe muy poca información acerca del comportamiento de otros COVs en LIs. Sin embargo, se han estudiado las solubilidades de compuestos fluorocarbonados de las series metano y etano en LIs imidazolios a temperaturas comprendidas entre 10 y 75 ºC y presiones de hasta 20 bar mediante termogravimetría (Shiflett y Yokozeki, 2006). Estos compuestos presentaban solubilidades más elevadas que sus análogos sin fluorar.

Cabe señalar que se ha evaluado la capacidad de emplear LIs en el diseño de bio-reactores multifásicos para el tratamiento de dimetilsulfato, dimetil disulfuro y tolueno utilizando [bmim][PF_6] y [bmim][NTf_2] como fase

no acuosa. Estos sistemas mostraron coeficientes de partición similares (o superiores, en el caso del tolueno) a los proporcionados por los disolvente orgánicos utilizados en este tipo de reactores (Quijano y col., 2011).

Además, recientemente se ha realizado un estudio computacional-experimental con el fin de seleccionar LIs apropiados para la absorción de tolueno mediante simulación molecular COSMO-RS, ensayos termogravimétricos y simulación de procesos ASPEN (Bedia y col., 2012). De acuerdo con los resultados obtenidos se han propuesto LIs imidazolio basados en anion [NTf_2] y con cadenas alquílicas largas asociadas al catión como disolventes adecuados para la absorción del tolueno, tanto desde el punto de vista termodinámico como cinético.

4. TÉCNICAS DE MEDIDA DE SOLUBILIDAD DE GASES EN LÍQUIDOS IÓNICOS

4. TÉCNICAS DE MEDIDA DE SOLUBILIDAD DE GASES EN LÍQUIDOS IÓNICOS

A continuación se describen las técnicas de medida más empleadas para determinar experimentalmente la solubilidad de gases en líquidos iónicos, las cuales incluyen la termogravimetría (TGA) a presión atmosférica y de alta presión, el empleo de la célula de presión y la aplicación de otros métodos como los de caída de presión o los volumétricos.

4.1. Termogravimetría a presión atmosférica

La técnica termogravimétrica consiste en registrar la variación que experimenta la masa de la muestra bajo una atmósfera controlada en función de la temperatura y del tiempo. La termogravimetría es una técnica rápida y eficaz que permite estudiar, no solo la termodinámica, sino también la cinética del proceso de absorción. Esta técnica se ha empleado para estudiar la capacidad de absorción (sobre todo química) y velocidad de absorción de CO_2 en LIs (Chen y col., 2011), así como la capacidad de absorción y difusividad de otros solutos con una elevada solubilidad en LIs, como el tolueno (Bedia y col, 2012).

Los experimentos se suelen realizar en una balanza termogravimétrica a presión atmosférica, en modo isotermo, controlando la temperatura mediante un baño termostático externo y estableciendo el flujo de gas que entra en contacto con la muestra. En estos experimentos, una cantidad conocida de LI, previamente secado a vacío, se carga en el crisol y se introduce en la termobalanza. Una vez cargada la muestra, el sistema se purga con un gas inerte para eliminar la posible humedad que haya podido absorber la muestra durante su manipulación. A continuación se corta el flujo de gas inerte y se introduce la corriente del gas de interés. Se considera que el sistema ha llegado al equilibrio cuando la masa registrada se mantiene prácticamente constante con el tiempo (<0,001 mg/h). Se han sugerido variaciones de esta técnica sin utilizar el equipo termogravimétrico propiamente dicho, sino burbujeando el

gas en la muestra contenida en un recipiente agitado y registrando la variación de peso antes y después del burbujeo (Zhang y col., 2009). Aunque esta práctica resulta un método accesible para evaluar la capacidad de absorción de un gas en un líquido, no proporciona un registro tan preciso de la variación de masa con el tiempo, resultando menos fiable el estudio de la cinética del proceso. La TGA a presión atmosférica ha sido la técnica utilizada en el presente trabajo para determinar la solubilidad y difusividad del NH_3 en LIs.

4.2. Termogravimetría de alta presión

La técnica termogravimétrica de alta presión permite registrar la variación del peso de la muestra bajo atmosfera controlada en función del tiempo a una temperatura y presión establecidas para determinar las isotermas o isobaras de absorción-desorción del sistema. Cabe señalar que la termogravimetría se presenta como un método eficaz y directo para determinar tanto la solubilidad como la difusividad del sistema, pero es necesario evaluar el efecto del empuje que ejerce el gas en el líquido cuando se opera a presiones elevadas para corregir los datos gravimétricos registrados por el equipo. Esta técnica ha sido ampliamente empleada para estudiar el proceso de absorción de gases en LIs a presiones de hasta 20-30 bar (Anthony y col., 2005; Anderson y col, 2007; Muldoon y col., 2007; Soriano y col., 2008; Shiflett y Yokozeki, 2005, 2006, 2007, 2009; Shifflet y col., 2008, 2010, 2012a, 2012b, 2012c). Asimismo, se ha utilizado para estimar la difusividad del CO_2 en LIs (Shifflet y Yokozeki, 2005).

Estos experimentos se realizan en termobalanzas de alta presión en las que habitualmente se opera en modo isotermo, de modo que se varía progresivamente la presión y se registra la variación de la masa en función de la presión y del tiempo. Las termobalanzas de alta presión pueden operar en modo dinámico y estático. La operación en modo dinámico proporciona un flujo continuo de gas a través de la celda en la que se encuentra la muestra, permitiendo un control exhaustivo de la presión a lo largo del proceso,

pudiéndose registrar así la masa de la muestra para los *set points* de temperatura y presión previamente establecidos. La medida estática es un procedimiento opcional, en el que se corta el flujo de gas una vez que el sistema alcanza el *set point* de temperatura y presión establecidos, de modo que la presión del sistema va disminuyendo lentamente y se considera que el sistema ha llegado al equilibrio cuando la masa y la presión registrada no varían con el tiempo. Una de las ventajas que incorporan las balanzas de alta presión es la posibilidad de medir directamente la densidad de la fase gaseosa que rodea la muestra, lo cual es necesario para evaluar los efectos de empuje que actúan sobre la muestra y así corregir los datos de masa registrados por el equipo, con el objetivo de determinar de manera precisa la termodinámica y cinética del proceso. De este modo, un procedimiento estándar de medida en una termobalanza de alta presión implica las siguientes etapas: a) calibrado del equipo para determinar la masa y el volumen del contenedor vacío de muestra; b) secado de cada nueva muestra introducida en el equipo; c) experimento para evaluar el efecto del empuje que ejerce la fases gaseosa a presión sobre la muestra liquida; d) experimento de absorción, en el que se registran los datos de masa en función de la presión y del tiempo; e) experimento de desorción. La TGA de alta presión ha sido la técnica utilizada en el presente trabajo para determinar la solubilidad y difusividad del CO_2 en LIs.

4.3. Célula de presión

Mediante esta técnica es posible obtener los datos de equilibrio líquido-vapor para una mezcla de composición conocida, registrando la presión de equilibrio del sistema a una temperatura fija. Esta técnica se ha empleado para estudiar la capacidad de absorción de CO_2 en LIs a elevadas presiones, incluso alcanzando condiciones supercríticas (Carvalho y col., 2009a, 2009b, 2009c, 2010; Mattedi y col., 2011). La célula de presión de volumen variable consiste en un cilindro hueco de acero inoxidable cerrado por un extremo con un pistón y por el otro extremo con una ventana de zafiro que permite la observación visual del

fluido. Detrás de la ventana de zafiro se coloca un sistema de adquisición de datos con video que reproduce en una pantalla de ordenador el comportamiento del fluido dentro de la célula de presión. La temperatura se mantiene constante mediante el paso de agua procedente de un baño termostático por el espacio anular concéntrico a la célula. Las muestras se preparan pesando cantidades precisas de LI seco, se introducen en la célula de presión y se procede a la evacuación del sistema. La masa del sistema se determina mediante una balanza de precisión. Entonces, el CO_2 es introducido a presión desde la bala de gas, que se conecta con la célula a través de un capilar de alta presión. Asimismo, la masa introducida de CO_2 se determina mediante pesada con la balanza de precisión. Una vez que la mezcla de composición conocida alcanza la temperatura deseada, la presión se reduce lentamente hasta que el sistema se homogeneiza. La presión a la cual la última burbuja desaparece representa la presión de equilibrio para la temperatura de trabajo.

4.4. Otras técnicas

Los métodos de caída de presión y volumétricos se utilizan habitualmente para determinar la solubilidad de gases en líquidos. En los métodos de caída de presión, el volumen se mantiene constante mientras se registra la disminución de presión que se produce en el sistema mientras el gas es absorbido en el líquido. En los métodos volumétricos, la presión se mantiene constante mientras se registra el cambio de volumen necesario para mantener la presión del sistema a medida que el gas es absorbido en el líquido. En ambos casos, las variables de presión, temperatura y volumen antes y después de la absorción son conocidas. Por tanto, la cantidad de gas absorbido por el líquido se calcula empleando ecuaciones de estado para determinar el número de moles a partir las mencionadas variables. Esta técnicas han sido empleadas por distintos grupos para estudiar la solubilidad de gases en LIs (Blanchard y col., 2001; Kamps y col., 2003; Kumelan y col., 2006a y 2006b; Aki y col., 2004; 2006; Brennecke y col., 2011).

5. SIMULACIÓN MOLECULAR COSMO-RS PARA LA SELECCIÓN Y DISEÑO DE LÍQUIDOS IÓNICOS

5. SIMULACIÓN MOLECULAR COSMO-RS PARA LA SELECCIÓN Y DISEÑO DE LÍQUIDOS IÓNICOS

El método COSMO-RS constituye un modelo químico cuántico para la predicción de propiedades termodinámicas de sustancias puras y mezclas en fase líquida empleando exclusivamente información estructural unimolecular del fluido. Una de las principales ventajas de esta metodología es que, a diferencia de los métodos clásicos utilizados tradicionalmente en Ingeniería Química, permite la predicción de las propiedades termodinámicas de los compuestos sin necesidad de datos experimentales para la definición de sus parámetros. Por ello, el método COSMO-RS resulta particularmente adecuado para la determinación de datos en sistemas de los que se dispone escasa información experimental, como es el caso de los líquidos iónicos, así como para el diseño de nuevos productos y procesos basados en estos disolventes.

5.1. Características generales del método COSMO-RS

El método COSMO-RS (Conductor-like Screaning Model for Real Solvents), desarrollado por A. Klamt y col. en 1995, constituye un modelo químico cuántico para la predicción de las propiedades termodinámicas de sustancias puras y mezclas en fase líquida usando exclusivamente información estructural uni-molecular del fluido (Klamt y Schüürmann, 1993; Klamt; 1995; Klamt y col., 1998; Klamt y Eckert, 2000a y 2000b; Eckert y Klamt, 2002; Klamt, 2005). Parte de reconocer que el estado termodinámico de un componente de una mezcla cualquiera en fase líquida depende de las interacciones moleculares que se establece en dicho medio y que estas interacciones, a nivel molecular, están determinadas fundamentalmente por la distribución de la densidad electrónica en la superficie de las moléculas interactuantes. Para determinar las propiedades macroscópicas de los fluidos a partir de la información mecano-cuántica de la distribución de la densidad local de carga en la superficie de las moléculas, el método COSMO-RS desarrolla un procedimiento de

termodinámica estadística para calcular los coeficientes de actividad de los componentes en la mezcla y, a partir de éstos, evaluar propiedades termodinámicas, termo-físicas y de equilibrio.

Los métodos COSMO son modelos de tipo solvatación continua. Esta clase de métodos permiten modelizar los efectos del solvente calculando una molécula individual, lo que reduce significativamente el tiempo de cálculo mecano-cuántico. El método COSMO establece que las moléculas en fase líquida son estructuras electrónicas polarizables y sitúa una de ellas en una cavidad del disolvente, describiendo a este último como un medio continuo de constante dieléctrica infinita. La molécula de soluto induce una polarización de la densidad de carga, σ, en la interfase con el medio conductor. Una vez calculada la distribución local de carga polarizada, el método COSMO divide la cavidad creada para representar la interacción soluto disolvente, tratando las moléculas como conjuntos de segmentos de superficie de carga polarizada.

Caracterizado el estado energético del soluto en la disolución a nivel mecano cuántico, el método COSMO-RS desarrolla un procedimiento de termodinámica estadística para calcular los coeficientes de actividad de los componentes en la mezcla y, a partir de éstos, evaluar propiedades termodinámicas, químicofísicas y de equilibrio. En primer lugar, el método COSMO-RS reúne la distribución de carga polarizada, $p^X(\sigma)$, sobre la superficie molecular en el campo de polaridad σ mediante el histograma denominado *σ-Profile*. A continuación, para determinar las propiedades termo-físicas (macroscópicas) del fluido a partir de la información electrónica (microscópica) de las moléculas, el método COSMO-RS desarrolla un tratamiento termodinámico estadístico en el que utiliza el *σ-Profile* como elemento de enlace.

El modelo COSMO-RS calcula la energía de interacción entre las moléculas de soluto y disolvente, $E(\sigma, \sigma')$, evaluando el contacto de una región de la superficie molecular de área efectiva a_{eff}, considerando que los segmentos

sobre las superficies de la molécula y la cavidad tienen densidades de carga polarizada σ y σ', respectivamente. La energía de interacción entre las moléculas del soluto y del disolvente se determina integrando, sobre toda la superficie de contacto, la energía necesaria para separar los segmentos de densidades de carga σ y σ' una distancia tal que el potencial eléctrico entre ambos segmentos de carga contraria se haga nulo. El método COSMO-RS establece que las interacciones entre moléculas en un fluido son de tres tipos: electrostáticas, de enlace de hidrógeno y de van der Waals, incluyendo para su formulación matemática cinco parámetros [a', c_{hb}, σ_{don}, σ_{acc} y $\tau(e)$], ajustados por comparación con datos experimentales. Una vez calculada la energía de interacción soluto/disolvente es posible evaluar en términos termodinámicos clásicos el estado termodinámico de los componentes en la mezcla. Para ello se recurre a un tratamiento termodinámico-estadístico cuya expresión de partida es la que define el potencial químico de un segmento de densidad de carga, σ, en el sistema S (*σ-Potencial*):

$$\mu_S(\sigma) = -R \cdot T \cdot \ln\left\{ \int p_S(\sigma') \cdot \exp\left(\frac{\mu_S(\sigma') - a_{eff} \cdot E(\sigma,\sigma')}{R \cdot T} \right) \cdot d\sigma' \right\} \quad [5.1.1.]$$

donde $\mu_S(\sigma)$ es una medida de la afinidad del sistema S por un segmento de superficie de polaridad σ. Formalmente, es el potencial químico de un área de contacto molecular promedio a_{eff} y densidad de carga polarizada σ en el conjunto S a la temperatura T. A partir de la expresión del *σ-potencial* se puede determinar el potencial químico de una molécula X en el líquido S (la energía libre parcial de Gibbs, G):

$$\mu_S^{X_i} = \mu_{C,S}^{X_i} + \mu_{R,S}^{X_i} = \int p^{X_i}(\sigma) \cdot \mu_S(\sigma) \cdot d\sigma - \lambda_C \cdot R \cdot T . \ln A_S \quad [5.1.2.]$$

donde los términos $\mu_{C,S}^{X_i}$ y $\mu_{R,S}^{X_i}$ son las contribuciones de tipo combinatorial y residual al potencial químico, λ_c es un parámetro ajustable y A_s es el valor promedio del área del disolvente. Finalmente, a partir del potencial químico se

puede determinar el coeficiente de actividad (γ) del soluto X en el disolvente S según:

$$\gamma_S^X = \exp\left(\frac{\mu_S^X - \mu_X^X}{R \cdot T}\right) \qquad [5.1.3.]$$

con lo que resulta accesible la descripción completa del estado termodinámico del soluto *X* en la disolución S.

En la Figura 5.1.1. se presenta un esquema del procedimiento COSMO-RS para el cálculo de las propiedades termo-físicas de los fluidos.

Los cálculos COSMO han sido implementados en diversos programas de química cuántica (Gaussian, Turbomole, etc.) para generar los archivos que contienen toda la información relativa a la distribución de carga polarizada sobre la superficie molecular y constituyen la entrada para los cálculos termodinámico estadísticos COSMO-RS, los cuales se llevan a cabo mediante el programa COSMOtherm.

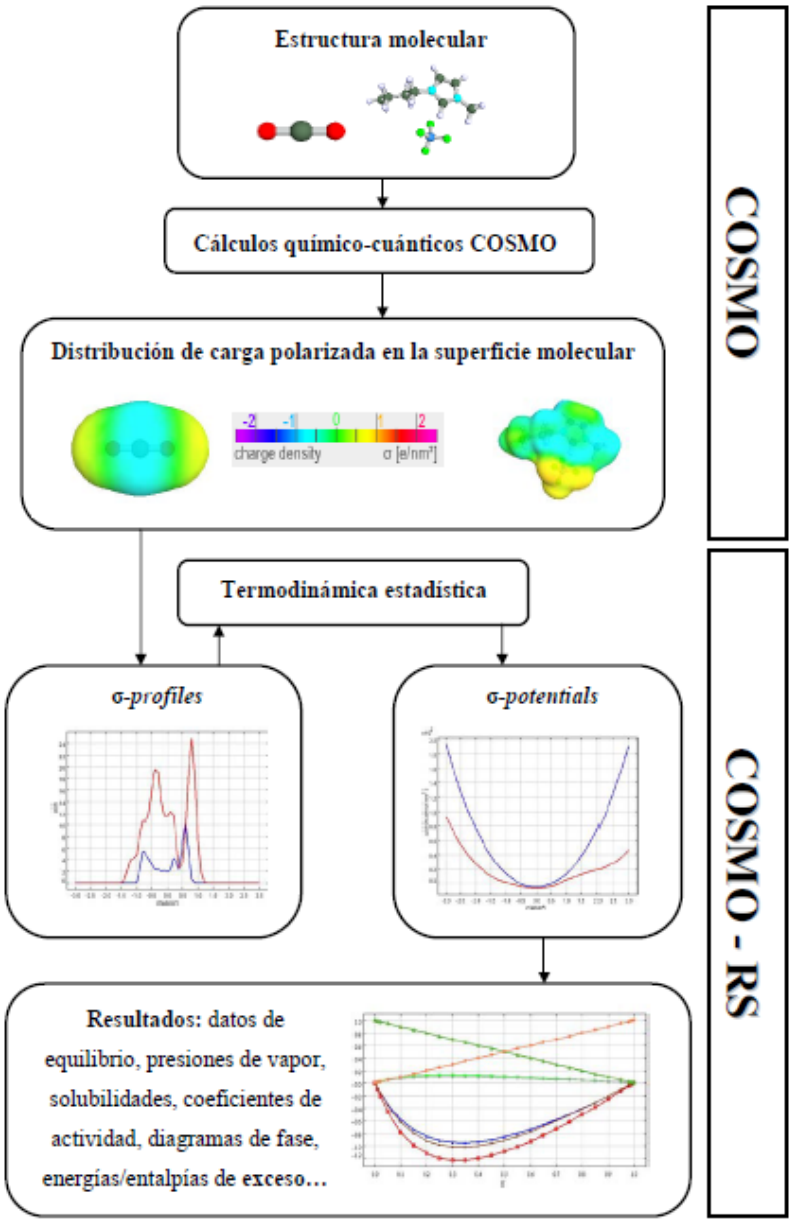

Figura 5.1.1. Procedimiento COSMO-RS para el cálculo de las propiedades termo-físicas de los fluidos. (Fuente: Adaptado de COSMOtherm, 2010)

5.2. Simulación molecular *COSMO-RS* para sistemas basados en líquidos iónicos

Como se ha expuesto con anterioridad, los líquidos iónicos están generando un creciente interés debido a sus peculiares propiedades y están siendo aplicados en una gran variedad de campos. Una de las principales ventajas asociadas a estos compuestos es que los iones que los constituyen pueden ser seleccionados para obtener LIs con las propiedades necesarias para aplicaciones específicas, por lo que son conocidos como "disolventes de diseño". Sin embargo, considerando que el número de combinaciones de contraiones posibles es del orden de 10^6 y teniendo en cuenta la escasez de datos experimentales disponibles, resulta de gran interés la aplicación de modelos predictivos para la estimación de las propiedades de los LIs. En este sentido, la metodología COSMO-RS ha mostrado un gran potencial en el campo de la simulación de mezclas multicomponentes (Klamt y col., 2010), incluyendo aquellas que presentan líquidos iónicos (Diedenhofen y Klamt, 2010).

Las ventajas más importantes aportadas por el método COSMO-RS frente a otros modelos utilizados habitualmente en Ingeniería Química son: a) predice propiedades termodinámicas sin necesidad de recurrir a datos experimentales; b) proporciona una descripción cualitativa y cuantitativa de las distintas interacciones químico-físicas entre las moléculas de los componentes puros y mezclas y, por tanto, contribuye a la interpretación del comportamiento de dichos fluidos; c) incluye en su cálculo los efectos asociados a las interacciones intramoleculares y los efectos de proximidad asociados a los enlaces de hidrógeno; d) permite resolver la diferencia entre isómeros y, por tanto, estimar su contribución a las propiedades de mezcla; y e) presenta una buena descripción de la dependencia de las propiedades con la temperatura.

Se han evaluado distintos métodos para la predicción del comportamiento de los sistemas con LIs, como ecuaciones de estado (Ally y col., 2004; Kroon, 2006; Wang, 2006; Andreu y Vega, 2007), métodos de contribución

de grupos (Kim y col., 2005) o modelos de coeficiente de actividad (Heintz, 2005). Sin embargo, los parámetros de estos modelos han de ser estimados a partir de datos experimentales. Por tanto, teniendo en cuenta la escasez de datos experimentales disponibles para la gran variedad de LIs posibles, resulta de gran utilidad el empleo de métodos que permitan estimar las propiedades termodinámicas de estos sistemas a partir de la información estructural de los compuestos involucrados.

En este sentido, la metodología COSMO-RS ha mostrado un buen comportamiento para el cálculo de las propiedades termodinámicas de los sistemas con LIs, como densidad (Palomar y col., 2007), presiones de vapor (Diedenhofen y col., 2007) coeficientes de actividad (Diedenhofen y col., 2003; Banerjee y Khanna, 2006), propiedades de exceso (Navas y col., 2009; Preiss y col., 2009) y equilibrio entre fases, incluyendo equilibrio líquido-vapor (Beste y col., 2005; Banerjee y col., 2006; Kato y col., 2005; Freire y col., 2008; Preiss y col., 2009), equilibrio líquido-líquido (Domanska y col., 2006; Lei y col., 2006; Banerjee y col., 2008; Freire y col., 2008; Kumar y col., 2009; Lapkin y col., 2010; Mohanty y col., 2010), equilibrio sólido-líquido (Palomar y col., 2009a; Rosol y col., 2009) y equilibrio gas-líquido involucrado en la absorción de gases mediante LIs (Zhang y col., 2008; Manan y col., 2009) y otros disolventes convencionales (Miltner y col., 2006; Miller y col., 2009). Por ello, la capacidad predictiva señalada confiere al método COSMO-RS un gran potencial para el diseño de nuevos LIs con propiedades adecuadas para su aplicación en procesos específicos de interés (Palomar y col., 2008 y 2009b; Bokhove y col., 2012; Gutierrez y col., 2012; Casas y col., 2013).

La aplicación de COSMO-RS en la selección y diseño de LIs resulta de gran utilidad para el progreso de las tecnologías de absorción de gases basadas en estos disolventes. En concreto, permite evaluar la solubilidad y la constante de Henry de los solutos gaseosos en los LIs, así como los coeficientes de actividad, las entalpías de mezcla y las interacciones intermoleculares,

pudiendo analizarse el efecto del catión, del anión y de los grupos funcionales en la capacidad absorbente del disolvente frente al soluto gaseoso para distintas condiciones de trabajo. Asimismo, permite el estudio de la selectividad del LI por un soluto específico en relación con otros gases (como, por ejemplo, es el caso del CO_2 en relación al CH_4 o el N_2 presentes en las corrientes de salida de las centrales termoeléctricas). Además, permite estimar parámetros de reacción, como constantes de equilibrio, energías libres de Gibbs y entalpías de reacción, de gran utilidad en los sistemas en los que el soluto presenta absorción química en el disolvente. A partir de estos estudios se pueden desarrollar modelos predictivos para el diseño y optimización de LIs con alta capacidad absorbente para un soluto específico, enfocándose así los esfuerzos experimentales posteriores hacia la caracterización de sistemas adecuados para la absorción de distintos compuestos, como CO_2, NH_3, COVs y otros solutos de interés.

6. RESULTADOS

6. RESULTADOS

En este capítulo se presentan los resultados obtenidos en el trabajo de investigación realizado durante la presente tesis doctoral. Estos resultados se estructuran en los siguientes bloques:

6.1. Absorción de dióxido de carbono con líquidos iónicos [Publicaciones 1-5]

6.2. Absorción de amoniaco con líquidos iónicos [Publicaciones 6 y 7]

6.3. Selección de líquidos iónicos para absorción de compuestos orgánicos volátiles (COVs) [Publicación 8]

A continuación se presenta un resumen de los resultados más relevantes obtenidos para cada uno de los bloques mencionados. Los artículos científicos publicados, los cuales se adjuntan en el Anexo I del presente documento, recogen la información detallada sobre los procedimientos de cálculo empleados, los métodos experimentales ensayados y los resultados obtenidos en cada uno de los distintos estudios.

6.1. Absorción de dióxido de carbono con líquidos iónicos

En este apartado se resumen los resultados obtenidos en relación con la absorción de dióxido de carbono con líquidos iónicos aplicada a las siguientes modalidades de captura:

- Absorción física de CO_2 con líquidos iónicos (LIs)
- Separación de CO_2/N_2 mediante membranas soportadas en LIs (SILMs)
- Absorción químico-física de CO_2 mediante LIs reversibles (RevILs)

Considerando el potencial de los LIs para absorber el CO_2 y la gran cantidad de combinaciones de contraiones posibles para constituir LIs, resulta necesario desarrollar métodos predictivos para seleccionar/diseñar LIs apropiados para tal fin. Para ello, en primer lugar se realizan una serie de estudios teóricos mediante simulación molecular para predecir el comportamiento termodinámico de los sistemas CO_2-LIs, comprender el origen de la absorción del soluto en el disolvente y, consecuentemente, proponer LIs con estructuras optimizadas para aumentar la capacidad de absorción de CO_2.

La Publicación 1 "Understanding the physical absorption of CO_2 in ionic liquids using the COSMO-RS method" se centra en: a) plantear una metodología para describir mediante simulación molecular el comportamiento termodinámico de los LIs para absorción de gases, particularizado para el caso del soluto CO_2; b) comprender el comportamiento de los sistemas CO_2-LIs según las interacciones energéticas que se establecen entre el soluto y el disolvente; y c) realizar un amplio *screening* computacional entre LIs comercialmente disponibles para seleccionar aquellos con mayor capacidad de absorción de CO_2 y proponer nuevos LIs con capacidades de absorción optimizadas. Los principales resultados obtenidos son los siguientes:

- Los distintos modelos de cálculo propuestos son capaces de proporcionar estimaciones cualitativas adecuadas para describir el

comportamiento experimental de los sistemas gas-LI. En el caso concreto del CO_2, si se considera el LI como par iónico a modo de agregado molecular y se optimiza la geometría de los compuestos considerando un entorno en fase gas el modelo puede proporcionar mejores resultados cuantitativos. Sin embargo, si se define el LI como par iónico y se optimizan los compuestos considerando un entorno en fase gas el modelo resulta más versátil y proporciona un mejor equilibrio entre capacidad predictiva y tiempo de cálculo requerido.

- Al analizar el estado energético de los sistemas CO_2-LI se observa que existe una relación entre la solubilidad del CO_2 en LIs y la entalpía de exceso de las especies en disolución. Las fuerzas atractivas de van der Waals constituyen la mayor contribución en el estado energético de los sistemas, mientras que las interacciones repulsivas electrostáticas suponen una contribución secundaria; los enlaces de hidrógeno resultan despreciables. Las fuerzas atractivas de van der Waals en la mezcla determinan en suma la disolución del CO_2 en el disolvente.

- El *screening* computacional de constantes de Henry de CO_2 en LIs pone de manifiesto que la solubilidad del CO_2 depende fundamentalmente del anión, mientras que el catión juega un papel secundario, aunque el aumento de la longitud de la cadena alquílica del catión favorece ligeramente la capacidad de absorción del CO_2. Además, se comprueba que los LIs comerciales que presentan una mayor capacidad de absorción de CO_2, como es el caso de los LIs fluorados, son aquellos que fomentan las interacciones de van der Waals con el soluto. Por ello, se proponen nuevos LIs altamente halogenados, concretamente LIs basados en aniones bromados, capaces de incrementar las fuerzas de van der Waals con el soluto y de favorecer en principio la absorción de CO_2.

Una vez seleccionado el modelo molecular más adecuado para simular los sistemas CO_2-LIs y validada la capacidad del método COSMO-RS para predecir el comportamiento termodinámico de los LIs para absorber físicamente el CO_2,

se plantea la posibilidad de aplicar la metodología COSMO-RS a otra modalidad de captura de CO_2, como es la de la separación de gases mediante membranas soportadas en LIs (SILMs).

En la Publicación 2 "CO_2/N_2 selectivity prediction in supported ionic liquid membranes (SILMs) by COSMO-RS" se realiza un estudio teórico para determinar mediante simulación molecular la selectividad del CO_2 con respecto al N_2 que idealmente proporcionarían las membranas soportadas en líquidos iónicos (SILMs). Otros objetivos del trabajo son la mejor comprensión del comportamiento de los sistemas mediante análisis energéticos, para así poder proponer LIs con características apropiadas para la separación selectiva de los gases, y la aplicación de una metodología para seleccionar LIs comerciales adecuados en la separación de gases realizando un amplio *screening* computacional. A continuación se exponen los principales resultados obtenidos en este trabajo:

- Es posible estimar la selectividad ideal CO_2/N_2 en SILMs según el ratio de solubilidad (en términos de constantes de Henry) de cada soluto en los LIs mediante cálculos COSMO-RS. La aproximación computacional empleada definiendo el LI como un par de contraiones independientes y optimizando la geometría de los compuestos en fase gas proporciona resultados cualitativos razonables, aunque sobreestima los valores predichos en relación con los experimentales. Por ello, se plantea una corrección de las estimaciones en función de las correlaciones obtenidas para los ajustes de los pares de datos experimentales-teóricos que proporciona una estimación más precisa de los valores de selectividad en SILMs.

- El aumento de la solubilidad del CO_2 y del N_2 en los LIs está relacionado con las entalpías de exceso exotérmicas de la disolución y con una mayor contribución de las fuerzas atractivas de van der Waals a dicha entalpía de exceso. Sin embargo, la solubilidad del CO_2 con respecto a la del N_2 en LIs

resulta notablemente superior en términos de constantes de Henry. Los LIs capaces de aumentar la selectividad son aquellos que proporcionan una baja solubilidad de ambos gases, pero que son capaces de incrementar las solubilidad del CO_2 con respecto al N_2 mediante fuerzas de van der Waals.

- Se proponen LIs comerciales basados en aniones $[SCN]^-$ para aumentar la selectividad ideal del CO_2 con respecto a la del N_2, de acuerdo con los resultados obtenidos mediante simulación molecular.

Considerando la capacidad del método COSMO-RS para predecir el comportamiento de sistemas basados en la absorción física de CO_2 con LIs, el siguiente reto es aplicar la metodología de simulación para estudiar sistemas basados en absorción química de CO_2 con LIs. Estos estudios se concretan en la Publicación 3 "COSMO-RS studies: structure-property relationships for CO_2 capture by reversible ionic liquids", la cual se centra en el estudio de los parámetros termodinámicos que caracterizan la absorción de CO_2 en LIs reversibles y en establecer relaciones estructura-propiedad con el fin de proponer nuevos disolventes con características apropiadas para capturar CO_2. Este trabajo se llevó a cabo en colaboración con el grupo de investigación de los profesores Dr. Eckert y Dr. Liotta durante la estancia predoctoral realizada en el Departamento de Ingeniería Química del Instituto Tecnológico de Georgia (Georgia Institute of Technology, Atlanta, E.E.U.U.). El principal objetivo del trabajo es desarrollar una guía que facilite la selección de nuevas estructuras de disolventes que presenten características adecuadas para ser aplicados en procesos de captura química de CO_2. Los LIs reversibles presentan una modalidad dual (física y química) de captura, de forma que los disolventes moleculares basados en sililaminas reaccionan químicamente con CO_2 para formar líquidos iónicos, que continúan capturando el CO_2 mediante absorción física. Posteriormente, el disolvente puede ser completamente regenerado a su forma original, esto es, líquido molecular, no iónico. Los parámetros termodinámicos básicos que caracterizan este tipo de LIs reversibles son: (1) la

entalpía de reacción, que da una idea de la energía necesaria para recuperar el líquido molecular; (2) la capacidad de absorción física, que se estudia en términos de la constante de Henry como medida de la solubilidad del CO_2 en el LI; y (3) la temperatura a la que se produce la reacción inversa para liberar el CO_2 y recuperar el líquido molecular, que se define como la temperatura a la que la constante de reacción de la sililamina con el CO_2 se aproxima a 10^{-1}. Las propiedades termodinámicas de los LIs reversibles, tanto para su reacción química con el CO_2 como para la absorción física del CO_2, se evalúan en función de las siguientes características estructurales del disolvente: (a) ventajas de incluir átomos de silicio en lugar de carbono; (b) longitud de los sustituyentes de la cadena alquílica unida al átomo de silicio; (c) longitud de la cadena alquílica que conecta la amina con el átomo de silicio; (d) efecto de la fluoración de la cadena alquílica; y (e) impedimento estérico mediante adición de grupos metilos en posiciones próximas al grupo funcional amina.

Tras evaluar las propiedades termodinámicas de los LIs reversibles basados en sililaminas para capturar el CO_2, las tendencias computacionales se validan empleando los valores experimentales publicados. Además, los resultados obtenidos para los LIs reversibles se comparan con los datos bibliográficos para el disolvente MEA, poniéndose de manifiesto la mayor capacidad de los LIs reversibles para capturar CO_2 y disminuir la energía requerida para la regeneración del disolvente. Además, se muestra que los LI reversibles presentan más afinidad por el CO_2 que por otros solutos presentes en las corrientes de salida de las plantas termoeléctricas, como CH_4, O_2 y N_2. Finalmente, esta metodología se aplica al diseño de un nueva sililamina fluorada con propiedades termodinámicas optimizadas para capturar el CO_2. Los resultados computaciones obtenidos están en consonancia con los datos experimentales disponibles. Esta serie de estudios demuestra que utilizar herramientas predictivas como guía puede reducir notablemente el tiempo y los costes asociados a la búsqueda de disolventes apropiados para absorber el CO_2.

Una vez realizados los estudios teóricos para comprender el comportamiento de los distintos sistemas CO_2-LI y proponer disolventes potencialmente adecuados para capturar el CO_2, el siguiente paso es determinar experimentalmente la capacidad, tanto termodinámica como cinética, de tales absorbentes. En concreto, se plantean dos trabajos de carácter experimental, los cuales se recogen en la Publicación 4 "Anion effects on kinetics and thermodynamics of CO_2 absorption in ionic liquids" y en la Publicación 5 "Solubility and diffusivity of CO_2 in [hxmim][NTf_2], [omim][NTf_2] and [dcmim][NTf_2] at T=(298.15, 308.15 and 323.15) K and pressures up to 20 bar". En la Publicación 4 se detalla la puesta a punto del método experimental y se estudia el efecto del anión para LIs de catión común ([bmim][PF_6], [bmim][NTf_2] y [bmim][FAP]), mientras que la Publicación 5 se centra en el estudio del efecto de la variación de la longitud de la cadena alquílica asociada al catión imidazolio en LIs de anión común ([hxmim][NTf_2], [omim][NTf_2] y [dcmim][NTf_2]). Por tanto, el principal objetivo de estos trabajos es poner a punto un procedimiento experimental basado en la termogravimetría de alta presión para estudiar el proceso de absorción de CO_2 en LIs y realizar un estudio sistemático de los datos termodinámicos y cinéticos sobre el efecto de la estructura del LI y de las condiciones de operación en el proceso de absorción física de CO_2.

En todos los casos, los experimentos termogravimétricos se llevan a cabo en una balanza de suspensión magnética de alta presión para determinar las isotermas de absorción y las curvas cinéticas de CO_2 en los seis LIs a las temperaturas de 25, 35 y 50 ^oC y presiones de hasta de 20 bar. Posteriormente, se analiza el efecto de la estructura del LI y de las condiciones de operación sobre la termodinámica (en términos de solubilidad y constantes de Henry) y la cinética (en términos de coeficientes de difusión) de la absorción de CO_2 en los LIs. La densidad de los disolventes, así como la solubilidad y las constantes de Henry del CO_2 en los LIs, se comparan con los datos bibliográficos disponibles

para validar el método experimental. A continuación, se determinan los coeficientes de difusión de CO_2 en cada uno de los LIs mediante un modelo de transferencia de materia por difusión. Además, se aplica la correlación empírica de Wilke-Chang para estimar los coeficientes de difusión de los sistemas y comparar los valores obtenidos por esta vía con aquellos calculados mediante el modelo de transferencia de materia por difusión. A continuación se exponen los principales resultados obtenidos en estos trabajos:

- Se realiza la puesta a punto de un procedimiento termogravimétrico empleando una balanza de suspensión magnética sometida a alta presión operando en modo dinámico; el método resulta rápido y preciso para determinar las isotermas de absorción y las curvas cinéticas del CO_2 en LIs.

- Las densidades de los LIs, que se encuentran en el orden de 1,2-1,6 g/cm^3, disminuyendo con la temperatura, presentan la siguiente tendencia con el catión: [bmim][FAP] > [bmim][NTf_2] > [bmim][PF_6]; sus valores son ligeramente menores conforme se aumenta la cadena alquílica del catión: [hxmim][NTf_2] > [omim][NTf_2] > [dcmim][NTf_2].

- La solubilidad del CO_2 en los LIs aumenta con la presión y disminuye con la temperatura. La tendencia encontrada con respecto al anión es la siguiente: [bmim][FAP] > [bmim][NTf_2] > [bmim][PF_6], alcanzándose fracciones molares máximas de CO_2 absorbido de 0,47, 0,40 y 0,29 a 25 ^oC (menor temperatura) y 20 bar (mayor presión), respectivamente. Asimismo, la solubilidad aumenta ligeramente con la longitud de la cadena alquílica del catión según el siguiente orden: [dcmim][NTf_2] > [omim][NTf_2] > [hxmim][NTf_2], alcanzándose fracciones molares máximas de CO_2 absorbido de 0,44, 0,43 y 0,42 a 25 ^oC y 20 bar, respectivamente.

- Los coeficientes de difusión del CO_2 en los LIs aumentan con la temperatura y la presión, presentando órdenes de magnitud comprendidos entre 10^{-10} y 10^{-11} m^2/s. Estos coeficientes muestran la siguiente tendencia con el

anión: [bmim][NTf_2] > [bmim][FAP] > [bmim][PF_6], disminuyendo su valor ligeramente al aumentar la cadena alquílica del cation: [hxmim][NTf_2] > [omim][NTf_2] > [dcmim][NTf_2]. Además, la correlación empírica de Wilke-Chang proporciona valores de los coeficientes de difusión de los sistemas comparables a los obtenidos experimentalmente, por lo que dicha correlación resulta viable para predecir el comportamiento cinético de los LIs para absorber el CO_2 en función de la temperatura.

Los resultados ponen de manifiesto el distinto comportamiento termodinámico y cinético que ofrece cada uno de los LIs para absorber el CO_2, por lo que resulta crítico evaluar ambos aspectos en el desarrollo de sistemas de absorción de CO_2 basados en LIs.

6.2. Absorción de amoniaco con líquidos iónicos

A continuación se presentan los resultados más significativos de los estudios realizados sobre absorción de amoniaco con líquidos iónicos, trabajo que se recoge en la Publicación 6 "Task-specific ionic liquids for efficient ammonia absorption" y en la Pubicación 7 "Screening ionic liquids as suitable NH_3 absorbents on the basis on thermodynamic and kinetic analysis", adjuntas en el Anexo I. Dichos estudios se centran en desarrollar una metodología de trabajo que combine la simulación molecular con los ensayos experimentales para proponer nuevos LIs optimizados para la absorción de NH_3, tanto desde el punto de vista termodinámico como cinético.

En primer lugar, se realizan estudios computacionales mediante el método químico cuántico COSMO-RS con el fin de preseleccionar un grupo de LIs con elevada capacidad absorbente de NH_3. Para ello, se evalúan las características estructurales de distintos disolventes comúnmente empleados para disolver amoniaco, así como las interacciones intermoleculares que se establecen entre el NH_3 y tales disolventes. Los resultados ponen de manifiesto que las interacciones atractivas de enlace de hidrogeno que se generan entre el soluto y el disolvente determinan la solubilidad del NH_3, sugiriendo la posibilidad de funcionalizar los LIs con grupos dadores de enlaces de hidrogeno, como grupos hidroxilo, para aumentar su capacidad de absorción de NH_3. A la vista de los resultados, se realiza un amplio *screening* computacional para evaluar la solubilidad del NH_3 en LIs comerciales, incluyendo aquellos funcionalizados con grupos ácidos que puedan incrementar la capacidad de absorción del LI.

Considerando los resultados obtenidos mediante simulación molecular se preseleccionan los siguientes líquidos iónicos, 1-2(-hidroxietil)-3-metilimidazolio tetrafluoroborato ([EtOHmim][BF_4]), choline bis(trifluorometilsulfonil)-imida ([choline][NTf_2]), tris(2-hidroxietil)metilamonio metilsulfato ([MTEOA]

[$MeSO_4$]) y 1-(2-hidroxietil)-3-metilimidazolio dicianamida ([EtOHmim][DCN]), además del 1-metil-3-butilimidazolio tetrafluoroborato ([bmim][BF_4]) tomado como referencia de la bibliografía. Los experimentos de absorción se llevan a cabo mediante termogravimetría a temperaturas comprendidas entre 20 y 40 ^oC y a presiones parciales de NH_3 de hasta 1 bar. Los resultados confirman que la solubilidad aumenta con la presión parcial del soluto y disminuye con la temperatura de trabajo. Los LIs seleccionados muestran una capacidad de absorción notablemente superior a la del líquido iónico [bmim][BF_4] de referencia, alcanzándose fracciones molares de absorción de NH_3 próximas a 0,7 con [MTEOA][MeSO4] a 20 ^oC y a 0,6 con [choline][NTf_2] a 40 ^oC para presiones de NH_3 de 1 bar, valores que vienen a duplicar la capacidad de absorción de NH_3 que proporciona el [bmim][BF_4]. Además, la regeneración completa de los LIs resulta posible sometiendo a la muestra a una corriente de gas inerte; no se observa disminución en la capacidad de absorción de los LIs regenerados en los sucesivos ciclos de absorción-desorción. Posteriormente, se estudia la cinética de la absorción aplicando un modelo de transferencia de materia por difusión mediante el que se obtienen coeficientes de difusión del NH_3 en los LIs del orden de 10^{-10} m^2/s, aumentando sus valores con la temperatura según la siguiente tendencia: [choline][NTf_2] > [EtOHmim][DCN] > [bmim][BF_4] > [EtOHmim][BF_4] > [MTEOA][$MeSO_4$].

Por último, con el objetivo de comparar el comportamiento de los distintos absorbentes en términos de termodinámica y cinética, se define un parámetro de eficiencia en función de la masa de NH_3 absorbida por unidad de masa de LI y por unidad de tiempo. Los resultados ponen de manifiesto que el [choline][NTf_2], el cual proporciona valores de eficiencia comprendidos entre 33,7 y 62,5 mmol NH_3/min·mol LI, resulta el LI más adecuado para la absorción de NH_3 en el intervalo de temperaturas estudiado en comparación con los valores de eficiencia proporcionados por los demás LIs ensayados, que están comprendidos entre 4,2 y 15 mmol NH_3/min·mol IL.

6.3. Selección de líquidos iónicos para absorción de compuestos orgánicos volátiles (COVs)

El objetivo de este trabajo es proponer una guía para seleccionar cationes y aniones que constituyan LIs con propiedades capaces de fomentar la solubilidad de COVs de distinta naturaleza en LIs. Para ello, se plantea una serie de análisis teóricos sistemáticos, tanto termodinámicos como energéticos, aplicando la metodología de simulación molecular COSMO-RS. Los estudios realizados se recogen en la Publicación 8 "Selection of ionic liquids for enhancing the gas solubility of volatile organic compounds" adjunta en el Anexo I de presente documento.

En primer lugar, se valida la capacidad de COSMO-RS para predecir la solubilidad de un amplio conjunto de solutos gaseosos en LIs, comparando los valores bibliográficos (en términos de constantes de Henry) con aquellos calculados para más de 125 sistemas.

A continuación, se analiza la relación existente entre los coeficientes de actividad a dilución infinita y la entalpía de exceso de las mezclas para más de 2.400 sistemas gas-LI con el objetivo de comparar la afinidad de los LIs por solutos con presiones de vapor muy diferentes. Según los resultados obtenidos, los compuestos gaseosos se clasifican atendiendo a la volatilidad de los solutos y a su coeficiente de actividad en los LIs, distinguiéndose diferentes casos, que comprenden desde compuestos alifáticos, los cuales muestran notables desviaciones positivas de la Ley de Raoult y baja solubilidad en LIs, hasta solutos orgánicos polares, que presentan significativas desviaciones negativas de la ley de Raoult y elevadas solubilidades en LIs.

Posteriormente, se realizan análisis sistemáticos aplicando COSMO-RS para estudiar la solubilidad y las interacciones energéticas de tres COVs de referencia: acetona, fenol y cloroformo. En concreto, se analiza la estructura química de los solutos y de los LIs en términos de la distribución de carga

polarizada en la superficie de las moléculas. A continuación, se llevan a cabo *screenings* de solubilidad de cada uno de los solutos en 270 LIs representativos. Seguidamente, se evalúan las contribuciones de las interacciones intermoleculares en las entalpías de exceso de las mezclas para comprender el origen de la solubilidad física de cada uno de los solutos en los diferentes LIs.

En el caso de la acetona, la solubilidad viene condicionada por la estructura de ambos contraiones. Los cationes capaces de aumentar la solubilidad de la acetona son aquellos funcionalizados con grupos de carácter ácido, como $[OH\text{-}emim]^+$ o $[choline]^+$, y aniones grandes con carga dispersa, como $[FAP]^-$ o $[NTf_2]^-$. Esto se explica teniendo en cuenta el carácter polar de la acetona y su comportamiento como aceptor de enlaces de hidrógeno, debido al oxigeno del grupo carbonilo de su estructura, que interacciona con los grupos de carácter ácido de los disolventes, dadores de enlaces de hidrogeno.

En cuanto al fenol, el anión juega el papel principal estableciendo enlaces de hidrógeno efectivos con el soluto, que incrementen su solubilidad. En este caso, la solubilidad del fenol aumenta en LIs con aniones con carácter básico, como el $[CH_3CO_2]^-$ o $[CH_3CO_2]^-$. Este comportamiento se atribuye al carácter dador de enlaces de hidrogeno del soluto, de modo que la afinidad entre el protón del grupo hidroxilo del fenol y los grupos aceptores de enlaces de hidrogeno del anión del LI controlan la solubilidad.

En cuanto al cloroformo, su solubilidad en LIs viene determinada por ambos contraiones. En este caso, las interacciones atractivas de enlaces de hidrogeno que controlan la solubilidad se establecen entre el protón ácido del cloroformo y los grupos básicos de los iones del disolvente. La solubilidad del cloroformo aumenta en LIs con elevada capacidad de actuar como aceptores de enlaces de hidrógeno, como aquellos que contienen aniones del tipo $[CH_3CO_2]^-$, y en cationes que no presentan grupos dadores de enlaces de hidrogeno, como por ejemplo el $[emmim]^+$, el $[bbbb\text{-}P]^+$ o el $[bbbb\text{-}N]^+$.

Por último, con el objetivo de realizar una evaluación generalizada de la influencia de la estructura del LI sobre la solubilidad de los COVs, los análisis computacionales se extienden a una muestra representativa de COVs con diferente naturaleza química. Como resultado de este estudio, se establecen las siguientes pautas generales que pueden ayudar a la selección de LIs potencialmente adecuados para ser empleados en procesos de absorción o separación de COVs.

(i) COVs que presentan una absorción favorable en LIs: solutos que contienen grupos funcionales fuertemente polares con marcado carácter dador o aceptor de enlaces de hidrógeno (fenol, acetona, cloroformo). Estos solutos presentan una fuerte desviación negativa de la Ley de Raoult y una elevada solubilidad en LIs, que viene determinada por la capacidad de establecer enlaces de hidrogeno efectivos entre el soluto y el disolvente. Por ello, la afinidad de los LIs por estos COVs se potencia seleccionando combinaciones de cationes y aniones que favorezcan tales enlaces de hidrogeno con el soluto en cuestión.

(ii) COVs que presentan moderada absorción en LIs: solutos que contienen cadenas alquílicas cortas o de carácter aromático (etano, eteno, benceno). Estos solutos presentan una desviación negativa de la Ley de Raoult moderada y solubilidades en LIs intermedias pero modulables, de tal forma que pueden ser significativamente favorecidas mediante una adecuada selección de los contraiones que constituyen el LI. En concreto, la solubilidad de estos solutos puede ser incrementada seleccionando LIs que favorezcan interacciones atractivas de van der Waals e interaciones electrostácticas polares entre el soluto y el disolvente. Los LIs más apropiados para incrementar la solubilidad de la mayoría de estos COVs son aquellos cationes con largas cadenas alquílicas y aniones grandes con carga dispersa como el $[FAP]^-$.

(iii) COVs que presentan absorción poco favorable en LIs: solutos alifáticos (hexano, octano) y compuestos perhalogenados (CCl_4). Estos solutos presentan desviaciones positivas de la Ley de Raoult, interacciones soluto-LI desfavorables y bajas solubilidades en LIs. La baja solubilidad de estos compuestos viene determinada por las interacciones electrostáticas de tipo repulsivo que se establecen entre el soluto y el disolvente. De este modo, la solubilidad de estos solutos en LIs disminuye notablemente seleccionando cationes pequeños y aniones polares como $[SCN]^-$ o $[DCN]^-$, que promueven interacciones electrostáticas repulsivas con los solutos no polares que se incluyen en este grupo de COVs. Estos LIs basados en $[SCN]^-$ o $[DCN]^-$ pueden ser aplicados como disolventes en técnicas de separación aromáticos/alifáticos, como por ejemplo en membranas soportadas en LIs.

En resumen, los estudios sistemáticos realizados mediante simulación molecular permiten analizar el comportamiento de los sistemas compuestos por COVs-LIs y justificar la solubilidad de tales solutos en los disolventes. De este modo, resulta posible establecer pautas que sirvan como guía en la selección racional de cationes y aniones que formen LIs con estructuras potencialmente óptimas para ser empleados como disolventes en los procesos de absorción o separación de COVs.

7. CONCLUSIONES

7. CONCLUSIONES

A partir de los resultados obtenidos en la investigación realizada se pueden extraer las siguientes conclusiones:

7.1. Absorción de dióxido de carbono con líquidos iónicos

(I) El método químico-cuántico COSMO-RS resulta una herramienta adecuada para predecir el comportamiento termodinámico de los solutos gaseosos en LIs y justificar el origen de dicho comportamiento en términos energéticos. El método COSMO-RS se ha aplicado satisfactoriamente para estudiar las siguientes modalidades de captura de CO_2:

- *Absorción física de CO_2 con líquidos iónicos (LIs):* Existe una relación entre la alta solubilidad del CO_2 en los LIs y la entalpía de exceso exotérmica de las especies en disolución. La solubilidad del CO_2 en los LIs viene determinada por las fuerzas atractivas de van der Waals que se establecen entre el soluto y el disolvente; las fuerzas repulsivas electrostáticas suponen una contribución secundaria; la contribución de los enlaces de hidrógeno resulta despreciable. La solubilidad del CO_2 depende fundamentalmente del anión, mientras que el catión juega un papel secundario, aunque el aumento de la longitud de su cadena alquílica favorece ligeramente la capacidad de absorción por parte del LI. Se proponen nuevos LIs altamente halogenados, como aquellos basados en aniones bromados, para favorecer la capacidad de absorción de los disolventes mediante el incremento de las fuerzas de van der Waals con el CO_2.

- *Separación de CO_2/N_2 mediante membranas soportadas en LIs (SILMs):* La selectividad ideal del CO_2 con respecto a la del N_2 en SILMs se puede estimar en función de las solubilidades (en términos de constantes de Henry) de cada uno de los solutos en los LIs. El aumento de la solubilidad del CO_2 y del N_2 en los LIs está relacionado con las entalpías de exceso exotérmicas de la disolución y con una mayor contribución de las fuerzas atractivas de van der Waals a dicha entalpía de exceso. Los LIs capaces de aumentar la selectividad son

aquellos que proporcionan una baja solubilidad de ambos gases, pero que incrementan la solubilidad del CO_2 con respecto al N_2 mediante fuerzas de van der Waals. Se proponen LIs comerciales basados en aniones $[SCN]^-$ para aumentar la selectividad ideal del CO_2 con respecto a la del N_2.

- *Absorción químico-física de CO_2 mediante LIs reversibles (RevILs):* Se ha desarrollado un mapa de relaciones estructura-propiedad que permite orientar el diseño de nuevos LIs reversibles basados en sililaminas para capturar CO_2 mediante absorción química y física. Empleando las relaciones estructura-propiedad obtenidas se ha propuesto una nueva sililamina fluorada con propiedades termodinámicas optimizadas para capturar el CO_2. Además, se ha determinado que los LIs reversibles presentan una mayor selectividad por el CO_2 que por otros solutos presentes en las corrientes de salida de las plantas termoeléctricas. Asimismo, se ha establecido que los LIs reversibles presentan una mayor capacidad para absorber CO_2 y un menor requerimiento energético para la regeneración del disolvente en comparación con las disoluciones amínicas empleadas para capturar CO_2 en post-combustión.

(II) Se ha puesto a punto un procedimiento experimental para estudiar el comportamiento de los LIs en la captura de CO_2 mediante termogravimetría de alta presión empleando una balanza de suspensión magnética operando en modo dinámico. Se han determinado las isotermas de absorción-desorción y las curvas cinéticas de CO_2 en los siguientes LIs halogenados: [bmim][PF_6], [bmim][FAP], [bmim][NTf_2], [hxmim][NTf_2], [omim][NTf_2] y [dcmim][NTf_2] a temperaturas comprendidas entre 25 y 50 ºC y presiones de hasta 20 bar. A partir de los resultados obtenidos, se ha evaluado el efecto de la estructura del LI y de las condiciones de operación sobre la termodinámica y la cinética del proceso de absorción, obteniéndose las siguientes conclusiones:

- Densidad de los LIs: Los valores de densidad de los LIs se encuentran entre 1,2 y 1,6 g/cm^3. Estos valores disminuyen con la temperatura y presentan las siguientes tendencias con respecto al anión: [bmim][FAP] > [bmim][NTf_2] > [bmim][PF_6]; y con respecto a la longitud de la cadena alquílica del catión: [hxmim][NTf_2] > [omim][NTf_2] > [dcmim][NTf_2].

- Solubilidad del CO_2 en los LIs: La solubilidad del CO_2 en los LIs aumenta con la presión y disminuye con la temperatura. Los valores de solubilidad muestran la siguiente tendencia con respecto al anión: [bmim][FAP] > [bmim][NTf_2] > [bmim][PF_6]; y aumentan ligeramente con la longitud de la cadena alquílica del catión en este orden: [dcmim][NTf_2] > [omim][NTf_2] > [hxmim][NTf_2]. La fracción molar maxima de CO_2 absorbido (0,47) se ha alcanzado mediante el LI [bmim][FAP] operando a 25 ºC (menor temperatura) y 20 bar (mayor presión).

- Coeficientes de difusión del CO_2 en los LIs: Los coeficientes de difusión del CO_2 en los LIs presentan órdenes de magnitud de 10^{-10} a 10^{-11} m^2/s. Estos valores aumentan con la temperatura y la presión y muestran las siguientes tendencias con respecto al anión: [bmim][NTf_2] > [bmim][FAP] > [bmim][PF_6], y con respecto al catión: [hxmim][NTf_2] > [omim][NTf_2] > [dcmim][NTf_2]. La correlación empírica de Wilke-Chang proporciona valores de los coeficientes de difusión del CO_2 en los LIs comparables a los obtenidos experimentalmente.

7.2. Absorción de amoniaco con líquidos iónicos

(I) El método químico-cuántico COSMO-RS ha sido empleado para estudiar las características estructurales de disolventes moleculares con elevada capacidad para absorber NH_3 y, en consecuencia, proponer nuevos LIs funcionalizados con estructuras optimizadas para absorber este soluto. Se ha determinado que las interacciones atractivas de enlaces de hidrogeno que se establecen entre el soluto y el disolvente condicionan la solubilidad del NH_3 y

se han propuestos LIs funcionalizados con grupos ácidos como candidatos para ser empleados como absorbentes de NH_3.

(II) Experimentalmente se han determinado las isotermas de absorción-desorción y las curvas cinéticas del NH_3 en LIs funcionalizados con grupos ácidos seleccionados, como [EtOHmim][BF_4], [choline][NTf_2], [MTEOA][$MeSO_4$] y [EtOHmim][DCN], y también en el LI [bmim][BF_4], tomado como referencia. Los experimentos se llevaron a cabo mediante termogravimetría a presión atmosférica a temperaturas comprendidas entre 20 y 40 ^oC y presiones parciales de NH_3 de hasta 1 bar, obteniéndose las siguientes conclusiones:

- Solubilidad del NH_3 en LIs: La solubilidad del NH_3 aumenta con la presión parcial del soluto y disminuye con la temperatura. Para presiones de NH_3 de 1 bar, el LI [MTEOA][MeSO4] proporciona la fracción molar máxima de absorción de NH_3 (0,7) a 20 ^oC (menor temperatura), mientras que el LI [choline][NTf_2] proporciona la fracción molar máxima de absorción de NH_3 (0,6) a 40 ^oC (máxima temperatura). Además se demostró que es posible la regeneración de los LIs en condiciones suaves de operación, sin que se observara disminución en la capacidad de absorción del LI tras su regeneración.

- Coeficientes de difusión del NH_3 en LIs: Los coeficientes de difusión del NH_3 en los LIs son del orden de 10^{-10} m^2/s. Estos valores aumentan con la temperatura y presentan la siguiente tendencia: [choline][NTf_2] > [EtOHmim][DCN] > [bmim][BF_4] > [EtOHmim][BF_4] > [MTEOA][$MeSO_4$]. Los valores de los coeficientes de difusión experimentales guardan un buen acuerdo con aquellos calculados mediante la correlación empírica de Wilke-Chang.

- Eficiencia de la absorción de NH_3 en los LIs: Se ha definido un parámetro de eficiencia que permite comparar el comportamiento de los distintos absorbentes en términos de termodinámica y de cinética. Según tal parámetro, el LI más adecuado para absorber NH_3 es el [choline][NTf_2], el cual proporciona un valor de eficiencia de 62,5 mmol NH_3/min·mol LI a la

temperatura de 40 ºC y presión de NH_3 de 1 bar, lo que supone un valor de eficiencia 6 veces superior al proporcionado por el LI de referencia [bmim][BF_4] en condiciones similares de trabajo.

7.3. Selección de líquidos iónicos para absorción de compuestos orgánicos volátiles (COVs)

(I) Se ha validado la capacidad del método COSMO-RS para predecir las tendencias generales de la solubilidad de un amplio intervalo de solutos gaseosos con distintas presión de vapor en LIs. Se ha observado una clara relación entre los coeficientes de actividad a dilución infinita de los solutos en los LIs y las entalpías de exceso de los compuestos en disolución.

(II) Se han realizado análisis sistemáticos termodinámicos y energéticos empleando el método químico-cuántico COSMO-RS con el objetivo de orientar la selección de cationes y aniones con características estructurales adecuadas para favorecer la absorción de COVs en LIs. Consecuentemente, se ha planteado una clasificación de los solutos atendiendo a su solubilidad en LIs y se han propuesto estructuras catiónicas y aniónicas con características optimizadas para ser empleadas como disolventes en procesos de absorción o separación de COVs en LIs, tal y como se resume a continuación:

- COVs que presentan una absorción favorable en LIs: solutos que contienen grupos funcionales fuertemente polares con marcado carácter dador o aceptor de enlaces de hidrógeno (fenol, acetona, cloroformo). Estos solutos presentan una elevada solubilidad en los LIs, que viene determinada por la capacidad de establecer enlaces de hidrogeno efectivos entre el soluto y el disolvente. El estudio individualizado de la solubilidad de estos tres solutos en LIs indica lo siguiente: a) la solubilidad de la acetona en LIs viene condicionada por la estructura de ambos contraiones y la capacidad de los mismos de actuar como dadores de enlaces de hidrógeno; los LIs cationes capaces de aumentar la solubilidad de la acetona son aquellos basados en cationes funcionalizados con

grupos de carácter ácido, como $[OH\text{-}emim]^+$ o $[choline]^+$, y en aniones grandes con carga dispersa ($[FAP]^-$, $[NTf_2]^-$); b) la solubilidad del fenol en LIs viene condicionada por la estructura del anión y aumenta en los LIs basados en aniones con carácter básico ($[CH_3CO_2]^-$ o $[CH_3CO_2]^-$); y c) la solubilidad del cloroformo en LIs viene determinada por ambos contraiones y aumenta en LIs con capacidad de actuar como aceptores de enlaces de hidrógeno, como aquellos basados en aniones de carácter básico como el $[CH_3CO_2]^-$ y cationes que no presentan grupos dadores de enlaces de hidrogeno como $[emmim]^+$, $[bbbb\text{-}P]^+$ o $[bbbb\text{-}N]^+$.

- COVs que presentan moderada absorción en LIs: solutos que contienen cadenas alquílicas cortas o de carácter aromático (etano, eteno, benceno). Estos solutos presentan solubilidades en LIs intermedias, las cuales pueden ser significativamente favorecidas seleccionando LIs que promuevan interacciones atractivas de van der Waals e interaciones electrostácticas polares entre el soluto y el disolvente, como aquellos basados en cationes con largas cadenas alquílicas y aniones grandes con carga dispersa, por ejemplo el $[FAP]^-$.

- COVs que presentan absorción poco favorable en LIs: solutos alifáticos (hexano, octano) y compuestos perhalogenados (CCl_4). Estos solutos presentan bajas solubilidades en LIs, que vienen determinadas por las interacciones electrostáticas de tipo repulsivo que se establecen entre el soluto y el disolvente. Se sugiere el empleo de tales LIs como disolventes en técnicas de separación basadas en membranas para, por ejemplo, separar mezclas de aromáticos/alifáticos, proponiéndose en este caso el uso de LI con cationes pequeños y aniones polares como $[SCN]^-$ o $[DCN]^-$, que disminuyan la solubilidad de estos compuestos en LIs y favorezcan la selectividad de la separación.

BIBLIOGRAFÍA

BIBLIOGRAFÍA

Aaron, D. y Tsouris, C. "Separation of CO_2 from flue gas: A review". *Separation Science and Technology* **2005**, *40*, 321−348.

Abrusci, C.; Palomar, J.; Pablos, J.L.; Rodriguez, F.; Catalina, F. "Efficient biodegradation of common ionic liquids by Sphingomonas paucimobilis bacterium". *Green Chemistry* **2011**, *13*, 709-717.

Abulhassani, J.; Manzoori, J.L.; Amjadi, M. "Hollow fiber based-liquid phase microextraction using ionic liquid solvent for preconcentration of lead and nickel from environmental and biological samples prior to determination by electrothermal atomic absorption spectrometry". *Journal of Hazardous Materials* **2009**, *81*, 481–486.

Aki, S. N. V. K.; Mellein, B. R.; Saurer, E. M.; Brennecke, J. F. "High-pressure phase behavior of carbon dioxide with imidazolium-based ionic liquids". *The Journal of Physical Chemistry B* **2004**, *108 (52)*, 20355–20365.

Ally, M.R.; Braunstein, J.; Baltus, R.E.; Dai, S. "Irregular ionic lattice model for gas solubilities in ionic liquids". *Industrial & Engineering Chemistry Research* **2004**, *43*, 1296-1301.

Almantariotis, D.; Gefflaut, T.; Padua, A.A.H.; Coxam, J.Y.; Costa-Gomes, M.F. "Effect of fluorination and size of the alkyl side-chain on the solubility of carbon dioxide in 1-alkyl-3-methylimidazolium bis(trifluoromethylsulfonyl)amide ionic liquids". *The Journal of Physical Chemistry B* **2010**, *114*, 3608–3617.

Alonso, L.; Arce, A.; Francisco, M.; Rodríguez, O; Soto, A. "Gasoline desulfurization using extraction with [C_8mim][BF_4] ionic liquid". *AIChE Journal* **2007**, *53 (12)*, 3108–3115.

Anderson, J.L.; Dixon, J.K.; Maginn, E.J.; Brennecke, J.F. "Measurement of SO_2 solubility in ionic liquids". *The Journal of Physical Chemistry B* **2006**, *110*, 15059-15062.

Anderson, J.L.; Dixon, J.K.; Brennecke, J.F. "Solubility of CO_2, CH_4, C_2H_6, C_2H_4, O_2, and N_2 in 1-hexyl-3-methylpyridinium bis(trifluoromethylsulfonyl)imide: comparison to other ionic liquids". *Accounts of Chemical Research* **2007**, *40*, 1208–1216.

Andreu, J.S. y Vega, L.F. "Capturing the solubility behavior of CO_2 in ionic liquids by a simple model". *The Journal of Physical Chemistry C* **2007**, *111*, 16028-16034.

Anthony, J.L.; Aki, S.; Maggin, E.J.; Brennecke, J.F. "Feasibility of using ionic liquids for carbon dioxide capture". *International Journal of Environmental Technology and Management* **2004**, *4 (1-2)*, 105-115.

Anthony, J.L.; Anderson, J.L.; Maggin, E.J.; Brennecke, J.F. "Anion effects on gas solubility in ionic liquids". *The Journal of Physical Chemistry B* **2005**, *109*, 6366-6374.

Arriaga, S.; Muñoz, R.; Hernandez, S.; Guieysse, B.; Revah, S. "Gaseous hexane biodegradation by Fusarium solani in two liquid phase packed-bed and stirred-tank bioreactors". *Environmental Science and Technology* **2006**, *40*, 2390–2395.

Baker, G.A. y Pandey, S. "Amphiphilic self organization in ionic liquids". *Ionic Liquids III A: Fundamentals, progress, challenges, and opportunities* **2005**, *901*, 234-243.

Baltus, R.E.; Counce, R.M.; Culbertson, B.H.; Luo, H.; DePaoli, W.; Dai, S.; Duckworth, D.C. "Examination of the potential of ionic liquids for gas separations". *Separation Science and Technology* **2005**, *40*, 525-541.

Banerjee, T. y Khanna, A. "Infinite dilution activity coefficients for trihexyltetradecyl phosphonium ionic liquids: measurements and COSMO-RS prediction". *Journal of Chemical & Engineering Data* **2006**, *51 (6)*, 2170–2177.

Banerjee, T.; Singh, M. K.; Khanna, A. "Prediction of binary VLE for imidazolium based ionic liquid systems using COSMO-RS". *Industrial & Engineering Chemistry Research* **2006**, *45 (9)*, 3207–3219.

Banerjee, T.; Verma, K. K.; Khanna, A. "Liquid-liquid equilibrium for ionic liquid systems using COSMO-RS: effect of cation and anion dissociation". *AIChE Journal* **2008**, *54 (7)*, 1874–1885.

Bara, J.E.; Carliste, T.K.; Gabriel, C.J.; Camper, D.; Finotello, A.; Gin, D.L.; Noble, R.D. "Guide to CO_2 separations in imidazolium-based room-temperature ionic liquids". *Industrial & Engineering Chemistry Research* **2009**, *48*, 2739-2751.

Bara, J.E.**;** Camper, D.E.; Gin, D.L.; Noble, R.D. "Room-temperature ionic liquids and composite materials: platform technologies for CO_2 capture". *Accounts of Chemical Research* **2010**, *43 (1)*, 152-159.

BASF, **2013**. <http://www.intermediates.basf.com/chemicals/ionic-liquids/processes>

Bates, E.D.; Mayton, R. D.; Ntai, I.; Davis, J.H. "CO_2 capture by a task-specific ionic liquid". *Journal of the American Chemical Society* **2002**, *124 (6)*, 926-927.

Bedia, J.; Ruiz, E.; de Riva, J.; Ferro, V.R.; Palomar, J.; Rodriguez, J.J. "Optimazed ionic liquids for toluene absorption". *AIChE Journal* **2012**. DOI: 10.1002/aic.13926.

Berenjian, A.; Chan, N.; Malmiri, H.J. "Volatile Organic Compounds removal methods: A review". *American Journal of Biochemistry and Biotechnology* **2012**, *8 (4)*, 220-229.

Beste, Y.; Eggersmann, M.; Schoenmakers, H. "Extractive distillation with ionic fluids". *Chemical Engineering & Technology* **2005**, *77 (11)*, 1800–1808.

Blanchard, L.A.; Gu, Z.; Brennecke, J.F. "High-pressure phase behavior of ionic liquid/CO_2 systems". *The Journal of Physical Chemistry B* **2001**, *105 (12)*, 2437–2444.

Blasucci, V.M.; Hart, R.; Mestre, V.L.; Hahne, D.J.; Burlager, M.; Huttenhower, H.; Thio, B. J. R.; Pollet, P.; Liotta, C. L.; Eckert, C.A. "Single component, reversible ionic liquids for energy applications". *Fuel* **2010**a, *89*, 1315−1319.

Blasucci, V.M.; Hart, R.; Pollet, P.; Liotta, C. L.; Eckert, C.A. "Reversible ionic liquids designed for facile separations". *Fluid Phase Equilibria* **2010**b, *294*, 1−6.

Bokhove, J.; Schuur, B.; de Haan, A. B. "Solvent design for trace removal of pyridines from aqueous streams using solvent impregnated resins". *Separation and Purification Technology* **2012**, *98*, 410-418.

Brennecke, J. F.; Goodrich, B. F.; de la Fuente, J. C.; Gurkan, B. E.; Lopez, Z. K.; Price, E. A.; Huang, Y. "Effect of water and temperature on absorption of CO_2 by amine-functionalized anion tethered ionic liquids". *The Journal of Physical Chemistry B* **2011**, *115 (29)*, 9140–9150.

Busca, G. y Pistarino, C. "Abatement of ammonia and amines from waste gases: a summary". *Journal of Loss Prevention in the Process Industries* **2003**, *16 (2)*, 157–163.

Camper, D.; Becker, C.; Koval, C.; Noble, R. "Low pressure hydrocarbon solubility in room temperature ionic liquids containing imidazolium rings interpreted using regular solution theory". *Industrial & Engineering Chemistry Research* **2005**, *44 (6)*, 1928-1933.

Camper, D.; Becker, C.; Koval, C.; Noble, R. "Diffusion and solubility measurements in room temperature ionic liquids". *Industrial & Engineering Chemistry Research* **2006**a, *45 (1)*, 445-450.

Camper, D.; Bara, J.; Koval, C.; Noble, R. "Bulk fluid solubility and membrane feasibility of R-mim-based room-temperature ionic liquids". *Industrial & Engineering Chemistry Research* **2006**b, *45 (18)*, 6279-6283.

Camper, D.; Bara, J.E.; Gin, D.L.; Noble, R.D. "Room-temperature ionic liquid-amine solutions: tunable solvents for efficient and reversible capture of CO_2". *Industrial & Engineering Chemistry Research* **2008**, *47*, 8496–8498.

Carvalho, P.J.; Alvarez, V.H.; Schroder, B.; Gil, A.M.; Marrucho, I.M.; Aznar, M.; Santos, L.M.N.B.F.; Coutinho, J.A P. "Specific solvation interactions of CO_2 on acetate and trifluoroacetate imidazolium based ionic liquids at high pressures". *The Journal of Physical Chemistry B* **2009**a, *113*, 6803−6812.

Carvalho, P.J.; Álvarez, V.H.; Machado, J.J.B.; Pauly, J.; Daridon, J.; Marrucho, I.M.; Aznar, M.; Coutinho, J.A.P. "High pressure phase behavior of carbon dioxide in 1-alkyl-3-methylimidazolium bis(trifluoromethylsulfonyl)imide ionic liquids". *Journal of Supercritical Fluids* **2009**b, *48*, 99–107.

Carvalho, P.J.; Alvarez, V.H.; Marrucho, I.M.; Aznar, M.; Coutinho, J.A.P. "High pressure phase behavior of carbon dioxide in 1-butyl-3-methylimidazolium bis(trifluoromethylsulfonyl)imide and 1-butyl-3-methylimidazolium dicyanamide ionic liquids". *Journal of Supercritical Fluids* **2009**c, *50*, 105–111.

Carvalho, P.J.; Alvarez, V.H.; Marrucho, I.M.; Aznar, M.; Coutinho, J.A.P. "High carbón dioxide solubilities in trihexyltetradecylphosphonium-based ionic liquids". *Journal of Supercritical Fluids* **2010**, *52*, 258–265.

Casas, A.; Oliet, M.; Alonso, M.V.; Rodríguez, F. "Dissolution of Pinus radiata and Eucalyptus globulus woods in ionic liquids under microwave radiation: Lignin regeneration and characterization". *Separation and Purification Tecnology* **2012**, *97*, 115-122.

Casas, A.; Omar, S.; Palomar, Jose; Oliet, M.; Alonso, M.V.; Rodriguez, F. "Relation between differential solubility of cellulose and lignin in ionic liquids and activity coefficients". *RSC Advances* **2013**, *3 (10)*, 3453-3460.

Chen, H.; Du, P.; Chen, J.; Hu, S.; Li, S.; Liu, H. "Separation and preconcentration system based on ultrasonic probe-assisted ionic liquid dispersive liquid–liquid microextraction for determination trace amount of chromium(VI) by electrothermal atomic absorption spectrometry". *Talanta* **2010**, *81*, 176–179.

Chen, Y.; Han, J.; Wang, T.; Mu, T. "Determination of absorption rate and capacity of CO_2 in ionic liquids at atmospheric pressure by thermogravimetric analysis". *Energy & Fuels* **2011**, *25*, 5810–5815

Chiang, Y.C.; Chiang, P.C.; Huang, C.P. "Effects of pore structure and temperature on VOC adsorption on activated carbon". *Carbon* **2011**, *39*, 523-534.

Chinn, D.; Vu, D. Q.; Driver, M. S.; Boudreau, L.C. "CO_2 removal from gas using ionic liquid absorbents". Patente Nº: US 2009/7527775, Mayo 5, **2009**.

Chowdhury, S.; Mohan, R.S.; Scott, J.L. "Reactivity of ionic liquids". *Tetrahedron* **2007**, *63*, 2363-2389.

Condemarin, R.A. y Scovazzo, P. "Gas permeabilities, solubilities, diffusivity, and diffusivity correlations for ammonium-based room temperature ionic liquids with comparison to imidazolium and phosphonium RTIL data". *Chemical Engineering Journal* **2009**, *147*, 51-57.

COSMOtherm, Users Manual, C2.1 Release 01.11; *GmbH&CoKG* (Leverkusen, Germany), **2010**. <http://www.cosmologic.de>.

Costa-Gomes, M.F. "Low-pressure solubility and thermodynamics of solvation of carbon dioxide, ethane, and hydrogen in 1-hexyl-3-methylimidazolium bis(trifluoromethylsulfonyl)amide between temperatures of 283 K and 343 K". *Journal of Chemical & Engineering Data* **2007**, *52 (2)*, 472–475.

Critoph, R.E. "Multiple bed regenerative adsorption cycle using the monolithic carbón-ammonia pair". *Applied Thermal Engineering* **2002**, *22*, 667–677.

D'Alessandro, D.M.; Smit, B.; Long, J.R. "Carbon dioxide capture: prospects for new materials". *Angewandte Chemie International Edition* **2010**, *49*, 6058-6082.

Daugulis, A.J. "Two-phasepartitioning bioreactors: a new technology platform for destroying xenobiotics". *Trends in Biotechnology* **2001**, *19*, 457–462.

Davis, J.H. "Task-specific ionic liquids". *Chemistry Letters* **2004,** *33 (9)*, 1072-1077.

Diedenhofen, M.; Eckert, F.; Klamt, A. "Prediction of infinite dilution activity coefficients of organic compounds in ionic liquids using COSMO-RS". *Journal of Chemical & Engineering Data* **2003**, *48 (3)*, 475–479.

Diedenhofen, M.; Klamt, A.; Marsh, K.; Schafer, A. "Prediction of the vapor pressure and vaporization enthalpy of 1-n-alkyl-3-methylimidazolium bis-(trifluoromethanesulfonyl) amide ionic liquids". *Physical Chemistry Chemical Physics* **2007**, *9 (33)*, 4653–4656.

Diedenhofen, M. y Klamt, A. "COSMO-RS as a tool for property prediction of IL mixtures – a review". *Fluid Phase Equilibria* **2010**, *294*, 31–38.

Domanska, U.; Pobudkowska, A.; Eckert, F. "(Liquid plus liquid) phase equilibria of 1-alkyl-3-methylimidazolium methylsulfate with alcohols, or ethers, or ketones". *The Journal of Chemical Thermodynamic* **2006**, *38 (6)*, 685–695.

Dou, B.; Zhang, M.; Gao, J.; Shen, W.; Sha, X. "High temperature removal of NH_3, organic sulphur, HCl and tar component from coal-derived gas". *Industrial & Engineering Chemistry Research* **2002**, *41*, 4195–4200.

Eckert, F. y Klamt, A. "Fast Solvent Screening via Quantum Chemistry: COSMO-RS approach". *AlChE Journal* **2002**, *48 (2)*, 369-385.

EEA, European Environmental Agency, **2013**a. <http://www.eea.europa.eu/data-and-maps/figures/sector-share-of-ammonia-emissions-eea-member-countries-3>

EEA, European Environmental Agency, **2013**b. <http://www.eea.europa.eu/data-and-maps/figures/emission-trends-of-ammonia-eea-member-countries-eu-27-member-states-3>

EEA, European Environmental Agency, **2013**c. <http://www.eea.europa.eu/data-and-maps/figures/change-in-emissions-of-ammonia-compared-with-the-2010-necd-and-gothenburg-protocol-targets-eea-member-countries-3>

Endres, F. y El Abedin, S.Z. "Air and water stable ionic liquids in physical chemistry". *Physical Chemistry Chemical Physics* **2006**, *8*, 2101-2116.

Endres, F.; MacFarlane, D.; Abbott, A. "Electrodeposition from ionic liquids". *Wiley-VCH* (Weinheim), **2008**.

EPA, The United States Environmental Proteccion Agency, **2012**a. <http://www.epa.gov/climatechange/ghgemissions/gases.html>

EPA, The United States Environmental Proteccion Agency, **2012**b. "Volatile Organic Compounds (VOCs) Technical Overview" <http://www.epa.gov/iaq/voc2.html>

Erisman, J.W.; Bleeker, A.; Galloway, J.; Sutton, M.A. "Reduced nitrogen in ecology and the environment". *Environmental Pollution* **2007**, *150*, 140–149.

EC, European Comision, **2001**. "Directive 2001/81/EC of the European Parliament and of the Council of 23 October 2001 on National Emission Ceilings for Certain Atmospheric Pollutants European Parliament and Council".

Faulkner, W.B. y Shaw, B.W. "Review of ammonia emission factors for United States animal agriculture". *Atmospheric Environment* **2008**, *42*, 6567–6574.

Figueroa, J.D.; Fout, T.; Plasynski, S.; McIlvried, H.; Srivastava, R.D. "Advances in CO_2 capture technology. The U.S. Department of Energy´s Carbon Sequestration Program". *International Journal of Greenhouse Gas Control* **2008**, *2 (1)*, 9-20.

Finotello, A.; Bara, J.E.; Camper, D.; Noble, R.D. "Room-temperature ionic liquids: temperature dependence of gas solubility selectivity". *Industrial & Engineering Chemistry Research* **2008**, *47*, 3453-3459.

Freire, M. G.; Ventura, S. P.; Santos, L. M.; Marrucho, I. M.; Coutinho, J. "Evaluation of COSMO-RS for the prediction of LLE and VLE of water and ionic liquids binary systems". *Fluid Phase Equilibria* **2008**, *268 (1-2)*, 74–84.

Galán, L.M.; Meindersma, G.W.; de Haan, A.B. "Solvent properties of functionalized ionic liquids for CO_2 absorption". *Chemical Engineering Research and Design* **2007**, *85 (1)*, 31-39.

Gang, L.; van Grondelle, J.; van Andersson, B.G.; Santen, R.A. "Selective low temperature NH_3 oxidation to N_2 on copper-based catalysts". *Journal of Catalysis* **1999**, *186*, 100–109.

García, S.; García, J.; Larriba, M.; Casas, A.; Rodríguez, F. "Liquid–liquid extraction of toluene from heptane by {[4bmpy][Tf_2N] + [emim][$CHF_2CF_2SO_3$]} ionic liquid mixed solvents". *Fluid Phase Equilibria* **2013**, *337*, 47-52.

Georgiadis, M.; Pistikopoulos, E.; Kikkinides, E.S. "Process Systems Engineering. Volume 5: Energy Systems Engineering". *Wiley-VCH* (Weinheim**), 2008**.

Giernoth, R. "Task-specific ionic liquids". *Angewandte Chemie International Edition* **2010**, *49*, 2834-2839.

Goodrich, B.F.; de la Fuente, J.C.; Gurkan, B.E.; Zadigian, D.J.; Price, E. A.; Huang, Y.; Brennecke, J.F. "Experimental measurements of amine-functionalized anion-tethered ionic liquids with carbon dioxide". *Industrial & Engineering Chemistry Research* **2011**, *50*, 111−118.

Gurau, G.; Rodriguez, H.; Kelley, S.P.; Janiczek, P.; Kalb, R. S.; Rogers, R.D. "Demonstration of chemisorption of carbon dioxide in 1,3-dialkylimidazolium acetate ionic liquids". *Angewandte Chemie International Edition* **2011**, *50*, 12024−12026.

Gurkan, B.E.; de la Fuente, J.; Mindrup, E.M.; Ficke, L.E.; Goodrich, B. F.; Price, E.A.; Schneider, W. F.; Brennecke, J.F. "Equimolar CO_2 absorption by anion-

functionalized ionic liquids". *Journal of the American Chemical Society* **2010**, *132*, 2116−2117.

Gutierrez, J.P.; Meindersma, G.W.; de Haan, A.B. "COSMO-RS-based ionic liquid selection for extractive distillation processes". *Industrial & Engineering Chemistry Research* **2012**, *51*, 11518-11529.

Han, X. y Armstrong, D.W. "Ionic liquids in separations". *Accounts of Chemical Research* **2007**, *40*, 1079-86.

Han, D. y Row, K.H. "Recent applications of ionic liquids in separation technology". *Molecules* **2010**, *15*, 2405-2426.

Hart, R.; Jessop, P.G.; Thomas, C.A.; Eckert, C.A.; Liotta, C.L. "The reaction of 1,8-diazabicyclo[5.4.0]undec-7-ene (DBU) with carbon dioxide". *The Journal of Organic Chemistry* **2005**, *70*, 5335−5338.

Heintz, A. "Recent developments in thermodynamics and thermophysics of non-aqueous mixtures containing ionic liquids. A review". *The Journal of Chemical Thermodynamics* **2005**, *37*, 525-535.

Heyems, F.; Peggy, M.D.; Charbit, F.; Fanlo, J.L.; Moulin, P. "A new efficient absorption liquid to treat exhaust air loaded with toluene". *Chemical Engineering Journal* **2006**, *115*, 225–231.

Holbrey, J.D. y Seddon, K.R. "Review: Ionic liquids". *Clean Products and Processes* **1999**a, *1*, 223-236.

Holbrey, J.D. y Seddon, K.R. "The phase behaviour of 1-alkyl-3-methylimidazolium tetrafluoroborates; ionic liquids and ionic liquid crystals". *Journal of the American Chemical Society, Dalton Transactions* **1999**b, *13*, 2133-2140.

Hong, J.H. y Park, K.J. "Compost biofiltration of ammonia gas from bin composting". *Bioresource Technology* **2005**, *96(6)*, 741–745.

Hong, G.; Jacquemin, J.; Deetlefs, M.; Hardacre, C.; Husson, P.; Costa, M.F. "Solubility of carbon dioxide and ethane in three ionic liquids based on the bis {(trifluoromethyl)sulfonil}imide anion". *Fluid Phase Equilibria* **2007**, 257, 27-34.

Huang, J.; Riisager, A.; Berg, R.W.; Fehrmann, R. "Tuning ionic liquids for high gas solubility and reversible gas sorption". *Journal of Molecular Catalysis A* **2008**, 279, 170–176.

Huang, J. y Rüther, T. "Why are ionic liquids attractive for CO_2 absorption? An overview". *Australian Journal of Chemistry* **2009**, *62*, 298-308.

Huddleston, J.G.; Visser, A.E.; Reichert, W.M.; Willauer, H. D.; Broker, G.A.; Rogers, R.D. "Characterization and comparison of hydrophilic and hydrophobic room temperature ionic liquids incorporating the imidazolium cation". *Green Chemistry* **2001**, *3*, 156-164.

IEA, International Energy Agency. "World Energy Outlook". Paris, **2010**.

IEA, International Energy Agency. "CO_2 Emission for fuel Combustion Highlights". Paris, **2012**.

Iolitech, **2013**. <http://www.iolitec.de/en/Ionic-Liquids/special-chemistry.html>

IPCC, Intergovernmental Panel on Climate Change. "In Climate Change 2007: The Physical Science Basis. Contribution of Working Group I to the Fourth Assessment Report of the Intergovernmental Panel on Climate Change". *Cambridge University Press* (Cambridge, Reino Unido), **2007**a.

IPCC, Intergovernmental Panel on Climate Change. "In Climate Change 2007: Mitigation. Contribution of Working Group III to the Fourth Assessment Report of the Intergovernmental Panel on Climate Change". *Cambridge University Press* (Cambridge, Reino Unido), **2007**b.

ISO 16000-6, **1989**. "Volatile organic compounds in air analysis".

Jacquemin, J.; Costa-Gomes, M.F.; Husson, P.; Majer, V. "Solubility of carbon dioxide, ethane, methane, oxygen, nitrogen, hydrogen, argon, and carbon monoxide in 1-butyl-3-methylimidazolium hexafluorophosphate". *Fluid Phase Equilibria* **2006**a, *240*, 87-95.

Jacquemin, J.; Costa-Gomes, M.F.; Husson, P.; Majer, V. "Solubility of carbone dioxide, ethane, methane, oxygen, nitrogen, hydrogen, argon, and carbon monoxide in 1-butyl-3-methylimidazolium tetrafluoroborate between temperatures 283 K and 343 K and at pressures close to atmospheric". *Journal of Chemical Thermodynamics* **2006**b, *38*, 490-502.

Jacquemin, J.; Husson, P.; Majer, V.; Costa, M.F. "Influence of the cation on the solubility of CO_2 and H_2 in ionic liquids based on the bis(trifluoromethylsulfonyl)imide anion". *Journal of Solution Chemistry* **2007**, 36, 967-979.

Jacquemin, J.; Husson, P.; Majer, V.; Padua, A.H.; Costa-Gomes, M.F. "Thermophysical properties, low pressure solubilities and thermodynamics of solvation of carbon dioxide and hydrogen in two ionic liquids based on the alkylsulfate anion". *Green Chemistry* **2008**, *10*, 944-950.

Jalili, A.H.; Rahmati-Rostami, M.; Ghotb, C.; Hosseini-Jenab, M.; Ahmadi, A.N. "Solubility of H_2S in ionic liquids [bmim][PF_6], [bmim][BF_4], and [bmim][Tf_2N]". *Journal of Chemical & Engineering* Data **2009**, *54 (6)*, 1844–1849.

Jarraya, S. Fourmentin, M. Benzina, S. Bouaziz. "VOC adsorption on raw and modified clay materials". *Chemical Geology* **2010**, *275*, 1-8.

Jessop, P. G.; Heldebrant, D. J.; Li, X.; Eckert, C. A.; Liotta, C.L. "Reversible nonpolar-to-polar solvent". *Nature* **2005**, *436*, 1102.

Kamps, A.P.S.; Tuma, D.; Xia, J. Z.; Maurer, G. "Solubility of CO_2 in the ionic liquid [bmim][PF_6]". *Journal of Chemical & Engineering Data* **2003**, *48 (3)*, 746-749.

Karadas, F.; Atilhan, M.; Aparicio, S. "Review on the use of ionic liquids (ILs) as alternative fluids for CO_2 capture and natural gas sweetening". *Energy Fuels* **2010**, *24*, 5817–5828.

Kato, R.; Gmehling, J. "Systems with ionic liquids: Measurement of VLE and gamma(infinity) data and prediction of their thermodynamic behavior using original UNIFAC, mod. UNIFAC(Do) and COSMO-RS(O1)". *The Journal of Chemical Thermodynamics* **2005**, *37 (6)*, 603–619.

Kelleher, B.P.; Leahy, J.J.; Henihan, A.M.; O'Dwyer, T.F.; Sutton, D.; Leahy, M.J. "Advances in poultry litter disposal technology, a review". *Bioresource Technology* **2002**, *83*, 27–36.

Kerlé, D.; Ludwig, R.; Geiger, A.; Paschek, D. "Temperature dependence of the solubility of carbon dioxide in imidazolium-based ionic liquids". *The Journal of Physical Chemistry B* **2009**, *113*, 12727-12735.

Kim, Y.S.; Choi, W.Y.; Lee, C.S.; "Measurements and calculation of the solubility of carbon dioxide in ionic liquid [bmim][PF_6]". *Proceedings of the 4th International Conference on Frontieres on Separation Science and Technology* **2004**, 19-22.

Kim, Y.S.; Choi, W. Y.; Jang, J.H.; Lee, C.S. "Solubility measurement and prediction of carbon dioxide in ionic liquids". *Fluid Phase Equilibria* **2005**, *228-229*, 439-445.

Klamt, A. y Schüürmann, G. "COSMO: A new approach to dielectric screening in solvents with explicit expressions for the screening energy and its gradient". *Journal of the Chemical Society, Perkin Transactions 2* **1993**, 799-805.

Klamt, A. "Conductor-like Screening Model for Real Solvents: a new approach to the quantitative calculation of solvation phenomena", *The Journal of Physical Chemistry* **1995**, *99 (7)*, 2224-2235.

Klamt, A.; V. Jonas; T. Bürger y J. C. W. Lohrenz. "Refinement and parameterization of COSMO-RS". *The Journal of Physical Chemistry A* **1998**, *102 (26)*, 5074–5085.

Klamt, A. y Eckert, F. "COSMO-RS: a novel and efficient method for the a priori prediction of thermophysical data of liquids". *Fluid Phase Equilibria* **2000**a, *172 (1)*, 43-72.

Klamt, A. y Eckert, F. "COSMO-RS: A quantum chemistry based alternative to group contribution methods for the prediction of activity coefficients in multi-component mixtures". *Fluid Phase Equilibria* **2000**b, *172*, 43-72.

Klamt, A. "COSMO-RS: from quantum chemistry to fluid phase thermodynamics and drug design". *Elsevier* (Amsterdam), First Edition, **2005**.

Klamt, A.; Eckert, F.; Arlt, W. "COSMO-RS: an alternative to simulation for calculating thermodynamic properties of liquid mixtures". *Annual Review of Chemical and Biomolecular Engineering* **2010**, *1*, 101–122.

Koornneef, J.; Ramirez, A.; van Harmelen, T.; van Horssen, A.; Turkenburg, W.; Faaij, A. "The impact of CO_2 capture in the power and heat sector on the emission of SO_2, NO_x, particulate matter, volatile organic compounds and NH_3 in the European Union". *Atmospheric Environment* **2010**, *44*, 1369–1385.

Kroon, M.C.; Karakatsani, E.K., Economou, I.G.; Witkamp, G.J.; Peters, C.J. "Modeling of the carbon dioxide solubility in imidazolium-based ionic liquids with the tPC-PSAFT equation of state". *The Journal of Physical Chemistry B* **2006**, *112*, 9262–9269.

Kumar, A.A.; Banerjee, T. "Thiophene separation with ionic liquids for desulphurization: a quantum chemical approach". *Fluid Phase Equilibria* **2009**, *278 (1-2)*, 1–8.

Kumelan, J.; Pérez Salado, A.; Tuma, D.; Maurer, G. "Solubility of CO_2 in the ionic liquids [bmim][CH_3SO_4] and [bmim][PF_6]". *Journal of Chemical & Engineering Data* **2006**a, 51, 1802-1807.

Kumelan, J.; Kamps, A.P.; Tuma, D.; Maurer, G. "Solubility of CO_2 in the ionic liquid [hmim][Tf_2N]". *Journal of Chemical & Engineering Data* **2006**b, *51*, 1802-1807.

Kumelan, J.; Kamps, A.P.; Tuma, D.; Maurer, G. "Solubility of the single gases methane and xenon in the ionic liquid [hmim][Tf_2N]". *Industrial & Engineering Chemistry Research* **2007**, *46*, 8236-8240.

Kumelan, J.; Kamps, A.P.; Tuma, D.; Yokozeki, A.; Shiflett, M.B.; Maurer, G. "Solubility of tetrafluoromethane in the ionic liquid [hmim][Tf_2N]". *The Journal of Physical Chemistry B* **2008**, *112*, 3040-3047.

Lapkin, A.A.; Peters, M.; Greiner, L.; Chemat, S.; Leonhard, K.; Liaw, M. A.; Leitner, W. "Screening of new solvents for artemisinin extraction process using ab initio methodology". *Green Chemistry* **2010**, *12 (2)*, 241–251.

Law, G. y Watson, W. P. "Surface tension measurements of N-alkylimidazolium ionic liquids". *Langmuir* **2001**, *17*, 6138-6141.

Lee, B. C. y Outcalt, S. L. "Solubilities of gases in the ionic liquid 1-n-butyl-3-methylimidazolium bis(trifluoromethylsulfonyl)imide". *Journal of Chemical & Engineering Data* **2006**, *51*, 892-897

Lei, Z. G.; Arlt, W.; Wasserscheid, P. "Separation of 1-hexene and n-hexane with ionic liquids". *Fluid Phase Equilibria* **2006**, *241 (1-2)*, 290–299.

Li, G.; Zhou, Q.; Zhang, X.; Wang, L.; Zhang, S.; Li, J. "Solubilities of ammonia in basic imidazolium ionic liquids". *Fluid Phase Equilibria* **2010**, *297*, 34–39.

Lietti, L.; Ramella, C.; Groppi, G.; Forzatti, P. "Oxidation of NH_3 and NO_x formation during the catalytic combustion of gasified biomasses fuels over Mn-hexaaluminate and alumina-supported Pd catalysts". *Applied Catalysis B: Environmental* **1999**, *21*, 89–101.

Lietti, L.; Ramis, G.; Busca, G.; Forzatti, P.; Bregani, F. "Characterization and reactivity of MoO_3/SiO_2 catalysts in the selective catalytic oxidation of ammonia to N_2". *Catalysis Today* **2000**, *61*, 187–195.

Lim, B.H.; Choe, W.H.; Shim, J.J.; Ra, C.S.; Tuma, D.; Lee, H.; Lee, C.S. "High-pressure solubility of carbon dioxide in imidazolium-based ionic liquids with aniones $[PF_6]$ and $[BF_4]$". *Korean Journal of Chemical Engineering* **2009**, *26 (4)*, 1130-1136.

Lintz, H.G. y Wittstock, K. "The oxidation of solvents in air on oxidic catalysts-formation of intermediates and reaction network". *Applied Catalysis A: General* **2001**, *216*, 217–225.

Liu, Y.; Jessop, P. G.; Cunningham, M.; Eckert, C. A.; Liotta, C. L. "Switchable surfactants". *Science* **2006**, *313*, 558−560.

Llamas, B. y Romero, E. "Tecnologías de lucha contra el cambio climático. Del carbón al carbono". *Universidad de Huelva* (España), **2006**.

Lozano, P. "Enzymes in neoteric solvents: from one-phase to multiphase systems". *Green Chemistry* **2010**, *12*, 555-569.

Manan, N. A.; Hardacre, C.; Jacquemin, J.; Rooney, D. W.; Youngs, T. G. "Evaluation of gas solubility prediction in ionic liquids using COSMOthermX". *Journal of Chemical & Engineering Data* **2009**, *54*, 2005–2022.

Marsh, K.N.; Boxall, J.A.; Lichtenthaler, R. "Room temperature ionic liquids and their mixtures - a review". *Fluid Phase Equilibria* **2004**, *219 (1)*, 93-98.

Meindersma, G.W.; Hansmeier, A.R.; de Haan, A.B. "Ionic liquids for aromatics extraction. Present status and future outlook". *Industrial & Engineering Chemistry Research* **2010**, *49*, 7530–7540.

Melse, RW.; Ogink, N.W.M.; Rulkens, W.H. "Overview of European and Netherlands' regulations on airborne emissions from intensive livestock production with a focus on the application of air scrubbers". *Biosystems Engineering* **2009**, *104*, 289–298.

Miller, M.B.; Chen, D.L.; Xie, H.B.; Luebke, D.R.; Johnson, J.K.; Enick, R.M. "Solubility of CO_2 in CO_2-philic oligomers; COSMOtherm predictions and experimental results". *Fluid Phase Equilibria* **2009**, *287*, 26–32.

Miltner, M.; Miltner, A.; Friedl, A. "Calculation of physical gas solubilities in various solvents with COSMO-RS". *Chemie Ingenieur Technik* **2006**, *78 (8)*, 1087–1092.

Mitsubishi Heavy Industries. "Large-scale carbon dioxide capture demonstration project at a coal-fired power plant in the USA". *Mitsubishi Heavy Industries Technical Review* **2012**, *49 (1)*, 37-43.

Mohanty, S.; Banerjee, T.; Mohanty, K. "Quantum chemical based screening of ionic liquids for the extraction of phenol from aqueous solution". *Industrial & Engineering Chemistry Research* **2010**, *49 (6)*, 2916–2925.

Moniruzzaman, M.; Nakashima, K.; Kamiya, N.; Goto, M. "Recent advances of enzymatic reactions in ionic liquids". *Biochemical Engineering Journal* **2010**, *48*, 295-314.

Muldoon, M.J.; Aki, S.N.V.K.; Anderson, J.L.; Dixon, J.K.; Brennecke, J.F. "Improving carbon dioxide solubility in ionic liquids". *The Journal of Physical Chemistry B* **2007**, *111*, 9001-9009.

Navas, A.; Ortega, J.; Vreekamp, R.; Marrero, E.; Palomar, J. "Experimental thermodynamic properties of 1-butyl-2-methylpyridinium tetrafluoroborate [$b_2$mpy][BF_4] with water and with alkan-1-ol and their interpretation with the COSMO-RS methodology". *Industrial & Engineering Chemistry Research* **2009**, *48 (5)*, 2678–2690.

Ndegwa, P.M.; Hristov, A.N.; Arogo, J.; Sheffield, R.E. "A review of ammonia emission mitigation techniques for concentrated animal feeding operations". *Biosystems Engineering* **2008**, *100*, 453–469.

NHMRC, National Health and Medical Research Council, **2002**. "Ambient air quality goals, national health and medical research council".

Ohno, H. "Electrochemical Aspects of Ionic Liquids". *John Wiley & Sons, Inc.* (Hoboken, NJ, USA), Second Edition, **2011**.

Olivier-Bourbigou, H., Favre, F., Forestière, A.; Hugues, F. "Ionic lquids and catalysis: the IFP Biphasic Difasol Process". *Handbook of Green Chemistry* **2010**, *1*, 101–126.

Orchillés, A.V.; Miguel, P.J; Vercher, E.; Martínez-Andreu, A. "Ionic liquids as entrainers in extractive distillation: isobaric vapor−liquid equilibria for acetone + methanol + 1-ethyl-3-methylimidazolium trifluoromethanesulfonate". *Journal of Chemical & Engineering Data* **2007**, *52 (1)*, 141–147.

Palgunadi, J.; Kang, J.E.; Nguyen, D.Q.; Kim, J.H.; Min, B.K.; Lee, S.D.; Kim, H.; Kim, H.S. "Solubility of CO_2 in dialkylimidazolium dialkylphosphate ionic liquids". *Thermochimica Acta* **2009**, *494*, 94-98.

Palomar, J.; Ferro, V.L.; Torrecilla, J.S.; Rodriguez, F. "Density and molar volume predictions using COSMO-RS for ionic liquids. An approach to solvent design". *Industrial & Engineering Chemistry Research* **2007**, *46 (18)*, 6041–6048.

Palomar, J.; Torrecilla, J.S.; Ferro, V.R.; Rodríguez, F. "Development of an a priori ionic liquid design tool 1: integration of a novel COSMO-RS molecular descriptor on neural networks". *Industrial & Engineering Chemistry Research* **2008**, *47*, 4523–4532.

Palomar, J.; Lemus, J.; Gilarranz, M. A.; Rodríguez, J. J. "Adsorption of ionic liquids from aqueous effluents by activated carbón". *Carbon* **2009**a, *47 (7)*, 1846–1856.

Palomar, J.; Torrecilla, J.S.; Ferro, V.R; Rodríguez, F. "Development of an a priori ionic liquid design tool 2: ionic liquid selection through the prediction of

COSMO-RS molecular descriptor by inverse neural network". *Industrial & Engineering Chemistry Research* **2009**b, *48*, 2257–2265.

Pandey, S. "Analytical applications of room-temperature ionic liquids: a review of recent efforts". *Analytica Chimica Acta* **2006**, *556 (1)*, 38-45.

Patel, D.D. y Lee, J.M. "Applications of ionic liquids". *The Chemical Record* **2012**, *12*, 329-355.

Pei, Y.; Wu, K.; Wang, J.; Fan, J. "Recovery of furfural from aqueous solution by ionic liquid based liquid–liquid extraction". *Separation Science and Technology* **2008**, *43*, 2090–2102.

Petkovic, M.; Seddon, K.R.; Rebelo, L.P.N.; Pereira, C.S. "Ionic liquids: a pathway to environmental acceptability". *Chemical Society Reviews* **2011**, *40 (3)*, 1383-1403.

Phan, L.; Chiu, D.; Heldebrant, D. J.; Huttenhower, H.; John, E.; Li, X.; Pollet, P.; Wang, R.; Eckert, C. A.; Liotta, C. L.; Jessop, P.G. "Switchable solvents consisting of amide/alcohol or guanidine/alcohol mixtures". *Industrial & Engineering Chemistry Research* **2008**, *47*, 539−545.

Plechkova, N.V. y Seddon, K.R. "Applications of ionic liquids in the chemical industry". *Chemical Society Reviews* **2008**, *37*, 123-150.

Polyakova, Y.; Jin, Y.Z.; Zheng, J.Z.; Row, K.H. "Effect of concentration of ionic liquid, 1-butyl-3-methylimidazolium tetrafluoroborate, for retention and separation of some amino and nucleic acids". *Journal of Pharmaceutical and Biomedical Analysis* **2006**, *29*, 1687–1701.

Preiss, U.; Jungnickel, C.; Thoming, J.; Krossing, I.; Luczak, J.; Diedenhofen, M.; Klamt, A. "Predicting the critical micelle concentrations of aqueous solutions of

ionic liquids and other ionic surfactants". *Chemistry - A European Journal* **2009**, *15 (35)*, 8880–8885.

Quijano, G. Hernandez, M. Thalasso, F. Muñoz, R. Villaverde, S. "Two-phase partitioning bioreactors in environmental biotechnology". *Applied Microbiology and Biotechnology* **2009**, *84*, 829-846.

Quijano, G.; Couvert, A.; Amrane, A.; Darracq, G.; Couriol, C.; Le Cloirec, P.; Paquin, L.; Carrié, D. "Potential of ionic liquids for VOC absorption and biodegradation in multiphase systems". *Chemical Engineering Science* **2011**, *66*, 2707-2712.

Raeissi, S. y Peters, C.J. "Carbon dioxide solubility in the homologous 1-alkyl-3-methylimidazolium bis(trifluoromethylsulfonyl)imide family". *Journal of Chemical & Engineering Data* **2009**a, *54*, 382-386.

Raeissi, S. y Peters, C.J. "A potential ionic liquid for CO_2-separating membranes: selection and gas solubility studies". *Green Chemistry* **2009**b, *11*, 185-192.

Ramdin, M.; de Loos, T.W.; Vlugt, T.H.J. "State-of-the-Art of CO_2 capture with ionic liquids". *Industrial & Engineering Chemistry Research* **2012**, *51*, 8149−8177.

Rao, C.S. "Environmental pollution control engineering". *New Age International* (New Delhi), Second Edition, **2007**.

Rao, A.B. and Rubin, E.A. "Technical, economic, and environmental assessment of amine-based CO_2 capture technology for power plant greenhouse gas control". *Environmental Science & Technology* **2002**, *36*, 4467−4475.

Rochelle, G.; Chen, E.; Dugas, R.; Oyenakan, B.; Seibert, F. "Solvent and process enhancements for CO_2 absorption/stripping". *Annual Conference on Capture and Sequestration* (Alejandria, Virginia, E.E.U.U.), **2005**.

Roe, S.M.; Spivey, M.D.; Lindquist, H.C.; Thesing, K.B.; Strait, R.P. "Estimating ammonia emissions from anthropogenic nonagricultural sources – Draft final report". *Emission Inventory Improvement Program*, **2004**.

Rogers, R.D. y Seddon, K.R. "Ionic liquids: Industrial applications for green chemistry". *ACS Symposium Series*, Vol. 818, *American Chemical Society* (Washington D.C.), **2002**.

Rogers, R.D. y Seddon, K.R. "Ionic liquids as green solvents: progress and prospects". *ACS Symposium Series*, Vol. 856, *American Chemical Society* (Washington D.C.), **2003**.

Rohan, A.L.; Switzer, J.R.; Flack, K.M.; Hart, R.; Sivaswamy, S.; Biddinger, E.J.; Talreja, M.; Manish; Verma, M.; Faltermeier, S.; Nielsen, P.T.; Pollet, Pamela; Schuette, G.F.; Eckert, C.A.; Liotta, C.L. "The synthesis and the chemical and physical properties of non-aqueous silylamine solvents for carbon dioxide capture". *ChemSusChem* **2012**, *5 (11)*, 2181-2187.

Rosol, Z. P.; German, N. J.; Gross, S. M. "Solubility, ionic conductivity and viscosity of lithium salts in room temperature ionic liquids". *Green Chemistry* **2009**, *11 (9)*, 1453–1457.

Roughton, B.C.; Christian, B.; White, J.; Camarda, K.V.; Gani, R. "Simultaneous design of ionic liquid entrainers and energy efficient azeotropic separation". *Computers & Chemical Engineering* **2012**, *42*, 248-262.

Schilderman, A.M.; Raeissi, S.; Peters, C.J. "Solubility of carbon dioxide in the ionic liquid 1-ethyl-3 methylimidazolium bis(trifluoromethylsulfonyl)imide". *Fluid Phase Equilibria* **2007**, *260 (1)*, 19-22.

Scovazzo, P. "Determination of the upper limits, benchmarks, and critical properties for gas separations using stabilized room temperature ionic liquid membranes (SILMs) for the purpose of guiding future research". *Journal of Membrane Science* **2009**, *343 (1-2)*, 199-211.

Seddon, K.R.; Stark, A.; Torres, M. J. "Influence of chloride, water, and organic solvents on the physical properti es of ionic liquids". *Pure and Applied Chemistry*, **2000**, *72 (12)*, 2275-2287.

Seddon, K.R.; Stark, A.; Torres, M.J. "Viscosity and density of 1-alkyl-3-methylimidazolium ionic liquids". *Clean solvents* **2002**, 34-49.

Sheridan, B.; Curran, T.; Dodd, V.; Colligan, J. "Biofiltration of odour and ammonia from a pig unit—a pilot-scale study". *Biosystems Engineering* **2002**, *82 (4)*, 441–453.

Shiflett, M.B. y Yokozeki, A. "Solubilities and diffusivities of carbon dioxide in ionic liquids: [bmim][PF_6] and [bmim][BF_4]". *Industrial & Engineering Chemistry Research* **2005**, 44 *(12)*, 4453–4464.

Shiflett, M.B. y Yokozeki, A. "Gaseous absorption of fluoromethane, fluoroethane, and 1,1,2,2-tetrafluoroethane in 1-butyl-3-methylimidazolium hexafluorophosphate". *Industrial & Engineering Chemistry Research* **2006**, *45*, 6375-6382.

Shiflett, M.B. y Yokozeki, A. "Solubility of CO_2 in room temperature ionic liquid [hmim][Tf_2N]". *The Journal of Physical Chemistry B* **2007**, *111*, 2070-2074.

Shiflett, M.B.; Kasprzak, D.J.; Junk, C.P. Yokozeki, A. "Phase behavior of carbon dioxide + [bmim][Ac] mixtures". *The Journal of Chemical Thermodynamics* **2008**, *40*, 25−31.

Shiflett, M.B. y Yokozeki, A. "Phase behavior of carbon dioxide in ionic liquids: [emim][acetate], [emim][trifluoroacetate], and [emim][acetate] + [emim][trifluoroacetate] mixtures". *Journal of Chemical & Engineering Data* **2009**, *54*, 108−114.

Shiflett, M.B.; Drew, D.W.; Cantini, R. A.; Yokozeki, A. "Carbon dioxide capture using ionic liquid 1-butyl-3-methylimidazolium acetate". *Energy Fuels* **2010**, *24*, 5781−5789.

Shiflett, M.B.; Elliott, B.A.; Lustig, S.R.; Sabesan, S.; Kelkar, M.S.; Yokozeki, A. "Phase Behavior of CO_2 in room-temperature ionic liquid 1-ethyl-3-ethylimidazolium acetate". *ChemPhysChem* **2012**a, *13 (7)*, 1806-1817.

Shiflett, M.B.; Niehaus, A.M.S.; Elliott, B.A.; Yokozeki, A. "Phase behavior of N_2O and CO_2 in room-temperature ionic liquids [bmim][Tf_2N], [bmim][BF_4], [bmim][$N(CN)_2$], [bmim][Ac], [eam][NO_3], and [bmim][SCN]". *International Journal of Thermophysics* **2012**b, *33 (3)*, 412-436.

Shiflett, M.B.; Elliott, B.A.; Yokozeki, A. "Phase behavior of vinyl fluoride in room-temperature ionic liquids [emim][Tf_2N], [bmim][$N(CN)_2$], [bmpy][BF_4], [bmim][HFPS] and [omim][TFES]". *Fluid Phase Equilibria* **2012**c, *316*, 147-155

Sommer, S.G. y Hutchings, N.J. "Techniques and strategies for the reduction of ammonia emission from agriculture". *Water Air and Soil Pollution* **1995**, *85*, 237–248.

Soriano, A.N.; Doma, B.T.; Li, M.H.; "Carbon dioxide solubility in 1-ethyl-3-methylimidazolium tetrafluoroborate". *Journal of Chemical & Engineering Data* **2008**, *53*, 2550-2555.

Soriano, A.N.; Doma, B.T.; Li, M.H. "Carbon dioxide solubility in some ionic liquids at moderate pressures". *Journal of the Taiwan Istitute of Chemical Engineers* **2009**a, *40*, 387-393.

Soriano, A.N.; Doma, B.T.; Li, M.H. "Carbon dioxide solubility in 1-ethyl-3-methylimidazolium trifluoromethanesulfonate". *The Journal of Chemical Thermodynamics* **2009**b, *41*, 525-529.

Sun, Y.; Clanton, C.J.; Janni, K.A.; Malzer, G.L. "Sulfur and nitrogen balances in biofilters for odorous gas emission control". *Transactions of the ASAE* **2000**, *43 (6)*, 1861–1875.

Sutton, M.A. y Fowler, D. "Introduction: fluxes and impacts of atmospheric ammonia on national, landscape and farm scales". *Environmental Pollution* **2002**, *119*, 7–8.

Sutton, M.A.; Erisman, J.W.; Dentener, F.; Möller, D. "Ammonia in the environment: from ancient times to the present". *Environmental Pollution* **2008**, *156*, 583–604.

Tang, B.; Bi, W.; Tian, M.; Ho Row, K. "Application of ionic liquid for extraction and separation of bioactive compounds from plants". *Journal of Chromatography B* **2012**, *904*, 1–21.

UNECE, The United Nations Economic Comission for Europe. Protocolo de Gotemburgo, **2013**. <http://www.unece.org/env/lrtap/multi_h1.html>

Van Meter, D.S.; Stuart, O.D.; Carle, A.B., Stalcup, A.M. "Characterization of a novel pyridinium bromide surface confined ionic liquid stationary phase for high-performance liquid chromatography under normal phase conditions via linear solvation energy relationships". *Journal of Chromatography A* **2008**, *1191*, 67–71.

Vancov, T.; Alston, A.S.; Brown, T.; McIntosh. "Use of ionic liquids in converting lignocellulosic material to biofuels". *Renewable Energy* **2012**, *45*, 1-6.

Vega, L.F. "El CO_2 como recurso. De la captura a los usos industriales". *Fundación Gas Natural* (España), **2010**.

Wang, X.; Daniels, R.; Baker, R.W. "Recovery of VOCs from high-volume low-VOC concentration air streams". *AIChE Journal* **2001**, *47*, 1094–1100.

Wang, T.F.; Peng, C.J.; Liu H.L.; Hu, Y. "Description of the pVT behavior of ionic liquids and the solubility of gases in ionic liquids using an equation of state". *Fluid Phase Equilibria* **2006**, *250*, 150–157.

Wang, C.; Luo, H.; Jiang, D.; Li, H.; Dai, S. "Carbon dioxide capture by superbase-derived protic ionic liquids". *Angewandte Chemie International Edition* **2010**a, *49*, 5978−5981.

Wang, C.; Mahurin, S. M.; Luo, H.; Baker, G. A.; Li, H.; Dai, S. "Reversible and robust CO_2 capture by equimolar task-specific ionic liquid-superbase mixtures". *Green Chemistry* **2010**b, *12*, 870−874.

Wang, C.; Luo, H.; Luo, X.; Li, H.; Dai, S. "Equimolar CO_2 capture by imidazolium-based ionic liquids and superbase systems". *Green Chemistry* **2010**c, *12*, 2019−2023.

Wang, C.; Luo, X.; Luo, H.; Jiang, D.; Li, H.; Dai, S. "Tuning the basicity of ionic liquids for equimolar CO_2 capture". *Angewandte Chemie International Edition* **2011**, *50*, 4918−4922.

Wasserscheid, P. y Keim, W. "Ionic liquids–new solutions for transition metal catalysis". *Angewandte Chemie International Edition* **2002**, *39*, 3772-3789.

Wasserscheid, P. y Welton, T. "Ionic Liquids in Synthesis". *Wiley-VCH* (Weinheim), First Edition, **2003**.

Welton, T. "Room-temperature ionic liquids. Solvents for synthesis and catalysis". *Chemical Reviews* **1999**, *99*, 2071-96.

Weyershausen, B. y Lehmann, K. "Industrial application of ionic liquids as performance additives". *Green Chemistry* **2005**, **7**, 15-19.

Yokozeki, A. y Shiflett, M.B. "Ammonia solubilities in room-temperature ionic Liquids". *Industrial & Engineering Chemistry Research* **2007**a, *46*, 1605–1610.

Yokozeki, A. y Shiflett, M.B. "Vapor–liquid equilibria of ammonia + ionic liquid Mixtures". *Applied Energy* **2007**b, *84*, 1258–1273.

Yokozeki, A. y Shiflett, M.B. "Hybrid vapor compression-absorption cycle". Patente Nº: US 2007/0019708A1. Enero 25, **2007**c.

Yokozeki, A. y Shiflett, M.B. "Absorption cycle utilizing ionic liquids and water as working fluids". Patente Nº: US 2007/0144186 A1. Junio 28, **2007**d.

Yuan, X.; Zhang, S.; Liu, J.; Lu, X.; "Solubilities of CO_2 in hydroxyl ammonium ionic liquids at elevated pressures". *Fluid Phase Equilibria*, **2007**, *257*, 195-200.

Zhang, X.; Hun, F.; Liu, Z.; Wang, W.; Shi, W.; Maginn, E.J.; "Absorption of CO_2 in the ionic liquid tris(pentafluoroethyl)trifluorophosphate ([hmim][FEP]): A

molecular view by computer simulations". *The Journal of Physical Chemistry B* **2009**, *113*, 7591-7598.

Zhang, X.; Liu, Z.; Wang, W.; "Screening of ionic liquids to capture CO_2 by COSMO-RS and experiments". *AIChE Journal* **2008**, *54 (10)*, 2717-2728.

Zhang, Y.; Zhang, S.; Lu, X.; Zhou, Q.; Fan, W.; Zhang, X. "Dual amino-functionalised phosphonium ionic liquids for CO_2 capture". *Chemistry: A European Journal* **2009**, *15*, 3003-3011.

Zhao, H. "Methods for stabilizing and activating enzymes in ionic liquids—a review". *Journal of Chemical Technology & Biotechnology* **2010**, *85*, 891–907.

ANEXO I.
Publicaciones

Publicación 1:

Palomar, J.; Gonzalez-Miquel, M.; Polo, A.; Rodriguez, F. **Understanding the physical absorption of CO_2 in ionic liquids using COSMO-RS method.** *Industrial & Engineering Chemical Research*, **2011**, *50*, 3452-346.

I&EC research
Industrial & Engineering Chemistry Research

ARTICLE

pubs.acs.org/IECR

Understanding the Physical Absorption of CO_2 in Ionic Liquids Using the COSMO-RS Method

Jose Palomar,*[,†] Maria Gonzalez-Miquel,[‡] Alicia Polo,[†] and Francisco Rodriguez[‡]

[†]Sección de Ingeniería Química, Departamento de Química Física Aplicada, Universidad Autónoma de Madrid, Cantoblanco, 28049 Madrid, Spain

[‡]Departamento de Ingeniería Química, Universidad Complutense de Madrid, 28040 Madrid, Spain

Supporting Information

ABSTRACT: The quantum chemical Conductor-like Screening Model for Real Solvents (COSMO-RS) method was evaluated as a theoretical framework to computationally investigate the application of room temperature ionic liquids (ILs) in absorptive technologies for capturing CO_2 from power plant emissions to efficiently reduce both experimental efforts and time consumption. First, different molecular models to simulate ILs and computational methods in geometry calculations were investigated to optimize the COSMO-RS capability to predict Henry's Law coefficients using a demanding solubility sample test with 35 gaseous solute-IL systems and 20 CO_2−IL systems. The simulation results were in good agreement with experimental data, indicating that using an ion-pair molecular model optimized in a gas-phase environment allows a finer COSMO-RS description of the IL structure influence on the CO_2 and other solutes solubilities. Moreover, the COSMO-RS methodology was used for the first time to achieve a deeper insight into the behavior of the solubility of CO_2 in ILs from a molecular point of view. For this purpose, further analyses of the energetic intermolecular interactions between CO_2 and ILs were performed by COSMO-RS, revealing that the van der Waals forces associated with the solute in the liquid phase determine the absorption capacity of CO_2 in ILs, which is measured in terms of Henry's Law coefficients. These findings were finally driven by a rational screening over 170 ILs with COSMO-RS to design new ILs that enhance CO_2 capture by physical absorption.

1. INTRODUCTION

There is growing concern that greenhouse gases are contributing to global climate change, and anthropogenic CO_2 emissions from fossil fuel power plants are being regarded as the main cause. Current CO_2 capture postcombustion technologies are based on chemical absorption methods employing aqueous solutions of amines, which involve several concerns, such as their corrosive nature and volatility, leading to high operational cost and environmental impact.[1] Therefore, it is necessary to develop absorption technologies using novel solvents capable of capturing CO_2 and overcoming the drawbacks associated with amine-based systems.

Room-temperature ionic liquids (ILs) are a broad category of organic salts that are typically liquid in their pure state, which have been regarded as potential environmentally benign solvents because of their unique properties, most notably their negligible vapor pressure. Moreover, an important feature associated with ILs is the possibility to design ones with the necessary properties for a specific application by tuning the structures of the ions, which has led to the term "designer solvents". Owing to these novel properties, ILs have generated significant interest across a wide variety of engineering applications,[2] with their use as media for CO_2 capture appearing specially promising.[1,3−6]

The use of ILs as solvents for CO_2 absorption has been of great interest in recent years, and much work is being carried out to explain the behavior of CO_2−ILs systems.[3−6] Studies regarding the effect of process conditions on the solubility of CO_2 in ILs have shown that the temperature has significant impact on the gas solubility, with decreasing solubilities as the temperature increases from 298 to 500 K.[7,8] The effect of pressure on CO_2 solubility has been measured at pressures from atmospheric to 32 MPa, finding that the gas solubility rapidly increased at low pressure, slowly increased above the pressures of 8 to 10 MPa and finally leveled off at approximately 30 MPa.[9] Apart from the process conditions, the nature of the anion seems to be the main factor dominating the dissolution of CO_2 in ILs, while cations are believed to play a secondary role.[10] The effect of the anion on gas solubility has been reported for different imidazolium-based ILs that contain anions such as tetrafluoroborate (BF_4^-),[9−15] hexafluorophosphate (PF_6^-),[9−12,14−18] bis(trifluoromethylsulfonil)-imide (NTf_2^-),[10,15,18−23] dicyanamide (DCN^-),[12] nitrate (NO_3^-),[13] trifluoromethanesulfonate ($CF_3SO_3^-$)[13,18,24] or a series of sulfates,[14,17] phosphates,[25] and acetates,[26] and results suggest that the anions containing fluorinated alkyl groups increase CO_2 solubility. Further screenings and experimental researches have demonstrated the capability of ILs containing increased fluoroalkyl chains, such as fluorinated phosphate anions (FEP), to improve CO_2 solubility in relation to the less fluorinated ILs previously studied.[27−29] Regarding the effect of the cation on CO_2 solubility, it is well agreed that a longer alkyl chain on an imidazolium ring is generally associated with a

Received: July 23, 2010
Accepted: January 21, 2011
Revised: January 5, 2011
Published: February 15, 2011

dx.doi.org/10.1021/ie101572m | *Ind. Eng. Chem. Res.* 2011, 50, 3452–3463

slightly higher solubility.[2,21,22,30] Although most of the ILs studied are based on imidazolium salts,[31] other cations, such ammonium,[32] phosphonium,[33] pyrrolidinium,[10,33,34] or thiouronium,[28] have also been studied, indicating that changing the cation has little effect on gas solubility.[10,28]

Considering the huge variety of theoretically possible ILs, predictive models capable of estimating the equilibrium thermodynamic properties are useful in the selection of ILs for specific applications. Several methods have been reported to predict the thermodynamic behavior of CO_2−ILs systems, such as Equation of States (EOS),[35,36] Group Contribution Models (GCM),[37] or Activity Coefficient Models (ACM).[38] However, the parameters of those models must be estimated using large quantities of experimental data. Considering the still scarcely available experimental data, it is of interest to devise methods by which the equilibrium thermodynamic properties can be estimated from structural information of the compounds. Molecular simulations based on physically founded models, such as COSMO-RS, have been largely applied as valuable tools to predict the physical and thermodynamic properties of ILs; their main advantage is that of providing a fundamental understanding at the molecular level.[39] The COSMO-RS (Conductor-like Screening Model for Real Solvents) method predicts the thermodynamic properties of mixtures on the basis of unimolecular quantum chemical calculations for the individual molecules.[40] COSMO-RS provides a unique a priori computational tool for designing ILs with specific properties.[41,42] Several publications have demonstrated the general suitability of the a priori COSMO-RS method to predict the properties of IL systems, such as density,[43] vapor pressure,[44] activity coefficients,[45−47] excess properties,[48,49] and phase equilibrium data (VLE,[49−54] LLE,[55−62] and SLE[63,64]). Very recently, the COSMO-RS method was used to evaluate the gas solubility of CO_2 and other gases in ILs[28,65] and in traditional solvents.[66−68] Thus, Zhang et al.[28] successfully performed a screening method of the Henry's Law constant of CO_2 in 408 ILs (imidazolium, pyrrolidinium, pyridinium, guanidinium, isouranium, and phosphonium) by COSMO-RS, selecting as a result three [FEP]-based ILs with optimized capacities for CO_2 absorption, which were afterward experimentally evaluated. The COSMO-RS method was additionally validated using the experimental data of [bmim][PF_6] and [bmim][BF_4] compounds at different temperatures. In addition, Rooney et al.[65] performed a detailed and systematic assessment of the predictive capacity of the COSMO-RS method for calculating gas solubility in ILs by changing the cation and anion constituting the IL, the solute, and the conditions of temperature and pressure. The results demonstrated that the a priori COSMO-RS method provided a qualitatively good prediction of gas solubility data in ILs without prior experimental knowledge of the compound's properties. In summary, previous works have stated the potential of the COSMO-RS computational approach to design suitable ILs for CO_2 capture technologies, such as physical absorption or membrane separation.

The standard procedure of COSMO-RS calculations consists of two major steps: (1) quantum chemical COSMO calculations for the molecular species involved and (2) COSMO-RS statistical calculations performed within the COSMOthermX program. In the first step, the geometries of the compound structures (i.e., gas solutes and ILs) are optimized at high-level quantum-chemical calculations. In this respect, the literature shows no general agreement on the best molecular model to simulate IL solvents with COSMO-RS. In most studies, mainly because of the computational simplicity, a molecular model of independent counterions ([C+A] model) was applied in the COSMO-RS calculation, in which ILs are treated as equimolar mixtures of cations and anions. A different computational approach considers the ion-paired structure ([CA] model) to simulate the IL compound, which is significantly more computationally demanding but includes the effects of counterion interactions in the calculations. Furthermore, the optimization of the geometry of ion-paired or ionic structures by quantum chemical calculations can be performed using the continuum solvation COSMO model or assuming a gas phase environment for the species. On the other hand, regarding the COSMO-RS statistical calculation step for gas−liquid equilibrium data, previous studies[65,68] showed that the predictive capability of COSMO-RS for gas solubility is clearly dependent on the correct description of the vapor pressure for the solutes. Vapor pressure in COSMOtherm can either be estimated using the gas-phase energy information (held in an *.energy file) or by using experimental data (through the semiempirical Antoine or Wagner equations). In general, the use of experimental vapor pressure to predict gas solubility is preferred when the system temperature is below or approximately equal to the critical temperature, whereas the energy value estimated by COSMO-RS is more accurate when the system temperature is much greater than the critical temperature.[66,68] However, Rooney et al.[65] concluded that COSMO-RS prediction of the gas solubility and the Henry's law constant of CO_2 in ILs and in common solvents is improved by using the energy value rather than the vapor pressure data in the calculations.

In summary, the literature has reported a variety of alternatives to perform COSMO-RS calculations of IL-based systems and some limitations regarding the definition of the gas phase (solute) and solvent phase for gas solubility predictions in ILs. For these reasons, the first aim of this study was to develop further optimization of the COSMO-RS approach to improve the prediction of gas solubility in ILs, with special attention to the case of the CO_2 solute. For this purpose, we evaluated the predictive capability of the COSMO-RS model using four different computational approaches ($[C+A]_{GAS}$, $[C+A]_{COSMO}$, $[CA]_{GAS}$, and $[CA]_{COSMO}$ models) through a comparison with experimental Henry's Law constants reported in the literature, including a wide sample data set of 20 different gases and 20 different ILs. The second objective of this work was to achieve a deeper insight into the CO_2 solubility behavior in ILs by using the COSMO-RS methodology to understand the role of the anion and cation nature on physical CO_2 absorption. For this purpose, the Henry's Law coefficient of CO_2 in ILs was successfully related to the excess enthalpy of CO_2−IL mixtures in solution predicted by COSMO-RS. The intermolecular interactions (electrostatic, hydrogen bonding, and van der Waals) between CO_2 and IL compounds in the liquid phase, quantified by COSMO-RS, were analyzed to contribute to the rational selection of ILs with favored characteristics for CO_2 separation. Finally, from a chemical engineering perspective, the COSMO-RS approach was tentatively used to design new ILs for CO_2 capture technology, which resulted from a computational screening over a wide number of IL compounds (imidazolium, pyridinium, pyrrolidinium, quinolinium, ammonium, phosphonium, and thioronium), including those with enhanced absorption capacity by bromination of the anion.

2. COMPUTATIONAL DETAILS

The COSMO-RS calculations were performed using four different computational approaches ($[C+A]_{GAS}$, $[C+A]_{COSMO}$,

$[CA]_{GAS}$, and $[CA]_{COSMO}$), following the steps of the standard method. First, the molecular geometry of all the molecular models (solutes and IL structures) was optimized using the quantum chemical Gaussian03 package.[69] In each case, vibrational frequency calculations were performed to confirm the presence of an energy minimum. The [C+A] and [CA] models used independent counterions and ion-paired structures, respectively, to simulate IL compounds in the COSMO-RS calculations. The GAS subscript denotes that the quantum-chemical geometry optimization of the chemical structures was performed in the ideal gas-phase at the B3LYP/6-31++G** computational level, whereas the COSMO subscript indicates that the optimization was performed using the continuum solvation COSMO model at the BVP86/TZVP/DGA1 computational level. Once the molecular models were optimized, Gaussiano03 was used to compute the COSMO files. The ideal screening charges on the molecular surface for each species were calculated by the continuum solvation COSMO model using the BVP86/TZVP/DGA1 level of theory. Subsequently, the COSMO files were used as an input in the COSMOthermX[70] code to calculate the thermodynamic properties (Henry's Laws constant and solubility of gaseous solutes in ILs, excess enthalpy of CO_2−IL mixtures and molecular volumes of ILs). According to our chosen quantum method, we used the corresponding parametrization (BP_TZVP_ C21_0108) that is required for the calculation of physicochemical data and that contains the intrinsic parameters of COSMOtherm.

The value of the pure compound's vapor pressure required for the calculation of the gas solubility was estimated either by COSMOthermX using the gas-phase energy information (held in an *.energy file) or by using experimental data through the Wagner correlation (held in a *.vap file). The experimental values of the pure CO_2 vapor pressures were used to determine the more accurate methodology to describe the solubility of the solute in ILs as a function of temperature.

A wide range of experimental values of Henry's Law coefficients in ILs has been collected from the IUPAC database[71] and recent publications (see Supporting Information, Tables S2 and S3). To increase the statistical evaluation of the four COSMO-RS approaches, data from more than 50 gas-IL systems, including 20 different gases (alkanes, alkenes, fluoroalkanes, SO_2, C_6H_6, and CO_2 solutes) and 20 different ILs (imidazolium, pyrrolidinium, and thioronium) were included in the analysis. The list and the abbreviations for each IL used herein are summarized in Supporting Information, Table S1.

The uncertainties in the gas solubility estimated by the different COSMO-RS approaches were determined by calculating the mean prediction error (MPE), as defined by eq 1:

$$\mathrm{MPE} = \frac{1}{N}\sum_{1}^{N}\frac{|K_H{}^{\mathrm{calc}} - K_H{}^{\mathrm{exp}}|}{K_H{}^{\mathrm{exp}}}\cdot 100 \qquad (1)$$

where N is the total number of data points used, $K_H{}^{\mathrm{calc}}$ is the Henry's Law constant calculated for a given IL at a given temperature, and $K_H{}^{\mathrm{exp}}$ is the corresponding value obtained from the experimental work reported previously.

3. RESULTS

3.1. Optimization of COSMO-RS Approach to Predict Henry's Law Constants of CO_2 in ILs. To optimize the capability of COSMO-RS to predict gas solubility in ILs, four different computational approaches ($[C+A]_{GAS}$, $[C+A]_{COSMO}$, $[CA]_{GAS}$, and $[CA]_{COSMO}$) to describe the IL solvent's nature were evaluated. The calculated Henry's Law coefficients, as a measure of gas solubility, were compared to the experimental data reported in the literature for a wide sample set that contained a variety of solutes (20) and ILs (20), which constitute demanding test cases for the predictive model.

Table 1. Statistical Results Obtained from the Comparison of Experimental and Predicted Henry's Law Constants (N = 35) of Common Solutes in ILs Using Different COSMO-RS Computational Approaches

	linear regression[a]				
model	A	B (Slope)	R^2	SD	MPE (%)
$[C+A]_{GAS}$	−0.14	0.91	0.95	0.035	31
$[C+A]_{COSMO}$	−0.26	0.86	0.93	0.040	34
$[CA]_{GAS}$	−0.37	0.96	0.95	0.038	33
$[CA]_{COSMO}$	−0.21	0.92	0.96	0.034	27

[a] $\mathrm{Ln}(1/K_H{}^{\mathrm{exp}}) = A + B\cdot\mathrm{Ln}(1/K_H{}^{\mathrm{COSMO\text{-}RS}})$

First, a general evaluation of the capability of the four COSMO-RS approaches to predict the solubility of gases in imidazolium-based ILs was performed by calculating the Henry's Law constants of 35 different solute-IL systems, including [bmim][BF_4], [bmim][PF_6], [emim][NTf_2], and [hmim][NTf_2], at near-ambient temperature (See Supporting Information, Figure S1 and Table S2). The experimental and calculated values were fitted by linear regression, and the results are reported in Table 1. Statistical analysis indicates that both the $[C+A]_{GAS}$ and $[C+A]_{COSMO}$ models tested are capable of qualitatively predicting the trend of Henry's Law constants of a great number of compounds (including alkanes, alkenes, fluorohydrocarbons, benzene, SO_2, and CO_2) in ILs. The results in Table 1 suggest that the computational approach using independent ionic structures optimized in the gas phase, the $[C+A]_{GAS}$ model, predicts gas solubility values that are in slightly better agreement with the experimental data (Slope = 0.91, $R^2 \approx 0.95$, and MPE = 31%) than those predicted using the continuum solvation COSMO method in the geometry optimization, that is, $[C+A]_{COSMO}$ model (Slope = 0.86, $R^2 \approx 0.93$, and MPE = 34%). In addition, the statistical results reported in Table 1 substantiate a sufficient accuracy as a whole for both IL molecular models of ion-paired structures, $[CA]_{GAS}$ and $[CA]_{COSMO}$, showing that the slopes and R^2 coefficients of the linear regressions improve slightly from the [C+A] model to the [CA] model. However, it should be noted that the four COSMO-RS approaches provide similar good capability to predict Henry's Law constants for a wide range of values for 35 gas-IL systems, including polar and non-polar solutes and imidazolium-based ILs with different anions.

The next purpose was to evaluate with more detail whether the molecular models implemented in COSMO-RS are able to describe the modification of the CO_2 solubility caused by the variation of the IL. Thus, the Henry's Law constants of CO_2 in 20 different ILs constituted by a variety of cations (12) and anions (6) were predicted by the COSMO-RS model and compared with the available experimental data, as shown in Figure 1 and Supporting Information, Table S3. An overall suitability of the four COSMO-RS approaches describing the tendencies of the CO_2 solubility in ILs, when either the nature of the cation or anion was modified, was observed in general good agreement

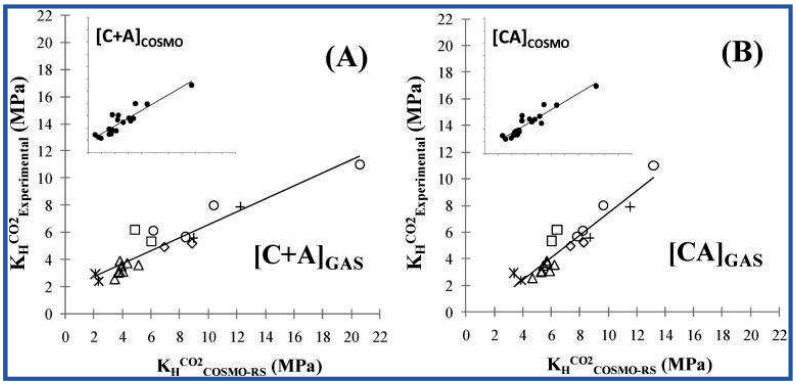

Figure 1. Comparison between the experimental and COSMO-RS-predicted Henry's law constants of CO_2 in ILs [* FEP^-, Δ NTf_2^-, □ PF_6^-, ◇ $CF_3SO_3^-$, ○ BF_4^-, + DCN^-] at near-ambient temperature, employing (A) $[C+A]_{GAS}$ and $[C+A]_{COSMO}$ models and (B) $[CA]_{GAS}$ and $[CA]_{COSMO}$ models.

with previous COSMO-RS studies.[28,65] Clearly from Figure 1, the interaction between the CO_2 molecules and the anion groups is the dominating factor in determining the K_H behavior in ILs, following the anion order of experimental CO_2 solubility in IL: $[FEP]^-$ > $[NTf_2]^-$ > $[CF_3SO_3]^-$ > $[PF_6]^-$ > $[BF_4]^-$ > $[DCN]^-$. Regarding the cation effect on K_H values, a longer alkyl chain on the imidazolium ring is generally associated with a slightly higher solubility, whereas the different head groups [imidazolium, pyrrolidinium, and thioronium] play a minor role in the CO_2 solubility. As it was stated in the literature,[27] the fluorination of anions ($[FEP]^-$ as example) or cations ($[C_8F_{13}H_4mim]^+$ as example) favors CO_2 dissolution in ILs, and it has been successfully used to improve the "CO_2-philicity" of ILs, whereas the presence of a polar group (as OH^-) in an IL decreases the CO_2 solubility in ILs (see Supporting Information, Table S3). The statistical results regarding the predictability of K_H constants for the four COSMO-RS approaches are summarized in Table 2. It should be noted that the best linear regression fit between the experimental and COSMO-RS calculated data was provided by the $[CA]_{GAS}$ model, with the slope closest to one (Slope = 0.84), the highest correlation coefficient ($R^2 \approx 0.88$), and the lowest standard deviation (SD = 0.79). Therefore, we conclude that the simulation of ILs with the counterion interactions by ion-paired structures, the [CA] models, described more accurately the effect of the anion and the cation on the CO_2 solubility in IL solvents. This conclusion is in agreement with that achieved by the molecular dynamic simulation, which evidenced somewhat cooperative behavior between the cation and the anion to capture CO_2.[29] In fact, we found that the COSMO-RS method using the $[CA]_{GAS}$ model adequately predicts the exceptions reported in the good behavior of the COSMO-RS predictability using the $[C+A]_{COSMO}$ model:[28,73] (i) the effect of substitution at the C(2) position on the imidazolium ring on gas solubility (Henry's Law coefficients at 298.13 K[83]: [Bmmim][PF_6] (Exp./Calc.): 6.2/6.4 > [Bmim][PF_6] (Exp./Calc.): 5.3/6.0); and (ii) the effect of changing the cation family on the K_H values from ammonium to pyrrolidinium to imidazolium at 298.4 K[21] ([Bmim][NTf_2] (Exp./Calc.): 3.70/5.6> [Bmpyrr][NTf_2] (Exp./Calc.): 3.9/5.7) > [N_{4111}][NTf_2] (Exp./Calc.): 3.25/5.4). However, it is noticeable that the $[CA]_{GAS}$ model showed the highest mean prediction error (MPE = 49%) because of a systematic overestimation of ~2 MPa in the Henry's Law coefficient values for the cases studied, which significantly influences the prediction error in the range of low K_H values. Yet, the $[C+A]_{GAS/COSMO}$ models generally provide higher accuracy in the quantitative prediction of K_H coefficients in ILs (MPE < 35%), especially in the low K_H value range, whereas $[C+A]_{GAS/COSMO}$ provided larger deviation with increasing K_H of CO_2 in ILs (see Figure 1).

Table 2. Statistical Results Obtained from the Comparison of Experimental and Predicted Henry's Law Constants (N = 20) of CO_2 in ILs Using Different COSMO-RS Computational Approaches

		linear regression[a]			
model	A	B (Slope)	R^2	SD	MPE (%)
$[C+A]_{GAS}$	1.76	0.48	0.87	0.82	33
$[C+A]_{COSMO}$	1.79	0.64	0.84	0.92	20
$[CA]_{GAS}$	−0.95	0.84	0.88	0.79	49
$[CA]_{COSMO}$	0.69	0.65	0.87	0.81	34

[a] $K_H^{exp} = A + B \cdot K_H^{COSMO\text{-}RS}$

Studies regarding the effect of temperature on the solubility of CO_2 in ILs have shown that Henry's Law constants vary with temperature by using an Arrhenius relationship. The four COSMO-RS computational approaches were evaluated in this study to determine if they were able to predict this trend. The standard procedure in the COSMOtherm software to calculate Henry's Law constants used the gas-phase energy information of the compounds held in *.energy files. Figure 2A compares the standard calculated K_H values in [hmim][NTf_2] to those of the experimental values reported in the literature at the 283.1−343.1 K temperature range. As can be seen, the four computational approaches provide a qualitative description of the solubility-temperature trend of CO_2 in ILs. In agreement with the aforementioned conclusions, the [C+A] models provide a more quantitative prediction of K_H values in the entire temperature range studied. Alternatively, Henry's Law constants can be estimated from the COSMO-RS calculation using the semiempirical Wagner equation to estimate the vapor pressure in the expression:

$$K_H = \gamma_i^{\infty} p_o^{vap} \quad (2)$$

where K_H, γ_i^{∞}, and p_o^{vap} are the Henry's Law constant, the activity coefficient at infinite dilution, and the vapor pressure of the

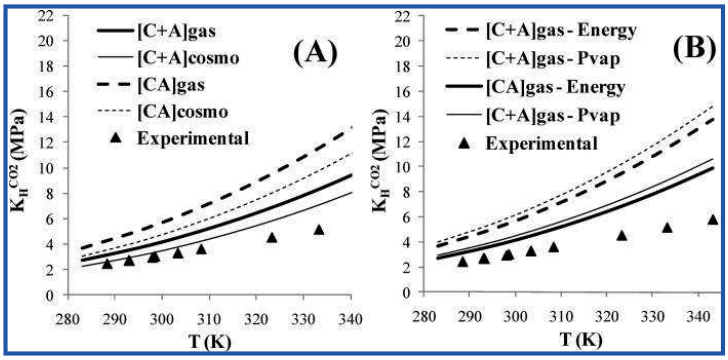

Figure 2. Comparison between the experimental and predicted Henry's law constants of CO_2 in [hmim][NTf_2] IL as a function of temperature, using for the COSMO-RS calculations: (A) energy file and (B) vapor pressure from the Wagner equation extrapolation.

pure gas, respectively. As is shown in Figure 2B for the example of [hmim][NTf_2] using the $[CA]_{GAS}$ and $[C+A]_{GAS}$ models in the COSMO-RS calculations, the K_H predictions are more accurate using the energy data rather than the p_o^{vap} values from the Wagner equation extrapolation. This general conclusion was achieved in the current analyses regardless of the ILs studied or the computational model used in the COSMO-RS calculations.

In summary, the results obtained show the capability of the four COSMO-RS computational approaches implemented to qualitatively predict the Henry's Law constants of CO_2 in ILs. In other words, the molecular model ([CA]/[C+A]) used to simulate the IL solvents or the environmental phase (GAS/SOLVENT) applied to the quantum-chemical optimization of the IL structures does not significantly influence the COSMO-RS predictions of the gas−liquid equilibrium data for IL systems, which is in contrast with the evidence reported for liquid−liquid and vapor−liquid−solid equilibria.[19,27] Nevertheless, it has been illustrated here that including the cation−anion interactions in the calculation for the ion-paired molecular model for IL species in the environmental phase, $[CA]_{GAS}$, allows a finer description of the IL's structural influence on the CO_2 solubility reported in the literature.

3.2. Analysis of CO_2 Solubility in ILs by COSMO-RS Methodology. The experimental variation of the Henry's Law constants of CO_2 in ILs with temperature has been used in the literature[28,58,65] to estimate the thermodynamic properties (Gibbs energy, enthalpy, and entropy) of solvation, which can be regarded as a good approximation for the thermodynamic solution parameters of gaseous solutes at low pressure. The results showed spontaneous absorption phenomena of CO_2 in ILs, exhibiting negative enthalpies of solution corresponding to an exothermic solvation behavior. The enthalpy of the physical CO_2 sorption is typically −10 to −20 kJ/mol for ILs. In fact, the empirically estimated heat of absorption, $\Delta_{sol}H^{\infty}$, seemed to gradually increase with the gas solubility of CO_2 in ILs for the anion series ([bmim][NTf_2]: −18 kJ/mol > [bmim][PF_6]: −16.1 > [bmim][DCN]: −15.0 kJ/mol).[72] Regarding the use of the molecular simulation in the energetic description of CO_2 absorption phenomena in ILs, Rooney et al.[65] demonstrated that K_H predictions by COSMO-RS of CO_2 in ILs at different temperatures can be successfully used to estimate $\Delta_{sol}G^{\infty}$, $\Delta_{sol}H^{\infty}$, and $\Delta_{sol}S^{\infty}$, with a relative absolute deviation of approximately 20%. In addition, Yokozeki et al.[73] used the thermodynamic excess Gibbs and enthalpy functions, estimated by an EOS model, to classify whether the absorption of CO_2 by ILs was of the physical or chemical type.

In this work, we hypothesize the potential relationship between the Henry's Law constant of CO_2 in ILs and the energy balance between the solute−solvent, solvent−solvent, and solute−solute interactions in the liquid mixture given by the excess enthalpy, H_m^E. The COSMO-RS method can be used to predict the excess enthalpy of a CO_2−IL liquid mixture, H_m^E, by summing the contribution of each component of the mixture, according to the expression:

$$H_m^E = x_{IL}\cdot H_{IL}^E + x_{CO2}\cdot H_{CO2}^E = x_{IL}\cdot[H_{IL,\,mixture} - H_{IL,\,pure}] + x_{CO2}\cdot[H_{CO2,\,mixture} - H_{CO2,\,pure}] \quad (3)$$

To analyze the possible relationship between the CO_2 solubility in ILs and the excess molar enthalpy of CO_2−IL mixtures, the COSMO-RS method was applied by using the $[CA]_{GAS}$ model to calculate the H_m^E values of the CO_2−IL mixtures at CO_2 concentrations corresponding to the solubility data in ILs at 298 K and 1 atm. Thus, Figure 3A compares the Henry's Law constants of CO_2 in 25 imidazolium-based ILs to the corresponding H_m^E calculated by the COSMO-RS/$[CA]_{GAS}$ approach at the temperature of 298.1 K (see Supporting Information, Table S4). As can be seen from the results, higher solubilities (decreasing K_H values) of CO_2 in ILs are associated with a higher exothermicity of the mixture, whereas low absorptions were found when the excess enthalpy for the CO_2−IL liquid mixtures was close to zero. To obtain a more realistic simulation of the solution of the gas compound in the liquid phase, we have considered canceling the term $H_{co2,pure}$ in eq 3 because the intermolecular interactions between the CO_2 molecules in the gas phase can be reasonably considered negligible with respect to the interactions in the liquid phase ($H_{co2,mixture} \gg H_{co2,pure}$). As a result, a more consistent expression for the excess enthalpy of the mixture, $H_m^{E'}$, to analyze CO_2 solubility in ILs would be as follows:

$$H_m^{E'} = x_{IL}\cdot H_{IL}^E + x_{CO2}\cdot H_{CO2}^{E'} = x_{IL}[H_{IL,\,mixture} - H_{IL,\,pure}] + x_{CO2}\cdot[H_{CO2,\,mixture}] \quad (4)$$

Figure 3B presents the relationship between the calculated K_H and $H_m^{E'}$ values of several representative imidazolium-based ILs with different anions and lengths of alkyl chain, which

dx.doi.org/10.1021/ie101572m |*Ind. Eng. Chem. Res.* 2011, 50, 3452–3463

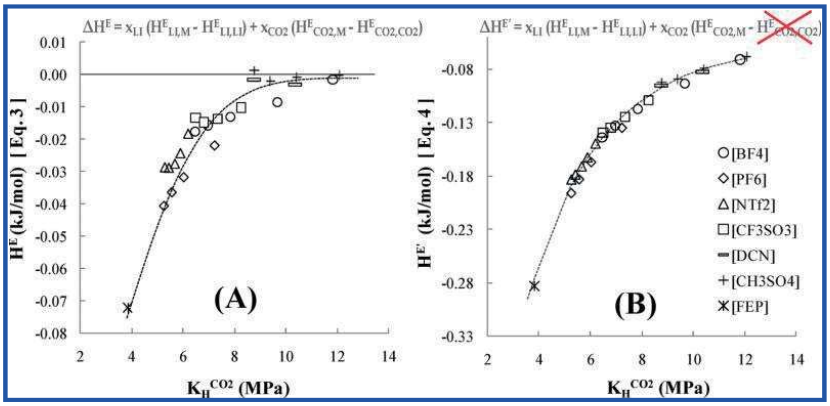

Figure 3. Comparison of Henry's law constants with the excess molar enthalpies of CO_2 in ILs at $T = 298.1$ K, calculated by the COSMO-RS/$[CA]_{GAS}$ computational approach using (A) eq 3 and (B) eq 4.

would be mathematically summarized by a quadratic regression model:

$$\mathrm{Log}[K_H] = 1.35 + 4.84 \cdot H_m^{E\prime} + 7.70 \cdot (H_m^{E\prime})^2$$
$$R^2 = 0.98 \qquad \mathrm{SD} = 0.017 \qquad (5)$$

An additional advantage of the COSMO-RS method is that it provides enthalpy estimations for the different intermolecular interactions [electrostatic (*Misfit*), van der Waals and hydrogen bonding] between the components of the mixture in the fluid phase. Therefore, as a relevant contribution, COSMO-RS was used to introduce the physicochemical solute−solvent and solvent−solvent interactions in the analysis with the aim of better understanding the CO_2 absorption in ILs from a molecular point of view.

The estimations of $H_m^{E\prime}$ in eq 4 by the COSMO-RS model can be also expressed by the sum of three contributions associated with the interactions of polar *Misfit*, hydrogen bonding, and van der Waals forces:

$$H_m^{E\prime} = H_m^{E\prime}(H\text{-}Bond) + H_m^{E\prime}(Misfit) + H_m^{E\prime}(VdW) \qquad (6)$$

Therefore, the COSMO-RS method can be tentatively used to analyze the Henry's Law coefficients of CO_2 in ILs in terms of the different intermolecular interactions of the solute−solvent contributions to the $H_m^{E\prime}$ values of the CO_2−IL systems reported in Figure 3B. Figure 4 illustrates that the van der Waals and electrostatic interactions, quantified by $H_m^{E\prime}(VdW)$ and $H_m^{E\prime}$-*(Misfit)*, determine the gas solubility of CO_2 in a series of more than 20 imidazolium-based ILs, evaluating such solubility in terms of Henry's Law constants at 298 K. Figure 4 shows that the dominant interaction is from the van der Waals forces, which contribute to the exothermicity of the CO_2−IL mixtures and, consequently, increase the solubility of the solute gas in the liquid phase. On the contrary, the electrostatic interactions (*Misfit*) between CO_2 and IL are repulsive, but the role of this contribution is minor for the IL series included in Figure 4. Finally, hydrogen-bonding interactions make negligible contributions to the excess values $H_m^{E\prime}$ of eq 6.

Previous molecular dynamic (MD) simulations[29,38,74] that were carried out to predict the CO_2 absorption isotherms in [hmim][FEP], [hmim][NTf_2], and [hmim][PF_6] ILs provided

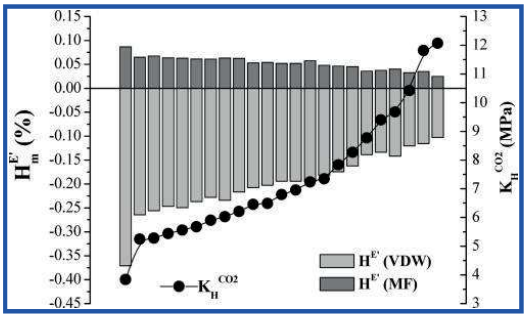

Figure 4. Comparison of the Henry's law constants with interaction energy contributions to excess molar enthalpies given by eq 6 for CO_2−IL mixtures at $T = 298.1$ K, calculated by the COSMO-RS/$[CA]_{GAS}$ computational approach.

similar conclusions to the current COSMO-RS analysis for a much higher number of different ILs. In these previous works, the good performance of [hmim][FEP] for CO_2 capture was mainly ascribed to the van der Waals contribution to the total interaction energy between the solute and solvent molecules, whereas electrostatic interactions contributed to a less extent.[29,38] In contrast to the COSMO-RS results, MD studies provided exothermic contributions for the electrostatic solute−solvent interaction to the energy. Interestingly, however, the MD results indicated that the CO_2 solubility decreases in the same order ($[FEP]^- > [NTf_2]^- > [PF_6]^-$) as the solute-anion electrostatic interactions increase. In fact, experimental evidence shows that the presence of strongly polar anions, such as $CF_3CO_2^-$ or DCN^-, with a high capacity to establish electrostatic interactions, does not improve CO_2 solubility in ILs, but they diminish the solubility with respect to other anions with more delocalized charges, such as [NTf_{2-}] [75,76]. Previous works in the literature do not provide a consistent explanation for the unexpected deviation from Pearson's "hard/soft acid/base" principles; thus, the basic character of the anion in ILs does not enhance the CO_2 physical absorption, even when stronger acid−base interactions between the CO_2 molecules and the anions have become

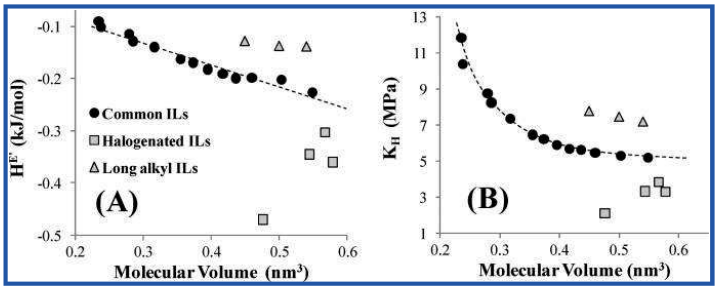

Figure 5. Comparison of (A) excess molar enthalpy for CO_2−IL mixtures given by eq 4 and (B) Henry's law constants of CO_2 in ILs to the molecular volume of ILs; all parameters were calculated at T = 298.1 K by the COSMO-RS/$[CA]_{GAS}$ computational approach.

apparent by spectroscopy.[77,78] This unexpected CO_2 solubility behavior of ILs with strongly basic anions was assigned by the COSMO-RS analysis to the global endothermic contribution of electrostatic solute−solvent/solvent−solvent interactions in CO_2−IL systems. However, the long-range of van der Waals forces between the IL and CO_2 have clear promotional effects on the gas solubility, but they are not able to significantly affect the intramolecular vibrations analyzed by infrared spectroscopy.[78] Recently, Coutinho et al.[79] suggested that the solubility of CO_2 in ILs increases with the increasing size difference between the gas solute and the solvent, assigning the non-ideal CO_2 solution behavior in ILs to the entropic contribution to the Gibbs free energy. Other works also related the larger size and asymmetry of the anion or cation to the capacity of leaving more "free" volume to accommodate CO_2, therefore, increasing the gas solubility in the ILs.[29]

In the following, we examine the possible role of the molecular size of ILs on their Henry's Law coefficients of CO_2 physical absorption. First, Figure 5A compares the COSMO-RS-calculated values of the excess enthalpy $H_m^{E'}$ of CO_2−IL mixtures (eq 4) to the molecular IL volumes for a selected sample with 20 IL compounds (see Supporting Information, Table S5), including an IL series with increased volumes caused by longer alkyl substituents and also by an increase in the number of halogenated atoms in the anion. As can be seen, most of the dispersed common ILs used in the CO_2 absorption studies present a linear relationship between the IL volume and the enthalpy of the interaction of the CO_2−IL mixtures, mainly because increasing the number of atoms in chemical systems always increases the attractive van der Waals intermolecular interactions. However, based on the COSMO-RS results shown in Figure 5A, the addition of alkyl groups increases the molecular volume to a larger extent than increasing the favorable van der Waals interactions reflected by $H_m^{E'}$ values, based on the results for the imidazolium series of alkylsulfate ILs (see Supporting Information, Table S5). In addition, the strong promotion of van der Waals interactions by including halogenated atoms (e.g., chlorine or bromine) in the IL structure clearly increases the exothermicity of the CO_2 and IL mixture because the molecular size of the IL is not linearly increased (see the fluorinated and brominated series reported in Figure 5A). As a consequence of the general linear relationship between $H_m^{E'}$ and V_{IL}, Figure 5B demonstrates that the use of large ILs implies lower Henry's Law coefficients (i.e., favorable impact of the CO_2 solubility) for most cases. However, there are significant exceptions of those ILs with high molecular volumes because of large alkyl chains (which present

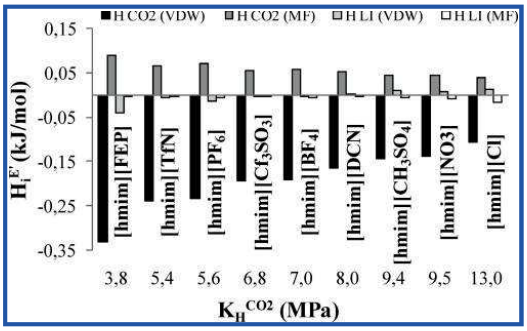

Figure 6. Description of the anion effect on Henry's law constants of CO_2 in ILs at T = 298.1 K using the interaction energy contributions to excess molar enthalpies given by eq 6, calculated by the COSMO-RS/$[CA]_{GAS}$ computational approach.

lower CO_2 solubility than expected based on their V_{IL}) and, on the contrary, those ILs that are strongly halogenated (which present significantly higher CO_2 solubilities than anticipated for their medium size), which deviated from the linear fit between $H_m^{E'}$ and V_{IL} in Figure 5A. We conclude that the COSMO-RS energy analysis consistently described the Henry's Law coefficient for the spontaneous mechanism of CO_2 dissolved in ILs dominated by the exothermic enthalpic effects associated with the attractive van der Waals interactions between the CO_2 solute and ionic species in the IL solvent, whereas the repulsive electrostatic interactions between the solute and the solvent play a minor role in determining the solubility of CO_2 in ILs at infinite dilution. Hydrogen bonding has a negligible effect on the CO_2 physical absorption by ILs based on the COSMO-RS results.

On the basis of the favorable results regarding the hypothesis of relating the $H_m^{E'}$ and K_H thermodynamic parameters in CO_2−IL systems, we analyzed in detail the effect of the chemical structure of ILs on their CO_2 solubility from the view of the intermolecular interaction description provided by the COSMO-RS/$[CA]_{GAS}$ computational approach. The nature of the anion has been demonstrated as the dominating factor in the dissolution of CO_2 in ILs.[3] Figure 6 presents the effect of the anions on the CO_2 solubility for several ILs based on common $[hmim]^+$ cations expressed in terms of K_H values calculated by the COSMO-RS/$[CA]_{GAS}$ method. In good agreement with previous experimental results, the solubilities of CO_2 in ILs are in the order

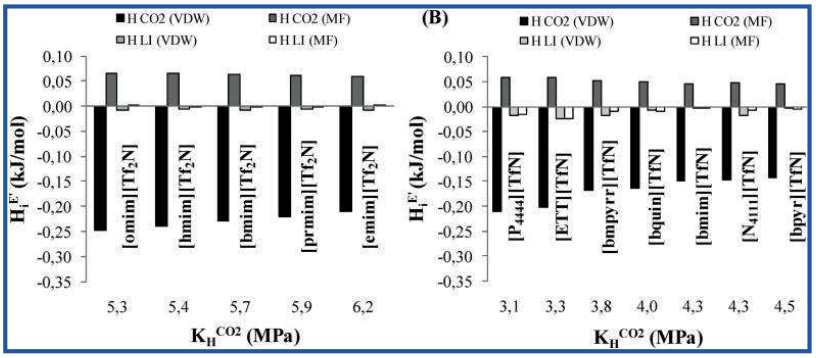

Figure 7. Description of the cation effect on Henry's law constants of CO_2 in ILs at T = 298.1 K using the interaction energy contributions to excess molar enthalpies given by eq 6, (A) Alkyl chain length was calculated by $[C+A]_{GAS}$ and (B) family cation type was calculated by the $[CA]_{GAS}$ computational approach in COSMO-RS.

$[FEP]^- > [NTf_2]^- > [PF_6]^- > [BF_4]^- > [DCA]^- > [CH_3SO_4]^- > [NO_3]^-$, covering a predicted K_H range of ~6 MPa. Figure 6 also presents the van der Waals and misfit interaction contributions of CO_2 and IL components to the excess enthalpy of the mixture given by eq 6. The results obtained illustrate that the solubility behavior described by the Henry's Law constant is mainly controlled by attractive van der Waals interactions between CO_2 and the anion. This conclusion is even more evident when the effect of the fluorination of the anion on the dissolution of CO_2 was analyzed in Figure 6. Thus, we can conclude that the presence of fluorinated entities in the anion improves the "CO_2−philicity" of ILs (solubility order $[FEP]^- > [PF_6]^- > [BF_4]^- > [Cl]^-$) because of the significant increase in the van de Waals interactions. However, Figure 6 shows that the repulsive electrostatic interactions between the anion and CO_2 solute play a secondary role, increasing this contribution with the same order as the van der Waals interactions but with lower quantitative variations. The hydrogen-bonding contributions were not reported in Figure 6 because they were only marginal.

On the other hand, it has also been demonstrated that the cations play a secondary role in the dissolution of CO_2 in ILs. Figure 7A shows for an IL series with the common $[NTf_2]^-$ anion that longer alkyl chains on the imidazolium ring are associated with a slightly higher solubility, expanding the K_H range by only 1 MPa for the solubility series $[omim]^+ > [hmim]^+ > [bmim]^+ > [prmim]^+ > [emim]^+$. Similar to the anion effects discussed, when the van der Waals contribution to the excess enthalpy of the CO_2−IL mixture is more negative, the solubility of CO_2 in IL is the higher but observes a lower variation in $H_{co2}^{E'}(VdW)$ with the cation alkyl chain than with the anion nature. The repulsive electrostatic interactions between the cation and CO_2 remain almost unaffected by the alkyl chain length of the cation. Additionally, the experimental[23,27] data displayed a minor influence of the cation family type on CO_2 solubility. Figure 7B shows the effect of the different cation type on the K_H values predicted by the COSMO-RS/$[CA]_{GAS}$ method for the IL series with a common $[NTf_2]^-$ anion. As can be seen, the CO_2 solubility covers a narrow K_H range from the most favorable types of cations (phosphonium and thioronium) to the least favorable type (pyridinium), which is in fairly good agreement with available experimental evidence.[10,28] Identical to previous results, the different CO_2 solubility capacities of the ILs included in

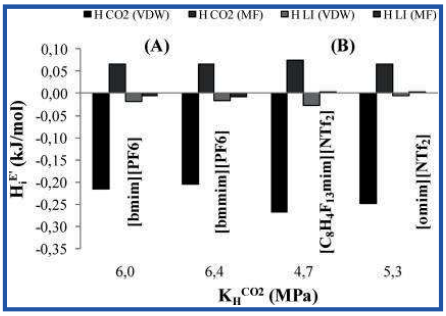

Figure 8. Description of the cation substituent effects [(A) Alkyl group at the C2 position and (B) Fluoroalkyl chain] on the Henry's law constants of CO_2 in ILs at T = 298.1 K using the interaction energy contributions to excess molar enthalpies given by eq 6, calculated by the COSMO-RS/$[CA]_{GAS}$ computational approach.

Figure 7B should be mainly ascribed to the contrary effects of attractive (van der Waals) and repulsive (electrostatic) intermolecular interactions between the ionic species of the IL and CO_2 solute. Regarding the cation substituent effects on the cation, it has been demonstrated that the substitution of the proton by a methyl group at the C2 position of the imidazolium ring slightly diminishes the CO_2 solubility, which is explained in terms of intermolecular interactions in Figure 8A. In addition, the fluorination of the alkyl chains of the cation has the same influence as that observed in the anions, as shown in Figure 8B, decreasing the K_H constant (higher solubility) from $[C_8H_4F_{13}mim][NTf_2]$ to $[omim][NTf_2]$. Again, these fluorination effects were mainly related to additional van der Waals interactions between the IL and CO_2 compounds. COSMO-RS provided the $H_{CO2}^{E'}(VdW)$ contribution of −0.33 kJ/mol for [hmim][FEP] (with 15 atoms of F) with respect to −0.27 kJ/mol for $[C_8H_4F_{13}mim][NTf_2]$, which explains the higher CO_2 solubility reported in the former IL.

In summary, these findings show that CO_2 solubility in ILs, described in terms of the infinite dilution K_H property, originates from intermolecular interactions of different natures, with the van der Waals forces between the solute and IL atoms being the dominating factor contributing to CO_2 physical absorption by ILs. As a consequence, the COSMO-RS analysis contributes to

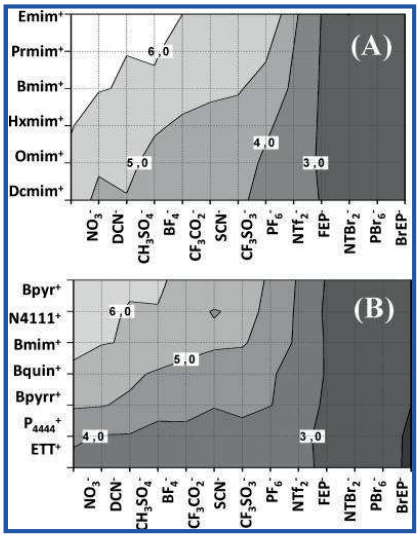

Figure 9. Screening of Henry's law constants of CO_2 in 170 ILs [(A) Imidazolium and (B) different cation family] at T = 298.1 K calculated by the COSMO-RS/$[C+A]_{GAS}$ computational approach (values corrected by the experimentally calculated linear correlation reported in Table 2).

understanding the underlying mechanism implied in the CO_2 dissolution process in ILs, and it could be implemented to rationally design ILs for CO_2 capture. For this purpose, we performed a COSMO-RS screening of K_H values, over 170 ILs, selecting counterion combinations with the criteria of enhancing the van der Waals forces and minimizing the electrostatic interactions. Because of the affordable computational cost, the screening of the Henry's Law coefficients of CO_2 was carried out using the $[C+A]_{GAS}$ approach, and the estimated COSMO-RS values that were corrected by the experimentally calculated linear correlation are shown in Table 2. The results of the COSMO-RS screening reported in Figures 9A and 9B show a distinguishable group of ILs with enhanced properties for the CO_2 physical absorption, which exhibit K_H < 3 MPa. The selected group includes ILs based on the $[FEP]^-$ anion and the new ILs with a remarkable bromination of the anion, that is, ILs based on $[BrEP]^-$, $[NTBr_2]^-$, and $[PBr_6]^-$ anions. One additional advantage of the potential use of brominated ILs is that, based on the simulation results, the solubility of CO_2 scarcely depends on the counterion structure (see Figure 9). Therefore, the cation family and alkyl substituent of the cation can be selected to tune other properties of interest in the design of the CO_2 separation process, such as density, viscosity, or selectivity, with respect to other gases in membrane-based operations. Future investigations will focus on attempting the synthesis and characterization of new ILs based on brominated anions and the experimental analysis of their feasibility in CO_2 capture technologies.

4. CONCLUSIONS

The capability of COSMO-RS has been evaluated by the implementation of four different computational approaches ($[C+A]_{GAS}$, $[C+A]_{COSMO}$, $[CA]_{GAS}$, and $[CA]_{COSMO}$) to predict the solubility of gaseous compounds, including CO_2, in ILs. The statistical results indicate that the four COSMO-RS approaches provide similar good capability to predict the experimental trends of the Henry's Law constants (slopes $\approx$ 0.9, R^2 > 0.9, and MPE < 50%) for a wide range of values of more than 50 gas-IL systems. Nevertheless, it was observed that the linear relationships between the experimental and theoretical data improve slightly from the [C+A] model to the [CA] model, thus, indicating the suitability of using an ion-pair model to describe intermolecular interactions of the ILs. This fact became more evident in the particular case of predicting the solubility of CO_2 in ILs, for which the $[CA]_{GAS/COSMO}$ models described more accurately the effect of the anion and the cation on CO_2 solubility in IL solvents. However, it should be noted that the $[CA]_{GAS}$ model showed ~2 MPa of systematic overestimation of the Henry's Law coefficient, increasing the prediction error in the range of low K_H values. Regarding the effect of temperature on the Henry's Law coefficients of CO_2 in ILs, the four computational approaches are able to provide a qualitative description of the solubility-temperature trends reported in the literature of CO_2 in ILs, which use energy information to estimate the vapor pressure of the solute preferred with respect to the extrapolation of the Wagner equation data.

After validating the capability of COSMO-RS to predict the solubility of CO_2 in ILs, an important challenge of this work was using this methodology for a deeper understanding of the behavior of CO_2−IL systems to contribute to the rational selection of ILs with favored characteristics for CO_2 absorption. To this end, the Henry's Law coefficient of CO_2 in ILs was successfully related to the excess enthalpy of CO_2−IL mixtures in solution, indicating that higher solubilities of CO_2 in ILs are associated with a higher exothermicity of the mixture. In addition, the intermolecular interactions (electrostatic, hydrogen bonding, and van der Waals) between the components of the mixture in the fluid phase were computed to determine the role of each contribution to the solubility of CO_2 in ILs. We determined that the attractive van der Waals forces associated with the compounds in the liquid phase dominate the behavior of the solubility of CO_2 in ILs, whereas the repulsive electrostatic interactions indicate a secondary contribution to the excess enthalpy of the dissolution, and the hydrogen bonds seem to be insignificant.

On the basis of the conclusion that ILs with a favored CO_2 absorption capacity are those capable of promoting van der Waals forces with the CO_2 solute, we have carried out a guided COSMO-RS screening. This screening resulted in the finding of new potential ILs with highly brominated anions capable of overcoming the known solubility limit range of ILs by the physical absorption of CO_2 that can be applied in membrane separation or other CO_2 gas−liquid capture technologies.

■ ASSOCIATED CONTENT

Ⓢ Supporting Information. Further details are given in Figure S1 and Tables S1−S5. This material is available free of charge via the Internet at http://pubs.acs.org.

■ AUTHOR INFORMATION

Corresponding Author

*Phone: 34 91 4976938. Fax: 34 91 4973516. E-mail: pepe.palomar@uam.es.

ACKNOWLEDGMENT

The authors are grateful to the "Ministerio Ciencia e Innovación" and "Comunidad de Madrid" for financial support (projects CTQ2008-01591, CTQ2008-05641 and S2009/PPQ-1545). We are very grateful to "Centro de Computación Científica de la Universidad Autónoma de Madrid" for computational facilities.

REFERENCES

(1) Figueroa, J. D.; Fout, T.; Plasynsky, S.; McIlvried, H.; Srivastava, R. D. Advances in CO_2 capture technology - The U.S. Department of Energy's Carbon Sequestration Program. *IJGGC* **2008**, *2*, 9–20.

(2) Wasserscheid, P.; Welton, T. *Ionic liquids in synthesis*; Wiley-VCH Verlag GmbH & Co. KGaA: Weinheim, Germany, 2008.

(3) Anthony, J. L.; Aki, S.; Maggin, E. J.; Brennecke, J. F. Feasibility of using ionic liquids for carbon dioxide capture. *IJETM* **2004**, *4* (1−2), 105–115.

(4) Bara, J. E.; Carliste, T. K.; Gabriel, C. J.; Camper, D.; Finotello, A.; Gin, D. L.; Noble, R. D. Guide to CO_2 separations in imidazolium-based room-temperature ionic liquids. *Ind. Eng. Chem. Res.* **2009**, *48*, 2739–2751.

(5) Huang, J.; Rüther, T. Why are ionic liquids attractive for CO_2 absorption? An overview. *Aust. J. Chem.* **2009**, *62*, 298–308.

(6) Bara, J. E.; Camper, D. E.; Gin, D. L.; Noble, R. D. Room-temperature ionic liquids and composite materials: platform technologies for CO_2 capture. *Acc. Chem. Res.* **2010**, *43* (1), 152–159.

(7) Kerlé, D.; Ludwig, R.; Geiger, A.; Paschek, D. Temperature dependence of the solubility of carbon dioxide in imidazolium-based ionic liquids. *J. Phys. Chem. B* **2009**, *113*, 12727–12735.

(8) Finotello, A.; Bara, J. E.; Camper, D.; Noble, R. D. Room-Temperature Ionic Liquids: Temperature Dependence of Gas Solubility Selectivity. *Ind. Eng. Chem. Res.* **2008**, *47*, 3453–3459.

(9) Lim, B. H.; Choe, W. H.; Shim, J. J.; Ra, C. S.; Tuma, D.; Lee, H.; Lee, C. S. High-pressure solubility of carbon dioxide in imidazolium-based ionic liquids with aniones $[PF_6]$ and $[BF_4]$. *Korean J. Chem. Eng.* **2009**, *26* (4), 1130–1136.

(10) Anthony, J. L.; Anderson, J. L.; Magín, E. J.; Brennecke, J. F. Anion effects on gas solubility in ionic liquids. *J. Phys. Chem. B* **2005**, *109*, 6366–6374.

(11) Chen, Y.; Zhang, S.; Yuan, X.; Zhang, Y.; Zhang, X.; Dai, W.; Mori, R. Solubility of CO_2 in imidazolium-based ionic liquids. *Thermochim. Acta* **2006**, *441*, 42–44.

(12) Soriano, A. N.; Doma, B. T.; Li, M. H. Carbon dioxide solubility in 1-ethyl-3-methylimidazolium tetrafluoroborate. *J. Chem. Eng. Data* **2008**, *53*, 2550–2555.

(13) Soriano, A. N.; Doma, B. T.; Li, M. H. Carbon dioxide solubility in some ionic liquids at moderate pressures. *J. Taiwan Inst. Chem. Eng.* **2009**, *40*, 387–393.

(14) Blanchard, L. A.; Gu, Z.; Brennecke, J. F. High-Pressure Phase Behavior of Ionic Liquid/CO_2 Systems. *J. Phys. Chem. B* **2001**, *105* (12), 2437–2444.

(15) Kim, Y. S.; Choi, W. Y.; Jang, J. H.; Yoo, K. P.; Lee, C. S. Solubility measurement and prediction of carbon dioxide in ionic liquids. *Fluid Phase Equilib.* **2005**, *228/229*, 439–445.

(16) Kim, Y. S.; Choi, W. Y.; Lee, C. S. Measurements and calculation of the solubility of carbon dioxide in ionic liquid $[bmim][PF_6]$. *Front. Sep. Sci. Technol.* **2004**, 19–22.

(17) Kumelan, J.; Pérez Salado, A.; Tuma, D.; Maurer, G. Solubility of CO_2 in the ionic liquids $[bmim][CH_3SO_4]$ and $[bmim][PF_6]$. *J. Chem. Eng. Data* **2006**, *51*, 1802–1807.

(18) Jalili, A. H.; Mehdizadeh, A.; Shokouhi, M.; Sakhaeinia, H.; Taghikhani, V. Solubility of CO_2 in 1-(2-hydroxyetyl)-3-methylimidazolium ionic liquids with different anions. *J. Chem. Thermodyn.* **2010**, *42*, 5787–5791.

(19) Shifflett, M. B.; Yokozeki, A. Solubility of CO_2 in room temperature ionic liquid $[hmim][TF_2N]$. *J. Phys. Chem. B* **2007**, *111*, 2070–2074.

(20) Schilderman, A. M.; Raeissi, S.; Peters, C. J. Solubility of carbon dioxide in the ionic liquid 1-ethyl-3 methylimidazolium bis(trifluoromethylsulfonyl)imide. *Fluid Phase Equilib.* **2007**, *260* (1), 19–22.

(21) Jacquemin, J.; Husson, P.; Majer, V.; Costa, M. F. Influence of the cation on the solubility of CO_2 and H_2 in ionic liquids based on the bis(trifluoromethylsulfonyl)imide anion. *J. Solution Chem.* **2007**, *36*, 967–979.

(22) Raeissi, S.; Peters, C. J. Carbon dioxide solubility in the homologous 1-alkyl-3-methylimidazolium bis(trifluoromethylsulfonyl)imide family. *J. Chem. Eng. Data* **2009**, *54*, 382–386.

(23) Hong, G.; Jacquemin, J.; Deetlefs, M.; Hardacre, C.; Husson, P.; Costa, M. F. Solubility of carbon dioxide and ethane in three ionic liquids based on the bis {(trifluoromethyl)sulfonil}imide anion. *Fluid Phase Equilib.* **2007**, *257*, 27–34.

(24) Soriano, A. N.; Doma, B. T.; Li, M. H. Carbon dioxide solubility in 1-ethyl-3-methylimidazolium trifluoromethanesulfonate. *J. Chem. Thermodyn.* **2009**, *41*, 525–529.

(25) Palgunadi, J.; Kang, J. E.; Nguyen, D. Q.; Kim, J. H.; Min, B. K.; Lee, S. D.; Kim, H.; Kim, H. S. Solubility of CO_2 in dialkylimidazolium dialkylphosphate ionic liquids. *Thermochim. Acta* **2009**, *494*, 94–98.

(26) Shifflett, M. B.; Yokozeki, A. Phase behavior of carbon dioxide in ionic liquids: [emim][acetate], [emim][trifluoroacetate] and [emim][acetate] + [emim][trifluoroacetate] mixtures. *J. Chem. Eng. Data* **2009**, *54*, 108–114.

(27) Muldoon, M. J.; Aki, S. N.; Anderson, J. L.; Dixon, J. K.; Brennecke, J. F. Improving carbon dioxide solubility in ionic liquids. *J. Phys. Chem. B* **2007**, *111*, 9001–9009.

(28) Zhang, X.; Liu, Z.; Wang, W. Screening of ionic liquids to capture CO_2 by COSMO-RS and experiments. *AIChE J.* **2008**, *54* (10), 2717–2728.

(29) Zhang, X.; Hun, F.; Liu, Z.; Wang, W.; Shi, W.; Maginn, E. J. Absorption of CO_2 in the ionic liquid tris(pentafluoroethyl)-trifluorophosphate ([hmim][FEP]): A molecular view by computer simulations. *J. Phys. Chem. B* **2009**, *113*, 7591–7598.

(30) Baltus, R. E.; Counce, R. M.; Culbertson, B. H.; Luo, H.; DePaoli, W.; Dai, S.; Duckworth, D. C. Examination of the potential of ionic liquids for gas separations. *Sep. Sci. Technol.* **2005**, *40*, 525–541.

(31) Yuan, X.; Zhang, S.; Liu, J.; Lu, X. Solubilities of CO_2 in hydroxyl ammonium ionic liquids at elevated pressures. *Fluid Phase Equilib.* **2007**, *257*, 195–200.

(32) Bates, E. D.; Mayton, R. D.; Ntai, I.; Davis, J. H. CO_2 capture by a task-specific ionic liquid. *J. Am. Chem. Soc.* **2002**, *124* (6), 926–927.

(33) Song, H. N.; Lee, B. C.; Lim, J. S. Measurement of CO_2 solubility in ionic liquids: [BMP][TfO] and [P14,6,6,6][Tf_2N] by measuring bubble-point pressure. *J. Chem. Eng. Data* **2010**, *55*, 891–896.

(34) Kumelan, J.; Tuma, D.; Kamps, A. P.; Maurer, G. Solubility of the single gases carbon dioxide and hydrogen in the ionic liquid [bmpy][Tf_2N]. *J. Chem. Eng. Data* **2010**, *55*, 165–172.

(35) Ally, M. R.; Braunstein, J.; Baltus, R. E.; Dai, S. Irregular ionic lattice model for gas solubilities in ionic liquids. *Ind. Eng. Chem. Res.* **2004**, *43*, 1296–1301.

(36) Andreu, J. S.; Vega, L. F. Capturing the solubility behavior of CO_2 in ionic liquids by a simple model. *J. Phys. Chem. C* **2007**, *111*, 16028–16034.

(37) Kim, Y. S.; Choi, W. Y.; Jang, J. H.; Lee, C. S. Solubility measurement and prediction of carbon dioxide in ionic liquids. *Fluid Phase Equilib.* **2005**, *228*−*229*, 439–445.

(38) Heintz, A. Recent developments in thermodynamics and thermophysics of non-aqueous mixtures containing ionic liquids. A review. *J. Chem. Thermodyn.* **2005**, *37*, 525–535.

(39) Maginn., E. J. Molecular simulation of ionic liquids: current status and future opportunities. *J. Phys.: Condens. Matter* **2009**, *21*, 37.

(40) Klamt, A. *COSMO-RS: From Quantum Chemistry to Fluid Phase Thermodynamics and Drug Design*; Elsevier: Amsterdam, The Netherlands, 2005.

(41) Palomar, J.; Torrecilla, J. S.; Ferro, V. R.; Rodríguez, F. Development of an a Priori Ionic Liquid Design Tool. 1. Integration of a Novel COSMO-RS Molecular Descriptor on Neural Networks. *Ind. Eng. Chem. Res.* **2008**, *47*, 4523–4532.

(42) Palomar, J.; Torrecilla, J. S.; Ferro, V. R.; Rodríguez, F. Development of an a Priori Ionic Liquid Design Tool. 2. Ionic Liquid Selection through the Prediction of COSMO-RS Molecular Descriptor by Inverse Neural Network. *Ind. Eng. Chem. Res.* **2009**, *48*, 2257–2265.

(43) Palomar, J.; Ferro, V. L.; Torrecilla, J. S.; Rodriguez, F. Density and molar volume predictions using COSMO-RS for ionic liquids. An approach to solvent design. *Ind. Eng. Chem. Res.* **2007**, *46* (18), 6041–6048.

(44) Diedenhofen, M.; Klamt, A.; Marsh, K.; Schafer, A. Prediction of the vapor pressure and vaporization enthalpy of 1-n-alkyl-3-methylimidazolium-bis-(trifluoromethanesulfonyl) amide ionic liquids. *Phys. Chem. Chem. Phys.* **2007**, *9* (33), 4653–4656.

(45) Simoni, L. D.; Brennecke, J. F.; Stadtherr, M. A. Asymmetric Framework for Predicting Liquid-Liquid Equilibrium of Ionic Liquid-Mixed-Solvent Systems. 1. Theory, Phase Stability Analysis, and Parameter Estimation. *Ind. Eng. Chem. Res.* **2009**, *48* (15), 7246–7256.

(46) Banerjee, T.; Khanna, A. Infinite dilution activity coefficients for trihexyltetradecyl phosphonium ionic liquids: Measurements and COSMO-RS prediction. *J. Chem. Eng. Data* **2006**, *51* (6), 2170–2177.

(47) Diedenhofen, M.; Eckert, F.; Klamt, A. Prediction of infinite dilution activity coefficients of organic compounds in ionic liquids using COSMO-RS. *J. Chem. Eng. Data* **2003**, *48* (3), 475–479.

(48) Navas, A.; Ortega, J.; Vreekamp, R.; Marrero, E.; Palomar, J. Experimental Thermodynamic Properties of 1-Butyl-2-methylpyridinium Tetrafluoroborate [b2mpy][BF4] with Water and with Alkan-1-ol and Their Interpretation with the COSMO-RS Methodology. *Ind. Eng. Chem. Res.* **2009**, *48* (5), 2678–2690.

(49) Preiss, U.; Jungnickel, C.; Thoming, J.; Krossing, I.; Luczak, J.; Diedenhofen, M.; Klamt, A. Predicting the Critical Micelle Concentrations of Aqueous Solutions of Ionic Liquids and Other Ionic Surfactants. *Chem.—Eur. J.* **2009**, *15* (35), 8880–8885.

(50) Freire, M. G.; Ventura, S. P.; Santos, L. M.; Marrucho, I. M.; Coutinho, J. Evaluation of COSMO-RS for the prediction of LLE and VLE of water and ionic liquids binary systems. *Fluid Phase Equilib.* **2008**, *268* (1−2), 74–84.

(51) Lei, Z. G.; Arlt, W.; Wasserscheid, P. Selection of entrainers in the 1-hexene/n-hexane system with a limited solubility. *Fluid Phase Equilib.* **2007**, *260*, 29–35.

(52) Banerjee, T.; Singh, M. K.; Khanna, A. Prediction of binary VLE for imidazolium based ionic liquid systems using COSMO-RS. *Ind. Eng. Chem. Res.* **2006**, *45* (9), 3207–3219.

(53) Kato, R.; Gmehling, J. Systems with ionic liquids: Measurement of VLE and gamma(infinity) data and prediction of their thermodynamic behavior using original UNIFAC, mod. UNIFAC(Do) and COSMO-RS(O1). *J. Chem. Thermodyn.* **2005**, *37* (6), 603–619.

(54) Beste, Y.; Eggersmann, M.; Schoenmakers, H. Extractive distillation with ionic fluids. *Chem. Eng. Technol.* **2005**, *77* (11), 1800–1808.

(55) Lapkin, A. A.; Peters, M.; Greiner, L.; Chemat, S.; Leonhard, K.; Liaw, M. A.; Leitner, W. Screening of new solvents for artemisinin extraction process using ab initio methodology. *Green Chem.* **2010**, *12* (2), 241–251.

(56) Mohanty, S.; Banerjee, T.; Mohanty, K. Quantum Chemical Based Screening of Ionic Liquids for the Extraction of Phenol from Aqueous Solution. *Ind. Eng. Chem. Res.* **2010**, *49* (6), 2916–2925.

(57) Kumar, A. A.; Banerjee, T. Thiophene separation with ionic liquids for desulphurization: A quantum chemical approach. *Fluid Phase Equilib.* **2009**, *278* (1−2), 1–8.

(58) Freire, M. G.; Carvalho, P. J.; Gardas, R. L.; Santos, L. M.; Marrucho, I. M.; Coutinho, J. Solubility of Water in Tetradecyltrihexylphosphonium-Based Ionic Liquids. *J. Chem. Eng. Data* **2008**, *53* (10), 2378–2382.

(59) Banerjee, T.; Verma, K. K.; Khanna, A. Liquid-liquid equilibrium for ionic liquid systems using COSMO-RS: Effect of cation and anion dissociation. *AIChE J.* **2008**, *54* (7), 1874–1885.

(60) Sahandzhieva, K.; Tuma, D.; Breyer, S.; Kamps, A. P.; Maurer, G. Liquid-liquid equilibrium in mixtures of the ionic liquid 1-n-butyl-3-methylimidazolium hexafluorophosphate and an alkanol. *J. Chem. Eng. Data* **2006**, *51* (5), 1516–1525.

(61) Lei, Z. G.; Arlt, W.; Wasserscheid, P. Separation of 1-hexene and n-hexane with ionic liquids. *Fluid Phase Equilib.* **2006**, *241* (1−2), 290–299.

(62) Domanska, U.; Pobudkowska, A.; Eckert, F. (Liquid plus liquid) phase equilibria of 1-alkyl-3-methylimidazolium methylsulfate with alcohols, or ethers, or ketones. *J. Chem. Thermodyn.* **2006**, *38* (6), 685–695.

(63) Palomar, J.; Lemus, J.; Gilarranz, M. A.; Rodríguez, J. J. Adsorption of ionic liquids from aqueous effluents by activated carbon. *Carbon* **2009**, *47* (7), 1846–1856.

(64) Rosol, Z. P.; German, N. J.; Gross, S. M. Solubility, ionic conductivity and viscosity of lithium salts in room temperature ionic liquids. *Green Chem.* **2009**, *11* (9), 1453–1457.

(65) Manan, N. A.; Hardacre, C.; Jacquemin, J.; Rooney, D. W.; Youngs, T. G. Evaluation of gas solubility prediction in ionic liquids using COSMOthermX. *J. Chem. Eng. Data* **2009**, *54*, 2005–2022.

(66) Franke, R.; Hannebauer, B.; Jung, S. A Case Study in the Pre-Calculation of Henry Coefficients. *Chem. Eng. Technol.* **2010**, *33* (2), 251–257.

(67) Miller, M. B.; Chen, D. L.; Xie, H. B.; Luebke, D. R.; Johnson, J. K.; Enick, R. M. Solubility of CO_2 in CO_2-philic oligomers; COSMOtherm predictions and experimental results. *Fluid Phase Equilib.* **2009**, *287*, 26–32.

(68) Miltner, M.; Miltner, A.; Friedl, A. Calculation of physical gas solubilities in various solvents with COSMO-RS. *Chem. Ing. Tech.* **2006**, *78* (8), 1087–1092.

(69) Frisch, M. J.; Trucks, G. W.; Schlegel, H. B.; Scuseria, G. E.; Robb,M. A.; Cheeseman, J. R.; Montgomery, J. A., Jr.; Vreven, T.; Kudin, K. N.; Burant, J. C.; Millam, J. M.; Iyengar, S. S.; Tomasi, J.; Barone, V.;Mennucci, B.; Cossi, M.; Scalmani, G.; Rega, N.; Petersson, G. A.;Nakatsuji, H.; Hada, M.; Ehara, M.; Toyota, K.; Fukuda, R.; Hasegawa, J.; Ishida, M.; Nakajima, T.; Honda, Y.; Kitao, O.; Nakai, H.; Klene, M.; Li, X.; Knox, J. E.; Hratchian, H. P.; Cross, J. B.; Bakken, V.; Adamo, C.; Jaramillo, J.; Gomperts, R.; Stratmann, R. E.; Yazyev, O.; Austin, A. J.; Cammi, R.; Pomelli, C.; Ochterski, J. W.; Ayala, P. Y.; Morokuma, K.;Voth, G. A.; Salvador, P.; Dannenberg, J. J.; Zakrzewski, V. G.; Dapprich, S.; Daniels, A. D.; Strain, M. C.; Farkas, O.; Malick, D. K.; Rabuck, A. D.; Raghavachari, K.; Foresman, J. B.; Ortiz, J. V.; Cui, Q.; Baboul, A. G.; Clifford, S.; Cioslowski, J.; Stefanov, B. B.; Liu, G.; Liashenko, A.; Piskorz, P.; Komaromi, I.; Martin, R. L.; Fox, D. J.; Keith, T.; Al-Laham, M. A.; Peng, C. Y.; Nanayakkara, A.; Challacombe, M.; Gill, P. M. W.; Johnson, B.; Chen, W.; Wong, M. W.; Gonzalez, C.; Pople, J. A. *Gaussian03*, revision B.05; Gaussian, Inc.: Wallingford, CT, 2004.

(70) *COSMOtherm*, C2.1 Release 01.08; COSMOlogic GmbH & Co. KG: Leverkusen, Germany, 2006; http://www.cosmologic.de

(71) Ionic Liquid Database-(ILthermo). *NIST Standard Reference Database* # 147; http://ilthermo.boulder.nist.gov/ILThermo/mainmenu.uix

(72) Chinn, D.; Vu, D.; Driver, M. S.; Boudreau, L. C. CO_2 removal from gas using ionic liquid absorbents. *Chevron Texaco Corporation*, 2005. U.S. Patent US2005/0129598A1.

(73) Yokoezi, A.; Shifflet, M. B.; Junk, C. P.; Grieco, L. M.; Foo, T. Physical and chemical absorptions of carbon dioxide in room-temperature ionic liquids. *J. Phys. Chem. B* **2008**, *112*, 16654–16663.

(74) Shah, J. K.; Maginn, E. J. Monte Carlo Simulations of Gas Solubility in the Ionic Liquid 1-n-Butyl-3-methylimidazolium Hexafluorophosphate. *J. Phys. Chem. B* **2005**, *109*, 10395–10405.

(75) Carvalho, P. J.; Coutinho, J. On the Nonideality of CO_2 Solutions in Ionic Liquids and Other Low Volatile Solvents. *J. Phys. Chem. Lett.* **2010**, *1* (4), 774–780.

(76) Carvalho, P. J.; Alvarez, V. H.; Marrucho, I. M.; Aznar, M.; Coutinho, J. High pressure phase behavior of carbon dioxide in 1-butyl-3-methylimidazolium bis(trifluoromethylsulfonyl)imide and 1-butyl-3-methylimidazolium dicyanamide ionic liquids. *J. Supercrit. Fluids* **2009**, *50* (2), 105–111.

(77) Kazarian, S. G.; Briscoe, B. J.; Welton, T. Combining ionic liquids and supercritical fluids: in situ ATR-IR study of CO_2 dissolved in

two ionic liquids at high pressures. *Chem. Commun.* **2000**, *20*, 2047–2048.

(78) Seki, T.; Grunwaldt, J. D.; Baiker, A. In situ attenuated total reflection infrared spectroscopy of imidazolium-based room-temperature ionic liquids under supercritical CO_2. *J. Phys. Chem B* **2009**, *113* (1), 114–122.

(79) Carvalho, P. J.; Álvarez, V. H.; Schroder, B.; Gil, A. M.; Marrucho, I. M.; Azanar, M.; Santos, L. M.; Coutinho, A. P. Specific salvation interaction of CO_2 on acetate and trifluoroacetate imidazolium based ionic liquids at high pressures. *J. Phys. Chem. B* **2009**, *113*, 6803–6812.

Publicación 2:

Gonzalez-Miquel, M.; Palomar, J.; Omar, S.; Rodriguez, F. **CO_2 / N_2 selectivity simulation in supported ionic liquid membranes (SILMs) by COSMO-RS**. *Industrial & Engineering Chemical Research*, **2011**, *50*, 5739–5748.

I&EC research
Industrial & Engineering Chemistry Research

ARTICLE

pubs.acs.org/IECR

CO_2/N_2 Selectivity Prediction in Supported Ionic Liquid Membranes (SILMs) by COSMO-RS

Maria Gonzalez-Miquel,[†] Jose Palomar,[*,‡] Salama Omar,[‡] and Francisco Rodriguez[†]

[†]Departamento de Ingeniería Química, Universidad Complutense de Madrid, 28040 Madrid, Spain

[‡]Sección de Ingeniería Química (Departamento de Química Física Aplicada), Universidad Autónoma de Madrid, Cantoblanco, 28049 Madrid, Spain

Supporting Information

ABSTRACT: The quantum chemical COSMO-RS method was applied to describe supported ionic liquid membranes (SILMs) with an enhanced capacity of selective separation of CO_2 from N_2, in order to contribute to the design of CO_2 postcombustion capture technologies based on ionic liquid (IL) solvents. First, the predictive capability of the COSMO-RS method was evaluated through a comparison with a wide range of selectivity experimental data, and a further optimization based on the Henry's Law constant of each solute in ILs was developed to improve the prediction of CO_2/N_2 selectivity in SILMs. Afterward, the optimized COSMO-RS approach was applied to design suitable SILM systems for CO_2/N_2 separation by driving a computational screening of 224 ILs, with results illustrating the capability of $[SCN^-]$-based ILs to enhance the selective separation of CO_2 from N_2. Finally, to better understand SILM behavior in CO_2 separation, the CO_2/N_2 selectivity differences among ILs were successfully related to the excess enthalpy of CO_2-IL and N_2-IL mixtures in solution predicted by COSMO-RS. In addition, the intermolecular interactions (electrostatic, hydrogen bonding, and van der Waals) between CO_2-IL and N_2-IL systems in the liquid phase, quantified by COSMO-RS, were analyzed in order to contribute to the rational selection of SILMs with positive characteristics for CO_2/N_2 selective separation.

1. INTRODUCTION

Carbon dioxide (CO_2) is regarded as the most important anthropogenic greenhouse gas, with its global atmospheric concentration increasing mainly as a result of fossil fuel power plant emissions.[1] The most promising near-term approach for mitigating the global warming effects caused by greenhouse gases involves direct CO_2 capture at power plants.[2,3] Conventional CO_2 postcombustion capture technologies are based on amine absorption processes, which involve several concerns such as their corrosive nature and volatility, leading to high operational cost and environmental impact.[3] Therefore, it is critical to develop innovative and cost-effective technologies capable of efficiently capturing CO_2, overcoming the drawbacks associated with commercially available systems.

Membrane gas separation technology represents an alternative mechanism by which CO_2 may be separated from flue gas of fossil power plants, largely composed of N_2, in postcombustion capture processes.[4] Polymeric membrane systems have been applied in gas separations, and they are more energy efficient and easier to operate than other technologies such as absorption.[3] In addition, it is possible to improve the selectivity and permeability of the gas separation process by applying a supported liquid membrane (SLM), which in general consists of a liquid phase—mostly an organic solvent—immobilized in a supporting porous membrane by capillary forces.[5] However, traditional SLMs are not stable enough, suffering from solvent evaporation of the liquid phase into the gas stream, which results in membrane degradation and a loss of selectivity.[6]

Room-temperature ionic liquids (ILs) are a broad category of organic salts typically liquid in their pure state, which have been regarded as potential environmentally benign solvents due to their unique properties, most notably their almost negligible vapor pressure. In addition, an important feature associated with ILs is the possibility to design one with the necessary properties for a specific application by tuning the structures of the ions, hence the term "designer solvents". Owing to these novel properties, ILs have generated significant interest across a wide variety of engineering applications,[7] with their use as media for CO_2 capture appearing to be especially promising.[3,8−11]

Innovative applications of ILs in supported membranes (SILMs) have been suggested to achieve a highly permeable and selective transport medium for CO_2 separation.[9−14] Research on using SILMs for gas separations has disclosed a competitive or superior performance relative to that of existing membrane materials, with theoretical and experimental data indicating selectivity versus permeability ratios for SILMs consistently above the Robeson plot upper bound for polymers.[15,16] Furthermore, the capability of IL membranes to be operated under industrial conditions without reducing the selectivities under mixed-gas operations with CO_2 partial pressures of 2 bar has been reported, and they are able to work under dry gas feed conditions and show long-term stability of up to 106 days under continuous flow operations without any detectable performance loss.[17] Previous literature indicates that the choice of the anion can have a more pronounced effect on CO_2

Received: December 8, 2010
Accepted: March 9, 2011
Revised: February 15, 2011
Published: March 23, 2011

solubility and CO_2/N_2 selectivity than the choice of the cation.[17,18] The performance of different imidazolium-based ILs containing anions such as bis(trifluoromethylsulfonil)imide [NTf_2^-],[15,17,20,21] trifluoromethanesulfonate [$CF_3SO_3^-$],[15,7,20] chloride [Cl^-],[15] dicyanamide [DCN^-],[15,17,20] hexafluorophosphate [PF_6^-],[21] tetrafluoroborate [BF_4^-],[17,20−22] or [$B(CN)_4^-$] has been evaluated ,[23] with results suggesting that anions containing nitrile groups increase CO_2/N_2 selectivities. In fact, [emim][DCN]-based SILMs have been reported to achieve a CO_2 permeability of 610 barrers combined with an ideal selectivity of 61 for CO_2/N_2.[15] Referring to the influence of the cation on gas separation performance, an evaluation of different salts based on imidazolium,[15,17,20−23] phosphonium,[12,24] sulphonium,[12,24] or ammonium[12] revealed better properties for imidazolium-based SILMs in terms of permeability and selectivity for CO_2/N_2 separation, with results suggesting that increasing the length of the alkyl chain on an imidazolium ring does not seem to enhance the CO_2/N_2 selectivity.[21,25] Another issue that should be highlighted is the effect of the functionalization of the ionic liquid by fluorination in gas separation properties, since the performance of a series of fluoroalkyl-functionalized imidazolium room-temperature ionic liquids was found to exhibit lower ideal selectivities for CO_2/N_2 than their alkyl-functionalized analogues,[25] to the contrary of what has been observed in the case of CO_2 absorption with bulk ionic liquids.[18,26−28] Therefore, due to the potential application of SILMs as an alternative mechanism to separate CO_2 from N_2 in industrial processes, and taking into account the huge variety of theoretically possible ILs that may be supported on the membrane material, the development of predictive models capable of estimating the gas separation performance of SILMs is of great interest.

The major driving force for selective separation of CO_2 from N_2 in SILMs is the solubility difference between these gases,[12,14] with literature results indicating that the mixed-gas selectivities are constant with feed partial pressures and can be described in terms of ideal selectivities.[17] Thus, the CO_2/N_2 selectivity, achieved for a certain SILM, could be estimated by determining of the solubility ratio between gases using the predicted solubility or the predicted Henry's Law constant of each gas in the ionic liquid. Several methods have been reported to predict the thermodynamic behavior of gases in ionic liquids, such as Equation of States (EOS),[29−32] Group Contribution Models (GCM),[33] or Activity Coefficient Models (ACM).[33] The parameters of these models must be determined by using a large amount of experimental data, which is not available for the vast majority of ionic liquids. Therefore, methods by which equilibrium thermodynamic properties can be estimated from structural information of the compounds are of great utility. At this point, the COSMO-RS (Conductor-like Screening Model for Real Solvents) model developed by Klamt[34] is regarded as a valuable method for predicting the thermodynamic properties of mixtures on the basis of unimolecular quantum chemical calculations for the individual molecules, providing an unique *a priori* computational tool for designing IL with specific properties.[35,36] The different interactions of molecules in a fluid (electrostatic interaction, hydrogen bonding, and dispersion) are represented as a function of surface polarities of the partners. Using an efficient thermodynamic solution for such pairwise surface interactions, COSMO-RS finally converts the molecular polarity information into standard thermodynamic data. Several publications have demonstrated the general suitability of the *a priori* COSMO-RS method to predict properties of IL systems, such as density,[37] vapor pressure,[38] activity coefficients,[39−41] excess properties,[42,43] and phase equilibrium data (VLE,[44−49] LLE,[50−59] and SLE[60,61]). In addition, the solubilities and Henry's Law constants of CO_2 and other gases in ILs have also been successfully estimated by COSMO-RS,[26,62] through a computational screening method for different operating conditions. Moreover, in our previous work,[63] we developed a further optimization of the COSMO-RS approach to improve the prediction of gas solubilities in ILs, with special attention given to the case of the CO_2 solute. Furthermore, we presented deeper insight into CO_2 solubility behavior in ILs using the COSMO-RS methodology in order to contribute to the rational selection of an IL with favorable characteristics for CO_2 absorption, with results revealing that van der Waals forces associated with the solute in the liquid phase determine the absorption capacity of CO_2 in ILs. In sum, the results showed that the *a priori* COSMO-RS method provides a qualitatively good prediction of gas solubility data in ILs, indicating a great potential to design a suitable IL for CO_2 capture. In addition, it has to be mentioned that a recent publication[64] predicted the solubilities and selectivities for CO_2/N_2 systems in eight ionic liquids based on 1-alkyl-methylimidazolium cations with [BF_4^-], [PF_6^-], [$CF_3SO_3^-$], [NTf_2^-], and [DCN^-] anions using a conductor like screening model based on activity coefficient, COSMO-SAC.

The aim of the present work is to extend the analysis for CO_2/N_2 selectivity predictions by COSMO-RS to a wide range of ILs reported in the literature under different operating conditions of temperature and pressure, in order to develop a further optimization of the model to improve the prediction of CO_2/N_2 selectivity in SILMs. The second objective of this work is to apply the optimized COSMO-RS approach to select suitable SILMs systems for CO_2/N_2 separation by driving a computational screening of 224 ILs based on 16 cations and 14 anions. Finally, our third objective is directed toward attaining a better understanding of CO_2/N_2 selectivity behavior in SILMs by using COSMO-RS methodology. For this, the CO_2/N_2 selectivity differences among ILs were analyzed in terms of Henry's Law coefficients of CO_2 and N_2, which were afterward successfully related to the excess enthalpy of CO_2−IL and N_2−IL mixtures in solution predicted by COSMO-RS. In addition, the intermolecular interactions (electrostatic, hydrogen bonding, and van der Waals) between CO_2−IL and N_2−IL systems in the liquid phase, quantified by COSMO-RS, were analyzed in order to contribute to the rational selection of SILMs with favorable characteristics for CO_2/N_2 selective separation.

2. COMPUTATIONAL DETAILS

The molecular geometries of all compounds (gaseous solutes and IL counterions) were optimized at the B3LYP/6-31++G** computational level in the ideal gas phase using the quantum chemical Gaussian 03 package.[65] A molecular model of independent counterions was applied in COSMO-RS calculations, where ILs are treated as an equimolar mixture of cations and anions.[26,63] Vibrational frequency calculations were performed in each case to confirm the presence of an energy minimum. Once molecular models were optimized, Gaussian 03 was used to compute the COSMO files. The ideal screening charges on the molecular surface for each species were calculated by the continuum solvation COSMO model using the BVP86/TZVP/DGA1 level of theory.[66,67] Subsequently, COSMO files were used as an input in the COSMOthermX[68] code to calculate the thermodynamic properties (Henry's Law constant and solubility of gaseous solutes

in ILs and detailed excess enthalpy contributions of CO_2−IL and N_2−IL mixtures). According to our chosen quantum method, the functional, and the basis set, we used the corresponding parametrization (BP_TZVP_C21_0108) that is required for the calculation of physicochemical data and contains intrinsic parameters of COSMOtherm, as well as specific parameters.

A wide range of experimental values of Henry's Law coefficients in ILs (see Table S1, Supporting Information, for the abbreviations of ILs) has been collected from the IUPAC database[69] and recent publications[70−79] (see Tables S2, S3, and S4, Supporting Information). To increase the statistical evaluation of the COSMO-RS approach, the data of gas-IL systems of 23 different solute gases (see Table S2, Supporting Information) and 20 different ILs (see Table S3, Supporting Information) were included in the analysis. The uncertainties in the Henry's Law constants and CO_2/N_2 selectivities estimated by the implemented COSMO-RS approach were determined by calculating the mean prediction error (MPE), as defined by eq 1:

$$\mathrm{MPE} = \frac{1}{N}\sum_{1}^{N}\frac{|X_{\mathrm{calc}} - X_{\mathrm{exp}}|}{X_{\mathrm{exp}}} \times 100 \qquad (1)$$

where N is the total number of data used, X_{calc} is the desired Henry's Law constant or CO_2/N_2 selectivity value calculated for a given IL at a given temperature, and X_{exp} is the corresponding value obtained from experimental work reported previously.

3. RESULTS

3.1. Optimization of COSMO-RS Approach to Predict CO_2/N_2 Selectivities in SILMs. The selective separation of CO_2 from N_2 in SILMs is determined by the solubility differences between gases,[12,14] with the mixed-gas selectivities being constant with feed partial pressures and similar to the ideal selectivities.[17] Thus, the CO_2/N_2 selectivity that may be achieved for a certain SILM, based on mole fraction, can be defined as follows:

$$S_{(\mathrm{CO_2/N_2})} = \frac{X_{\mathrm{CO_2}}}{X_{\mathrm{N_2}}} \qquad (2)$$

where X_i is the solubility of compound i in the ionic liquid supported in the membrane.

In addition, the indicated mole fraction of gas in solution, X_i, is related with the Henry's Law constants of the gaseous solute in the ionic liquid, K_H, by the following expression:

$$K_H = \frac{P_i}{X_i} \qquad (3)$$

where P_i is the partial pressure of gas above the solution.

Thus, the CO_2/N_2 selectivity achieved for a certain SILM can be determined by estimating the Henry's Law constant of each gas in the ionic liquid, as indicated in eq 4, which results from a combination of eq 2 and eq 3.

$$S_{(\mathrm{CO_2/N_2})} = \frac{K_{H_{\mathrm{N2}}}}{K_{H_{\mathrm{CO2}}}} \qquad (4)$$

In order to evaluate the capability of COSMO-RS to predict the Henry's Law constants of the gases in the IL, the calculated Henry's Law coefficients were compared to experimental data reported in the literature for a wide sample set of solutes (21) and ILs (20). First, a general evaluation of the capability of COSMO-RS to predict the solubility of gases in ILs was performed with the calculation of Henry's constant values of 42 solute−IL systems,

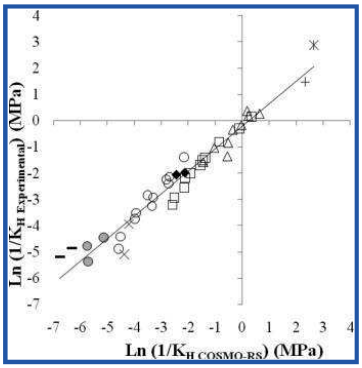

Figure 1. Comparison between the experimental and COSMO-RS predicted Henry's Law constants of common solutes [○ alkanes, □ alkenes, △ fluoroalkanes, + SO_2; ∗ C_6H_6, ♦ CO_2, × O_2, H_2 (denoted by the gray circles), and — N_2] in ILs at near-ambient temperature.

which include different compounds (alkanes, alkenes, fluorohydrocarbons, benzene, SO_2, H_2, O_2, N_2, and CO_2) in several ILs ([bmim][BF_4], [bmim][PF_6], [emim][NTf_2], and [hmim][NTf_2]; see Table S2, Supporting Information). Due to the large solubility value range, from benzene in [bmim][BF_4] (K_H = 0.056 MPa) to N_2 in [bmim][BF_4] (K_H = 179.1 MPa), it was decided to plot the data as the logarithmic inverse of the Henry's constant [$\mathrm{Ln}(1/K_H)$] to present the whole collection of values adequately, as in Figure 1. Experimental and calculated values were fitted by linear regression, and the results are reported in eq 5. The accuracy of the equation was indicated by the correlation coefficient (R^2 = 0.98), the standard deviation (SD = 0.42), and the mean prediction error MPE = 26%. In order to complete the statistical analysis, Figure 3A reports the residuals from the linear regression model in eq 5. Given that the R^2 between residuals and $\mathrm{Ln}(1/K_H)$ values is less than 0.008, no mathematical dependence between them can be found.

$$\ln(1/K_{H\mathrm{exp}}) = -0.21(\pm 0.09) + 0.86(\pm 0.03) \times \ln(1/K_{H\mathrm{COSMO\text{-}RS}}) \qquad (5)$$

Therefore, the statistical results indicated the suitability of the implemented COSMO-RS approach to provide reasonable predictions of the Henry's Law constants of a great number of compounds in ILs, including N_2 and CO_2. However, the generally larger deviation of COSMO-RS predictions when the K_H value increases should be noted; this is for gases (N_2, H_2, O_2, etc.) scarcely soluble in ILs, as can be seen in Table S2 (Supporting Information). In addition, for a further optimization of the solubility predictions for the particular case of CO_2 in ILs, Henry's constants of CO_2 in 20 different ILs constituted by a variety of cations (including imidazolium, pyrrolidium, thiouronium, and functionalized ones) and anions ([BF_4^-], [PF_6^-], [NTf_2^-], [$CF_3SO_3^-$], [DCN^-], [FEP^-]) were computed using COSMO-RS and compared with the available experimental data, given in Figure 2 and Table S3 (Supporting Information). The linear regression fit between experimental and calculated K_H data is provided by eq 6, with statistical results of R^2 = 0.87, SD = 0.82, and MPE = 33%, suggesting the capability of the COSMO-RS approach to predict qualitatively the trend of Henry's constants

of CO_2 in a great diversity of ILs. Again, the residual analysis reported in Figure 3B from the linear regression model in eq 6 evidences no mathematical dependence between the correlated data.

$$K_{H\text{exp}} = 1.8(\pm 0.3) + 0.48(\pm 0.04) \times K_{H\text{COSMO-RS}} \quad (6)$$

The next step was to evaluate the capability of the COSMO-RS method to predict the CO_2/N_2 selectivity in SILMs. To this purpose, much selectivity experimental data including 14 imidazolium ILs based on anions $[BF_4^-]$, $[CF_3SO_3^-]$, $[NTf_2^-]$, $[DCN^-]$, $[B(CN)_4^-]$, and $[C(CN)_3^-]$ were compared to the bulk selectivity values estimated by the application of eq 4 and a previous computation of the Henry's Law constants of the compounds in ILs by COSMO-RS. Despite the evidenced COSMO-RS capability to provide qualitative predictions of the gas solubility trends in ILs, the slopes of the linear regression fittings in eqs 5 and 6 suggest an overestimation of the predicted values in comparison to the experimental ones. Therefore, with the aim of providing an optimization of the methodology to describe the CO_2/N_2 selectivity in SILMs, we propose to correct the computed COSMO-RS Henry's Law constants of CO_2 and N_2 by the utilization of the adjustment eqs 5 and 6. The corrected K_H values (see Tables S2 and S3, Supporting Information) are quantitatively closer to the experimental ones than the standard COSMO-RS predictions, especially for high K_H values. The experimental vs the estimated values of CO_2/N_2 selectivity (see Table S4, Supporting Information) are plotted in Figure 4A and B, from the respective estimations of the bulk selectivity values by K_H prediction with standard and corrected COSMO-RS approaches. Linear regression analyses in Table 1 showed a reasonable capability of COSMO-RS to predict the CO_2/N_2 selectivity trends in SILMs. The slopes of the linear regression fittings and the mean error for standard and optimized COSMO-RS methods sustain the larger suitability of the latter to provide a more accurate description of the CO_2/N_2 selectivity behavior in SILMs. Thus, the optimized COSMO-RS computational approach (with Henry's Law constant values estimated using the experimental−calculated linear correlations reported in eqs 5 and 6) will be applied in further analysis as an optimized methodology for the estimation of CO_2/N_2 bulk selectivity to simulate this property in SILMs.

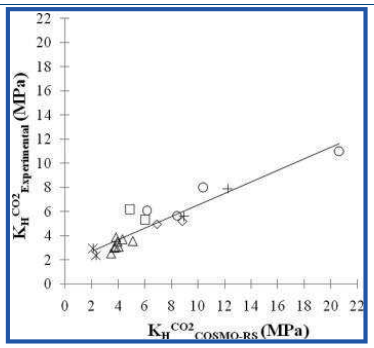

Figure 2. Comparison between the experimental and COSMO-RS predicted Henry's Law constants of CO_2 in ILs [∗ FEP^-, △ NTf_2^-, □ PF_6^-, ◇ CF_3SO_3, ○ BF_4^-, + DCN^-] at near-ambient temperature.

3.2. Screening of CO_2/N_2 Selectivities in SILMs by COSMO-RS Methodology. The next objective of this work was to apply the corrected COSMO-RS approach to design suitable SILM systems for the selective separation of CO_2 from N_2, with the aim of reducing the range of preliminary experimental measurements for SILM-based process development. To this purpose, a computational screening of CO_2/N_2 selectivities was performed for 224 ILs based on different cations (imidazolium, pyridinium, pyrrolodinium, quinolinium, ammonium, phosphonium, thioronium) and anions ($[FEP^-]$, $[NTf_2^-]$, $[FeCl_4^-]$, $[CF_3SO_3^-]$, $[CF_3CO_3^-]$, $[B(CN)_4^-]$, $[NO_3^-]$, $[CH_3CO_2^-]$, $[CH_3SO_3^-]$, $[CH_3SO_4^-]$, $[C(CN)_3^-]$, $[DCN^-]$, $[BF_4^-]$, $[SCN^-]$). The results of the CO_2/N_2 selectivity screening in ILs using the optimized COSMO-RS approach are presented in Figure 5. In general, it can be observed that the anions mainly determine the selective separation of CO_2 from N_2 in SILMs, while the cations play a secondary role, as it is reported in the literature.[17,18] In addition, regarding the structure of the cations, it is noticeable that neither a longer alkyl chain attached to an imidazolium ring nor the functionalization by fluorination seem to improve the CO_2/N_2 selectivity in SILMs, which is in good agreement with experimental evidence.[21,25] These findings may be surprising since contrary behavior has been observed in the particular case of CO_2 solubility in bulk ILs.[18,26−28] Regarding the influence of the anion structure on CO_2/N_2 selectivity, it can be observed that well-known anions for enhancing the solubility of

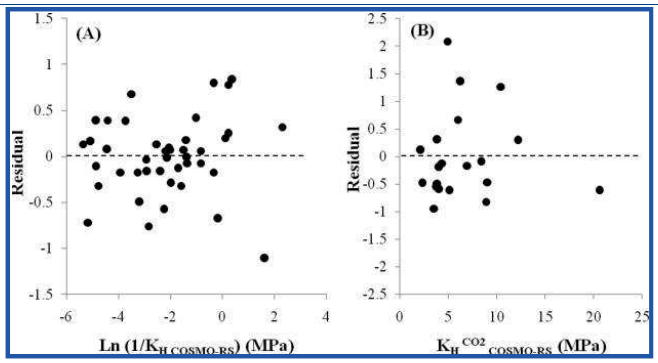

Figure 3. Graphical analysis of residuals obtained from a comparison between the experimental and COSMO-RS Henry's Law constants of (A) common solutes including N_2 and (B) CO_2 in ILs at near-ambient temperature.

dx.doi.org/10.1021/ie102450x |*Ind. Eng. Chem. Res.* 2011, 50, 5739–5748

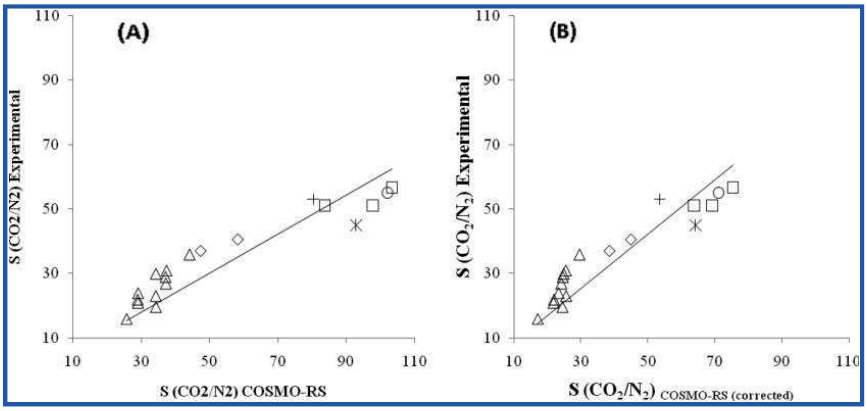

Figure 4. Comparison between experimental and predicted CO_2/N_2 selectivities in SILMs [○ BF_4^-, □ DCN^-, ◇ $CF_3SO_3^-$, △ NTf_2^-, ∗ $C(CN)_3^-$, and + $B(CN)_4^-$] at near-ambient temperature, using Henry's Law constants predicted by (A) standard COSMO-RS and (B) optimized COSMO-RS.

Table 1. Statistical Results Obtained from Comparison of Experimental and Predicted CO_2/N_2 Selectivities in SILMs (N = 19)

	linear regression[a]			
model	B (slope)	R^2	SD	MPE (%)
COSMO-RS	0.60	0.95	6.6	50
Optimized COSMO-RS	0.84	0.95	6.5	16

[a] $S_{CO2/N2,\,exp} = B \times S_{CO2/N2,COSMO\text{-}RS}$

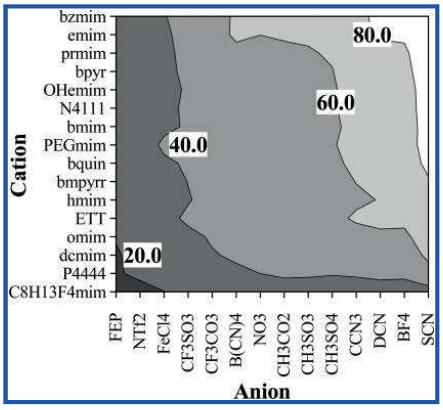

Figure 5. Screening of CO_2/N_2 selectivity in 224 SILMs at T = 298.1 K calculated by optimized COSMO-RS approach.

CO_2 in bulk ILs, such as $[NTf_2^-]$ or $[FEP^-]$, do not seem to represent a good choice for designing SILMs suitable for the separation of CO_2 from N_2; meanwhile, less fluorinated anions such as $[BF_4^-]$ or anions containing nitrile groups such as $[DCN^-]$ are a better option to improve the CO_2/N_2 selectivity in SILMs, as it is shown in the literature.[15,17,20−22] The CO_2/N_2 selectivity screening presented in this paper suggested the proposal of a novel type of SILM based on the SCN^- anion, which has not been reported before and that may be capable of achieving CO_2/N_2 selectivities up to 90 under ambient operating conditions, based on optimized COSMO-RS results. Moreover, an important feature associated with the potential application of $[SCN^-]$-based SILMs is that, on the basis of simulation, the CO_2/N_2 selectivity significantly depends on the counteranion structure, in contrast to the cases of ILs with $[NTf_2^-]$ or $[FEP^-]$ anions. Therefore, the cation family and the alkyl substituent of the cation can be selected to tune CO_2/N_2 selectivity and other properties of interest of the ILs, such as density or viscosity, to optimize the CO_2/N_2 separation process based in membrane technology. Hence, taking into account that ILs based on the $[SCN^-]$ anion are already commercially available, future investigations will be focused on the experimental analysis of $[SCN^-]$-based SILMs to evaluate their feasibility on the selective separation of CO_2 from N_2.

3.3. Analysis of CO_2/N_2 Selectivities in SILMs by COSMO-RS Methodology. The third objective of this work was to achieve a further understanding of CO_2/N_2 selectivity behavior in SILMs by applying COSMO-RS methodology. To this end, the CO_2/N_2 selectivity differences among ILs, computed by using eq 4, were analyzed in terms of Henry's Law coefficients of CO_2 and N_2, i.e., by using an optimized COSMO-RS approach. Series of imidazolium cations paired with $[FEP^-]$, $[NTf_2^-]$, $[BF_4^-]$, $[CF_3SO_3^-]$, $[DCN^-]$, and $[SCN^-]$ anions were selected as representative ILs to perform the CO_2/N_2 selectivity analysis in SILMs. The comparison of the CO_2/N_2 selectivity in SILMs with the Henry's Law constants of each gas in the ILs is plotted in Figure 6. The large difference between K_H values of CO_2 and N_2 in ILs (i.e., $K_{H\ (CO2/[emim][SCN])}$ = 5.5; $K_{H\ (N2/[emim][SCN])}$ = 553.6) makes it necessary to plot the K_H parameter on a logarithmic scale to present the whole range of data, as in Figure 6. Such differences between the Henry's Law constants of CO_2 and N_2 in ILs (over 2 orders of magnitude) make clear the distinct solubility of each solute in the solvent, with the former being much soluble in the ILs than the latter. However, the results indicate that the solubility of CO_2 in ILs does not determine the CO_2/N_2 selectivity in SILMs. In fact, ILs based on $[FEP^-]$ and $[NTf_2^-]$ anions present the largest solubility of both CO_2 and N_2 (see Figure 6), but they also present the lowest CO_2/N_2 selectivity to be applied in membrane

technology. On the contrary, anions such as [BF_4^-] or [DCN^-], which provide much lower solubilities of CO_2 in bulk ILs, are clearly better alternatives for enhancing the selective separation of CO_2 from N_2 in SILMs. As can be seen in Figure 6, larger differences between the Henry's Law constant values of CO_2 and N_2 are found when generally the gas solubility decreases in ILs. In this respect, the ILs based on the [SCN^-] anion, proposed in this work to improve the CO_2/N_2 selectivity in SILMs, provide larger differences between the solubilities of CO_2 and N_2 in ILs, which may result in a higher CO_2/N_2 selectivity when they are applied in separation processes based on membranes.

Once it was exhibited that the CO_2/N_2 selectivity behavior in SILMs can be explained in terms of the difference between K_H values of CO_2 and N_2 in the specific IL, we analyzed Henry's Law constants of CO_2 and N_2 in terms of the excess enthalpy, H_m^E, for CO_2/N_2 solute and bulk IL mixtures, based on the relationship found in a previous work.[63] The COSMO-RS method was used to predict the excess enthalpy of a gas-IL liquid mixture, H_m^E, by summing the contributions of each component of the mixture, according to the expression

$$H_m^E = x_{IL}H_{IL}^E + x_{gas}H_{gas}^E = x_{IL}\cdot[H_{IL,\,mixture} - H_{IL,\,pure}] + x_{gas}[H_{gas,\,mixture} - H_{gas,\,pure}] \quad (7)$$

However, the suitability of canceling the term $H_{gas,pure}$ in eq 7 has been demonstrated[63] in the case of physical absorption of CO_2 in ILs, in order to obtain a more realistic simulation of the solution of the gas compound in the liquid phase, since the intermolecular interactions between the molecules in the gas phase can be reasonably considered to be negligible with respect to the interactions in the liquid phase. Thus, the above approach was extended to both gaseous solutes in this work to obtain a more consistent expression (eq 8) for excess enthalpy of the mixture, $H_m^{E'}$, to analyze CO_2 and N_2 solubilities in ILs:

$$H_m^{E'} = x_{IL}[H_{IL,\,mixture} - H_{IL,\,pure}] + x_{gas}[H_{gas,\,mixture}] \quad (8)$$

Thus, the excess molar enthalpy for mixtures of CO_2 or N_2 and bulk IL was calculated using the COSMO-RS method at solute concentrations corresponding to the solubility data in ILs at 298.1 K and 1 atm. As a result, Figure 7A and B compare the Henry's Law constants of CO_2 and N_2 in 35 imidazolium-based ILs to the corresponding H_m^E calculated by COSMO-RS (see Table S5, Supporting Information). Higher solubilities (decreasing K_H values) of CO_2 and N_2 in ILs are associated with a higher exothermicity (decreasing H_m^E values) of the mixture, whereas lower solubilities of the solutes in the ILs are related with enthalpy values of the liquid mixtures close to zero. Note the much higher absorption enthalpies for CO_2 in ILs with respect to the case of N_2−IL mixtures, which makes the distinct intermolecular interactions of each solute with the IL solvent clear. In addition, it can be appreciated that ILs with positive characteristics for the absorption of both gases, those that provide low CO_2/N_2 selectivities in membranes, such as [FEP^-]-based ILs, show pronounced exothermicity behavior for CO_2 absorption and less marked but also exothermic behavior for N_2 dissolution (i.e., [emim][FEP]: $\Delta H_{CO2}^E = -0.218$ kJ/mol; $\Delta H_{N2}^E = -0.002$ kJ/mol); meanwhile, ILs that enhance CO_2/N_2 selectivity, such as those based on the [DCN^-] anion, exhibit much lower exothermicity behavior for CO_2 dissolution and positive values of the absorption enthalpy of

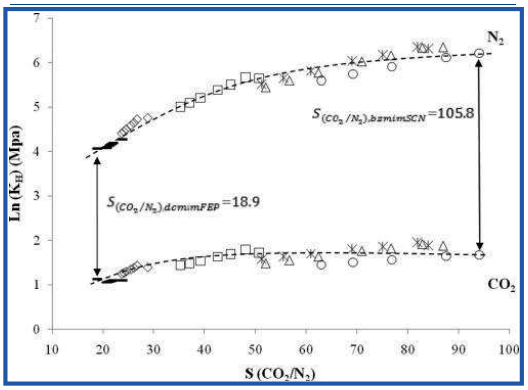

Figure 6. Comparison of Henry's law constants of CO_2 and N_2 in ILs with CO_2/N_2 selectivity in SILMs [○ SCN^-, △ BF_4^-, ∗ DCN^-, □ $CF_3SO_3^-$, ◊ NTf_2^- and — FEP^-] at T = 298.1 K calculated by optimized COSMO-RS.

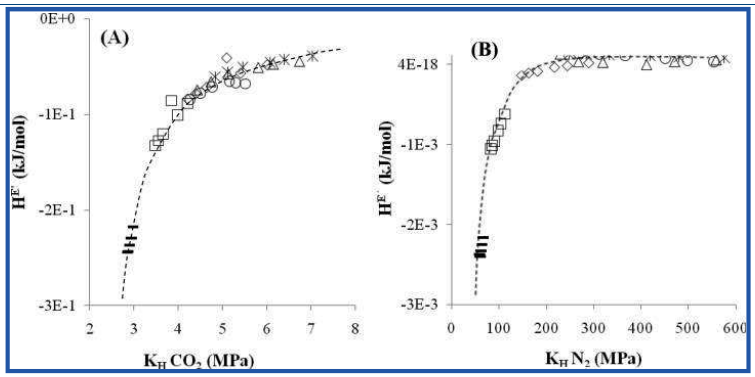

Figure 7. Comparison of Henry's Law constants with the excess molar enthalpies [○ SCN^-, △ BF_4^-, ∗ DCN^-, □ $CF_3SO_3^-$, ◊ NTf_2^- and — FEP^-] at T = 298.1 K calculated using a corrected COSMO-RS. (A) CO_2−IL systems and (B) N_2−IL systems.

dx.doi.org/10.1021/ie102450x |Ind. Eng. Chem. Res. 2011, 50, 5739–5748

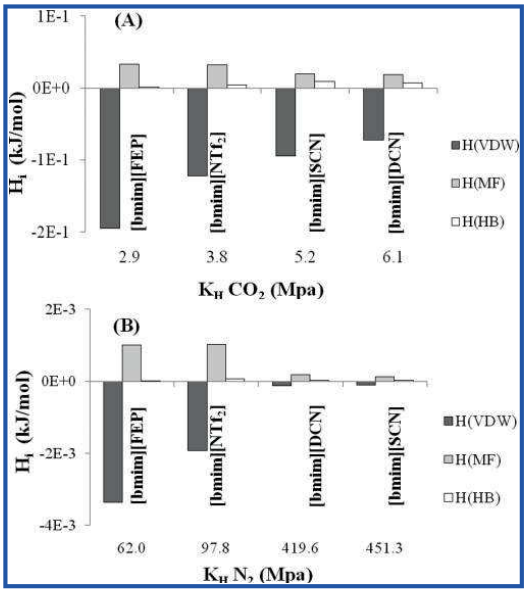

Figure 8. Description of the anion effect on Henry's Law constants of CO_2 and N_2 in ILs at T = 298.1 K by using the interaction energy contributions [electrostatic, H(MF); van der Waals H(VDW); and hydrogen-bonding, H(HB)] to excess molar enthalpies calculated by corrected COSMO-RS (A) CO_2−IL systems and (B) N_2−IL systems.

N_2 in the ILs, which indicates no affinity for the N_2 solute (i.e., [emim][DCN]: ΔH_{CO2}^{E} = −0.039 kJ/mol; ΔH_{N2}^{E} = 0.00003 kJ/mol). In this respect, it has to be noticed that the [SCN$^-$]-based SILMs proposed in this work possess favorable characteristics for the CO_2/N_2 separation in terms of energetic balance, since they exhibit even less affinity for N_2 while enhancing CO_2 solubility in the IL (i.e., [emim][SCN]: ΔH_{CO2}^{E} = −0.068 kJ/mol; ΔH_{N2}^{E} = 0.00008 kJ/mol) in comparison to those suggested in the literature, such as [DCN$^-$]-based SILMs.[15]

Following the CO_2/N_2 selectivity analysis in SILMs from an energetic point of view, the last step is an attempt at understanding the role of the different intermolecular interaction contributions [electrostatic (misfit), hydrogen-bonding, and van der Waals] between CO_2 or N_2 and ILs in the fluid phase by applying a COSMO-RS methodology.[63] Considering that the estimations of $H_m^{E'}$ in eq 8 can be expressed by the sum of the intermolecular interaction contributions

$$H_m^{E'} = H_m^{E'}(\text{H-bond}) + H_m^{E'}(\text{misfit}) + H_m^{E'}(\text{VdW}) \quad (9)$$

COSMO-RS was used to analyze the Henry's Law coefficients of CO_2 and N_2 in ILs in terms of the different solute−solvent interaction contributions to the $H_m^{E'}$ values of the CO_2−IL and N_2−IL systems, as reported in Figure 8. Series of an imidazolium cation paired with [FEP$^-$], [NTf$_2^-$], [DCN$^-$], and [SCN$^-$] were selected as representative ILs to illustrate the diverse CO_2/N_2 selectivity behaviors in SILMs. In general, it can be seen that the van der Waals forces determine the gas solubility of CO_2 and N_2 in ILs, while the electrostatic interactions play a repulsive but secondary role, and the hydrogen bonding interactions make a negligible contribution to the excess values of $H_m^{E'}$. The dominant interactions of van der Waals in the case of the fluorinated ions [FEP$^-$] and [NTf$_2^-$] are very significant, which contributes to the exothermicity of CO_2−IL and N_2−IL mixtures, increasing the solubility of both gaseous solutes in the liquid phase, hence diminishing the CO_2/N_2 selectivity in SILMs. On the contrary, ILs based on [DCN$^-$] and [SCN$^-$] anions exhibit lower exothermic behavior for CO_2 and N_2 absorptions, with minor van der Walls contributions related to the solubility of CO_2 in the solvent and showing no affinity for the N_2 solute, as indicated in the insignificant energetic contributions to the absorption enthalpy of N_2−ILs systems. Note that the results presented in Figure 8 support the proposal of using [SCN$^-$]-based SILMs to improve the CO_2/N_2 selective separation, since the ILs based on [SCN$^-$] anions are capable of increasing the CO_2 solubility by enhancing the van der Walls intermolecular interactions between the CO_2 and the IL, while exhibiting even less affinity for the N_2 solute than the [DCN$^-$]-based ILs.

4. CONCLUSIONS

The CO_2/N_2 selectivity in SILMs was estimated by the solubility ratio between gases in terms of the Henry's Law constant of each solute in the specific IL calculated by COSMO-RS. A general evaluation of the capability of COSMO-RS to predict the Henry's Law constants of gases in ILs was performed by the implementation of an ion-independent molecular model, with results indicating the capability of the computational approach to provide qualitative predictions of the solubility trends of a wide diversity of solutes in ILs, although suggesting an overestimation of the predicted values in comparison to the experimental ones. Therefore, the experimental-calculated correlations obtained by linear regression fitting of the data were applied to correct the computed Henry's Law constants of gaseous solutes in order to obtain a more accurate estimation of the CO_2/N_2 selectivity values in SILMs.

A relevant contribution of the CO_2/N_2 selectivity screening presented in this paper is the proposal of a novel type of SILMs based on [SCN$^-$] anions, which have not been reported before and that may be capable of achieving high CO_2/N_2 selectivities under ambient operating conditions, on the basis of simulation results. Moreover, an important feature associated with the potential application of the commercially available [SCN$^-$]-based ILs in membrane technology is that the CO_2/N_2 selectivity also depends on the counteranion structure, which makes it possible to select the cation family and its alkyl substituent to tune CO_2/N_2 selectivity and other properties of interest of the ILs, such as density or viscosity, to optimize the CO_2/N_2 separation in SILMs.

Finally, for a deeper understanding of the CO_2/N_2 selectivity behavior in SILMs, the Henry's Law constants of each solute in the ILs were successfully related to the excess enthalpy of CO_2−IL and N_2−IL mixtures in solution predicted by COSMO-RS, with results indicating that higher solubilities of CO_2 and N_2 in ILs are associated with a higher exothermicity of the mixture and higher contributions of the van der Waals intermolecular interactions to the excess enthalpy of absorption. However, the ILs that may improve the CO_2/N_2 selectivities in SILMs, such as [SCN$^-$]-based ILs, are those with generally low gas solubilities but capable of increasing the CO_2 solubility by enhancing the van der Waals intermolecular interactions of CO_2 in the mixture while exhibiting no affinity for N_2.

■ ASSOCIATED CONTENT

Supporting Information. List of ionic liquids, experimental and estimated Henry constants, experimental and predicted CO_2/N_2 selectivities, comparison of corrected Henry's law constants with excess molar enthalpies (Tables S1−S5). This material is available free of charge via the Internet at http://pubs.acs.org.

■ AUTHOR INFORMATION

Corresponding Author

*Phone: 34 91 4976938. Fax: 34 91 4973516. E-mail: pepe.palomar@uam.es.

■ ACKNOWLEDGMENT

The authors are grateful to the "Ministerio de Ciencia e Innovación" and "Comunidad de Madrid" for financial support (projects CTQ2008-01591, CTQ2008-05641, and S2009/PPQ-1545). We are very grateful to "Centro de Computación Científica de la Universidad Autónoma de Madrid" for computational facilities.

■ REFERENCES

(1) IPCC, 2007: Summary for Policymakers. In *Climate Change 2007: The Physical Science Basis. Contribution of Working Group I to the Fourth Assessment Report of the Intergovernmental Panel on Climate Change*; Solomon, S., Qin, D., Manning, M., Chen, Z., Marquis, M., Averyt, K. B., M., Tignor Miller, H. L., Eds.; Cambridge University Press: Cambridge, U. K.

(2) Pennlinea, H. W.; Luebkea, D. R.; Jonesa, K. L.; Myersa, C. R.; Morsib, B. I.; Heintzb, Y. J.; Ilconichc, J. B. Progress in carbon dioxide capture and separation research for gasification-based power generation point sources. *Fuel Process. Technol.* **2008**, *89*, 897–907.

(3) Figueroa, J. D.; Fout, T.; Plasynsky, S.; McIlvried, H.; Srivastava, R. D. Advances in CO_2 capture technology - The U.S. Department of Energy's Carbon Sequestration Program. *IJGGC* **2008**, *2*, 9–20.

(4) Favre, E. Carbon dioxide recovery from post-combustion processes: Can gas permeation membranes compete with absorption? *J. Membr. Sci.* **2007**, *294*, 50–59.

(5) Kocherginsky, N. M.; Yang, Q.; Seelam, L. Recent advances in supported liquid membrane technology. *Sep. Purif. Technol.* **2007**, *53*, 171–177.

(6) Teramoto, M.; Sakaida, Y.; Fu, S. S.; Ohnishi, N.; Matsuyama, H.; Maki, T.; Fukui, T.; Arai, K. An attempt for the stabilization of supported liquid membrane. *Sep. Purif. Technol.* **2000**, *21*, 137–144.

(7) Wasserscheid, P.; Welton, T. *Ionic Liquids in Synthesis*; Wiley-VCH Verlag GmbH & Co. KGaA: Weinheim, Germany, 2008.

(8) Anthony, J. L.; Aki, S.; Maggin, E. J.; Brennecke, J. F. Feasibility of using ionic liquids for carbon dioxide capture. *IJETM* **2004**, *4* (1−2), 105–115.

(9) Bara, J. E.; Carliste, T. K.; Gabriel, C. J.; Camper, D.; Finotello, A.; Gin, D. L.; Noble, R. D. Guide to CO_2 separations in imidazolium-based room-temperature ionic liquids. *Ind. Eng. Chem. Res.* **2009**, *48*, 2739–2751.

(10) Shiflett, M. B.; Yokozeki, A. Solubilities and Diffusivities of Carbon Dioxide in Ionic Liquids: [bmim][PF_6] and [bmim][BF_4]. *Ind. Eng. Chem. Res.* **2005**, *44* (12), 4453–4464.

(11) Huang, J.; Rüther, T. Why are ionic liquids attractive for CO_2 absorption? An overview. *Aust. J. Chem.* **2009**, *62*, 298–308.

(12) Scovazzo, P. Determination of the upper limits, benchmarks, and critical properties for gas separations using stabilized room temperature ionic liquid membranes (SILMs) for the purpose of guiding future research. *J. Membr. Sci.* **2009**, *343* (1−2), 199–211.

(13) Hassib-ur-Raman, M.; Siaj, M.; Larachi, F. Ionic liquids for CO_2 capture-development and progress. *Chem. Eng. Proc.* **2010**, 313–322.

(14) Bara, J. E.; Camper, D. E.; Gin, D. L.; Noble, R. D. Room-temperature ionic liquids and composite materials: platform technologies for CO_2 capture. *Acc. Chem. Res.* **2010**, *43* (1), 152–159.

(15) Scovazzo, P.; Kieft, J.; Finan, D. A.; Koval, C.; DuBois, D.; Noble, R. Gas separation using non-hexafluorophosphate $[PF_6]^-$ anion supported ionic liquids membranes. *J. Membr. Sci.* **2004**, *238*, 56–63.

(16) Camper, D.; Bara, J.; Koval, C.; Noble, R. Bulk-fluid solubility and membrane feasibility of Rmim-based room temperature ionic liquids. *Ind. Eng. Chem. Res.* **2006**, *45*, 6279–6283.

(17) Scovazzo, P.; Havard, D.; McShea, M.; Mixon, S.; Morgan, D. Long-term, continuous mixed-gas dry fed CO_2/CH_4 and CO_2/N_2 separation performance and selectivities for room temperature ionic liquid membranes. *J. Membr. Sci.* **2009**, *327*, 41–48.

(18) Anthony, J. L.; Anderson, J. L.; Magín, E. J.; Brennecke, J. F. Anion effects on gas solubility in ionic liquids. *J. Phys. Chem. B* **2005**, *109*, 6366–6374.

(19) Jacquemin, J.; Husson, P.; Majer, V.; Costa, M. F. Influence of the cation on the solubility of CO_2 and H_2 in ionic liquids based on the bis(trifluoromethylsulfonyl)imide anion. *J. Sol. Chem.* **2007**, *36*, 967–979.

(20) Finotello, A.; Bara, J. E.; Narayan, S.; Camper, D.; Noble, R. D. Ideal gas solubilities and solubility selectivities in a binary mixture of room-temperature ionic-liquids. *J. Phys. Chem. B* **2008**, *112*, 2335–2339.

(21) Neves, L. A.; Crespo, J. G.; Coelhoso, I. M. Gas permeation studies in supported ionic liquids membranes. *J. Membr. Sci.* **2010**, *357*, 160–170.

(22) Zhao, W.; He, G.; Zhang, L.; Ju, J.; Dou, H.; Nie, F.; Li, C.; Liu, H. Effect of water in ionic liquid on the separation performance of supported ionic liquid membrane for CO_2/N_2. *J. Membr. Sci.* **2010**, *350*, 279–285.

(23) Mahurin, S. M.; Lee, J. S.; Baker, G. A.; Luo, H.; Dai, S. Performance of nitrile-containing anions in task-specific ionic liquids for improved CO_2/N_2 separation. *J. Membr. Sci.* **2010**, *353*, 177–183.

(24) Cserjesi, P.; Nemestothy, N.; Bako, K. B. Gas separation properties of supported liquid membranes prepared with unconventional ionic liquids. *J. Membr. Sci.* **2010**, *349*, 6–11.

(25) Bara, J. E.; Gabriel, C. J.; Carlisle, T. K.; Camper, D. E.; Finotello, A.; Gin, D. L.; Noble, R. D. Gas separations in fluoroalkyl-functionalized room-temperature ionic liquids using supported liquid membranes. *Chem. Eng. J.* **2009**, *147*, 43–50.

(26) Zhang, X.; Liu, Z.; Wang, W. Screening of ionic liquids to capture CO_2 by COSMO-RS and experiments. *AIChE J.* **2008**, *54* (10), 2717–2728.

(27) Muldoon, M. J.; Aki, S. N.; Anderson, J. L.; Dixon, J. K.; Brennecke, J. F. Improving carbon dioxide solubility in ionic liquids. *J. Phys. Chem. B* **2007**, *111*, 9001–9009.

(28) Zhang, X.; Hun, F.; Liu, Z.; Wang, W.; Shi, W.; Maginn, E. J. Absorption of CO_2 in the ionic liquid tris(pentafluoroethyl)-trifluorophosphate ([hmim][FEP]): A molecular view by computer simulations. *J. Phys. Chem. B* **2009**, *113*, 7591–7598.

(29) Ally, M. R.; Braunstein, J.; Baltus, R. E.; Dai, S. Irregular ionic lattice model for gas solubilities in ionic liquids. *Ind. Eng. Chem. Res.* **2004**, *43*, 1296–1301.

(30) Kroon, M. C.; Karakatsani, E. K.; Economou, I. G.; Witkamp, G. J.; Peters, C. J. Modeling of the carbon dioxide solubility in imidazolium-based ionic liquids with the tPC-PSAFT equation of state. *J. Phys. Chem. B* **2006**, *112*, 9262–9269.

(31) Wang, T. F.; Peng, C. J.; Liu, H. L.; Hu, Y. Description of the pVT behavior of ionic liquids and the solubility of gases in ionic liquids using an equation of state. *Fluid Phase Equilib.* **2006**, *250*, 150–157.

(32) Andreu, J. S.; Vega, L. F. Capturing the solubility behavior of CO_2 in ionic liquids by a simple model. *J. Phys. Chem. C* **2007**, *111*, 16028–16034.

(33) Kim, Y. S.; Choi, W. Y.; Jang, J. H.; Lee, C. S. Solubility measurement and prediction of carbon dioxide in ionic liquids. *Fluid Phase Equilib.* **2005**, *228−229*, 439–445.

(34) Klamt, A. *COSMO-RS: From Quantum Chemistry to Fluid Phase Thermodynamics and Drug Design*; Elsevier: Amsterdam, 2005.
(35) Palomar, J.; Torrecilla, J. S.; Ferro, V. R.; Rodríguez, F. Development of an a Priori Ionic Liquid Design Tool. 1. Integration of a Novel COSMO-RS Molecular Descriptor on Neural Networks. *Ind. Eng. Chem. Res.* **2008**, *47*, 4523–4532.
(36) Palomar, J.; Torrecilla, J. S.; Ferro, V. R.; Rodríguez, F. Development of an a Priori Ionic Liquid Design Tool. 2. Ionic Liquid Selection through the Prediction of COSMO-RS Molecular Descriptor by Inverse Neural Network. *Ind. Eng. Chem. Res.* **2009**, *48*, 2257–2265.
(37) Palomar, J.; Ferro, V. L.; Torrecilla, J. S.; Rodriguez, F. Density and molar volume predictions using COSMO-RS for ionic liquids. An approach to solvent design. *Ind. Eng. Chem. Res.* **2007**, *46* (18), 6041–6048.
(38) Diedenhofen, M.; Klamt, A.; Marsh, K.; Schafer, A. Prediction of the vapor pressure and vaporization enthalpy of 1-n-alkyl-3-methylimidazolium-bis-(trifluoromethanesulfonyl) amide ionic liquids. *Phys. Chem. Chem. Phys.* **2007**, *9* (33), 4653–4656.
(39) Simoni, L. D.; Brennecke, J. F.; Stadtherr, M. A. Asymmetric Framework for Predicting Liquid-Liquid Equilibrium of Ionic Liquid-Mixed-Solvent Systems. 1. Theory, Phase Stability Analysis, and Parameter Estimation. *Ind. Eng. Chem. Res.* **2009**, *48* (15), 7246–7256.
(40) Banerjee, T.; Khanna, A. Infinite dilution activity coefficients for trihexyltetradecyl phosphonium ionic liquids: Measurements and COSMO-RS prediction. *J. Chem. Eng. Data* **2006**, *51* (6), 2170–2177.
(41) Diedenhofen, M.; Eckert, F.; Klamt, A. Prediction of infinite dilution activity coefficients of organic compounds in ionic liquids using COSMO-RS. *J. Chem. Eng. Data* **2003**, *48* (3), 475–479.
(42) Navas, A.; Ortega, J.; Vreekamp, R.; Marrero, E.; Palomar, J. Experimental Thermodynamic Properties of 1-Butyl-2-methylpyridinium Tetrafluoroborate [b2mpy][BF4] with Water and with Alkan-1-ol and Their Interpretation with the COSMO-RS Methodology. *Ind. Eng. Chem. Res.* **2009**, *48* (5), 2678–2690.
(43) Preiss, U.; Jungnickel, C.; Thoming, J.; Krossing, I.; Luczak, J.; Diedenhofen, M.; Klamt, A. Predicting the Critical Micelle Concentrations of Aqueous Solutions of Ionic Liquids and Other Ionic Surfactants. *Chem.—Eur. J.* **2009**, *15* (35), 8880–8885.
(44) Freire, M. G.; Ventura, S. P.; Santos, L. M.; Marrucho, I. M.; Coutinho, J. Evaluation of COSMO-RS for the prediction of LLE and VLE of water and ionic liquids binary systems. *Fluid Phase Equilib.* **2008**, *268* (1−2), 74–84.
(45) Lei, Z. G.; Arlt, W.; Wasserscheid, P. Selection of entrainers in the 1-hexene/n-hexane system with a limited solubility. *Fluid Phase Equilib.* **2007**, *260*, 29–35.
(46) Freire, M. G.; Santos, L. M.; Marrucho, I. M.; Coutinho, J. Evaluation of COSMO-RS for the prediction of LLE and VLE of alcohols plus ionic liquids. *Fluid Phase Equilib.* **2007**, *255* (2), 167–178.
(47) Banerjee, T.; Singh, M. K.; Khanna, A. Prediction of binary VLE for imidazolium based ionic liquid systems using COSMO-RS. *Ind. Eng. Chem. Res.* **2006**, *45* (9), 3207–3219.
(48) Kato, R.; Gmehling, J. Systems with ionic liquids: Measurement of VLE and gamma(infinity) data and prediction of their thermodynamic behavior using original UNIFAC, mod. UNIFAC(Do) and COSMO-RS(O1). *J. Chem. Thermodyn.* **2005**, *37* (6), 603–619.
(49) Beste, Y.; Eggersmann, M; Schoenmakers, H. Extractive distillation with ionic fluids. *Chem. Ing. Tech.* **2005**, *77* (11), 1800–1808.
(50) Lapkin, A. A.; Peters, M.; Greiner, L.; Chemat, S.; Leonhard, K.; Liaw, M. A.; Leitner, W. Screening of new solvents for artemisinin extraction process using ab initio methodology. *Green Chem.* **2010**, *12* (2), 241–251.
(51) Mohanty, S.; Banerjee, T.; Mohanty, K. Quantum Chemical Based Screening of Ionic Liquids for the Extraction of Phenol from Aqueous Solution. *Ind. Eng. Chem. Res.* **2010**, *49* (6), 2916–2925.
(52) Kumar, A. A.; Banerjee, T. Thiophene separation with ionic liquids for desulphurization: A quantum chemical approach. *Fluid Phase Equilib.* **2009**, *278* (1−2), 1–8.
(53) Freire, M. G.; Carvalho, P. J.; Gardas, R. L.; Santos, L. M.; Marrucho, I. M.; Coutinho, J. Solubility of Water in Tetradecyltrihexylphosphonium-Based Ionic Liquids. *J. Chem. Eng. Data* **2008**, *53* (10), 2378–2382.
(54) Freire, M. G.; Carvalho, P. J.; Gardas, R. L.; Marrucho, I. M.; Santos, L. M.; Coutinho, J. A. Mutual solubilities of water and the [C(n)mim][Tf2N] hydrophobic ionic liquids. *J. Phys. Chem. B* **2008**, *112* (6), 1604–1610.
(55) Banerjee, T.; Verma, K. K.; Khanna, A. Liquid-liquid equilibrium for ionic liquid systems using COSMO-RS: Effect of cation and anion dissociation. *AIChE J.* **2008**, *54* (7), 1874–1885.
(56) Sahandzhieva, K.; Tuma, D.; Breyer, S.; Kamps, A. P.; Maurer, G. Liquid-liquid equilibrium in mixtures of the ionic liquid 1-n-butyl-3-methylimidazolium hexafluorophosphate and an alkanol. *J. Chem. Eng. Data* **2006**, *51* (5), 1516–1525.
(57) Lei, Z. G.; Arlt, W.; Wasserscheid, P. Separation of 1-hexene and n-hexane with ionic liquids. *Fluid Phase Equilib.* **2006**, *241* (1−2), 290–299.
(58) Domanska, U.; Pobudkowska, A.; Eckert, F. (Liquid plus liquid) phase equilibria of 1-alkyl-3-methylimidazolium methylsulfate with alcohols, or ethers, or ketones. *J. Chem. Thermodyn.* **2006**, *38* (6), 685–695.
(59) Jork, C.; Kristen, C.; Pieraccini, D.; Stark, A.; Chiappe, C.; Beste, Y. A.; Arlt, W. Tailor-made ionic liquids. *J. Chem. Thermodyn.* **2005**, *37* (6), 537–558.
(60) Palomar, J.; Lemus, J.; Gilarranz, M. A.; Rodríguez, J. J. Adsorption of ionic liquids from aqueous effluents by activated carbon. *Carbon* **2009**, *47* (7), 1846–1856.
(61) Rosol, Z. P.; German, N. J.; Gross, S. M. Solubility, ionic conductivity and viscosity of lithium salts in room temperature ionic liquids. *Green Chem.* **2009**, *11* (9), 1453–1457.
(62) Manan, N. A.; Hardacre, C.; Jacquemin, J.; Rooney, D. W.; Youngs, T. G. Evaluation of gas solubility prediction in ionic liquids using COSMOthermX. *J. Chem. Eng. Data* **2009**, *54*, 2005–2022.
(63) Palomar, J.; Gonzalez-Miquel, M.; Polo, A.; Rodriguez, F. Understanding the physical absorption of CO_2 in ionic liquids using the COSMO-RS method. *Ind. Eng. Chem. Res.* **2011**, *50*, 3452−3463.
(64) Shimoyama, Y.; Ito, A. Prediction of cation and anion effects on solubilities, selectivities and permeabilities for CO_2 in ionic liquids using COSMO based activity coefficient model. *Fluid Phase Equilib.* **2010**, *297*, 178–182.
(65) Franke, R.; Hannebauer, B.; Jung, S. A Case Study in the Pre-Calculation of Henry Coefficients. *Chem. Eng. Technol.* **2010**, *33* (2), 251–257.Frisch, M. J.; Trucks, G. W.; Schlegel, H. B.; Scuseria, G. E.; Robb, M. A.; Cheeseman, J. R.; Montgomery, J. A., Jr.; Vreven, T.; Kudin, K. N.; Burant, J. C.; Millam, J. M.; Iyengar, S. S.; Tomasi, J.; Barone, V.; Mennucci, B.; Cossi, M.; Scalmani, G.; Rega, N.; Petersson, G. A.; Nakatsuji, H.; Hada, M.; Ehara, M.; Toyota, K.; Fukuda, R.; Hasegawa, J.; Ishida, M.; Nakajima, T.; Honda, Y.; Kitao, O.; Nakai, H.; Klene, M.; Li, X.; Knox, J. E.; Hratchian, H. P.; Cross, J. B.; Bakken, V.; Adamo, C.; Jaramillo, J.; Gomperts, R.; Stratmann, R. E.; Yazyev, O.; Austin, A. J.; Cammi, R.; Pomelli, C.; Ochterski, J. W.; Ayala, P. Y.; Morokuma, K.; Voth, G. A.; Salvador, P.; Dannenberg, J. J.; Zakrzewski, V. G.; Dapprich, S.; Daniels, A. D.; Strain, M. C.; Farkas, O.; Malick, D. K.; Rabuck, A. D.; Raghavachari, K.; Foresman, J. B.; Ortiz, J. V.; Cui, Q.; Baboul, A. G.; Clifford, S.; Cioslowski, J.; Stefanov, B. B.; Liu, G.; Liashenko, A.; Piskorz, P.; Komaromi, I.; Martin, R. L.; Fox, D. J.; Keith, T.; Al-Laham, M. A.; Peng, C. Y.; Nanayakkara, A.; Challacombe, M.; Gill, P. M. W.; Johnson, B.; Chen, W.; Wong, M. W.; Gonzalez, C.; Pople, J. A. *Gaussian 03*, revision B.05; Gaussian, Inc.: Wallingford, CT, 2004.
(66) Sosa, C. J.; Andzelm, B. C.; Elkin, E.; Wimmer, K.; Dobbs, D.; Dixon, D. A. A local density functional study of the structure and vibrational frequencies of molecular transition-metal compounds. *J. Phys. Chem. A* **1992**, *96*, 6630.
(67) Schaefer, A.; Huber, C.; Ahlrichs, R. Fully optimized contracted Gaussian basis sets of triple zeta valence quality for atoms Li to Kr. *J. Chem. Phys.* **1994**, *100*, 5829.
(68) *COSMOtherm C2.1*, release 01.08; GmbH&CoKG: Leverkusen, Germany, 2006. http://www.cosmologic.de (accessed March 2011).
(69) Ionic Liquid Database − (ILthermo). NIST Standard Reference Database # 147. http://ilthermo.boulder.nist.gov/ILThermo/mainmenu.uix ((accessed March 2011).

(70) Shiflett, M. B.; Yokozeki, A. Gaseous absorption of fluoromethane, fluoroethane, and 1,1,2,2-tetrafluoroethane in 1-butyl-3-methylimidazolium hexafluorophosphate. *Ind. Eng. Chem. Res.* **2006**, *45*, 6375–6382.

(71) Anderson, J. L.; Dixon, J. K.; Maginn, E. J.; Brennecke, J. F. Measurement of SO_2 solubility in ionic liquids. *J. Phys. Chem. B* **2006**, *110*, 15059–15062.

(72) Shokouhi, M.; Adibi, M.; Jalili, A. H.; Hosseini-Jenab, M.; Mehdizadeh, A. Solubility and Diffusion of H_2S and CO_2 in the Ionic Liquid 1-(2-hydroxyethyl)-3-methylimidazolium tetrafluoroborate. *J. Chem. Eng. Data* **2010**, *55*, 1663–1668.

(73) Almantanotis, D.; Gefflent, T.; Pádua, A. A.; Coxam, J. Y.; Costa-Gomes, M. F. Effect of fluorination and size of the alkyl side-chain on the solubility of carbon dioxide in 1-alkyl-3-methylimidazolium bis(trifluoromethylsulfonyl)amide ionic liquids. *J. Phys. Chem. B* **2010**, *114*, 3608–3617.

(74) Carvalho, P. J.; Alvarez, V. H.; Marrucho, I. M.; Aznar, M.; Coutinho, J. High pressure phase behavior of carbon dioxide in 1-butyl-3-methylimidazolium bis(trifluoromethylsulfonyl)imide and 1-butyl-3-methylimidazolium dicyanamide ionic liquids. *J. Supercrit. Fluids* **2009**, *50* (2), 105–111.

(75) Baltus, R. E.; Counce, R. M.; Culbertson, B. H.; Luo, H.; DePaoli, W.; Dai, S.; Duckworth, D. C. Examination of the potential of ionic liquids for gas separations. *Sep. Sci. Technol.* **2005**, *40*, 525–541.

(76) Kumełan, J.; Kamps, A. P. S.; Urukova, I.; Tuma, D.; Maurer, G. Solubility of oxygen in the ionic liquid [bmim][PF6]: Experimental and molecular simulation results. *J. Chem. Thermodyn.* **2005**, *37*, 595–602.

(77) Jacquemin, J.; Costa-Gomes, M. F.; Husson, P.; Majer, V. Solubility of carbon dioxide, ethane, methane, oxygen, nitrogen, hydrogen, argon, and carbon monoxide in 1-butyl-3-methylimidazolium tetrafluoroborate between temperatures 283 and 343 K and at pressures close to atmospheric. *J. Chem. Thermodyn.* **2005**, *38*, 490–502.

(78) Kumełan, J.; Kamps, A. P. S.; Urukova, I.; Tuma, D.; Maurer, G. Solubility of H_2 in the ionic liquid [bmim][PF6]. *J. Chem. Eng. Data* **2006**, *51*, 11–14.

(79) Kumełan, J.; Kamps, A. P. S.; Urukova, I.; Tuma, D.; Maurer, G. Solubility of H_2 in the ionic liquid [hmim][Tf_2N]. *J. Chem. Eng. Data* **2006**, *51*, 1364–1367.

Publicación 3:

Gonzalez-Miquel, M.; Talreja, M.; Ethier, A.L.; Flack, K.; Switzer, J.R.; Biddinger, E.J.; Pollet, P.; Palomar, J.; Rodriguez, F.; Eckert, C.A.; Liotta, C.L. **COSMO-RS Studies: Structure−property relationships for CO_2 capture by reversible ionic liquids.** *Industrial & Engineering Chemical Research,* **2012**, *51*, 16066−16073.

I&EC research
Industrial & Engineering Chemistry Research

Article

pubs.acs.org/IECR

COSMO-RS Studies: Structure–Property Relationships for CO_2 Capture by Reversible Ionic Liquids

Maria Gonzalez-Miquel,*[,†] Manish Talreja,[‡,§] Amy L. Ethier,[‡,§] Kyle Flack,[§,∥] Jackson R. Switzer,[‡,§] Elizabeth J. Biddinger,[‡,§] Pamela Pollet,[§,∥] Jose Palomar,[⊥] Francisco Rodriguez,[†] Charles A. Eckert,[‡,§,∥] and Charles L. Liotta*[,‡,§,∥]

[†]Departamento de Ingeniería Química, Universidad Complutense de Madrid, 28040 Madrid, Spain

[‡]School of Chemical & Biomolecular Engineering, [∥]School of Chemistry and Biochemistry, and [§]Specialty Separations Center, Georgia Institute of Technology, Atlanta, Georgia 30332, United States

[⊥]Sección de Ingeniería Química (Departamento de Química Física Aplicada), Universidad Autónoma de Madrid, 28049 Madrid, Spain

Supporting Information

ABSTRACT: The quantum-chemical approach COSMO-RS was used to develop structure–property relationships of reversible ionic-liquid (RevIL) solvents for CO_2 capture. Trends predicted for the thermodynamic properties of the RevILs using COSMO-RS, such as CO_2 solubility, solvent regeneration enthalpy, and solvent reversal temperature, were verified by experimental data. This method was applied to a range of structures, including silylamines with varying alkyl chain lengths attached to the silicon and amine functionality, silylamines with fluorinated alkyl chains, sterically hindered silylamines and carbon-based analogues. The energetics of CO_2 capture and release and the CO_2 capture capacities are compared to those of the conventional capture solvent monoethanolamine. The results of this study suggest that the simple COSMO-RS computational approaches reported herein can act as a guide for designing new RevILs. COSMO-RS allows for the determination of the relative thermodynamic properties of CO_2 in these and related systems.

1. INTRODUCTION

CO_2 emissions from fossil-fuel-fired power plants are a major contributor to global climate change.[1] Because energy use will continue to increase and coal will remain a major energy source, such emissions will continue to be an important issue.[2] Conventional technologies for CO_2 capture are based on amine solutions, namely, 30% aqueous monoethanolamine (MEA).[3,4] This technique, however, requires much parasitic energy in solvent regeneration,[3−6] so a more benign and cost-effective method is required.

Advanced aqueous amine-based systems are being developed to overcome the drawbacks of the conventional technologies.[7] Additionally, significant efforts are underway to develop new CO_2 capture technologies that offer substantial economic advantages, including chemical reaction and physical absorption using solvents, swing adsorption with metal–organic frameworks, zeolites, membrane technology, and chemical looping. The Eckert–Liotta research group has developed a new class of silicon-based, nonaqueous solvents deemed reversible ionic liquids (RevILs) that eliminate the parasitic energy penalty of heating the water used in aqueous ethanolamine systems. These RevILs are derived from silylamines, which react with carbon dioxide (reversibly) to form ionic liquids.[8−12] RevILs capture CO_2 by a dual mechanism: chemical reaction and physical absorption. Two moles of silylamine solvent react with one mole of CO_2 to form a carbamate and an ammonium ion pair (Scheme 1), in a process that is readily reversed by heating or sparging with an inert gas. The RevIL formed is then capable of additional CO_2 capture through physical absorption. Note that the recycling of the solvents is a critical issue for the development of any CO_2 capture technology aiming to be economically viable.

Rather than synthesizing silylamines with a wide variety of structural modifications, COSMO-RS[13−15] has been employed to provide direction for the synthesis of promising structures. This approach is both faster and cheaper. The overall goal in using COSMO-RS, therefore, is to provide a roadmap for synthesizing novel solvent structures for developing sustainable CO_2 capture processes.

2. BACKGROUND OF REVERSIBLE IONIC LIQUIDS

2.1. Reversible Ionic Liquids for CO_2 Capture. The thermodynamics of the RevIL-CO_2 systems reported herein includes the following aspects:

(1) Physical absorption capacity of CO_2: The solubility of CO_2 in each RevIL (Scheme 1) is measured in terms of the Henry's law constant of CO_2 ($K_H^{CO_2}$) in the ionic liquid. This approach is valid as long as the self-interactions of the dissolved gas are negligible.

(2) Enthalpy of regeneration: The enthalpy required for regeneration of the molecular liquid (ΔH_{reg}) is the sum of the enthalpies associated with the removal of both the chemically reacted (ΔH_{reac}) and the physically absorbed ($\Delta H_{dissolution}$)

Received: September 11, 2012
Revised: November 14, 2012
Accepted: November 17, 2012
Published: November 30, 2012

Scheme 1. Reaction of Silylamine with CO_2 to Form Reversible Ionic Liquids

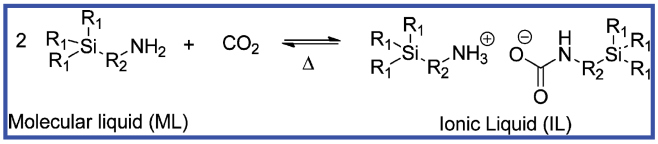

CO_2. Because bond-breaking is involved in one of the steps in the regeneration of the CO_2, the heat or enthalpy of reaction, ΔH_{reac}, is the main contributor to the overall heat required. Thus, the following approximation is employed: $\Delta H_{reg} \approx \Delta H_{reac}$.

$$\Delta H_{reg} = \Delta H_{reac} + \Delta H_{dissolution} \quad (1)$$

(3) Reversal temperature: Reversal temperature refers to the reverse reaction of the RevIL to form the molecular liquid and CO_2. It is defined for each RevIL as the temperature at which the equilibrium constant of reaction of the silylamine with CO_2 to form RevIL approaches 10^{-1}, that is, $K_{reac} \rightarrow 10^{-1}$. The heat required to raise the ionic liquid to the regeneration (reversal) temperature (T_{rev}) for releasing the chemically absorbed CO_2 is

$$Q = mC_p\Delta T = mC_p(T_{rev} - T_{cap}) \quad (2)$$

where m is the mass of the ionic liquid, C_p is the heat capacity of the solvent mixture, and T_{cap} is the capture temperature of CO_2. T_{cap} is determined by the temperature of the flue gas stream (typically 40 °C), and T_{rev} is a function of the structure of molecular liquid.

2.2. Structures of the Molecular Precursors. The structure–property relationships fall into two categories of RevILs: (1) unhindered silylamines with no additional methyl groups attached to the alkyl chain containing the amine functionality and (2) hindered silylamines with methyl groups attached to the alkyl chain containing the amine functionality (Tables S1 and S2, Supporting Information). The thermodynamic properties of RevILs for both chemical reaction with CO_2 and physical absorption of CO_2 were evaluated focusing on the following structural characteristics:

(a) silicon versus carbon atoms,
(b) length of the alkyl chain substituents attached to the silicon atom,
(c) length of the alkyl chain connecting the amine to the silicon atom,
(d) fluorine versus hydrogen on the carbon backbone, and
(e) steric hindrance proximate to the amine functionality.

The molecular precursor (3-aminopropyl)triethylsilane (TEtSA) was used as the reference compound to compare the effects of changing the molecular liquid structure on the CO_2 capture properties of the silylamines.

3. THEORY: COSMO-RS

COSMO-RS (Conductor-like Screening Model for Real Solvents) is a predictive method developed by Klamt and coworkers for thermodynamic equilibria of fluids and liquid mixtures that uses a statistical thermodynamics approach based on the results of unimolecular quantum chemical calculations.[14] It is a valuable tool for providing a fundamental understanding (at the molecular level) of the systems for which prior experimental knowledge is not available. Several publications have demonstrated the capabilities of the a priori COSMO-RS method in successfully predicting the properties of a wide variety of systems,[13−20] including those containing CO_2 and other gases in ionic liquids[21−26] and traditional solvents.[27,28] In this work, COSMO-RS is used for the first time to predict the thermodynamic properties of RevILs for CO_2 capture.

Here, we first optimized the molecular geometries of all of the compounds (solutes, molecular liquids, and ionic liquids) at the B3LYP/6-31++G** computational level in the ideal-gas phase using the quantum chemical Gaussian 03 package.[29] We applied a molecular model of independent counterions in the COSMO-RS calculations, where RevILs were treated as equimolar mixtures of cations and anions. We performed the vibrational frequency calculations for each case to confirm the presence of an energy minimum.

Then, we applied the following two-step procedure for COSMO-RS calculations. First, Gaussian 03 was used to compute the necessary COSMO files. The ideal screening charges on the molecular surface for each species were calculated by the continuum solvation COSMO model using the BVP86/TZVP/DGA1 level of theory. Subsequently, COSMO files were used as input to the COSMOtherm[30] statistical thermodynamic code to calculate the thermodynamic properties. Version C21_0111 of COSMOthermX was used to perform all of the calculations. The parametrization scheme BP_TZVP_ C21_0108[31] was used for the calculation of the Henry's law constants of CO_2 in the solvents and the excess enthalpies of the liquid mixtures, $H^{E'}$, which were determined using the corrected expression[22]

$$H^{E'} = x_{IL}H^{E'}_{IL} + x_{CO_2}H^{E'}_{CO_2} \approx x_{IL}(H^{E'}_{IL,mixture} - H^{E'}_{IL,pure}) + x_{CO_2}(H^{E'}_{CO_2,mixture}) \quad (3)$$

This scheme was chosen in accordance with the chosen quantum method (functional and basis set) and has been previously validated for predicting the solubility trends of gases in ionic liquids.[22,23]

To compute the solvent regeneration enthalpy, Gibbs free energy, and equilibrium constants of the chemical reaction of CO_2 with the silylamines, we applied the advanced feature of the latest release of COSMOtherm, the parametrization BP_TZVP_ C21_0111, which contains intrinsic parameters obtained considering thermodynamic parameters of reaction (equilibrium constants, free energies, and enthalpies) in their optimization.[33]

Reference 32 describes the calculation of Henry's law constants ($K_H^{CO_2}$) using COSMOtherm, and ref 33 provides the procedure for estimating the enthalpy of reaction (ΔH_{reac}) and the equilibrium constant (K_{reac}).

4. RESULTS AND DISCUSSION

4.1. Thermodynamic Properties of CO_2 Capture with Reversible Ionic Liquids. *4.1.1. CO_2 Physical Absorption Capacity of Reversible Ionic Liquids.* The CO_2 physical absorption capacities of the RevILs were evaluated in terms of

dx.doi.org/10.1021/ie302449c | Ind. Eng. Chem. Res. 2012, 51, 16066−16073

the Henry's law constants of CO_2 solubility in the ionic liquids ($K_H^{CO_2}$) (Figures 1 and 2). Decreasing values of the Henry's law constants imply increasing solubility of the solute (CO_2) in the solvent (RevIL). It is clear that the solubility trends predicted by COSMO-RS match the experimental observations.[12] However, COSMO-RS overestimates the Henry's constants of CO_2 in the RevILs. Recent publications[22,23] have also reported that COSMO-RS systematically overestimates the Henry's constant of CO_2 in classical ILs but provides a reasonable linear fit between calculated and experimental values.

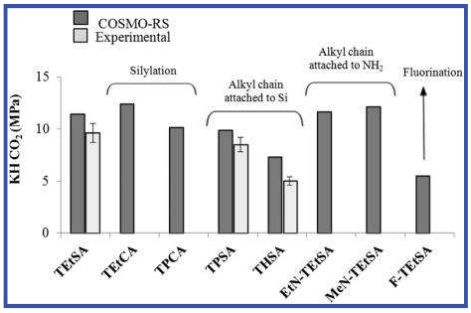

Figure 1. Henry's law constants of CO_2 in regular silylamines (in their corresponding ionic-liquid forms) calculated by COSMO-RS and comparison with experimental results[12] at T = 35 °C. (The Henry's law constant of CO_2 in MEA is 144.1 MPa calculated by COSMO-RS at T = 35 °C.)

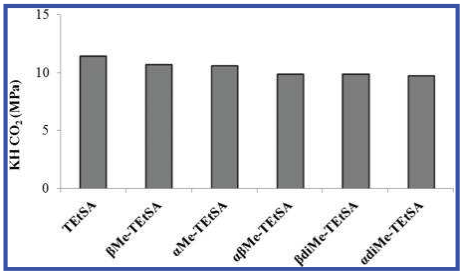

Figure 2. Henry's law constants of CO_2 in hindered silylamines (in their corresponding ionic-liquid forms) calculated by COSMO-RS at T = 35 °C.

The substitution of a silicon atom (TEtSA, TPSA) for a carbon atom (TEtCA, TPCA) in the molecular liquid could contribute to an increase in the CO_2 physical absorption capacity of the ionic liquid, as illustrated in Figure 1. Also, increasing the length of the alkyl chain attached to the silicon atom significantly enhances the CO_2 solubility, as shown by the $K_H^{CO_2}$ trend from ethyl (TEtSA) to propyl (TPSA) to hexyl (THSA). Increasing the length of the alkyl chain separating the amine from the silicon atom also results in an increase in the CO_2 solubility. The effect of changing the length of the alkyl chain attached to the amine group is less pronounced than the effect of changing the length of the alkyl chain attached to the silicon. This is probably due to the fact that there is a single chain on the amine compared to the three side chains on the silicon. It has been reported that fluorine-containing compounds interact favorably with CO_2.[33−38] The COSMO-RS calculations indicate that the $K_H^{CO_2}$ value for F-TEtSA is smaller than that of the base compound TEtSA.

Figure 2 illustrates the steric effects on the physical absorption of CO_2 associated with introducing methyl groups at various positions on TEtSA backbone. The results show that increasing the number of methyl groups attached to the alkyl chain separating the amine functionality from the silicon slightly increases the CO_2 solubility. The position of the methyl groups does not appear to exhibit a significant effect on the $K_H^{CO_2}$ values, although it seems that introducing methyl groups in the α-position slightly increases the CO_2 solubility. The comparison between the Henry's law constants of CO_2 in silylated RevILs and in MEA ($K_H^{CO_2}$ < 15 MPa versus $K_H^{CO_2}$ = 144.1 MPa, as computed by COSMO-RS) indicates the superior CO_2 physisorption behavior of the silylated RevILs discussed in this article. Similar solubility trends were observed for CO_2 in the RevILs in a study of the Henry's law constants in units of bar·(mol/L) (Figures S1 and S2 and Table S3, Supporting Information).

In addition to high CO_2 solubility, an optimum solvent for CO_2 capture should also display a high selectivity for CO_2. Figure 3 shows that the Henry's law constants (in RevILs) of other flue-gas components or components present in methane−CO_2 mixtures were much higher than that of CO_2, indicating that the RevILs will preferentially absorb CO_2.

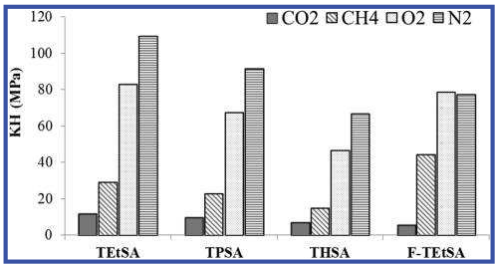

Figure 3. Henry's law constants of major flue gas components in RevILs calculated by COSMO-RS at T = 35 °C.

It has been validated that an energetic analysis based on the enthalpic effects caused by the specific intermolecular interactions between the solute and the IL solvent is able to explain the solubility behavior of CO_2 (and other solutes) for the cases of dilute solutions. Recently, we studied the relationship between the Henry's law constants of CO_2 and the excess enthalpies of the mixture for a series of imidazolium-based ILs paired with different anions such as [BF_4], [PF_6], [NTf_2], [CF_3SO_3], [FEP], and [DCN], with the results showing that the higher solubility of CO_2 in the ILs is associated with higher exothermicity of the CO_2−IL mixtures.[22−24] Figure 4A shows this relationship between the Henry's law constants and the excess enthalpies of CO_2 in classical ionic liquids and RevILs as calculated by COSMO-RS. Silylated RevILs are as good physical absorbents as classical ionic liquids. The contributions of the different intermolecular interactions (electrostatic "misfit", hydrogen bond, and van der Waals) to excess enthalpies are shown in Figure 4B. The attractive van der Waals forces determine the structure−property relationships of the Henry's law constants of CO_2 in

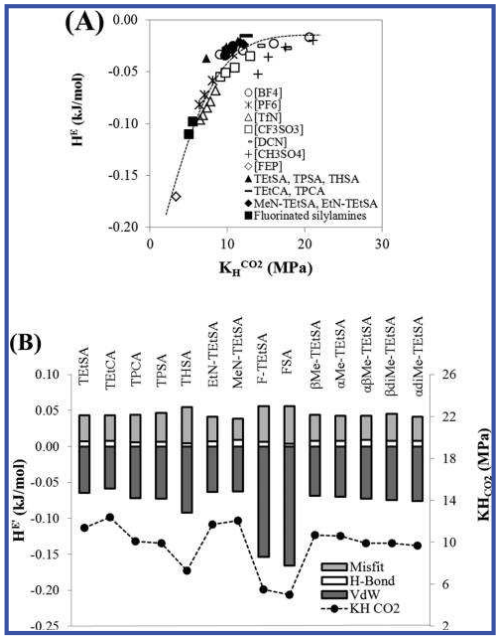

Figure 4. (A) Comparison of Henry's law constants ($K_H^{CO_2}$) and excess enthalpies ($H^{E,}$) (eq 3) of CO_2 in classical imidazolium-based ionic liquids (ILs) and reversible ionic liquids (RevILs) calculated by COSMO-RS at T = 35 °C. (B) Comparison of Henry's law constants ($K_H^{CO_2}$) with the interaction energy contributions to excess enthalpies (H_i^E) of CO_2 in reversible ionic liquids (RevILs) calculated by COSMO-RS at T = 35 °C.

RevILs, increasing in the following order: fluorination > length of alkyl chain > steric hindrance > silicon versus carbon.

4.1.2. Heat of Regeneration. Figure 5 compares the enthalpies of reaction (ΔH_{reac}) of silylamines with the available

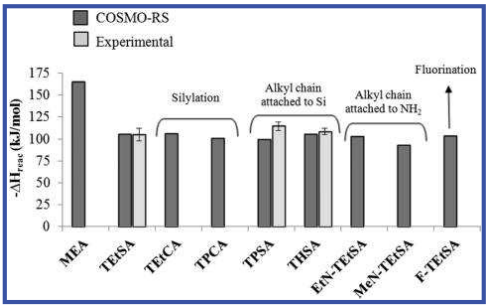

Figure 5. Heats of reaction of regular silylamines calculated by COSMO-RS and comparison with experimental results.[12]

experimental data.[12] For all of the experimentally tested silylamines, ΔH_{reac} for CO_2 capture was nearly −100 kJ/mol, with COSMO-RS values quantitatively matching the experimental calorimetric measurements made using differential scanning calorimetry. The heat of reaction calculated by COSMO-RS for neat MEA (nonaqueous) is −165 kJ/mol of CO_2 captured. Therefore, according to COSMO-RS, a higher energy input is required for the regeneration of neat MEA than for the regeneration of the RevILs. The heat of reaction between CO_2 and aqueous MEA has been reported to be within the range from −72 to −85 kJ/mol of CO_2 at 40 °C.[39,40] This enthalpy value, however, is a sum of enthalpies associated with several reactions involving formation of carbamates, carbonates, bicarbonates, and ammonium and hydronium ions in addition to physical absorption. Hence, the direct comparison between COSMO-RS calculations and experimental values is inappropriate. Although the additional reactions decrease the absorption energy, considerable amounts of parasitic energy is spent on heating water during the regeneration step for aqueous MEA. In fact, it has been reported that, during regeneration, thermal energy (about 165 kJ/mol of CO_2) is added to the solution to release the CO_2. A large amount of water in the amine solution must be heated to the regeneration temperature,[39] so advanced alternative stripper configurations are being investigated with the aim of reducing the energy consumption in conventional CO_2 capture processes.[41] It should be noted that RevILs (like almost any solvent) will absorb water from the flue gas stream. Additional research is needed to determine the solubility of water in the RevILs under capture and release conditions.

The heats of reaction of the unhindered silylamines do not exhibit a strong structural dependence with respect to the length of the alkyl chain, carbon versus silicon analogues, or the presence of fluorine containing substituents. Only a slight decrease in the reaction enthalpy for the silylamine MeN-TEtSA was observed in comparison to TEtSA, possibly because of the proximity of the silicon to the amine functionality.

The heats of reaction of the hindered silylamines are illustrated in Figure 6. The steric effects, due to the increasing

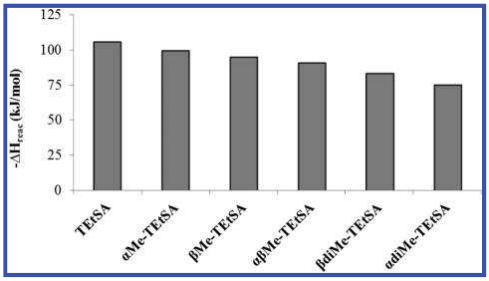

Figure 6. Heats of reaction of hindered silylamines calculated by COSMO-RS.

number of methyl groups attached to the alkyl chain containing the amine functionality, decrease the heat of the reaction. The position of methylation does not affect the calculated ΔH_{reac} of the monomethylated compounds. In contrast, disubstitued RevILs, where two methyl groups are attached to the same carbon, have a more pronounced effect on ΔH_{reac}. Dimethylation in the α-position decreases the calculated heat of reaction by 25% as compared to that of TEtSA.

4.1.3. Reversal Temperature. Figures 7 and 8 compare the COSMO-RS and experimental values[12] for the reversal temperatures of the unhindered and the hindered RevILs. The COSMO-RS calculations reported here used a specific definition of the reversal temperature. Reversal temperature is

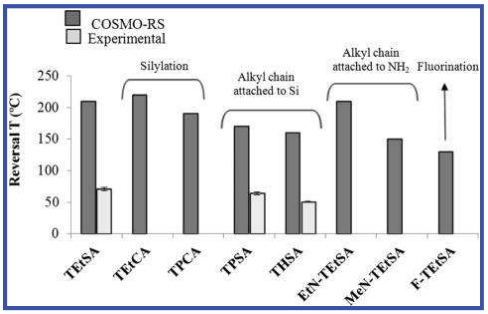

Figure 7. Reversal temperatures of regular silylamines calculated by COSMO-RS and comparison with experimental results.[12]

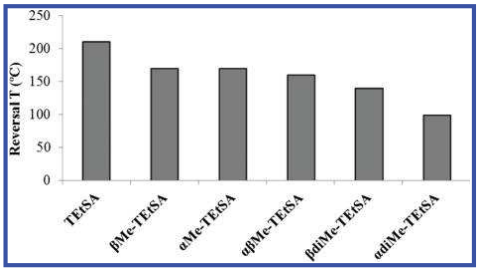

Figure 8. Reversal temperatures of hindered silylamines calculated by COSMO-RS.

defined as the temperature at which the equilibrium constant of the CO_2 capture reaction approaches 10^{-1} ($K_{reac} \rightarrow 10^{-1}$). The experimental reversal temperature was determined by differential scanning calorimetry (DSC) and is defined as the onset temperature of the reverse reaction of the RevIL releasing the chemically absorbed CO_2. Although the COSMO-RS results for the reversal temperature deviate from the experimental values obtained by DSC measurements, the trends are similar. It should be understood that there is always an equilibrium between the liquid- and gas-phase CO_2 dictated by temperature and CO_2 pressure. The reversal temperatures shown here present the relative behaviors of the solvents and do not represent complete reversal of the RevIL to the molecular liquid.

Figure 7 indicates that the reversal temperatures of the ionic liquids decrease slightly with the substitution of a silicon for a carbon atom in the molecular precursors, that is, TEtCA–TEtSA and TPCA–TPSA. In addition, the reversal temperatures of the silylamines decrease with increasing length of the alkyl chain attached to the silicon atom or increasing distance of the amine functionality from the silicon atom. Moreover, adding fluorinated groups to the molecular liquid precursor also decreases the reversal temperature, as illustrated with the fluorinated analogue F-TEtSA.

The effect of introducing steric hindrance proximate to the amine functionality on the molecular liquid is shown in Figure 8. As the number of methyl groups attached to the alkyl chain separating the amine functionality from the silicon atom increases, the reversal temperature decreases. Most notably, the addition of two methyl groups in the α-position decreases the reversal temperature of TEtSA significantly. These results are supported by several works reporting that sterically hindered amines, such as 2-amino-2-methyl-L-propanol (AMP), offer higher capacities and reaction rates than those obtained with conventional unhindered amines such as MEA. This was attributed to the lower stability constants of the carbamate reaction product between CO_2 and the hindered amines.[42,43]

4.2. Structure–Property Relationships for Designing Novel Reversible Ionic Liquid for CO_2 Capture. A COSMO-RS calculation on a novel silylamine-based solvent for CO_2 capture, (3-aminopropyl) diisopropyl(1H,1H,2H,2H-perfluoropentyl)silane (FSA) (Table 1), was performed.

It was anticipated that, because of the combined presence of a silicon atom, a polyfluororalkyl chain, and a long alkyl chain attached to the silicon atom, the molecule would be expected to present a higher physical absorption capacity, a similar heat of reaction to other silylamines (value close to −100 kJ/mol of CO_2), and a lower reversal temperature than TEtSA. Table 2 summarizes the thermodynamic properties related to CO_2 capture for the silylamine FSA computed by applying the COSMO-RS methodology and compared with the experimental values.[12]

Table 2. Predicted and Experimental Thermodynamic Properties of the RevIL FSA for CO_2 Capture and Comparison to Those of the RevIL TEtSA

	FSA		TEtSA	
thermodynamic property	predicted (COSMO-RS)	experimental[12]	predicted (COSMO-RS)	experimental[12]
Henry constant of CO_2 (MPa) (T = 35 °C)	5.0	4.5	11.4	9.6
heat of reaction (kJ/mol)	−96.6	−106.9	−105.6	−105.0
reversal temperature (°C)	130	54	210	70

Table 1. Structure of the Molecular Precursor FSA

Molecular Liquid	Acronym	Structure
(3-aminopropyl) diisopropyl(1H,1H,2H,2H-perfluoropentyl)silane	FSA	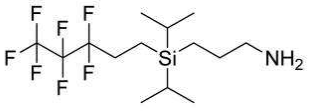

dx.doi.org/10.1021/ie302449c | Ind. Eng. Chem. Res. 2012, 51, 16066–16073

The Henry's law constants for CO_2 indicate higher physical absorption capacity of the FSA ionic liquid in comparison not only to TEtSA but also to the other RevILs considered in this study. In fact, the CO_2 solubility in FSA is greater than that in F-TEtSA, despite a lesser number of fluorine atoms. This could be due to the longer side chain attached to the silicon atom. The heat of reaction calculated for the molecular liquid FSA is similar to those for TEtSA and the other unhindered silylamines. Finally, the predicted reversal temperature of the FSA ionic liquid was found to be lower than that for TEtSA. This example illustrates the importance of establishing structure−property relationships and using them to design molecules with favorable properties. This approach is valuable for guiding the design of new CO_2 capture solvents and hence supplementing the experimental research.

The structure−property relationships to predict property changes developed from the results in the previous section are summarized below.

(a) Substitution of silicon for carbon: The substitution of silicon for carbon in the molecular precursors enhances the CO_2 physical absorption capacity of the ionic liquids and lowers the temperature at which the chemically reacted CO_2 is released.

(b) Length of the alkyl chain attached to silicon: Increasing the length of the alkyl chain attached to silicon enhances the CO_2 solubility in the RevILs, mainly because of the increased of van der Waals interaction, as was demonstrated for common ionic liquids. The reversal temperature of the RevILs decreases with increasing length of the alkyl chain substituents.

(c) Fluorination: Fluoroalkyl substituents attached to the silicon of the molecular liquid appear to have a large impact on improving the CO_2 physisorption capacity. This is likely due to the CO_2-philic nature of fluorine-containing compounds. The electronic effects on the compound due to the presence of the fluorine atoms decrease the reversal temperature of the RevIL. It is noted the presence of a fluoroalkyl substituent does not have a significant effect on ΔH_{reac}. Hence, there is little effect on the heat input required for the regeneration of the molecular liquid.

(d) Steric hindrance: The physical absorption capacity is slightly enhanced with increasing number of methyl groups attached to the alkyl chain connecting the amine functionality to the silicon atom. The steric impediment has a clear effect on the heat of the reaction. In general, the effect of introducing steric hindrance through methyl substitution near the amine functionality results in a gradual decrease of the reversal temperature of the ionic liquids. In particular, increasing the methylation of the molecular precursors, especially dimethylation at the α-position to the amine, has the most significant effect.

3. CONCLUSIONS

The quantum-chemical approach employing COSMO-RS has helped map structure−property relationships that can improve the design of novel solvents for sustainable CO_2 capture processes by both chemical and physical absorption. The method was applied to evaluate the thermodynamic properties of the silylamine-based RevILs for CO_2 capture. The predicted trends were validated against available experimental data.

As a result of the COSMO-RS analysis reported here, the effects of (a) silicon substitution for carbon, (b) the length of the alkyl chain attached to the silicon group, (c) the length of the alkyl chain connecting the amine functionality to the silicon, (d) the presence of fluoroalkyl substituents attached to the silicon atom, and (e) steric hindrance imparted by methyl groups attached to the alkyl chain connecting the amine to the silicon were addressed for the (1) CO_2 physical absorption capacities, (2) heats of reaction, and (3) reversal temperatures of the RevILs for CO_2 capture. In addition, the results were compared to those for the conventional solvent aqueous MEA, showing the superior ability of the RevILs to enhance the overall CO_2 capture capacity and to lower the energy input required. Finally, the COSMO-RS calculations were applied to predict the behavior of a new silylated fluorinated RevIL with optimized thermodynamic properties for CO_2 capture. The theoretical property estimations were in good agreement with the available experimental results. Thus, using theoretical tools as a guide, the time and expense associated with the synthesis of large numbers of potential structures for CO_2 capture can be dramatically reduced.

■ ASSOCIATED CONTENT

Supporting Information

Structures of regular and hindered silylamines (Tables S1 and S2); Henry's law constants of CO_2 [bar·(mol/L)] in regular and hindered silylamines calculated by COSMO-RS at T = 35 °C (Figures S1 and S2); and data estimated by COSMO-RS, i.e., Henry's law constants of CO_2 and molecular weights and densities of the RevILs (Table S3). This material is available free of charge via the Internet at http://pubs.acs.org.

■ AUTHOR INFORMATION

Corresponding Author

*E-mail: mgonzalezmiquel@quim.ucm.es (M.G.-M), charles.liotta@chemistry.gatech.edu (C.L.L.).

Notes

The authors declare no competing financial interest.

■ ACKNOWLEDGMENTS

The Spanish authors are grateful to the "Ministerio de Economía y Competitividad" and "Comunidad de Madrid" for financial support (Projects CTQ2011-26758 and S2009/PPQ-1545, respectively). The U.S. authors also acknowledge support from Philips 66.

■ REFERENCES

(1) *Climate Change 2007: The Physical Science Basis. Contribution of Working Group I to the Fourth Assessment Report of the Intergovernmental Panel on Climate Change*; Cambridge University Press: New York, 2007.

(2) *International Energy Outlook Report 2008*; Report DOE/EIA-0484; Energy Information Administration, U.S. Department of Energy: Washington, DC, 2008.

(3) Rao, A. B.; Rubin, E. A. Technical, economic, and environmental assessment of amine-based CO_2 capture technology for power plant greenhouse gas control. *Environ. Sci. Technol.* **2002**, *36*, 4467−4475.

(4) Aaron, D.; Tsouris, C. Separation from flue gas: A review. *Sep. Sci. Technol.* **2005**, *40*, 321−348.

(5) Figueroa, J. D.; Fout, T.; Plasynsky, S.; McIlvried, H.; Srivastava, R. D. Advances in CO_2 Capture Technology—The U.S. Department of Energy's Carbon Sequestration Program. *Int. J. Greenhouse Gas Control* **2008**, *2*, 9−20.

(6) Huang, J.; Rüther, T. Why are ionic liquids attractive for CO_2 absorption? An overview. *Aust. J. Chem.* **2009**, *62*, 298−308.
(7) MHI's Energy Efficient Flue Gas CO_2 Capture Technology and Large Scale CCS Demonstration Test at Coal-Fired Power Plants in USA. *Mitsubishi Heavy Ind. Tech. Rev.* **2011**, *48* (1), 26−32. Available at https://www.mhi.co.jp/technology/review/pdf/e481/e481026.pdf (accessed November 2012).
(8) Blasucci, V.; Dilek, C.; Huttenhower, H.; John, E.; Llopis-Mestre, V.; Pollet, P.; Eckert, C. A.; Liotta, C. L. One-component, switchable ionic liquids derived from siloxylated amines. *Chem. Commun.* **2009**, 116−118.
(9) Hart, R.; Pollet, P.; Hahne, D. J.; John, E.; Llopis-Mestre, V.; Blasucci, V.; Huttenhower, H.; Leitner, W.; Eckert, C. A.; Liotta, C. L. Benign coupling of reactions and separations with reversible ionic liquids. *Tetrahedron* **2010**, *66*, 1082−1090.
(10) Blasucci, V. M.; Hart, R.; Pollet, P.; Liotta, C. L.; Eckert, C. A. Reversible ionic liquids designed for facile separations. *Fluid Phase Equilib.* **2010**, *294*, 1−6.
(11) Blasucci, V.; Hart, R.; Llopis-Mestre, V.; Hahne, D. J.; Burlager, M.; Huttenhower, H.; Joo, B.; Thio, R.; Pollet, P.; Liotta, C. L.; Eckert, C. A. Single component, reversible ionic liquids for energy applications. *Fuel* **2010**, *89*, 1315−1319.
(12) Rohan, A. L.; Switzer, J. R.; Flack, K. M.; Hart, R. J.; Sivaswamy, S.; Biddinger, E. J.; Talreja, M.; Verma, M.; Faltermerier, S.; Nielsen, P. T.; Pollet, P.; Schuette, G. F.; Eckert, C. A.; Liotta, C. L. The Synthesis and the Chemical and Physical Properties of Non-Aqueous Silylamine Solvents for CO_2 Capture. *ChemSusChem* **2012**, *5*, 2181−2187.
(13) Eckert, F.; Klamt, A. Fast solvent screening via quantum chemistry: COSMO-RS approach. *AIChE J.* **2002**, *48* (2), 369−385.
(14) Klamt, A. *COSMO-RS: From Quantum Chemistry to Fluid Phase Thermodynamics and Drug Design*; Elsevier Science Ltd.: Amsterdam, The Netherlands, 2005.
(15) Klamt, A.; Frank Eckert, F.; Arlt, W. COSMO-RS: An alternative to simulation for calculating thermodynamic properties of liquid mixtures. *Annu. Rev. Chem. Biol. Eng.* **2010**, *1*, 101−122.
(16) Palomar, J.; Ferro, V. R.; Torrecilla, J. S.; Rodríguez, F. Density and Molar Volume Predictions Using COSMO-RS for Ionic Liquids. An Approach to Solvents Design. *Ind. Eng. Chem. Res.* **2007**, *46*, 6041−6048.
(17) Palomar, J.; Torrecilla, J. S.; Ferro, V. R.; Rodríguez, F. Development of an a Priori Ionic Liquid Design Tool. 1. Integration of a Novel COSMO-RS Molecular Descriptor on Neural Network. *Ind. Eng. Chem. Res.* **2008**, *47*, 4523−4532.
(18) Palomar, J.; Torrecilla, J. S.; Ferro, V. R.; Rodríguez, F. Development of an a Priori Ionic Liquid Design Tool. 2. Ionic Liquid Selection through the Prediction of COSMO-RS Molecular Descriptor by Inverse Neural Network. *Ind. Eng. Chem. Res.* **2009**, *48*, 2257−2265.
(19) Klamt, A. The COSMO and COSMO-RS solvation models. *WIREs Comput. Mol. Sci.* **2011**, *1*, 699−709.
(20) Diedenhofen, M.; Klamt, A. COSMO-RS as a tool for property prediction of IL mixtures—A review. *Fluid Phase Equilib.* **2010**, *294*, 31−38.
(21) Zhang, X.; Liu, Z.; Wang, W. Screening of ionic liquids to capture CO_2 by COSMO-RS and experiments. *AIChE J.* **2008**, *54* (10), 2717−2728.
(22) Palomar, J.; Gonzalez-Miquel, M.; Polo, A.; Rodriguez, F. Understanding the physical absorption of CO_2 in ionic liquids using the COSMO-RS method. *Ind. Eng. Chem. Res.* **2011**, *50*, 3452−3463.
(23) Gonzalez-Miquel, M.; Palomar, J.; Omar, S.; Rodriguez, F. CO_2/N_2 selectivity prediction in supported ionic liquid membranes (SILMs) by COSMO-RS. *Ind. Eng. Chem. Res.* **2011**, *50*, 5739−5748.
(24) Palomar, J.; Gonzalez-Miquel, M.; Bedia, J.; Rodriguez, F.; Rodríguez, J. J. Task-specific ionic liquids for efficient ammonia absorption. *Sep. Purif. Technol.* **2011**, *82*, 43−52.
(25) Bedia, J.; Palomar, J.; Gonzalez-Miquel, M.; Rodriguez, F.; Rodríguez, J. J. Screening ionic liquids as suitable ammonia absorbents on the basis of thermodynamic and kinetic analysis. *Sep. Purif. Technol.* **2012**, *95*, 188−195.
(26) Miller, M. B.; Chen, D. L.; Xie, H. B.; Luebke, D. R.; Johnson, J. K.; Enick, R. M. Solubility of CO_2 in CO_2-philic oligomers; COSMOtherm predictions and experimental results. *Fluid Phase Equilib.* **2009**, *287*, 26−32.
(27) Franke, R.; Hannebauer, B.; Jung, S. A case study in the pre-calculation of Henry coefficients. *Chem. Eng. Technol.* **2010**, *33* (2), 251−257.
(28) Miltner, M.; Miltner, A.; Friedl, A. Calculation of physical gas solubilities in various solvents with COSMO-RS. *Chem. Ing. Tech.* **2006**, *78* (8), 1087−1092.
(29) Frisch, M. J.; Trucks, G. W.; Schlegel, H. B.; Scuseria, G. E.; Robb, M. A.; Cheeseman, J. R.; Montgomery, J. A., Jr.; Vreven, T.; Kudin, K. N.; Burant, J. C.; Millam, J. M.; Iyengar, S. S.; Tomasi, J.; Barone, V.; Mennucci, B.; Cossi, M.; Scalmani, G.; Rega, N.; Petersson, G. A.; Nakatsuji, H.; Hada, M.; Ehara, M.; Toyota, K.; Fukuda, R.; Hasegawa, J.; Ishida, M.; Nakajima, T.; Honda, Y.; Kitao, O.; Nakai, H.; Klene, M.; Li, X.; Knox, J. E.; Hratchian, H. P.; Cross, J. B.; Bakken, V.; Adamo, C.; Jaramillo, J.; Gomperts, R.; Stratmann, R. E.; Yazyev, O.; Austin, A. J.; Cammi, R.; Pomelli, C.; Ochterski, J. W.; Ayala, P. Y.; Morokuma, K.; Voth, G. A.; Salvador, P.; Dannenberg, J. J.; Zakrzewski, V. G.; Dapprich, S.; Daniels, A. D.; Strain, M. C.; Farkas, O.; Malick, D. K.; Rabuck, A. D.; Raghavachari, K.; Foresman, J. B.; Ortiz, J. V.; Cui, Q.; Baboul, A. G.; Clifford, S.; Cioslowski, J.; Stefanov, B. B.; Liu, G.; Liashenko, A.; Piskorz, P.; Komaromi, I.; Martin, R. L.; Fox, D. J.; Keith, T.; Al-Laham, M. A.; Peng, C. Y.; Nanayakkara, A.; Challacombe, M.; Gill, P. M. W.; Johnson, B.; Chen, W.; Wong, M. W.; Gonzalez, C.; Pople, J. A. *Gaussian 03*, revision B.05; Gaussian, Inc.: Wallingford, CT, 2004.
(30) *COSMOtherm*, C2.1 Release 01.11; COSMOlogic GmbH & Co. KG: Leverkusen, Germany, 2010; http://www.cosmologic.de (accessed September 2012).
(31) Eckert, F. *COSMOtherm Users Manual, C2.1 Release 01.08*; COSMOlogic GmbH & Co. KG: Leverkusen, Germany, 2007.
(32) Eckert, F. *COSMOtherm Users Manual, C2.1 Release 01.11*; COSMOlogic GmbH & Co. KG: Leverkusen, Germany, 2010.
(33) Jacquemin, J.; Husson, P.; Majer, V.; Costa, M. F. Influence of the cation on the solubility of CO_2 and H_2 in ionic liquids based on the bis(trifluoromethylsulfonyl)imide anion. *J. Solution Chem.* **2007**, *36*, 967−979.
(34) Hong, G.; Jacquemin, J.; Deetlefs, M.; Hardacre, C.; Husson, P.; Costa, M. F. Solubility of carbon dioxide and ethane in three ionic liquids based on the bis{(trifluoromethyl)sulfonil}imide anion. *Fluid Phase Equilib.* **2007**, *257*, 27−34.
(35) Raeissi, S.; Peters, C. J. Carbon dioxide solubility in the homologous 1-alkyl-3-methylimidazolium bis-(trifluoromethylsulfonyl)imide family. *J. Chem. Eng. Data* **2009**, *54*, 382−386.
(36) Muldoon, M. J.; Aki, S. N.; Anderson, J. L.; Dixon, J. K.; Brennecke, J. F. Improving carbon dioxide solubility in ionic liquids. *J. Phys. Chem. B* **2007**, *111*, 9001−9009.
(37) Zhang, X.; Hun, F.; Liu, Z.; Wang, W.; Shi, W.; Maginn, E. J. Absorption of CO_2 in the ionic liquid tris(pentafluoroethyl)-trifluorophosphate ([hmim][FEP]): A molecular view by computer simulations. *J. Phys. Chem. B* **2009**, *113*, 7591−7598.
(38) Galán, L. M.; Meindersma, G. W.; de Haan, A. B. Solvent properties of functionalized ionic liquids for CO_2 absorption. *Trans. Inst. Chem. Eng. A* **2007**, *85* (A1), 31−39.
(39) Yeh, J. T.; Pennline, H. W. Study of CO_2 Absorption and Desorption in a Packed Column. *Energy Fuels* **2001**, *15*, 274−278.
(40) Kim, I.; Svendsen, H. F. Heat of Absorption of Carbon Dioxide (CO_2) in Monoethanolamine (MEA) and 2-(Aminoethyl)-ethanolamine (AEEA) Solutions. *Ind. Eng. Chem. Res.* **2007**, *46*, 5803−5809.
(41) Van Wagener, D. H.; Rochelle, G. T. Stripper configurations for CO_2 capture by aqueous monoethanolamine. *Chem. Eng. Res. Des.* **2011**, *15* (274−278), 1639−1646.
(42) Sartori, G.; Savage, D. W. Sterically hindered amines for CO_2 removal from gases. *Ind. Eng. Chem. Fundam.* **1983**, *22*, 239−249.

(43) Xu, S.; Wang, Y. W.; Otto, F. D.; Mather, A. E. Kinetics of the reaction of carbon dioxide with 2-amino-2-methyl-1-propanol solutions. *Chem. Eng. Sci.* **1996**, *51* (6), 841−850.

Publicación 4:

Gonzalez-Miquel, M.; Bedia, J.; Abrusci, C.; Palomar, J.; Rodriguez F. **Anion effects on kinetics and thermodynamics of CO_2 absorption in ionic liquids.** *The Journal of Physical Chemistry B*, **2013**, *117*, 3398−3406.

THE JOURNAL OF PHYSICAL CHEMISTRY B

Article

pubs.acs.org/JPCB

Anion Effects on Kinetics and Thermodynamics of CO_2 Absorption in Ionic Liquids

Maria Gonzalez-Miquel,[†] Jorge Bedia,[‡] Concepcion Abrusci,[§] Jose Palomar,*[,‡] and Francisco Rodriguez[†]

[†]Departamento de Ingeniería Química, Universidad Complutense de Madrid, 28040 Madrid, Spain

[‡]Departamento de Química Física Aplicada (Sección de Ingeniería Química), Universidad Autónoma de Madrid, Cantoblanco, 28049 Madrid, Spain

[§]Departamento de Biología Molecular, Universidad Autónoma de Madrid, Cantoblanco, 28049 Madrid, Spain

Supporting Information

ABSTRACT: A thermogravimetric technique based on a magnetic suspension balance operating in dynamic mode was used to study the thermodynamics (in terms of solubility and Henry's law constants) and kinetics (i.e., diffusion coefficients) of CO_2 in the ionic liquids [bmim][PF_6], [bmim][NTf_2], and [bmim][FAP] at temperatures of 298.15, 308.15, and 323.15 K and pressures up to 20 bar. The experimental technique employed was shown to be a fast, accurate, and low-solvent-consuming method to evaluate the suitability of the ionic liquids (ILs) to be used as CO_2 absorbents. Thermodynamic results confirmed that the solubility of CO_2 in the ILs followed the order [bmim][FAP] > [bmim][NTf_2] > [bmim][PF_6], increasing with decreasing temperatures and increasing pressures. Kinetic data showed that the diffusion coefficients of CO_2 in the ILs followed a different order, [bmim][NTf_2] > [bmim][FAP] > [bmim][PF_6], increasing with increasing temperatures and pressures. These results evidenced the different influence of the IL structure and operating conditions on the solubility and absorption rate of CO_2, illustrating the importance of considering both thermodynamic and kinetic aspects to select adequate ILs for CO_2 absorption. On the other hand, the empirical Wilke−Chang correlation was successfully applied to estimate the diffusion coefficients of the systems, with results indicating the suitability of this approach to foresee the kinetic performance of ILs to absorb CO_2. The research methodology proposed herein might be helpful in the selection of efficient absorption solvents based on ILs for postcombustion CO_2 capture.

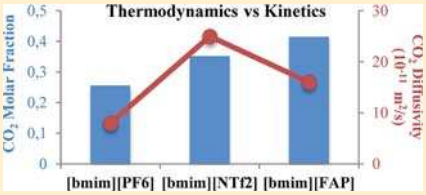

1. INTRODUCTION

CO_2 emissions from fossil-fuel-fired power plants are considered the main contributor to global climate change.[1] Conventional technologies for CO_2 postcombustion capture are based on amine solutions, which involve several concerns, such as their corrosive nature and volatility, high operational cost, and environmental impact.[2]

Over the last years, ionic liquids (ILs) have generated increasing attention in a wide variety of engineering applications, including their role as alternative solvents in gas absorption/separations processes owing to their unique physicochemical properties such as low vapor pressure and tailorability.[3−6] In particular, ILs have been proposed as potential candidates for CO_2 postcombustion capture in order to develop novel absorption technologies capable of overcoming the drawbacks associated with the amine-based systems.[7−10]

The thermogravimetric technique has been proven to be an effective method to accurately determine the absorption isotherms of CO_2 in ILs.[11−13] Indeed, this method has been intensively used by different research groups to provide systematic information about the thermodynamics of CO_2 in ILs considering the effect of the solvent structure and operating conditions.[14−22] The main results of CO_2 absorption in ILs emphasize that the anion plays a major role in the solvent structure for CO_2 absorption, with fluorination helping to increase the physical solubility of CO_2 in ILs,[15,17,23,24] and report the effect of the absorption temperature and pressure on the CO_2 solubility.[14,25−28]

The importance of the diffusion coefficients in mass transfer operations, such as the process of CO_2 absorption, is well recognized. However, although great efforts are being carried out to explain the solubility behavior of CO_2−IL systems, scarce kinetic data are available. Shifflet and Yokozeki reported the diffusion coefficients of CO_2 in [bmim][PF_6] and [bmim][BF_4] from thermogravimetric time-dependent absorption data by using a simple diffusion model.[11] Chen et al. characterized the kinetics of CO_2 in various ILs by defining an absorption rate parameter through thermogravimetric analysis.[13] A few other methods have been studied to determine the diffusion coefficients of CO_2 in ILs, such as the semi-infinitive volume approach reported by Camper et al.,[29] the employment of a lag-time technique over immobilized ILs suggested by Morgan et al.,[30] the use of a transient thin-liquid method

Received: January 23, 2013
Revised: February 18, 2013
Published: February 26, 2013

   dx.doi.org/10.1021/jp4007679 | J. Phys. Chem. B 2013, 117, 3398−3406

described by Moganty and Baltus,[31] and the use of online FTIR measurements proposed by Kortenbruck et al.,[32] whose results show that the values of the diffusion coefficients are significantly dependent on the measurement technique, although they present concordant orders of magnitude.

In our previous works, a multiscale research methodology was followed to study gas separation processes based on ILs. The absorption behavior of several gases in ILs, such as CO_2,[24,33,34] NH_3,[35,36] toluene,[37] and other VOCs,[38] was analyzed from a molecular point of view based on quantum-chemical COSMO-RS simulations to preliminarily select a set of absorbents with favorable characteristics. Moreover, thermodynamic and kinetic data were determined from thermogravimetric measurements at atmospheric pressure for the cases of NH_3[35,36] and toluene.[37] The results showed a remarkably different dependence of gas solubility and absorption rates on IL structure and operating conditions. As a consequence, it is of great interest to set up experimental procedures that accurately measure both thermodynamic and kinetic data of CO_2 in ILs, which provide the design parameters (i.e., gas−liquid equilibrium data and diffusion coefficients) required for gas separation process development. In addition, the application of a theoretical approach to foresee the absorption rate of CO_2 in IL may be helpful to consider kinetic criteria in the preliminary selection of the absorbent. In this sense, the empirical Wilke−Chang model was successfully applied to predict the diffusion coefficients of NH_3[36] and toluene[37] in ILs. Hence, by using the overall research methodology, which combines both theoretical and experimental studies, a selection of potential ILs to absorb CO_2 can be made, taking into account both thermodynamic and kinetic aspects for further development of CO_2 absorption processes.

In particular, the first aim of this contribution is to present an experimental procedure to provide accurate experimental information about the thermodynamic and kinetic behavior of CO_2 absorption in ILs as a function of the structure of the anion at different operating conditions of temperature and pressure. The second aim is to evaluate the possibility of using an empirical correlation to predict the diffusion coefficient of CO_2 in ILs. Experimental thermogravimetric measurements were performed in dynamic mode to determine the absorption isotherms and kinetic curves of CO_2 in three ionic liquids, i.e., [bmim][PF_6], [bmim][NTf_2], and [bmim][FAP], at temperatures of 298.15, 308.15, and 323.15 K and pressures up to 20 bar. These ILs have been selected because of their thermodynamically favorable CO_2 absorption capabilities.[24,33] First, the effect of the anion and the operating conditions on the thermodynamic (in terms of solubility and Henry's law constants) and kinetic (in terms of diffusion coefficients) performances of the ILs for CO_2 absorption was analyzed. In order to do so, the density of the solvents and the solubility and Henry's law constants of CO_2 in ILs were determined and compared to the available reported results to validate the experimental procedure, and the diffusion coefficients of CO_2 in each one of the solvents were determined by using a simplified diffusion mass model. Afterward, the empirical correlation of Wilke−Chang was used to estimate the diffusion coefficients of the systems, and the values were compared to those experimentally determined to evaluate the viability of using this approach to predict the kinetic behavior of a specific IL for CO_2 absorption.

2. EXPERIMENTAL PROCEDURE

2.1. Materials. Carbon dioxide, CO_2, and nitrogen, N_2, were obtained from Praxair, Inc., with a minimum purity of 99.999%. The ionic liquids 1-butyl-3-methylimidazolium hexafluorophosphate, [bmim][PF_6], and 1-butyl-3-methylimidazolium tris(pentafluoroethyl)trifluorophosphate, [bmim][FAP], were obtained from Merck, and the ionic liquid 1-butyl-3-methylimidazolium bis(trifluoromethanesulfonil)imide [bmim][NTf_2] was obtained from Io-Li-Tec (Ionic Liquid Technologies), all of them with a minimum purity of 99%.

2.2. Experimental Setup. The gas solubility measurements were performed with a Gravimetric High Pressure Sorption Analyzer (ISOSORP GAS LP-flow, Rubotherm). The sorption measuring instrument with magnetic suspension balance (MSB) has a measuring load of 0−10 g, and the resolution of the mass reading is 0.01 mg with a reproducibility (standard deviation) of (±) 0.03 mg and an uncertainty <0.002%. The MSB can operate in the pressure range between 10^{-6} bar (ultrahigh vacuum or UHV) and 30 bar and in the temperature range from room temperature up to 150 °C. The temperature in the sample is regulated by an external thermostat circulating bath filled with silicone oil (Julabo F25-ME), and the temperature in the measuring cell is recorded with a Pt 100 probe. The Rubotherm sorption analyzer equipment provides precise computer control and measurement of weight, pressure, and temperature to accurately determine the gas absorption−desorption isotherms and isobars. In particular, the magnetic suspension coupling control and the peripherals, which consist of the SARTORIUS Balance, JUMO DICON 400 temperature gauge, Julabo F25-ME Thermostat, DPI 282 Pressure Gauges, RUBOTHERM Gas-Dosing Unit, and BROOKS Mass Flow controller (FlowBus), are regulated by the supplied MessPro software to control the Rubotherm MSB and monitor the fully automatic process. The MSB can operate in both dynamic and static modes. Dynamic gas dosing provides a continuous flow of gas through the measuring cell and complete control of the pressure of the system. The static measurement is an optional procedure, where all dynamic mass flows and pressure control stop. All the absorption measurements in this work were performed in dynamic mode in order to ensure an exhaustive control of the set-point pressure. It should be noted that a main feature of this sorption instrument with magnetic suspension balance is the possibility of directly measuring the density of the gas phase surrounding the sample in an extremely high accuracy, which is necessary to correct the buoyancy effects acting on the sample in order to obtain reliable thermodynamic and kinetic data.

2.3. Experimental Measurements. *2.3.1. Blank Measurement.* A blank measurement was performed with the MSB in order to determine the mass and the volume of the sample container (m_{SC} and V_{SC}). The blank measurement was carried out as an adsorption isotherm without sample in the MSB (at a temperature of 298.15 K and starting from vacuum, the pressure was increased stepwise up to 20 bar with an inert gas, i.e., N_2, setting a gas flow rate of 100 mL/min). From the experimental data recorded during the blank measurement, the following linear relationship between the balance reading (m_{BAL}) and the gas density (ρ) can be written:

$$m_{BAL} = m_{SC} - \rho \cdot V_{SC} \quad (1)$$

The above linear function is the mass of the sample container in a vacuum (m_{SC}) minus the buoyancy effect ($\rho \cdot V_{SC}$). The

dx.doi.org/10.1021/jp4007679 | J. Phys. Chem. B 2013, 117, 3398−3406

experimental data recorded during the blank measurement are the balance reading (m_{BAL}) and the temperature (T) and pressure (P) of the gas from which the density of the gas (ρ) can be calculated. Therefore, from the results of this blank measurement, the weight of the empty sample container (m_{SC}) and the volume of the sample container (V_{SC}) were determined.

2.3.2. Reactivation of Sample. The reactivation of the sample was performed every time after a new sample was loaded into the MSB in order to reduce its content of water and volatiles. The sample container was filled with the ionic liquid sample (≈50 mg) and loaded into the MSB. Then, the samples were dried and degassed at a temperature higher than 323.15 K while the pressure was maintained in a vacuum until the changes in mass were <0.001 mg/h.

The weight of the sample container loaded with sample (m_{SC+S}) is measured by the MSB during the reactivation procedure in a vacuum (when $P = 0$ and $\rho = 0$, then $m_{SC} = m_{BAL}$). From this data, the mass of the reactivated sample (m_S) can be calculated by subtracting from it the mass of the empty sample container ($m_S = m_{SC+S} - m_{SC}$).

2.3.3. Buoyancy Measurements. The mass of sample weighed with the MSB during the adsorption experiment needs to be corrected for the buoyancy effect acting on it in the gas phase. The buoyancy effect (B) is proportional to the product of the density and the volume of the body ($\rho \cdot V$), and becomes considerable at low temperature and high pressure.

The holding force (H), which is determined by the balance, is dependent on the equilibrium forces acting on the sample, i.e., the gravitational force (F_G) acting on the sample in earth's gravity field (g = acceleration of gravity) and the buoyancy force (B) acting on the body in the opposite direction:

$$H = F_G - B = m \cdot g - (\rho \cdot V) \cdot g \tag{2}$$

As a result of that, the balance reading ($m_{BAL} = H/g$) is equal to

$$m_{BAL} = \frac{H}{g} = m - \rho \cdot V = m_{SC+S} - \rho \cdot V_{SC+S} \tag{3}$$

The above linear function is the mass of the sample container and the sample in a vacuum (m_{SC+S}) minus the buoyancy effect, which is due to the volume of the empty sample container plus the volume of the sample (V_{SC+S}).

The buoyancy measurements were performed like absorption isotherms in the MSB (stepwise increase of pressure at constant temperature) with each one of the ionic liquids at each temperature (298.15, 308.15, and 323.15 K) under inert gas atmosphere (i.e., N_2, setting a gas flow rate of 100 mL/min). Afterward, the balance reading during the buoyancy measurement (m_{BAL}) was plotted as a function of the density of the gas (ρ) measured with the MSB. From the linear regression of the measured data, the sum of the volumes of the sample container and the sample (V_{SC+S}) is determined. Therefore, the results of the buoyancy measurement are the volume of the loaded sample container (V_{SC+S}), the volume of the sample itself ($V_S = V_{SC+S} - V_{SC}$), and the true density of the sample under the operating conditions ($\rho_S = m_S/V_S$).

2.3.4. Absorption Measurements. After the buoyancy measurement was performed, the MSB and the sample were evacuated and the isothermal absorption measurement was carried out. In particular, the CO_2 absorption isotherms in each one of the ionic liquids were determined at temperatures of 298.15, 308.15, and 323.15 K and pressures up to 20 bar. First, the system was kept under inert gas atmosphere at the set temperature until the sample mass was constant (weight change rate <0.001 mg/h). Subsequently, the CO_2 gas was introduced into the MSB (gas flow rate = 100 mL/min) and the pressure of the gas was increased stepwise at constant temperature up to the set pressure, and the increment in the sample weight was monitored and recorded. The ionic liquid and the gas were considered to have reached equilibrium when at constant pressure no further weight change was observed throughout time (weight change rate <0.001 mg/h). Afterward, the recorded balance reading (m_{BAL}) in the absorption measurement was corrected for the buoyancy effect acting on the sample and the sample container as follows:

$$m_{BAL,CORR} = m_{BAL} + \rho \cdot V_{SC+S} \tag{4}$$

This buoyancy corrected mass ($m_{BAL,CORR}$) is the mass of the sample container (m_{SC}) and the mass of the sample with absorbed gas ($m = m_S + m_{CO_2}$). Then, the mass of the sample with absorbed gas is determined by subtracting the mass of the empty sample container from this ($m = m_{BAL,CORR} - m_{SC}$), the mass of absorbed gas is calculated by subtracting the mass of reactivated sample from the mass of sample with absorbed gas ($m_{CO_2} = m - m_S$), and the molar fraction of gas absorbed is determined as follows:

$$X_{CO_2} = \frac{m_{CO_2}/M_{CO_2}}{m_s/M_{IL}} \tag{5}$$

where M_{CO_2} and M_{IL} are, respectively, the molar masses of CO_2 and the ionic liquid.

After absorption, the ionic liquids were regenerated. For the regeneration, the system was set and kept in a vacuum until the mass stabilized (weight change rate <0.001 mg/h). It was verified that the mass of the ionic liquid samples at the end of each experiment was the same as the mass initially loaded (weight change <0.2%), which was attained in less than 20 min for all the systems studied.

In this work, the temperature and the pressure were respectively controlled with uncertainties corresponding to ±0.01 K and ±0.01 bar. The maximum uncertainty of the isothermal ionic liquid density data is estimated to be below 0.002 g/cm^3, and the maximum uncertainty of the measured CO_2 mole fraction absorbed in ILs was estimated to be below 0.005.

3. RESULTS

3.1. Density. As it was exposed above, the Rubotherm sorption analyzer provides the possibility of directly measuring the density of the gas phase surrounding the sample to accurately determine the density of the solvents from the buoyancy measurements, and afterward correct the absorption data. Figure 1 shows the results obtained for the isothermal density of the ionic liquids [bmim][PF_6], [bmim][NTf_2], and [bmim][FAP] over the temperature range 298.15–323.15 K. Comparison of the ionic liquid density measurements with the available published data shows agreement within about 0.3–1.3% over the temperatures studied. Overall densities of the three ionic liquids are in the order of 1.3–1.6 g/cm^3 and present the following trend: [bmim][FAP] > [bmim][NTf_2] > [bmim][PF_6].

3.2. Thermodynamics. Experimental isothermal solubility data for CO_2 in [bmim][PF_6], [bmim][NTf_2], and [bmim]-

dx.doi.org/10.1021/jp4007679 | J. Phys. Chem. B 2013, 117, 3398–3406

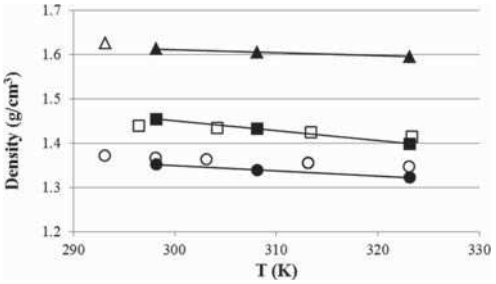

Figure 1. Density data of ionic liquids. [bmim][PF_6], measured in this work (●) and reported[39] (○); [bmim][NTf_2], measured in this work (■) and reported[50] (□); [bmim][FAP], measured in this work (▲) and reported[40] (△).

[FAP] at temperatures of 298.15, 308.15, and 323.15 K and pressures up to 20 bar are plotted in Figures 2, 3, and 4.

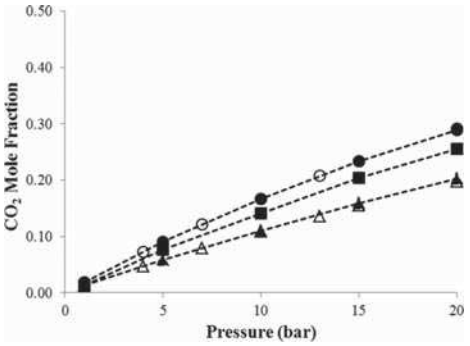

Figure 2. Isothermal solubility data of the system CO_2 and [bmim][PF_6]: measured in this work (●) and reported[11] (○) at 298.15 K; measured in this work (■) at 308.15 K; measured in this work (▲) and reported[11] (△) at 323.15 K.

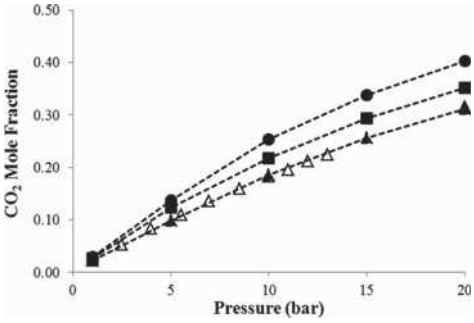

Figure 3. Isothermal solubility data of the system CO_2 and [bmim][NTf_2]: measured in this work (●) at 298.15 K; measured in this work (■) at 308.15 K; measured in this work (▲) and reported[17,41] (△) at 323.15 K.

Comparison of the measured solubilities with the previously reported values for CO_2 in [bmim][PF_6][11] and CO_2 in

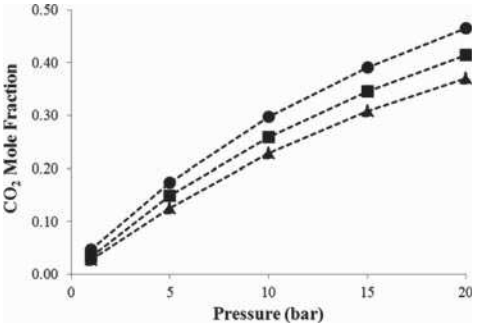

Figure 4. Isothermal solubility data of the system CO_2 and [bmim][FAP] measured in this work at (●) 298.15 K, (■) 308.15 K, and (▲) 323.15 K.

[bmim][NTf_2][17,41] determined by thermogravimetric techniques shows in Figures 2 and 3 that our data seem consistent with the available published data, and validate our experimental procedure for further solubility analyses. The obtained absorption isotherms confirm that the CO_2 solubility increases with decreasing temperature and increasing pressure for all the ILs studied. Regarding the effect of the structure of the anion, results show that the solubility of the CO_2 in the ILs containing [bmim] as a common cation follows the subsequent trend: [FAP] > [NTf_2] > [PF_6], being possible to achieve maximum molar fractions of absorbed CO_2 corresponding to 0.47, 0.40, and 0.29, respectively, at 298.15 K and 20 bar.

The Henry's law constant, K_H, is frequently used as a parameter for evaluating the solubility of a gaseous solute in a dilute solution, and it can be calculated using the following expression:

$$K_H = \lim_{x_{CO_2} \to 0} \left(\frac{P}{x_{CO_2}} \right) \quad (6)$$

where X_{CO_2} is the mole fraction of CO_2 in the IL and P is the equilibrium pressure.

According to eq 6, the measured data can be used to estimate the Henry's law constants at infinite dilution. In particular, the Henry's law constants were calculated as the slope from a linear fit of the solubility data at relatively low pressures (up to 5 bar), which provided a correlation coefficient higher than 0.99. The obtained values of the Henry's law constant of CO_2 in [bmim][FAP], [bmim][NTf_2], and [bmim][PF_6] at temperatures of 298.15, 308.15, and 323.15 K are represented in Figure 5. The results illustrate how K_H increases with the temperature and with the type of anion as follows: [FAP] < [NTf_2] < [PF_6] (note that increasing the values of the Henry's law constant involves decreasing the solubility of CO_2 in terms of molar fraction units). In addition, a comparison between the values of Henry's law constants obtained in this work and those available in the literature is shown in Figure 6, illustrating that the data determined in the present study is in agreement with the previously reported values. The measurement procedure based on the thermogravimetric technique operating in dynamic mode provides fast and accurate determination of the absorption data of CO_2 in the studied ILs, being possible to achieve the thermodynamic equilibrium of the systems in approximately 2 h for each T, P set-point.

dx.doi.org/10.1021/jp4007679 | J. Phys. Chem. B 2013, 117, 3398−3406

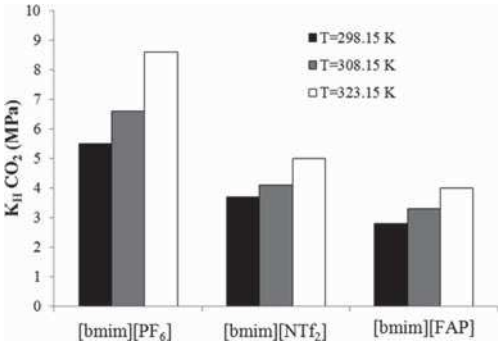

Figure 5. Henry's law constants of CO_2 in the ILs [bmim][PF_6], [bmim][NTf_2], and [bmim][FAP] at 298.15, 308.15, and 323.15 K estimated from solubility data of this work.

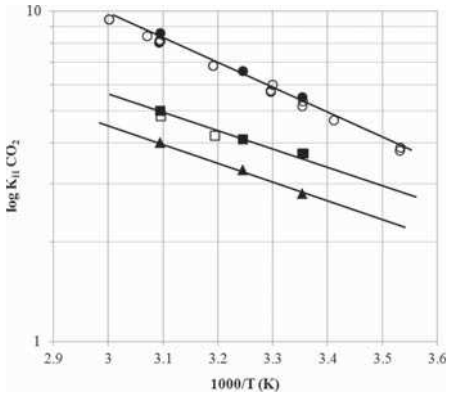

Figure 6. Comparison of estimated and reported Henry's law constants of CO_2 in ILs at different temperatures. [bmim][PF_6], estimated in this work (●) and reported[14,42−44] (○); [bmim][NTf_2], estimated in this work (■) and reported[45] (□); [bmim][FAP], estimated in this work (▲).

3.3. Kinetics. In order to evaluate the kinetics of the absorption of CO_2 in ILs, the diffusion coefficients were estimated from the time-dependent absorption data collected with the Rubotherm sorption analyzer for each one of the systems. The diffusion coefficients were estimated by applying a mass diffusion model reported by Shifflet and Yokozeki for CO_2−IL systems.[11] This model has also been used in our previous works for studying the kinetics of other gaseous solutes in ILs such as NH_3[36] and toluene.[37] Briefly, this model makes the following assumptions: the gas is dissolved in the liquid through a one-dimensional (vertical) diffusion process; the thermodynamic equilibrium is instantly established with the saturation concentration in a thin boundary layer between the gas and liquid phases; the saturation concentration, the temperature, and pressure are kept constant; and the gas−liquid system is considered a dilute solution in which the thermophysical properties of the solution do not change. Therefore, the process of gas dissolving in liquid may be described by one-dimensional mass diffusion due to the local concentration difference. The CO_2 mass balance can be written as

$$\frac{\partial C}{\partial t} = D\cdot\frac{\partial^2 C}{\partial z^2} \tag{7}$$

with an initial condition $C = C_0$ when $t = 0$ and $z < 0 < L$ and boundary conditions (i) $C = C_s$ when $t > 0$ and $z = 0$ and (ii) $\partial C/\partial z = 0$ at $z = L$. C is the concentration of gas dissolving in the IL as a function of time, t, and vertical location, z. L is the depth of IL in the container (estimated for each case using the mass of the IL sample and the corresponding density value previously determined in the buoyancy measurements), and C_0 is the initial concentration of the dissolving gas at each temperature and pressure. D is the diffusion coefficient, that is assumed to be constant. However, despite assuming a dilute solution, the CO_2 gas absorbed into the ionic liquid cannot be regarded as being highly dilute, so the diffusion coefficients must be taken as "effective" diffusion constants.

The experimentally measured quantity at a specified time is the total concentration (mass per unit volume) of dissolved gas in IL. This space-averaged concentration at a given time, $\overline{C}$, can be calculated from the equations

$$\overline{C} = \frac{1}{L}\int_0^L C\ \mathrm{d}z \tag{8}$$

$$\overline{C} = C_s\left[1 - 2\left(1 - \frac{C_0}{C_s}\right)\sum_{n=0}^{\infty}\frac{\exp(-\lambda_n{}^2 Dt)}{L^2\lambda_n{}^2}\right] \tag{9}$$

Although the last equation contains an infinite summation, only the first few terms are sufficient in practical applications. Fitting the experimental data to this equation by nonlinear regression, the saturation concentration, C_s, and the diffusion coefficient, D, were determined for each T, P set-point. Parts A, B, and C of Figure 7, respectively, present the diffusion coefficients of CO_2 in [bmim][PF_6], [bmim][NTf_2], and [bmim][FAP] determined from the isothermal data at 298.15, 308.15, and 323.15 K and pressures from 1.0 to 20.0 bar. The order of magnitude of the diffusion coefficients is 10^{-10} to 10^{-11} m^2/s, which agrees with the available data reported by Shifflet and Yokozeki for CO_2 in [bmim][PF_6] and [bmim][BF_4] by using the thermogravimetric technique operating in static mode, under similar conditions of temperature, pressure, and mass sample.[11] The trends in the diffusivity coefficients of CO_2 in the ILs can be explained in terms of the changes in viscosities of the ILs and the CO_2−IL mixtures with the IL structure and the operating conditions. Regarding the effect of the anion, the diffusion coefficients exhibit the following order: [bmim][NTf_2] > [bmim][FAP] > [bmim][PF_6], a trend which agrees with the viscosity data reported for the pure ILs (Table 1). As it can be seen in the figures, in all cases, the diffusion coefficients of CO_2 in the ILs increase with absorption temperature, which can be justified from the decreasing viscosities of the solvents with increasing temperatures; however, the CO_2 solubility decreases with temperature, resulting in large but more moderate decrease in the IL viscosities,[47] which accounts for a milder increase in the diffusivity coefficients. The increase in the diffusivity coefficients with increasing operating pressures may be ascribable to the reported decreasing viscosities of the CO_2−IL mixtures with increasing CO_2 partial pressures.[47,48]

In order to compare the experimental effective diffusion coefficients with those estimated by empirical equations, the

dx.doi.org/10.1021/jp4007679 | J. Phys. Chem. B 2013, 117, 3398−3406

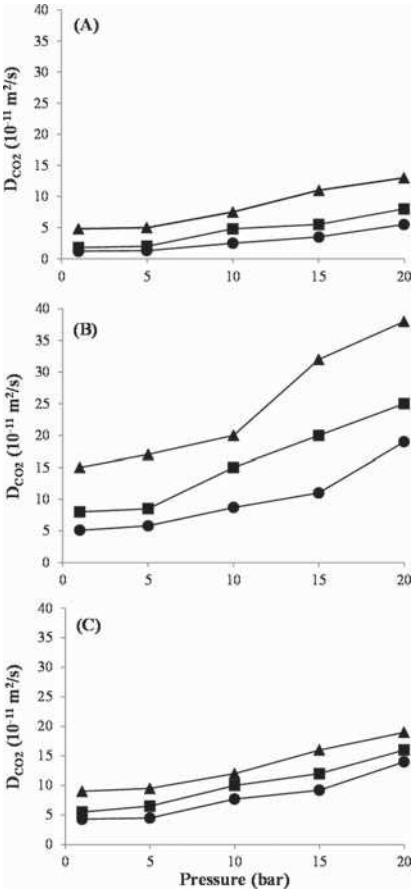

Figure 7. Diffusion coefficient of CO_2 in (A) [bmim][PF_6], (B) [bmim][NTf], and (C) [bmim][FAP] determined from thermogravimetric isothermal data from 1.0 to 20.0 bar by applying eqs 7–9: (●) 298.15 K; (■) 308.15 K; (▲) 323.15 K.

Table 1. Viscosity of the Studied ILs and the Diffusion Coefficients of CO_2 in Them Estimated by the Wilke–Chang Equation

ionic liquid	molar weight (g/mol)	T (K)	viscosity (Pa·s)	D_{CO_2} (m²/s)
[bmim][PF_6]	284.18	293.6	0.3759[a]	1.2×10^{-11}
		302.6	0.2091[a]	2.2×10^{-11}
		312.2	0.1350[a]	3.5×10^{-11}
		321.9	0.0916[a]	5.3×10^{-11}
[bmim][NTf_2]	419.37	293.4	0.0598[a]	9.0×10^{-11}
		302.9	0.0406[a]	1.4×10^{-10}
		312.4	0.0287[a]	2.0×10^{-10}
[bmim][FAP]	584.23	293.0	0.0930[b]	6.8×10^{-11}

[a]From ref 46. [b]From ref 40.

diffusion coefficients of CO_2 in ILs were also calculated using the empirical Wilke–Chang correlation[49]

$$D = 7.4 \times 10^{-8} \frac{(\phi \cdot M_{IL})^{0.5} \cdot T}{\mu \cdot V_{CO_2}^{0.6}} \quad (10)$$

where D is the diffusion coefficient (cm²/s); M_{IL} is the molecular weight of the solvent; T is the temperature (K); μ is the dynamic viscosity of the solution (cP), which will be approximated to the viscosity of the ionic liquid assuming a dilute solution; V_{CO_2} is the molal volume of solute at normal boiling point (cm³/mol); and ϕ is the association parameter with value unity for unassociated solvents.

The diffusion coefficients of CO_2 in [bmim][PF_6], [bmim][NTf_2], and [bmim][FAP] estimated by applying the Wilke–Chang equation at different temperatures are collected in Table 1. In Figure 8, the new estimated diffusion coefficients of CO_2 in the three ILs are compared to the experimental data obtained averaged over pressures (1–20 bar). This figure shows that the diffusivity values estimated by Wilke–Chang are in reasonable agreement with the experimental data obtained for the ILs in the temperature range studied. Hence, the Wilke–Chang equation can be used as an *a priori* approach to evaluate the kinetic behavior of a potential IL candidate for CO_2 absorption.

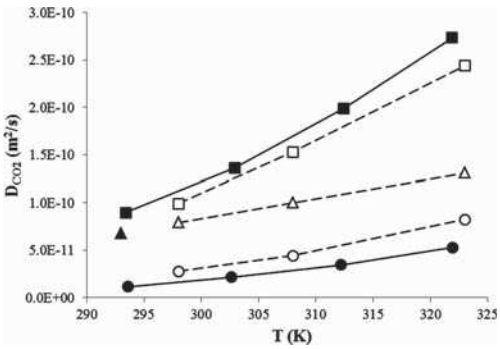

Figure 8. Comparison of diffusion coefficients of CO_2 in ILs obtained from experiments (open symbols) and estimated from Wilke–Chang correlation (filled symbols): (●) [bmim][PF6]; (■) [bmim][NTf_2]; (▲) [bmim][FAP].

3.4. Discussion: Thermodynamics vs Kinetics. The performance of the solvent in an absorption process depends on both thermodynamic and kinetic aspects at the operating conditions; therefore, both of them would need to be considered in the selection of suitable ILs as potential CO_2 absorbents. Figures 9–11 depict the molar fraction of CO_2 absorbed and the corresponding diffusion coefficients to illustrate the effect of the IL structure, temperature, and pressure on the CO_2 absorption process.

Figure 9 shows that the solvent which presents the best absorption capacity (i.e., [bmim][FAP]) is not the one exhibiting the highest CO_2 diffusivity (this is [bmim][NTf_2]). Figure 10 indicates that the temperature is a crucial parameter to optimize in the absorption process, since decreasing temperature increases the amount of CO_2 absorbed but decreases diffusion rates. Figure 11 shows that, for a given temperature, operating at higher pressures improves both the absorption capacity and the diffusivity. Current results indicate that the selection of the IL structure and the operating conditions should be considered in the process optimization to

dx.doi.org/10.1021/jp4007679 | J. Phys. Chem. B 2013, 117, 3398–3406

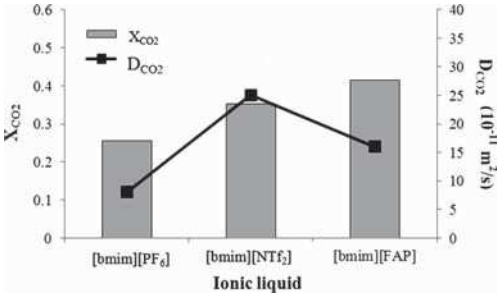

Figure 9. Effect of the anion on the solubility (mole fraction, X_{CO_2}) and diffusivity of CO_2 in ILs (T = 308.15 K and P = 20 bar).

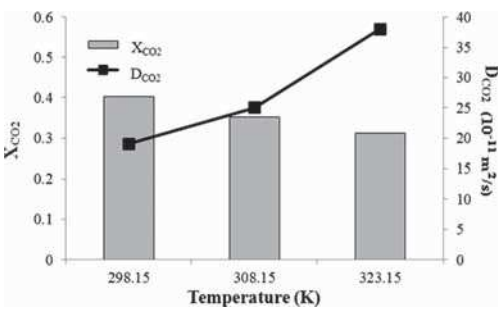

Figure 10. Effect of the temperature on the solubility (mole fraction, X_{CO_2}) and diffusivity of CO_2 in [bmim][NTf$_2$] at P = 20 bar.

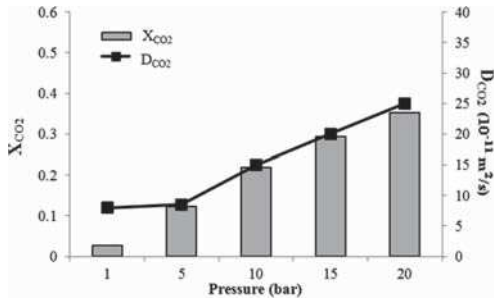

Figure 11. Effect of the pressure on the solubility (mole fraction, X_{CO_2}) and diffusivity of CO_2 in [bmim][NTf$_2$] at T = 308.15 K.

obtain the best balance between absorption capacity and rate in CO_2 capture operations.

4. CONCLUSIONS

A thermogravimetric technique based on a magnetic suspension balance operating in dynamic mode was used to study the thermodynamics and kinetics of CO_2 in the ionic liquids (ILs) [bmim][PF$_6$], [bmim][NTf$_2$], and [bmim][FAP] at temperatures ranging from 298.15 to 323.15 K and pressures up to 20 bar. The effect of the operating conditions and the structure of the anion on the solubility and diffusion data was reported. The proposed technique was shown to be a fast and accurate method to determine the absorption data of CO_2 in ILs, providing the possibility of directly determining the density of the samples to obtain reliable thermodynamic and kinetic data.

The isothermal densities of the ionic liquids were in the order of 1.3−1.6 g/cm^3, decreasing with increasing temperature and showing the following trend: [bmim][FAP] > [bmim][NTf$_2$] > [bmim][PF$_6$]. The solubility of CO_2 in the ionic liquids increased with decreasing temperatures and increasing pressures and followed the subsequent trend: [bmim][FAP] > [bmim][NTf$_2$] > [bmim][PF6], reaching maximum molar fractions of absorbed CO_2 corresponding to 0.47, 0.40, and 0.29, respectively, at 298.15 K and 20 bar. The diffusion coefficients of CO_2 in the ILs increased with increasing temperatures and pressures and showed the following trend: [bmim][NTf$_2$] > [bmim][FAP] > [bmim][FAP], presenting orders of magnitude from 10^{-10} to 10^{-11} m^2/s. Finally, the empirical Wilke−Chang correlation was successfully applied as an alternative to the diffusion model to estimate the diffusion coefficients of the systems. The results indicated the suitability of using this approach to foresee the kinetic behavior of the ILs for CO_2 absorption.

Experimental and theoretical results in this work illustrate the different thermodynamic and kinetic performance of a specific IL in the CO_2 absorption process, being a critical issue to assess both aspects in the development of industrial operations based on ILs for CO_2 capture. The methodology proposed in this work and the results obtained thereby might be helpful in the selection of appropriate solvents to develop novel absorption processes based on ILs.

■ ASSOCIATED CONTENT

Supporting Information

Table S1: Experimental isothermal density data of ionic liquids. Tables S2−S4: Experimental solubility data, Henry's law constants and diffusion coefficients of CO_2 in ionic liquids. This material is available free of charge via the Internet at http://pubs.acs.org.

■ AUTHOR INFORMATION

Corresponding Author

*Phone: 34 91 4976938. Fax: 34 91 4973516. E-mail: pepe.palomar@uam.es.

Notes

The authors declare no competing financial interest.

■ ACKNOWLEDGMENTS

The authors are grateful to the "Ministerio de Economía y Competitividad" and "Comunidad de Madrid" for financial support (projects CTQ2011-26758 and S2009/PPQ-1545, respectively).

■ REFERENCES

(1) IPCC. *In Climate Change 2007: The Physical Science Basis. Contribution of Working Group I to the Fourth Assessment Report of the Intergovernmental Panel on Climate Change*; Cambridge University Press: Cambridge, U.K., and New York, 2007.

(2) Rao, A. B.; Rubin, E. A. A Technical, Economic, and Environmental Assessment of Amine-Based CO_2 Capture Technology for Power Plant Greenhouse Gas Control. *Environ. Sci. Technol.* **2002**, *36*, 4467−4475.

(3) Wasserscheid, P.; Welton, T. *Ionic Liquids in Synthesis*; Wiley-VCH: Weinheim, Germany, 2003.

(4) Plechkova, N. V.; Seddon, K. R. Applications of Ionic Liquids in the Chemical Industry. *Chem. Soc. Rev.* **2008**, *37*, 123−150.
(5) Palomar, J.; Torrecilla, J. S.; Ferro, V.; Rodriguez, F. Development of an a Priori Ionic Liquid Design Tool. 1. Integration of a Novel COSMO-RS Molecular Descriptor on Neural Networks. *Ind. Eng. Chem. Res.* **2008**, *47*, 4523−4532.
(6) Palomar, J.; Torrecilla, J. S.; Ferro, V.; Rodriguez, F. Development of an a Priori Ionic Liquid Design Tool. 2. Ionic Liquid Selection through the Prediction of COSMO-RS Molecular Descriptor by Inverse Neural Network. *Ind. Eng. Chem. Res.* **2009**, *48*, 2257−2265.
(7) Huang, J.; Rüther, T. Why Are Ionic Liquids Attractive for CO_2 Absorption? An Overview. *Aust. J. Chem.* **2009**, *62*, 298−308.
(8) Bara, J. E.; Carliste, T. K.; Gabriel, C. J.; Camper, D.; Finotello, A.; Gin, D. L.; Noble, R. D. Guide to CO_2 Separations in Imidazolium-Based Room-Temperature Ionic Liquids. *Ind. Eng. Chem. Res.* **2009**, *48*, 2739−2751.
(9) Karadas, F.; Atilhan, M.; Aparicio, S. Review on the Use of Ionic Liquids (ILs) as Alternative Fluids for CO_2 Capture and Natural Gas Sweetening. *Energy Fuels* **2010**, *24*, 5817−5828.
(10) Ramdin, M.; de Loos, T. W.; Vlugt, T. H. J. State-of-the-Art of CO_2 Capture with Ionic Liquids. *Ind. Eng. Chem. Res.* **2012**, *51*, 8149−8177.
(11) Shiflett, M. B.; Yokozeki, A. Solubilities and Diffusivities of Carbon Dioxide in Ionic Liquids: [bmim][PF_6] and [bmim][BF_4]. *Ind. Eng. Chem. Res.* **2005**, *44*, 4453−4464.
(12) Soriano, A. N.; Doma, B. T.; Li, M. H. Carbon Dioxide Solubility in Some Ionic Liquids at Moderate Pressures. *J. Taiwan Inst. Chem. Eng.* **2009**, *40*, 387−393.
(13) Chen, Y.; Han, J.; Wang, T.; Mu, T. Determination of Absorption Rate and Capacity of CO_2 in Ionic Liquids at Atmospheric Pressure by Thermogravimetric Analysis. *Energy Fuels* **2011**, *25*, 5810−5815.
(14) Anthony, J. L.; Maginn, E. J.; Brennecke, J. F. Solubilities and Thermodynamic Properties of Gases in the Ionic Liquid 1-n-Butyl-3-methylimidazolium hexafluorophosphate. *J. Phys. Chem. B* **2002**, *106* (29), 7315−7320.
(15) Anthony, J. L.; Anderson, J. L.; Maginn, E. J.; Brennecke, J. F. Anion Effects on Gas Solubility in Ionic Liquids. *J. Phys. Chem. B* **2005**, *109*, 6366−6374.
(16) Anderson, J. L.; Dixon, J. K.; Brennecke, J. F. Solubility of CO_2, CH_4, C_2H_6, C_2H_4, O_2, and N_2 in 1-Hexyl-3-methylpyridinium Bis(trifluoromethylsulfonyl)imide: Comparison to Other Ionic Liquids. *Acc. Chem. Res.* **2007**, *40*, 1208−1216.
(17) Muldoon, M. J.; Aki, S. N.; Anderson, J. L.; Dixon, J. K.; Brennecke, J. F. Improving Carbon Dioxide Solubility in Ionic Liquids. *J. Phys. Chem. B* **2007**, *111*, 9001−9009.
(18) Zhang, X.; Liu, Z.; Wang, W. Screening of Ionic Liquids to Capture CO_2 by COSMO-RS and Experiments. *AIChE J.* **2008**, *54* (10), 2717−2728.
(19) Soriano, A. N.; Doma, B. T.; Li, M. H. Solubility of Carbon Dioxide in 1-Ethyl-3-methylimidazolium 2-(2-Methoxyethoxy)-ethylsulfate. *J. Chem. Thermodyn.* **2008**, *40*, 1654−1660.
(20) Soriano, A. N.; Doma, B. T.; Li, M. H. Carbon Dioxide Solubility in 1-Ethyl-3-methylimidazolium Tetrafluoroborate. *J. Chem. Eng. Data* **2008**, *53*, 2550−2555.
(21) Soriano, A. N.; Doma, B. T.; Li, M. H. Carbon Dioxide Solubility in 1-Ethyl-3-methylimidazolium Trifluoromethanesulfonate. *J. Chem. Thermodyn.* **2009**, *41*, 525−529.
(22) Yokozeki, A.; Shiflett, M. B. Separation of Carbon Dioxide and Sulfur Dioxide Gases Using Room-Temperature Ionic Liquid [hmim][Tf_2N]. *Energy Fuels* **2009**, *23*, 4701−4708.
(23) Zhang, X.; Hun, F.; Liu, Z.; Wang, W.; Shi, W.; Maginn, E. J. Absorption of CO_2 in the Ionic Liquid 1-n-Hexyl-3-methylimidazolium Tris(pentafluoroethyl)trifluorophosphate ([hmim][FEP]): A Molecular View by Computer Simulations. *J. Phys. Chem. B* **2009**, *113*, 7591−7598.
(24) Palomar, J.; Gonzalez-Miquel, M.; Polo, A.; Rodriguez, F. Understanding the Physical Absorption of CO_2 in Ionic Liquids Using the COSMO-RS Method. *Ind. Eng. Chem. Res.* **2011**, *50*, 3452−3463.
(25) Finotello, A.; Bara, J. E.; Camper, D.; Noble, R. D. Room-Temperature Ionic Liquids: Temperature Dependence of Gas Solubility Selectivity. *Ind. Eng. Chem. Res.* **2008**, *47*, 3453−3459.
(26) Kerlé, D.; Ludwig, R.; Geiger, G.; Paschek, D. Temperature Dependence of the Solubility of Carbon Dioxide in Imidazolium-Based Ionic Liquids. *J. Phys. Chem. B* **2009**, *113*, 12727−12735.
(27) Lim, B. H.; Choe, W. H.; Shim, J. J.; Ra, C. S.; Tuma, D.; Lee, H.; Lee, C. S. High-Pressure Solubility of Carbon Dioxide in Imidazolium-Based Ionic Liquids with Anions [PF_6] and [BF_4]. *Korean J. Chem. Eng.* **2009**, *26* (4), 1130−1136.
(28) Carvalho, P. J.; Alvarez, V. H.; Marrucho, I. M.; Aznar, M.; Coutinho, J. A. P. High Pressure Phase Behavior of Carbon Dioxide in 1-Butyl-3-methylimidazolium Bis(trifluoromethylsulfonyl)imide and 1-Butyl-3-methylimidazolium Dicyanamide Ionic Liquids. *J. Supercrit. Fluids* **2009**, *50*, 105−111.
(29) Camper, D.; Becker, C.; Koval, C.; Noble, R. Diffusion and Solubility Measurements in Room Temperature Ionic Liquids. *Ind. Eng. Chem. Res.* **2006**, *45* (1), 445−4450.
(30) Morgan, D.; Ferguson, L.; Scovazzo, P. Diffusivities of Gases in Room-Temperature Ionic Liquids: Data and Correlations Obtained Using a Lag-Time Technique. *Ind. Eng. Chem. Res.* **2005**, *44*, 4815−4823.
(31) Moganty, S. S.; Baltus, R. E. Diffusivity of Carbon Dioxide in Room-Temperature Ionic Liquids. *Ind. Eng. Chem. Res.* **2010**, *49*, 9370−9376.
(32) Kortenbruck, K.; Pohrer, B.; Schluecker, E.; Friedel, F.; Ivanovic-Burmazovic, I. Determination of the Diffusion Coefficient of CO_2 in the Ionic Liquid [emim][NTf_2] Using Online FTIR Measurements. *J. Chem. Thermodyn.* **2012**, *47*, 76−80.
(33) Gonzalez-Miquel, M.; Palomar, J.; Omar, S.; Rodríguez, F. CO_2/N_2 Selectivity Prediction in Supported Ionic Liquid Membranes (SILMs) by COSMO-RS. *Ind. Eng. Chem. Res.* **2011**, *50*, 5739−5748.
(34) Gonzalez-Miquel, M.; Talreja, M.; Ethier, A. L.; Flack, K.; Switzer, J. R.; Biddinger, E. J.; Pollet, P.; Palomar, J.; Rodriguez, F.; Eckert, C. A.; et al. COSMO-RS Studies: Structure−Property Relationships for CO_2 Capture by Reversible Ionic Liquids. *Ind. Eng. Chem. Res.* **2012**, *51*, 16066−16073.
(35) Palomar, J.; Gonzalez-Miquel, M.; Bedia, J.; Rodriguez, F.; Rodriguez, J. J. Task-Specific Ionic Liquids for Efficient Ammonia Absorption. *Sep. Purif. Technol.* **2011**, *82*, 43−52.
(36) Bedia, J.; Palomar, J.; Gonzalez-Miquel, M.; Rodriguez, F.; Rodriguez, J. J. Screening ILs as Suitable NH_3 Absorbents on the Basis on Thermodynamic and Kinetic analysis. *Sep. Purif. Technol.* **2012**, *95*, 188−195.
(37) Bedia, J.; Ruiz, E.; de Riva, J.; Ferro, V. R.; Palomar, J.; Rodriguez, J. J. Optimized Ionic Liquids for Toluene Absorption. *AIChE J.* **2012**, DOI: 10.1002/aic.13926.
(38) Gonzalez-Miquel, M.; Palomar, J.; Rodriguez, F. Selection of Ionic Liquids for Enhancing the Gas Solubility of Volatile Organic Compounds. *J. Phys. Chem. B* **2013**, *117*, 296−306.
(39) Harris, K. R.; Woolf, L. A.; Kanakubo, M. Temperature and Pressure Dependence of the Viscosity of the Ionic Liquid 1-Butyl-3-methylimidazolium Hexafluorophosphate. *J. Chem. Eng. Data* **2005**, *50*, 1777−1782.
(40) Merck Millipore, 2012. http://www.merckmillipore.com/showBrochure/200910.245.ProNet.pdf.
(41) Sedláková, Z.; Wagner, Z. High-pressure Phase Equilibria in Systems Containing CO_2 and Ionic Liquid of the [Cnmim][Tf_2N] type. *Chem. Biochem. Eng. Q.* **2012**, *26* (1), 55−60.
(42) Camper, D.; Scovazzo, P.; Koval, C.; Noble, R. Gas Solubilities in Room Temperature Ionic Liquids. *Ind. Eng. Chem. Res.* **2004**, *43* (12), 3049−3054.
(43) Jacquemin, J.; Husson, P.; Majer, V.; Costa Gomes, M. F. C. Low-pressure Solubilities and Thermodynamics of Solvation of Eight Gases in 1-Butyl-3-methylimidazolium Hexafluorophosphate. *Fluid Phase Equilib.* **2006**, *240* (1), 87−95.
(44) Shiflett, M. B.; Yokozeki, A. Solubility and Diffusivity of Hydrofluorocarbons in Room-Temperature Ionic Liquids. *AIChE J.* **2006**, *52* (3), 1205−1219.

(45) Zhang, J.; Zhang, Q.; Qiao, B.; Deng, Y. Solubilities of the Gaseous and Liquid Solutes and Their Thermodynamics of Solubilitation in the Novel Room-Temperature Ionic Liquids at Infinite Dilution by Gas Chromatography. *J. Chem. Eng. Data* **2007**, *52*, 2277−2283.
(46) Jacquemin, J.; Husson, P.; Padua, A. A. H.; Majer, V. Density and Viscosity of Several Pure and Water-Saturated Ionic Liquids. *Green Chem.* **2006**, *8*, 172−180.
(47) Ahosseinia, A.; Ortegab, E.; Sensenichc, B.; Scurtoa, A. M. Viscosity of n-Alkyl-3-methyl-imidazolium Bis-(trifluoromethylsulfonyl)amide Ionic Liquids Saturated with Compressed CO_2. *Fluid Phase Equilib.* **2009**, *286*, 72−78.
(48) Tomida, D.; Kenmochi, S.; Qiao, K.; Bao, Q̃; Yokoyama, C. Viscosity of Ionic Liquid Mixtures of 1-Alkyl-3-methylimidazolium Hexafluorophosphate + CO_2. *Fluid Phase Equilib.* **2011**, *307*, 185−189.
(49) Wilke, C. R.; Chang, P. Correlation of Diffusion Coefficients in Dilute Solutions. *AIChE J.* **1955**, 264−270.
(50) Fredlake, C. P.; Crosthwaite, J. M.; Hert, D. H.; Aki, S. N. V. K.; Brennecke, J. F. Thermophysical Properties of Imidazolium-Based Ionic Liquids. *J. Chem. Eng. Data* **2004**, *49*, 954−964.

Publicación 5:

Gonzalez-Miquel, M.; Bedia, J.; Palomar, J.; Rodriguez, F. **Solubility and diffusivity of CO_2 in [hxmim][NTf_2], [omim][NTf_2] and [dcmim][NTf_2] at T=(298.15, 308.15 and 323.15) K and pressures up to 20 bar.** *Journal of Chemical & Engineering Data*, **2013** (*Submitted*)

Solubility and Diffusivity of CO_2 in [hxmim][NTf_2], [omim][NTf_2] and [dcmim][NTf_2] at T=(298.15, 308.15 and 323.15) K and pressures up to 20 bar

Maria Gonzalez-Miquel[a], *Jorge Bedia*[b], *Jose Palomar**[b], *Francisco Rodriguez*[a]

[a]Departamento de Ingeniería Química, Universidad Complutense de Madrid, 28040 Madrid, Spain.

[b]Departamento de Química Física Aplicada (Sección de Ingeniería Química), Universidad Autónoma de Madrid, Cantoblanco, 28049 Madrid, Spain.

ABSTRACT

Solubilities and diffusion coefficients of CO_2 absorption in the ionic liquids (ILs) [hxmim][NTf_2], [omim][NTf_2] and [dcmim][NTf_2] at temperatures of 298.15, 308.15 and 323.15 K, and pressures up to 20 bar were obtained by thermogravimetric measurements using a high pressure sorption analyzer with magnetic suspension balance operating in dynamic mode. The effect of the length of the alkyl side chain of the imidazolium cation and the operating conditions on the thermodynamics and kinetics of the CO_2 absorption process in ILs were evaluated. Absorption data confirmed that the CO_2 solubility in ILs increases with increasing length of the alkyl side chain of the cation, and with decreasing temperatures and increasing pressures. The diffusion coefficients of CO_2, calculated by applying a mass diffusion model, decrease with increasing lengths of the alkyl side chain of the cation, and increase with both temperature and pressure of absorption. These results illustrate the importance of considering both thermodynamic and kinetic aspects in the selection of an IL as absorbent and the operating conditions for developing absorption processes based on ILs. In addition, the empirical correlation of Wilke-Chang was successfully applied as an alternative to estimate the diffusion coefficients of the systems.

1. INTRODUCTION

The increasing CO_2 atmospheric concentration and its relationship to the greenhouse effect and global warming has become a major concern nowadays[1]. Fossil fuel combustion is regarded as the main contributor to CO_2 emissions to the atmosphere, and it is expected to remain as the principal source of power generation in the upcoming years[2,3]. Current technologies for post-combustion CO_2 capture are based on amine solvents, which are energy intensive and has negative environmental impact due to their corrosive nature and volatility[4]. Therefore, the development of more environmentally friendly technologies for CO_2 emissions reduction is urgently needed.

Ionic liquids (ILs) are a broad category of organic salts which have been extensively proposed as alternative to the conventional volatile solvents due to their unique properties, such as their negligible vapor pressure and their tailorability[5-8]. In particular, the use of ILs as absorbents for CO_2 capture has generated increasing interest in recent years[9-13], with numerous studies reporting the effect of the solvent molecular structure[14-17] and the process conditions[18-23] on the behavior of CO_2-ILs systems. However, research on CO_2 capture with ionic liquids mostly focuses on solubility data, and there is lack of other physicochemical and kinetic information which is highly required to evaluate the performance of the solvent to absorb the gaseous solute[13].

In order to address this issue, previous works of our group have been dealing with the development of property predicting tools, and/or experimental research on both thermodynamics and kinetics of several gases in ILs, including NH_3[24,25], toluene[26], and VOCs[27]. Specifically, in the case of CO_2[28-31], we have conducted theoretical research based on quantum-chemical simulations and empirical diffusion models to provide further insights in understanding the behavior of CO_2 absorption in ILs. Moreover, we have recently reported and validated a procedure based on thermogravimetric measurements to evaluate the thermodynamics and kinetics of CO_2 absorption in imidazolium based-ILs paired with different anions, i.e. [PF_6], [NTf_2] and [FAP], with results showing different trends for absorption capacities and diffusivities of CO_2 in ILs as function of IL structure, temperature and pressure[31]. In current paper, we aim to further study the performance of the imidazolium-[NTf_2] ILs by evaluating the effect of the length of the alkyl side chain of the imidazolium ring on the absorption process.

In this contribution, thermogravimetric measurements were performed to determine the absorption isotherms of CO_2 in the ionic liquids [hxmim][NTf_2], [omim][NTf_2] and [dcmim][NTf_2], at temperatures of 298.15, 308.15 and 323.15 K, and pressures up to 20 bar. Afterwards, the effect of the length of the alkyl side chain of the cation and the operating conditions on the thermodynamics and kinetics of the absorption process of CO_2 in ILs was studied. Firstly, the density of the solvents and the solubility and Henry´s law constants of CO_2 in the ILs were determined. Afterwards, the diffusion coefficients of CO_2 in each one of the ILs at the different temperatures were calculated from the time-dependent absorption data by using a diffusion mass model. In addition, the empirical correlation of Wilke-Chang was used as an alternative to estimate the diffusion coefficients of the systems, and the suitability of using this equation to predict the kinetic behavior of the ILs for CO_2 absorption was evaluated.

2. EXPERIMENTAL PROCEDURE

2.1 Materials

Carbon dioxide, CO_2, and nitrogen, N_2, were obtained from Praxair, Inc., with a minimum purity of 99.999%. The ionic liquids 1-hexyl-3-methylimidazolium bis(trifluoromethanesulfonil)imide [hxmim][NTf_2], 1-octyl-3-methylimidazolium bis(trifluoromethanesulfonil)imide [omim][NTf_2], and 1-decyl-3-methylimidazolium bis(trifluoromethanesulfonil)imide [dcmim][NTf_2], were obtained from Io-Li-Tec (Ionic Liquid Technologies), all of them with a minimum purity of 99%.

2.2 Experimental set-up

A Gravimetric High Pressure Sorption Analyzer (ISOSORP GAS LP-flow, Rubotherm) operating in dynamic mode was used to perform the gas solubility measurements of CO_2 in the ILs.

The Rubotherm sorption analyzer equipment is controlled with the software Messpro, which allows for the absorption process to be fully monitored and provides a precise control of the measurement of weight, pressure, and temperature required to determine the gas absorption-desorption isotherms and isobars.

The sorption measuring analyzer with magnetic suspension balance (MSB) presents a measuring load of 0-10 g and a resolution of the mass reading of 0.01 mg, with a reproducibility of ± 0.03 mg and an uncertainty < 0.002%. The equipment can operate at pressures ranging from 10^{-6} bar (ultra-high vacuum, UHV) to 30 bar. The pressure is controlled with an uncertainty corresponding to ± 0.01 bar. The temperature of the sample is regulated by an external thermostat with circulating bath (Julabo F25-ME), which can operate from room temperature up to 150º C. The temperature is controlled with an uncertainty corresponding to ± 0.01 K.

It is worth mentioning that a main advantage of this sorption analyzer is the possibility of measuring the density of the sample, which is required to correct the buoyancy effects acting on the sample in order to accurately determine the thermodynamic and kinetic data.

The procedure followed to perform the gravimetric measurements (i.e. buoyancy and absorption experiments) with the Rubotherm magnetic suspension balance and the treatment of the collected data to determine the densities of the solvents and the solubilities of CO_2 in the ILs is explained in our previous work[31]. The maximum uncertainty of the measured ionic liquid density data is estimated to be below 0.002 g/cm^3, and the maximum uncertainty of the measured absorbed CO_2 mole fraction is estimated to be below 0.005.

3. RESULTS

The density data of the ionic liquids was determined from the buoyancy measurements performed with the Rubotherm sorption analyzer following the procedure exposed in our previous work[31]. The results obtained for the isothermal densities of the ionic liquids [hxmim][NTf_2], [omim][NTf_2] and [dcmim][NTf_2] at temperatures ranging from 298.15 to 323.15 K are plotted in Figure 1. These results are in agreement with the available reported data[32,33] within about 0.3-1.8% over the temperatures studied. Overall densities of the ILs are in the order of 1.2-1.4 g/cm^3, decreasing with increasing temperatures and with the length of the alkyl chain in the subsequent order: [hxmim][NTf_2] > [omim][NTf_2] > [dcmim][NTf_2].

Figures 2, 3 and 4 show respectively the absorption isotherms of CO_2 in [hxmim][NTf_2], [omim][NTf_2] and [dcmim][NTf_2] at temperatures of 298.15, 308.15 and 323.15 K, and pressure ranging from 1 to 20 bar. The thermodynamic equilibrium of the systems was reached in approximately 2 h for each *T,P* set-point. In addition, the recovery of the solvents after each one of the experiments was achieved in less than 20 min under vacuum for all the systems studied. In all cases, it was verified that the final mass of the IL was the same as the mass initially loaded (weight change < 0.2%). Our results are in agreement with the available reported values of CO_2 solubility in [hxmim][NTf_2][34] measured by a similar thermogravimetric technique. Note that the small shift between the absorption isotherms observed in this work and those previously published (Fig. 2) is due to the slightly different absorption temperatures (298.15 and 323.15 in this work, and 297.3 and 322.9 K in the reported work). As expected, the obtained results confirm that the absorbed CO_2 mole fraction increases with decreasing temperature and increasing pressure for all the ILs studied. Moreover, results show that the CO_2 solubility in the ILs slightly decreases with decreasing length of the alkyl chain of the cation as follows: [dcmim][NTf_2]>[omim][NTf_2]>[hxmim][NTf_2]. As an additional parameter for evaluating the CO_2 solubility trends in the studied solvents, the Henry´s law constant (K_H) of CO_2 in the ILs were estimated from the slopes of the linear fits of the collected solubility data at low pressures. Figure 5 illustrates that the Henry´s law constants of CO_2 decrease with decreasing absorption temperatures and with increasing length of the alkyl side chain of the cation, as higher values of K_H indicate lower CO_2 solubilities.

The diffusion coefficients of CO_2 in the ILs were estimated from the time-dependent absorption data by applying a mass diffusion model, following the procedure exposed in our previous work[31]. This approach was successfully applied by Shifflet and Yokoezi for studying the kinetics of CO_2 in ILs[18], and has also been used by our group for determining the diffusion coefficients of several gaseous solutes in ILs, including NH_3[25], toluene[26] and CO_2[31]. The diffusion coefficients of CO_2 in the ionic liquids [hxmim][NTf_2], [omim][NTf_2] and [dcmim][NTf_2] as a function of the temperature and pressure are plotted in Fig 6. The order of magnitude of the diffusion coefficients are about from 10^{-10} to 10^{-11} m^2/s. In all cases, the diffusion coefficients increase with the

absorption temperature and pressure. The observed trends can be explained from the changes in the viscosities of the ILs and the CO_2-IL mixtures with the operating conditions[35,36]. Regarding the effect of the structure of the cation, the diffusion coefficients of CO_2 decrease with increasing lengths of the alkyl side chain of the imidazolium ring, as follows: [hxmim][NTf_2] > [omim][NTf_2] > [dcmim][NTf_2]. This behavior agrees with the viscosity trends of the solvents (see Table 1).

In our previous works, the empirical correlation of Wilke-Chang has also been used to estimate the diffusion coefficients of several gaseous solutes[25,26,31] in ILs as an alternative to the diffusion mass model to study the kinetic behavior of the systems. Following, the empirical correlation of Wilke-Chang will be applied to estimate the diffusion coefficients of CO_2 in the studied ILs, and the results will be compared to those previously calculated from the experimental data by applying the diffusion mass model. The empirical correlation of Wilke-Chang[38] can be written as follows,

$$\mathrm{D} = 7.4 \cdot 10^{-8} \frac{(\phi \cdot M_{IL})^{0.5} \cdot T}{\mu \cdot V_{CO_2}^{0.6}}$$

where D is the diffusion coefficient (cm^2/s); M_{IL} is the molecular weight of the IL; T is the temperature (K); μ is the dynamic viscosity of the IL (cP); V_{CO_2} is the molal volume of the solute at normal boiling point (cm^3/mol); and ϕ is the association parameter with value unity for unassociated solvents. The diffusion coefficients of CO_2 in ILs estimated by applying the Wilke-Chang equation are presented in Table 1. Comparison of the estimated diffusion coefficients with those calculated by applying the diffusion mass model over pressures (1-20 bar) is plotted in Figure 7. This figure shows that the diffusivity values estimated by both approaches follow similar trends.

In order to evaluate the performance of the studied ILs for CO_2 absorption from both thermodynamic and kinetic aspects, Figures 8-10 illustrate the absorbed CO_2 molar fractions and the corresponding diffusion coefficients as function of the IL structure and operating conditions. Figure 8 shows that increasing the alkyl side chain of the imidazolium cation results in slightly higher CO_2 absorption capacities but lower diffusion rates. Figure 9 illustrates that increasing the absorption temperature, decrease the CO_2 solubility but notably increase the CO_2 diffusivity. Figure 10 indicates that

increasing the absorption pressure both enhance the CO_2 absorption capacity and diffusion rate. These results suggest that the selection of the IL molecular structure and the operating conditions are key parameters to optimize the development of absorption processes for CO_2 capture based on ILs.

4. CONCLUSIONS

A high-pressure sorption analyzer operating in dynamic mode was used to perform thermogravimetric measurements of CO_2 in the ionic liquids [hxmim][NTf_2], [omim][NTf_2] and [dcmim][FAP] at temperatures ranging from 298.15 to 323.15 K and pressures up to 20 bar. The absorption isotherms and the Henry´s laws constants of the systems were determined, and from the time-dependent absorption data the diffusion coefficients of the systems were calculated by applying a mass diffusion model. Based on the obtained thermodynamic and kinetic data, the effects of the length of the alkyl side chain of the imidazolium cation and the operating conditions on the CO_2 absorption process were evaluated.

The isothermal densities of the ionic liquids were in the order of 1.2-1.4 g/cm^3, decreasing with increasing temperatures and with the length of the alkyl side chain of the cation. The solubility of CO_2 in ILs increases with increasing lengths of the alkyl side chain of the cation, and with decreasing temperatures and increasing pressures. The diffusion coefficients of CO_2 decreases with increasing lengths of the alkyl side chain of the cation, and increases with both temperature and pressure of absorption. These results illustrate that the solvent structure and the process conditions need to be optimize in order to obtain the best balance between the thermodynamic and kinetic performance of the ILs to be used in the development of absorption processes.

In addition, the empirical correlation of Wilke-Chang was successfully applied as an alternative to the diffusion mass model to determine the diffusion coefficients of the systems. This approach might be helpful to anticipate the kinetic behavior of potential ILs for CO_2 absorption.

ASSOCIATED CONTENT

Supporting Information. Table S1: Experimental isothermal density data of ionic liquids. Tables S2-S4: Experimental solubility data, Henry´s law constants and diffusion coefficients of CO_2 in ionic liquids. This material is available free of charge via the Internet at http://pubs.acs.org.

AUTHOR INFORMATION

Corresponding Author

* Tel.: 34 91 4976938. Fax: 34 91 4973516. E-mail: pepe.palomar@uam.es

Notes

The authors declare no competing financial interest.

ACKNOWLEDGMENTS

The authors are grateful to the "Ministerio de Economía y Competitividad" and "Comunidad de Madrid" for financial support (Projects CTQ2011-26758 and S2009/PPQ-1545, respectively).

REFERENCES

(1) IPCC. In Climate Change 2007: The Physical Science Basis. Contribution of Working Group I to the Fourth Assessment Report of the Intergovernmental Panel on Climate Change. *Cambridge University Press*: Cambridge, U.K., and New York, NY, USA, **2007**.

(2) CO_2 Emissions from Fuel Combustion Highlights; *International Energy Agency*: Paris, **2012**.

(3) World Energy Outlook; *International Energy Agency*: Paris, **2012**.

(4) Rao, A.B. and Rubin, E.A. Technical, economic, and environmental assessment of amine-based CO_2 capture technology for power plant greenhouse gas control. *Environ. Sci. Technol.* **2002**, *36*, 4467-4475.

(5) Wasserscheid, P. and Welton, T. *Ionic Liquids in Synthesis*. *Wiley-VCH*, Weinheim (Second Edition), **2008**.

(6) Plechkova, N.V. and Seddon, K.R. Applications of ionic liquids in the chemical industry. *Chem. Soc. Rev.* **2008**, *37*, 123-150

(7) Palomar, J.; Torrecilla, J.S.; Ferro, V.R.; Rodriguez, F. Development of an a priori ionic liquid design tool. 1. Integration of a novel COSMO-RS molecular descriptor on neural networks. *Ind. Eng. Chem. Res.* **2008**, *47*, 4523–4532.

(8) Palomar, J.; Torrecilla, J.S.; Ferro, V.R.; Rodriguez, F. Development of an a priori ionic liquid design tool. 2. Ionic liquid selection through the prediction of COSMO-RS molecular descriptor by inverse neural network. *Ind. Eng. Chem. Res.* **2009**, *48*, 2257-2265.

(9) Huang, J. and Reuther, T. Why are ionic liquids attractive for CO_2 absorption? An overview. *Aust. J. Chem.* **2009**, *62*, 298–308.

(10) Bara, J. E.; Carliste, T. K.; Gabriel, C.J.; Camper, D.; Finotello, A.; Gin, D. L.; Noble, R. D. Guide to CO_2 separations in imidazoliumbased room-temperature ionic liquids. *Ind. Eng. Chem. Res.* **2009**, *48*, 2739–2751.

(11) Brennecke, J.F. and Gurkan, B.E. Ionic Liquids for CO_2 capture and emission reduction. *J. Phys. Chem. Lett.* **2010**, *1 (24)*, 3459-3464.

(12) Karadas, F.; Atilhan, M.; Aparicio, S. Review on the use of ionic liquids (ILs) as alternative fluids for CO_2 capture and natural gas sweetening, *Energy Fuels* **2010**, *24*, 5817–5828.

(13) Ramdin, M.; de Loos, T.W.; Vlugt, T.H.J. State-of-the-Art of CO_2 capture with ionic liquids. *Ind. Eng. Chem. Res.* **2012**, *51*, 8149−8177.

(14) Anthony, J.L.; Maginn, E.J.; Brennecke, J.F. Solubilities and thermodynamic properties of gases in the ionic liquid 1-n-butyl-3-methylimidazolium hexafluorophosphate. *J. Phys. Chem. B.* **2002**, *106 (29)*, 7315-7320.

(15) Anthony, J.L.; Anderson, J.L.; Magín, E.J.; Brennecke, J. F. Anion effects on gas solubility in ionic liquids. *J. Phys. Chem. B* **2005**, *109*, 6366–6374.

(16) Muldoon, M. J.; Aki, S. N.; Anderson, J. L.; Dixon, J. K.; Brennecke, J. F. Improving carbon dioxide solubility in ionic liquids. *J. Phys. Chem. B* **2007**, *111*, 9001–9009.

(17) Zhang, X.; Hun, F.; Liu, Z.; Wang, W.; Shi, W.; Maginn, E. J. Absorption of CO_2 in the ionic liquid tris(pentafluoroethyl)- trifluorophosphate ([hmim][FEP]): A molecular view by computer simulations. *J. Phys. Chem. B* **2009**, *113*, 7591–7598.

(18) Shiflett, M.B. and Yokozeki, A. Solubilities and diffusivities of carbon dioxide in ionic liquids: [bmim][PF_6] and [bmim][BF_4]. *Ind. Eng. Chem. Res.* **2005**, *44*, 4453-4464.

(19) Jacquemin, J.; Husson, P.; Majer, V.; Costa Gomes, M.F.C. Low-pressure solubilities and thermodynamics of solvation of eight gases in 1-butyl-3-methylimidazolium hexafluorophosphate. *Fluid Phase Equilib.* **2006**, *240 (1)*, 87-95.

(20) Finotello, A.; Bara, J. E.; Camper, D.; Noble, R. D. Room- Temperature Ionic Liquids: temperature dependence of gas solubility selectivity. *Ind. Eng. Chem. Res.* **2008**, *47*, 3453–3459.

(21) Kerlé, D.; Ludwig, R.; Geiger, A.; Paschek, D. Temperature dependence of the solubility of carbon dioxide in imidazolium-based ionic liquids. *J. Phys. Chem. B* **2009**, *113*, 12727–12735.

(22) Soriano, A.N.; Doma, B.T.; Li, M.H. Carbon dioxide solubility in some ionic liquids at moderate pressures. *J. Taiwan Inst. Chem. Eng.* **2009**, *40*, 387-393.

(23) Mattedi, S.; Carvalho, P.J.; Coutinho, J.A.P.; Alvarez, V.H. Iglesias, M. High pressure CO_2 solubility in N-methyl-2-hydroxyethylammonium protic ionic liquids. *J. Supercrit. Fluids* **2011**, *56*, 224–230.

(24) Palomar, J.; Gonzalez-Miquel, M.; Bedia, J.; Rodriguez, F.; Rodriguez, J.J. Task-specific ionic liquids for efficient ammonia absorption. *Sep. Pur. Technol*. **2011**, *82*, 43–52.

(25) Bedia, J.; Palomar, J.; Gonzalez-Miquel, M.; Rodriguez, F.; Rodriguez, J.J. Screening ILs as suitable NH_3 absorbents on the basis on thermodynamic and kinetic analysis. *Sep. Pur. Technol.*, **2012**, *95*, 188-195.

(26) Bedia, J.; Ruiz, E.; de Riva, J.; Ferro, V.R.; Palomar, J.; Rodriguez, J.J. Optimized ionic liquids for toluene absorption. *AIChE J.*, **2012**, DOI: 10.1002/aic.13926.

(27) Gonzalez-Miquel, M.; Palomar, J.; Rodriguez, F. Ionic liquids for enhancing the gas solubility of volatile organic compounds. *J. Phys. Chem. B*, **2013**, 117, 296−306.

(28) Palomar, J.; Gonzalez-Miquel, M.; Polo, A.; Rodriguez, F. Understanding the physical absorption of CO_2 in ionic liquids using the COSMO-RS method. *Ind. Eng. Chem. Res.* **2011**, *50*, 3452–3463

(29) Gonzalez-Miquel, M.; Palomar, J.; Omar, S.; Rodríguez, F. CO_2/N_2 selectivity prediction in supported ionic liquid membranes (SILMs) by COSMO-RS. *Ind. Eng. Chem. Res.* **2011**, *50*, 5739−5748.

(30) Gonzalez-Miquel, M.; Talreja, M.; Ethier, A.L.; Flack, K.; Switzer, J.R.; Biddinger, E.J.; Pollet, P.; Palomar, J.; Rodriguez, F.; Eckert, C.A.; Liotta, C.L. COSMO-RS

Studies: Structure-Property Relationships for CO_2 Capture by Reversible Ionic Liquids. *Ind. Eng. Chem. Res.* **2012**, *51*, 16066−16073.

(31) Gonzalez-Miquel, M.; Bedia, J.; Abrusci, C.; Palomar, J.; Rodriguez, F. Anion Effects on Kinetics and Thermodynamics of CO_2 Absorption in Ionic Liquids. *J. Phys. Chem. B* **2013**, DOI: 10.1021/jp4007679

(32) Tokuda, H.; Hayamizu, K.; Ishii, K.; Susan, M.A.B.H.; Watanabe, M.J. Physicochemical properties and structures of room temperature ionic liquids. 2. Variation of Alkyl Chain Length in Imidazolium Cation. *J. Phys. Chem. B* **2005**, *109 (13)*, 6103-6110.

(33) Tome, L.I.N.; Carvalho, P.J.; Freire, M. G.; Marrucho, I. M.; Fonseca, I. M. A.; Ferreira, A. G. M.; Coutinho, J. A. P.; Gardas, R. L.J. Measurements and correlation of high-pressure densities of imidazolium-based ionic liquids. *Chem. Eng. Data* **2008**, *53*, 1914-1921.

(34) Shiflett, M.B. and Yokozeki, A. Solubility of CO2 in room temperature ionic liquid [hmim][Tf_2N]. *J. Phys. Chem. B* **2007**, 111, 2070-2074.

(35) Ahosseini, A.; Ortega, E.; Sensenich, B.; Scurto, A.M. Viscosity of n-alkyl-3-methyl-imidazolium bis(trifluoromethylsulfonyl)amide ionic liquids saturated with compressed CO_2. *Fluid Phase Equilib.* **2009**, *286*, 72–78.

(36) Tomida, D.; Kenmochi, K.; Qiao, K.; Bao, Q., Yokoyama, C. Viscosity of ionic liquid mixtures of 1-alkyl-3-methylimidazolium hexafluorophosphate+CO_2. *Fluid Phase Equilib*. **2011**, *307*, 185–189.

(37) Gan, Q.; Xue, ML; Rooney, D. A study of fluid properties and microfiltration characteristics room temperature ionic liquids [C_{10}min][NTf_2] and [N_{8881}][NTf_2] and their polar solvent mixtures. *Sep Purif Technol.* **2006**, *51*, 185-192.

(38) Wilke, C.R. and Chang, P. Correlation of diffusion coefficients in dilute solutions. *A1ChE J.* **1955**, 264-270.

Figures and tables

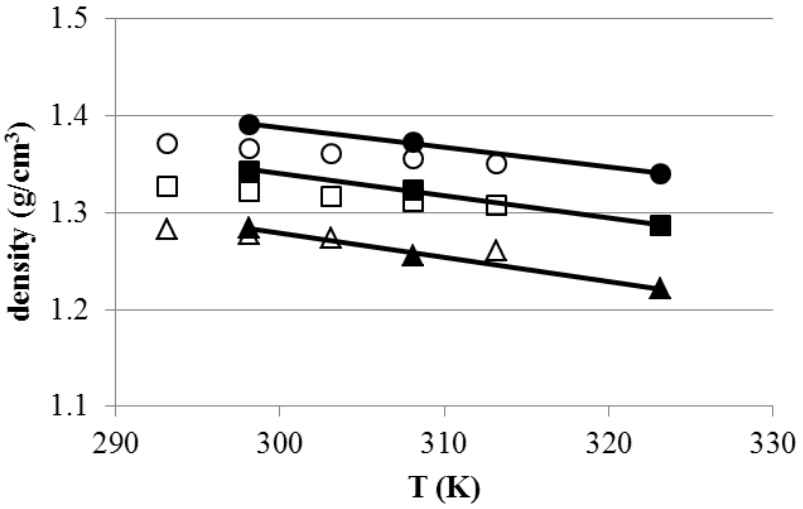

Figure 1: Density data of ionic liquids. [hxmim][NTf_2]: measured in this work (●), and reported[32] (○);. [omim][NTf_2]: measured in this work (■), and reported[32] (□); [dcmim][NTf_2]: measured in this work (▲) and reported[33] (△).

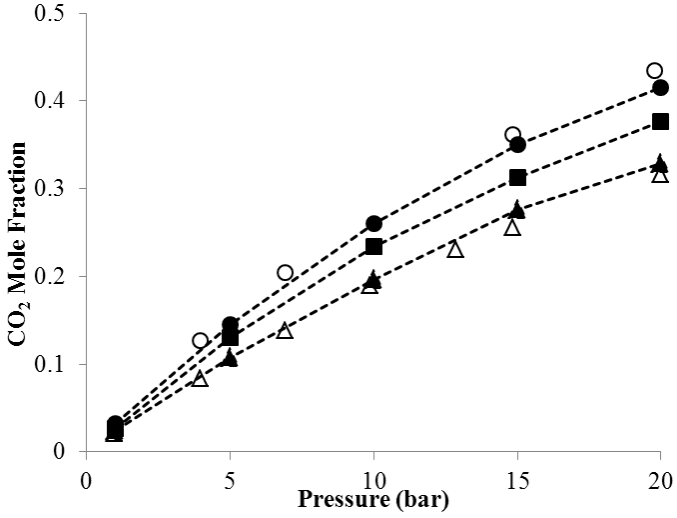

Figure 2. Isothermal solubility data of the system CO_2 and [hxmim][NTf_2]: measured in this work (●) at 298.15 K, and reported[34] (○) at 297.3 K; measured in this work (■) at 308.15 K; measured in this work (▲) at 323.15 K, and reported[34] (△) at 322.9 K.

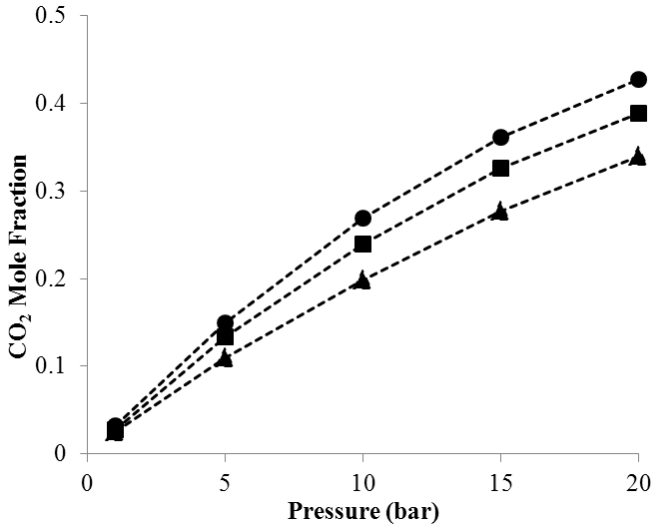

Figure 3. Isothermal solubility data of the system CO_2 and [omim][NTf_2]: measured in this work at (●) 298.15 K, (■) 308.15 K and (▲) 323.15 K.

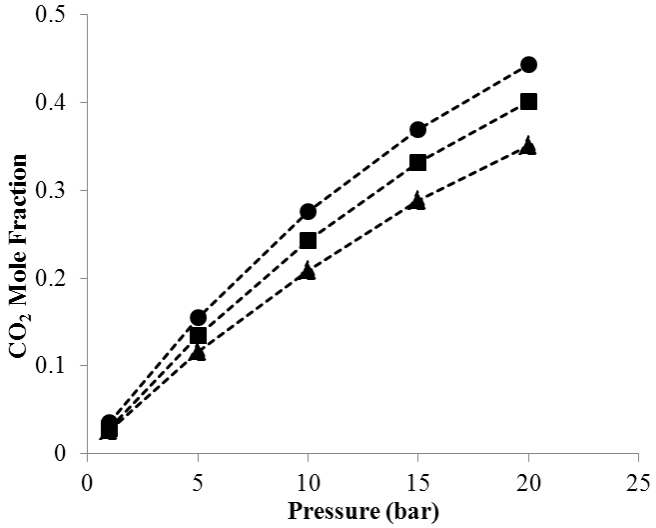

Figure 4. Isothermal solubility data of the system CO_2 and [dcmim][NTf_2]: measured in this work at (●) 298.15 K, (■) 308.15 K and (▲) 323.15 K.

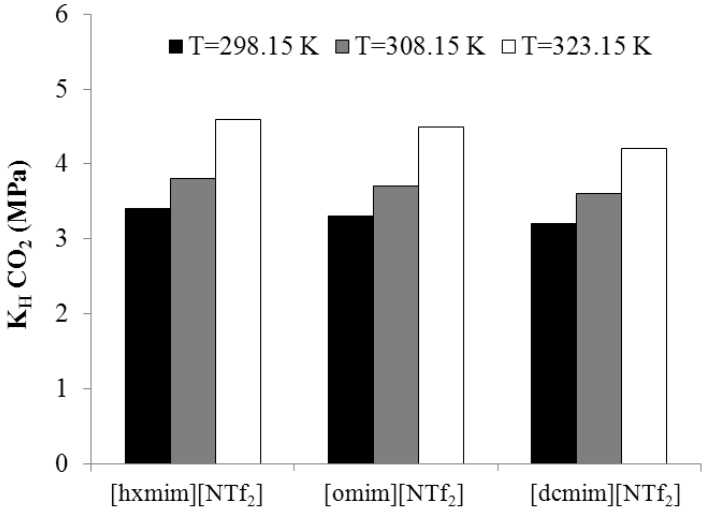

Figure 5. Henry´s law constants of CO_2 in the ILs [hxmim][NTf_2], [omim][NTf_2], and [dcmim][NTf_2] at 298.15, 308.15 and 323.15 K estimated from the solubility data measured in this work.

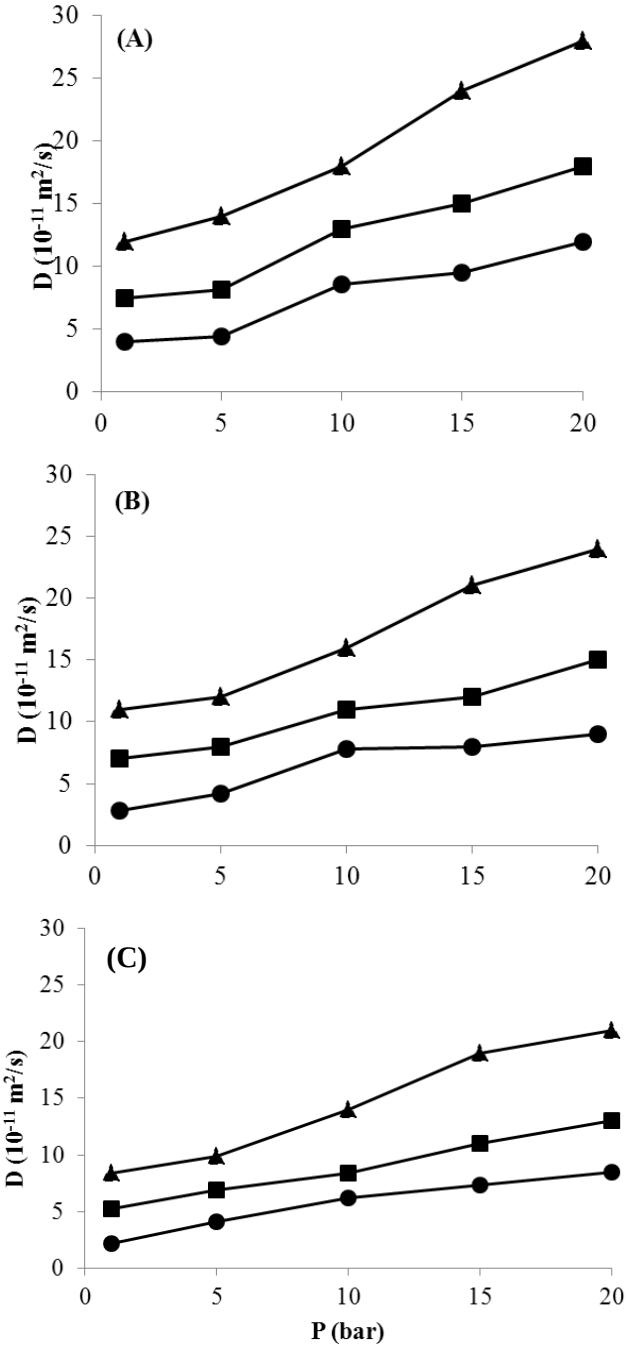

Figure 6. Diffusion coefficient of CO_2 in (A) [hxmim][NTf_2], (B) [omim][NTf_2], and (C) [dcmim][NTf_2] determined from thermogravimetric data from 1.0 to 20.0 bar by applying the mass diffusion model.(●) 298.15 K; (■) 308.15 K; and (▲) 323.15 K.

Table 1. Diffusion coefficients of the systems CO_2 in [hxmim][NTf_2], [omim][NTf_2] and [dcmim][NTf_2], estimated by Wilke-Chang ecuation.

Ionic liquid	Molar weight (g/mol)	T (K)	Viscosity (Pa·s)*	D_{CO2} (m^2/s)
[hxmim][NTf_2]	447.42	293.15	0.08717 [a]	$6.24 \cdot 10^{-11}$
		303.15	0.05372 [a]	$1.05 \cdot 10^{-10}$
		313.15	0.03547 [a]	$1.64 \cdot 10^{-10}$
[omim][NTf_2]	475.47	293.15	0.11885 [a]	$4.71 \cdot 10^{-11}$
		303.15	0.07116 [a]	$8.14 \cdot 10^{-11}$
		313.15	0.04585 [a]	$1.30 \cdot 10^{-10}$
[dcmim][NTf_2]	503.53	293.15	0.1420 [b]	$4.06 \cdot 10^{-11}$
		298.15	0.1202 [b]	$4.88 \cdot 10^{-11}$
		303.15	0.0985 [b]	$6.05 \cdot 10^{-11}$
		313.15	0.0728 [b]	$8.46 \cdot 10^{-11}$
		323.15	0.0515 [b]	$1.23 \cdot 10^{-10}$

[a]: from reference 32; [b]: from reference 37.

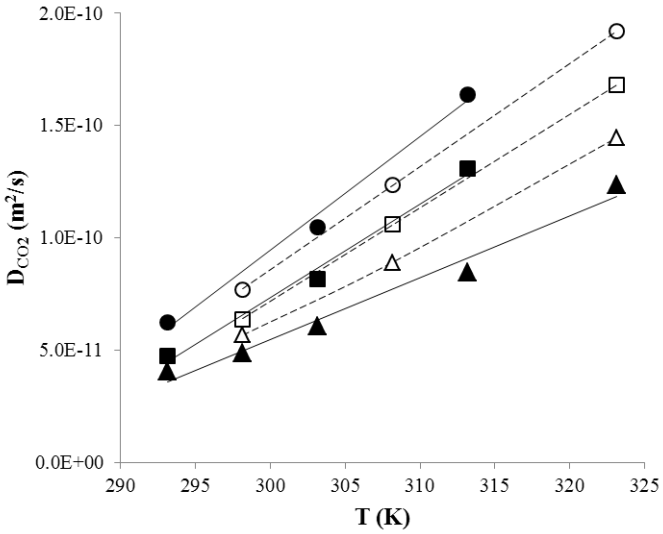

Figure 7. Comparison of diffusion coefficients of CO_2 in ILs obtained from experiments (open symbols) and estimated by Wilke-Chang correlation (filled symbols): (●) [hxmim][NTf_2]; (■) [omim][NTf_2]; and (▲) [dcmim][NTf_2].

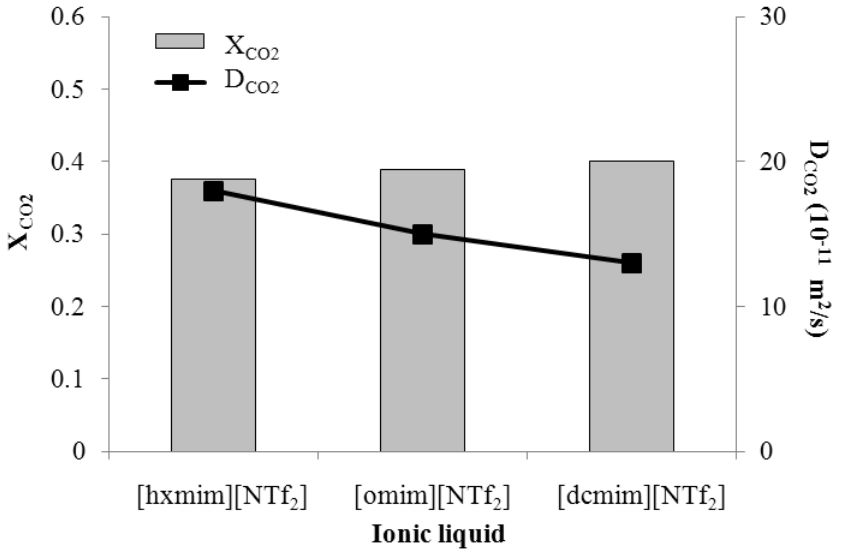

Figure 8. Effect of the length of the alkyl chain of the cation on the solubility and diffusivity of CO_2 in ILs (T=308.15 K and P=20 bar).

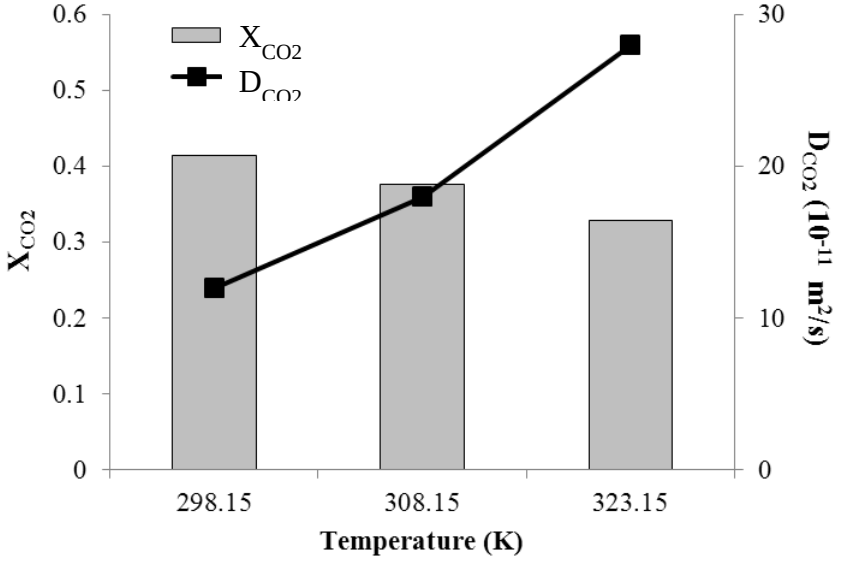

Figure 9. Effect of the temperature on the solubility and diffusivity of CO_2 in [hxmim][NTf_2] at P=20 bar.

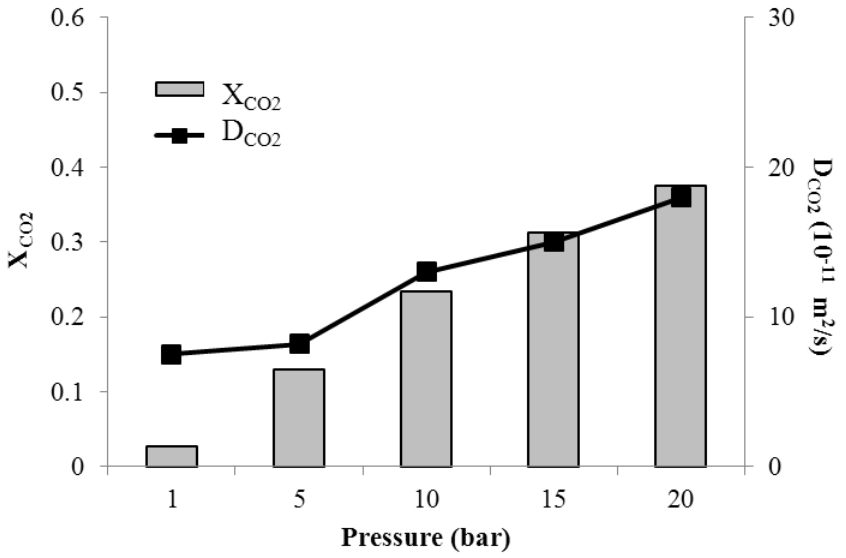

Figure 10. Effect of the pressure on the solubility and diffusivity of CO_2 in [hxmim][NTf_2] at T=308.15 K.

Publicación 6:

Palomar, J.; Gonzalez-Miquel, M.; Bedia, J. Rodriguez, F.; Rodriguez, J.J. **Task-specific ionic liquids for efficient ammonia absorption**. *Separation and Purification Technology*, **2011**, *82*, 43-52.

Separation and Purification Technology 82 (2011) 43–52

Contents lists available at SciVerse ScienceDirect

Separation and Purification Technology

journal homepage: www.elsevier.com/locate/seppur

Task-specific ionic liquids for efficient ammonia absorption

Jose Palomar [a,*], Maria Gonzalez-Miquel [b], Jorge Bedia [a], Francisco Rodriguez [b], Juan J. Rodriguez [a]

[a] Sección de Ingeniería Química (Departamento de Química Física Aplicada), Universidad Autónoma de Madrid, Cantoblanco, 28049 Madrid, Spain
[b] Departamento de Ingeniería Química, Universidad Complutense de Madrid, 28040 Madrid, Spain

ARTICLE INFO

Article history:
Received 5 May 2011
Received in revised form 11 August 2011
Accepted 15 August 2011
Available online 27 August 2011

Keywords:
Ionic liquids
Ammonia, NH_3
Absorption
COSMO-RS

ABSTRACT

A computational–experimental study was carried out to select ionic liquids with optimized properties for absorption of ammonia (NH_3). Firstly, a quantum-chemical COSMO-RS analysis was performed to analyze the solute–solvent intermolecular interactions determining the gas–liquid equilibrium data. Subsequently, a rational COSMO-RS screening of Henry's law coefficient of NH_3 over 272 ionic liquids was done to select potential high-capacity ammonia solvents. Finally, further experimental studies were carried out to evaluate the suitability of selected ILs as NH_3 absorbents, in terms of thermal stability, liquid-phase window and ammonia solubility. Experimentally was demonstrated that both absorption and desorption proceed quite rapidly and complete desorption was achieved at room temperature. From the results obtained we propose two commercially available task-specific ILs, [EtOHmim][BF_4] and [choline][NTf_2], whose characteristics would allow using new easy-to-regenerate NH_3 absorption systems operating in absorption–desorption cycles at near-ambient temperature and atmospheric pressure.

1. Introduction

Ammonia (NH_3) emissions are important contributors to atmospheric pollution, leading to a wide range of different environmental problems which include the formation of fine particulate matter, eutrophication of ecosystems, acidification of soils and alteration of the global greenhouse balance [1–3]. Agricultural sector has been identified as a primary contributor to atmospheric ammonia emissions (i.e., fertilizer application, livestock operations and dairy industry) [4,5]. However, increased attention is being paid to ammonia releases from anthropogenic nonagricultural sources (i.e., losses due to the volatilization of ammonia refrigeration system or intensive livestock animal production) for contributing to atmospheric reactive nitrogen [6,7]. Eventually large-scale implementation of post-combustion technology for CO_2 capture in power plants may also result in higher NH_3 emission, due to the oxidative degradation of the amine-based solvents, estimating the potential increase of the power sector contribution from 0.5% to 13% of total ammonia emissions [8]. Consequently, air quality policies, such as The National Emission Ceiling Directive of the European Commission [9], are being formulated to set national emission levels for key air pollutants including NH_3. Therefore, the development of techniques capable of capturing nitrogen reactive pollutants or reducing the volatility of ammonia-containing systems is of great interest, including separation by novel absorbents [10] and adsorbents [11] or elimination by dielectric barrier discharge reactors [12].

Room-temperature ionic liquids (ILs) are a novel type of solvents entirely composed by ions, which exhibit distinctive properties, most notably their negligible vapor pressure [13]. Moreover, an important feature is the possibility of designing "task-specific ILs" with the required properties for a particular application by tuning the structure of the ions, hence the term "designer solvents" [14,15]. Owing to their unique properties, ILs have generated significant interest across a wide variety of engineering applications, including their use as absorbents in gas separation processes [16], such as CO_2 capture [17–20], absorption of SO_2 [21–23] and hydrofluorocarbons [24–27] and reactive absorption of propylene [28–30]. Although studies regarding the behavior of NH_3-ILs systems are still scarce, the results reported so far suggest a great potential of ILs to be used in ammonia absorption systems. The solubilities of ammonia in imidazolium-based ionic liquids paired with different anions, including tetrafluoroborate [BF_4^-], hexafluorophosphate [PF_6^-], bis(trifluoromethylsulfonil)imide [NTf_2^-], nitrate [NO_3^-], trifluoromethanesulfonate [$CF_3SO_3^-$], clorure [Cl^-], acetate [$CH_3CO_2^-$] and tyocianate [SCN^-] have been studied at temperatures ranging from 283 to 353 K and pressures up to 5 MPa, the results indicating a favorable absorption behavior at high pressure and near-ambient temperature [31,32]. In addition, the absorption of ammonia in guanidinium-based ILs has been showed even more efficient than that observed with imidazolium-based ILs at room temperature and atmospheric pressure, indicating the main role played by the cation in the IL absorption capacity [33]. Recently, the effect of the length of the alkyl chain of cation in the solubility of NH_3 has been studied for series of imidazolium ILs [34], the results showing that longer alkyl chains, associated

* Corresponding author. Tel.: +34 91 4976938; fax: +34 91 4973516.
E-mail address: pepe.palomar@uam.es (J. Palomar).

1383-5866/$ - see front matter © 2011 Elsevier B.V. All rights reserved.
doi:10.1016/j.seppur.2011.08.014

to the imidazolium ring, cause a slight increase of the NH_3 solubility. The high solubility observed for NH_3 in conventional ILs, compared with other organic solvents [35,36], suggests the opportunity of designing task-specific ILs with optimized properties for NH_3 capture, allowing the potential application of ILs in cooling/heating cycles [6], in air scrubbers for end-of-pipe treatment technologies in livestock farming [7] or as new solvents in additional treatment options to mitigate the emission of ammonia from CO_2 capture systems in power plants [8].

Considering the huge variety of cation and anion combinations for possible ILs and taking into account the still limited available experimental data, computational methods by which equilibrium thermodynamic properties can be estimated from structural information of the compounds are of great utility. Thus, Flory–Huggins model [37] and generic van der Waals equation of state [38] have been successfully applied to predict the solubility of NH_3 in ILs from the available experimental data [31,32,34]. At this point, COSMO-RS (Conductor-like Screening Model for Real Solvents) model developed by Klamt and co-workers [39] is regarded as a valuable method for predicting the thermodynamic properties of ILs mixtures on the basis of unimolecular quantum chemical calculations for the individual molecules [40], providing an unique *a priori* computational tool for designing ILs with specific properties [41,42]. In fact, several publications have demonstrated the general suitability of COSMO-RS method to predict properties of IL systems, including the solubilities and Henry's law constants of several gases in ILs [43–46]. Moreover, an important feature is that the different intermolecular interactions (electrostatic forces, hydrogen bonding and van der Waals forces) between the mixture components can be quantified by COSMO-RS, contributing to the rational selection of ILs with improved characteristics for specific applications [47]. Indeed, in our previous works [45,46] novel ILs with optimum characteristics for CO_2 separation were designed, on the basis of an energetic analysis performed for the excess enthalpies of CO_2–IL mixtures and the COSMO-RS description of the intermolecular interactions between CO_2 and the IL compounds.

The aim of this work is to propose novel task-specific ILs with high capacities and adequate properties for absorbing ammonia. To accomplish that, we propose to develop a research strategy based on a two-step procedure illustrated in Scheme 1. Firstly, a computational thermodynamic analysis is performed to select a set of ILs with convenient properties by applying COSMO-RS. Secondly, further experimental studies are carried out to evaluate the suitability of selected ILs as NH_3 absorbents, in terms of thermal stability, liquid-phase window and ammonia solubility. For this purpose, COSMO-RS is used to formerly analyze the intermolecular interactions between NH_3 solute and conventional ILs and other benchmark solvents (as water), in order to elucidate the structural characteristic or functional groups which enhance the solubility of NH_3 in ILs. These findings are then driven by a COSMO-RS screening of the Henry's law constants (as a measure of solubility) of NH_3 over 272 ILs, in order to select a group of task-specific ILs as potential high-capacity ammonia absorbents. Subsequently, experimental studies are performed to determine the thermal stability and liquid-phase windows of the selected ILs in order to discard those solvents unstable or solid within the temperature range tested. Finally, the gas–liquid equilibrium data of NH_3 in two selected-as-adequate task-specific ILs and a conventional IL (used as reference) are measured at atmospheric pressure and temperatures of 293 and 313 K, obtaining finally the solubility of NH_3 in the IL at these conditions. As a result, we propose two commercially available task-specific ILs based on ammonium and imidazolium cations which allow NH_3 uptake as high as 0.65 (molar fraction) at near-ambient temperature and pressure conditions. In addition, the absorption–desorption rate curves have obtained at near-ambient temperatures and atmospheric pressures, in order to evaluate the regeneration of the proposed absorbents, point of interest for the application of ILs in operations based on ammonia absorption in liquid solvents.

2. Procedure

2.1. Computational details

The molecular geometry of all compounds (NH_3 and ILs counterions, see the list and the abbreviations for each IL used in Table S1) were optimized at the B3LYP/6-31++G** computational level in the ideal gas phase using the quantum chemical Gaussian03 package [48]. A molecular model of independent counterions was applied in COSMO-RS calculations, where ILs are treated as equimolar mixture of cation and anion [49]. Vibrational frequency calculations were performed in each case to confirm the presence of an energy minimum. Once molecular models were optimized, Gaussian03 was used to compute the COSMO files. The ideal screening charges on the molecular surface for each species were calculated by the continuum solvation COSMO model using BVP86/TZVP/DGA1 level of theory. Subsequently, COSMO files were used as an input in COSMOthermX [50] code to calculate the thermodynamic properties (Henry's laws constant of NH_3 in ILs and detailed excess enthalpies contributions of NH_3–IL mixtures). According to our chosen quantum method, the functional and the basis set, we used the corresponding parameterization (BP_TZVP_C21_0108) that is required for the calculation of physicochemical data and contains intrinsic parameters of COSMOtherm, as well as specific parameters.

2.2. Materials

High-purity anhydrous ammonia (purity > 99.999%) was purchased from Praxair Technology, Inc. and was used without further purification. The ILs used in this study as absorbates were the following: 1-butyl-3-methylimadazolium tetrafluoroborate [bmim][BF_4], 1-2(-hydroxyethyl)-3-methylimadazolium tetrafluoroborate [EtOH mim][BF_4], 1-2(-hydroxyethyl)-3-methylimadazolium chloride [EtOHmim][Cl], methylammonium nitrate [N-Me][NO_3], dimethylammonium nitrate [N-1,2-Me][NO_3], choline bis(trifluoromethylsulfonyl)imide [choline][NTf_2] and *n*-2-hydroxyethyl ammonium formiate [N-EtOH][CHOO] supplied by Io-Li-Tec (Ionic Liquid

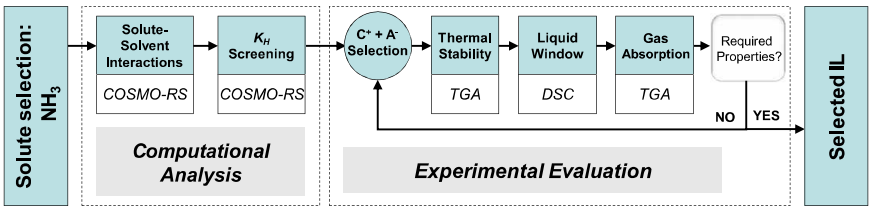

Scheme 1. Research strategy.

Technologies), in the highest purity available (purity > 97–98%). The ILs were used also without previous purification.

2.3. Physical property measurements

Density measurements were performed using an Anton Paar DMA-5000 oscillating U-tube densimeter. The effect of the viscosity on density determination was automatically corrected by a factor depending on the viscosity of the sample. Prior to each measurement, density measurements of Millipore quality water were made in order to check the calibration of the densimeter. The repeatability and the uncertainty in measurements were estimated to be less than $\pm 1 \cdot 10^{-6}$ g/cm^{-3} and $\pm 1 \cdot 10^{-5}$ g/cm^{-3}, respectively. Dynamic viscosities of ILs were determined using an Anton Paar Automated Micro Viscometer (AMVn). The temperature was controlled by a Pt100 temperature sensor with a resolution of ±0.01 K. The measurement method of this instrument was the falling ball principle. It consists of the determination of the ball's rolling time in a calibrated glass capillary filled with sample. The calibration of the capillary was performed by the manufacturer using viscosity standard fluids. The estimated experimental uncertainty was estimated to be less than ±0.5% and the repeatability was less than ±0.1%. The water content of ILs used in absorption experiments (after drying them under vacuum of 10^{-3} Torr at 298 K over 24 h) were determined with a Mettler Toledo DL31 Karl Fischer titrator and using the one component technique. The polarizing current for the potentiometric end-point determination was 20 A and the stop voltage 100 mV. The end-point criterion was the drift stabilization ($3\ \mu_{H_2O}\ min^{-1}$) or maximum titration time (10 min). The measurement was corrected for the baseline drift, defined as the residual or penetrating water that the apparatus removes per minute. The uncertainty in experimental measurements has been found to be less than 7%. Table 1 collects the measured density and dynamic viscosity at 293.15 and 313.15 K and the water content of used ILs.

The presence of water undoubtedly affects the viscosity of ILs. However, as can be seen in Table 1, we have operated with ILs with very low water content. Thus, the mass fraction of water in [EtOHmim][BF_4] ($1.65 \cdot 10^{-4}$) is as five times smaller than the lowest water content used by other authors ($8 \cdot 10^{-4}$–$3 \cdot 10^{-2}$) to check its influence on the viscosity of [EtOHmim][BF_4] in the 288.15–328.15 K temperature range [51]. The viscosity variation of [bmim][BF_4] with water content from zero to the concentration studied at 313.15 K is less than 5 mPa s according to a previous study carried out in the 303.15–353.15 K temperature range [52]. The [choline][NTf_2] at room temperature is not miscible with water, but above 345.25 K an one-phase system is formed [53]. The water content in the [choline][NTf_2] used in this work is <60 ppm; therefore, in the temperature range studied, the water should not significantly affect to the absorption capacity and other properties of this IL, as in fact we have found.

2.4. Absorption/desorption experimental procedures

The thermal stability of the ILs was studied by non-isothermal thermogravimetric analyses carried out in a thermogravimetric analyzer (TGA/SDTA851^e Mettler Toledo International Inc.) under nitrogen flow (100 cm^3 STP/min). The IL temperature was increased from room temperature up to 673 K at a heating rate of 10 K/min. We also studied the stability of the ILs by analyzing the weight loss in isothermal TGA experiments performed at 323 K under nitrogen flow (100 cm^3 STP/min). Differential scanning calorimetry (DSC) experiments were run on a DSC calorimeter (DSC823^e Mettler Toledo International Inc.). In order to provide the same thermal history, about 10 mg of sample were placed in the aluminum pan and then covered by an aluminum lid, then heated from 298 to 398 K at 1 K/min in a nitrogen atmosphere.

Fig. 1 shows a scheme of the setup used for the ammonia absorption experiments. Before each experiment, ILs were dried under vacuum (10^{-3} Torr) at 298 K over at least 24 h. Ammonia absorption equilibrium and kinetic experiments were carried out in the aforementioned TGA analyzer at atmospheric pressure and temperatures of 293 and 313 K using 20 mg of IL sample amount. The balance has a weight range of 0–1000 mg with a resolution of 0.1 μg. The temperature of the sample was maintained constant with a regulated external thermostat bath (Huber minisat 125). Gas–liquid equilibrium data of ammonia in ILs were obtained by setting the partial pressure of ammonia in the NH_3/N_2 gas flow (100 cm^3 STP/min) and monitoring the increment on weight of the sample. Blank experiments were carried out with neat N_2 gas (in absence of NH_3 solute), without obtaining measurable weight increment in IL sample by TGA equipment, consistently with the reported low solubility of N_2 in imidazolium-based ILs (<10^{-3} molar fraction at 1 atm and 313 K) [54]. The IL and the gas seemed to have reached equilibrium when at constant pressure no further weight change was observed throughout time (weight change rate <0.001 mg h^{-1}). The time required for reaching equilibrium at each pressure level depended on the IL (typically around 2 h).

The absorption–desorption rate curves were also obtained in the aforementioned thermogravimetric system (at 293 K). Ammonia absorption was performed under continuous NH_3 gas flow (100 cm^3 STP/min) at 0.1 MPa. The increment of weight was monitored and once the IL and the gas seem to have reached equilibrium (weight change rate <0.001 mg h^{-1}), desorption was carried out at the absorption temperature under dry nitrogen flow (100 cm^3 STP/min).

3. Results

3.1. Preliminary selection of ILs for NH_3 absorption by COSMO-RS methodology

COSMO-RS method calculates the thermodynamic properties of fluid mixtures by using the 3D molecular surface polarity

Table 1
Physical properties and water content of used ILs.

Ionic liquid	T (K)	Density[a] (g cm^{-3})	Viscosity[a] (mPa s)	Water content[a] (ppm)
[bmim][BF_4]	293.15	1.203	123.41	250 ppm (180 ppm)[b]
	313.15	1.189	48.25	
[EtOHmim][BF_4]	293.15	1.365	149.34	200 ppm (165 ppm)[b]
	313.15	1.350	54.09	
[choline][NTf_2]	293.15	1.522	95.54	60 ppm (∼60 ppm)[b]
	313.15	1.512	61.75	

[a] Commercial IL as purchased.
[b] Dried IL at under vacuum (10^{-3} Torr) at 298.15 K over 24 h.

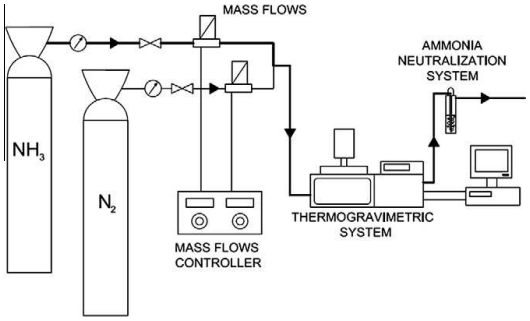

Fig. 1. Schematic diagram of the atmospheric pressure system for ammonia absorption measurements.

distributions of their individual compounds resulting from quantum chemical calculations, data easily visualized in the histogram function σ-profile [39]. Therefore, based on COSMO-RS methodology, the σ-profile of one compound includes the main chemical information necessary to predict its possible interactions in a fluid phase. The COSMO-RS histogram can be qualitatively divided in three main regions upon the following cut-off values: hydrogen bond donor ($\sigma < -0.0082$ e/Å^2) and acceptor ($\sigma > +0.0082$ e/Å^2) regions and the non-polar region ($-0.0082 < \sigma < +0.0082$ e/Å^2). Fig. 2 shows the σ-profile of the ammonia solute, which is dominated by a series of peaks located at the positive polar region. The highly polarized charge at 0.028 e/Å^2 is assigned to the nitrogen fragment (red colored polar surface of the NH_3 in Fig. 2), indicating its ability to act as strong hydrogen bond acceptor (basic character). In addition, the two prominent peaks at -0.011 and -0.007 e/Å^2 correspond to the hydrogen atoms of ammonia molecule (reflected in weak blue and green color in the polar surface of the compound, Fig. 2). Therefore, these hydrogen groups are described as weak hydrogen bond donors (acidic character) by COSMO-RS. On the other hand, the σ-profile of water – solvent of reference for NH_3 absorption – is dominated by polarized charge density from the electron lone-pairs of the oxygen (peaks located around +0.018 e/Å^2) and from the two very polar hydrogen atoms (peaks located around -0.016 e/Å^2). This reflects the amphoteric character of water molecule, with excellent ability to act as a donor as well as an acceptor for hydrogen bonding. It is well stated that NH_3 mainly participates as base/hydrogen bond acceptor of the acidic species/groups of H_2O molecules in aqueous solution [55]. To evaluate this finding, we introduced 2,2-difluoeroethanol in current COSMO-RS analysis as an alcohol with enhanced hydrogen bond donor properties. The σ-profile of 2,2-difluoeroethanol in Fig. 2 shows the peak of the hydroxyl hydrogen atom located at a more negative position (-0.018 e/Å^2) in the polar scale than the acidic groups of water, i.e., COSMO-RS description indicated an even stronger acidic character for 2,2-difluoroethanol, in good agreement with experimental and theoretical evidences [56]. In previous studies, COSMO-RS was successfully applied to analyze the solubility of gaseous solutes in ILs in terms of the contributions of the different intermolecular interactions between solute and solvent to the excess enthalpy, H^E, values of the liquid phase [45,46]. Therefore, COSMO-RS are here used to predict the excess enthalpy of a NH_3–water mixture, H^E, by summing the contribution of each component of the mixture, according to the expression:

$$H^E = x_{solvent} \cdot H^E_{solvent} + x_{NH_3} \cdot H^E_{NH_3} \quad (1)$$

The estimations of H^E in Eq. (1) by the COSMO-RS model can be also expressed by the sum of three contributions associated with the intermolecular interactions of polar *Misfit*, hydrogen bonding and van der Waals forces between the mixture components:

$$H^E = H^E\ (H\text{-}Bond) + H^E\ (Misfit) + H^E\ (VdW) \quad (2)$$

Then, the next aim was to relate the gas solubility of NH_3 in representative solvents to the different intermolecular interactions between the solute and solvent molecules. Fig. 3 presents the Henry's law constants of NH_3 in water, 2,2-difluoroethanol and conventional ILs at $T = 298.15$ K, together with the interaction energies contributions to the excess molar enthalpies of the corresponding NH_3–solvent system, both computed by COSMO-RS. It is shown that the attractive hydrogen bonding interactions (negative H^E values), determine the increasing gas solubility of NH_3 in the solvents (decreasing K_H values), in good agreement with previous computational analysis by molecular dynamics [57]. Meanwhile, the attractive electrostatic interactions (*Misfit*) between NH_3 and the solvents play a secondary role. At last, van der Waals interactions make almost negligible contributions to the H^E excess enthalpy values of these systems. As can be seen, polar solvents such as water are capable to increase the solubility of NH_3 acting as a hydrogen bonding donor (K_H of NH_3 in $H_2O \approx 0.013$ MPa *vs* the value of 11.6 MPa in [bmim][BF_4]). Indeed, polar solvents with strong acid character, i.e., 2,2-difluoroethanol, present even higher absorption capacities than water (K_H of NH_3 in 2,2-difluoroethanol ≈ 0.002 MPa). However, it can be appreciated that conventional ILs, which behave mostly as hydrogen bond acceptors [47], do not possess the ability to form effective hydrogen bonds with the NH_3 solute, hence do not seem optimum structures for ammonia absorption (K_H of NH_3 in conventional ILs ≈ 0.1 MPa). In sum, COSMO-RS analysis allows concluding that inclusion of acid groups in the ILs may enhance the absorption capacity of the ammonia solute in the solvent.

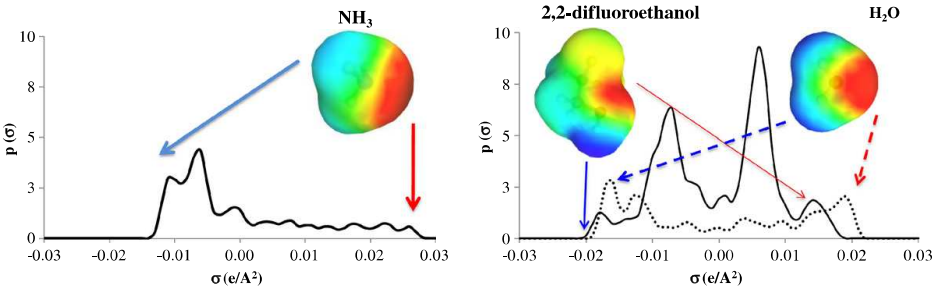

Fig. 2. σ-Profiles and polarized charge surfaces of ammonia, water and 2,2-difluoroethanol computed by COSMO-RS.

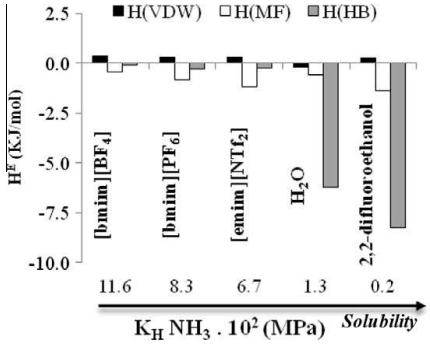

Fig. 3. Description of the solvent effect on Henry's law constants of NH_3 at T = 298.15 K by using the interaction energies contributions [electrostatic, H(MF); Van der Waals H(VDW); and hydrogen-bonding, H(HB)] to excess molar enthalpies of solute–solvent mixture computed by COSMO-RS.

In order to design suitable task-specific ILs for NH_3 absorption, COSMO-RS method was applied for driving a rational screening of Henry's law constants of NH_3 in 272 ILs at 298.15 K. The computational screening was performed over ILs based on different cations (imidazolium, pyridinium, pyrrolodinium, quinolinium, ammonium, phosphonium, thioronium) and anions ([FEP$^-$], [NTf_2^-], [$FeCl_4^-$], [$CF_3SO_3^-$], [$CF_3CO_2^-$], [$B(CN)_4^-$], [NO_3^-], [$CH_3CO_3^-$], [$CH_3SO_3^-$], [$CH_3SO_4^-$], [$C(CN)_3^-$], [DCN$^-$], [BF_4^-], [SCN$^-$], [PF_6^-], [CHOO$^-$], [Cl$^-$]). Note that ILs based on hydroxyl functionalized cations such as [choline$^+$], [N-EtOH$^+$] or [EtOHmim$^+$] were included in the screening as suggested by the preliminary analyses performed above. The results from the COSMO-RS screening of the Henry's law constants of NH_3 in ILs are presented in Fig. 4. In general, it is observed that the ammonia absorption capacity of ILs is more determined by the cation than by the anion, in good agreement with previous experimental [31–34] and theoretical conclusions [57]. Regarding the cation family effect, ILs based on ammonium and imidazolium seem to improve the NH_3 absorption capacity in comparison to ILs based on other cations such as pyrrolodinium, quinolinium, phosphonium or thioronium. In addition, it should be pointed out that ILs based on hydroxyl functionalized cations, such as [EtOHmim$^+$] or [choline$^+$], significantly enhance the NH_3 absorption capacity in relation to their non-functionalized analogs. On the other hand, Fig. 4 indicates that highly fluorinated anions such as [NTf_2^-] or [FEP$^-$] improve the absorption capacity of NH_3 in ILs

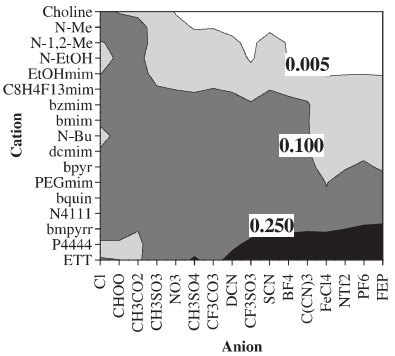

Fig. 4. Screening of predicted Henry's law constants (MPa) of NH_3 in 272 ILs at T = 298.15 K calculated by COSMO-RS.

including cations with acidic character, leading to the solvents with the highest NH_3 solubility values in the COSMO-RS screening.

The last objective of the computational study is the selection of potential ILs with adequate characteristics for NH_3 absorption, with the aim of reducing the range of preliminary experimental measurements. To accomplish that, the predicted Henry's law constants of NH_3 in series of ILs (see Table S2), including those conventional ILs previously studied in bibliography [31–34,37] as well as those hydroxyl-functionalized task-specific ILs suggested in the above analysis, were related to the excess enthalpy H^E of the NH_3–IL systems estimated by COSMO-RS, as it is shown in Fig. 5. As a general trend, higher solubilities (decreasing K_H values) of NH_3 in ILs are associated with higher exothermicity (decreasing H^E values) of the mixture, whereas lower solubilities of the solute in the ILs are related with enthalpy values of the mixtures close to zero. The reason is evidenced in Fig. 6 where the NH_3 absorption behavior (in terms of the Henry's law constants) in ILs can be analyzed in terms of the intermolecular interaction contributions to the H^E values of the NH_3–IL systems. It illustrates that the significant increase of the NH_3 solubility in ILs based on hydroxyl functionalized cations, such as [choline$^+$] or [EtOHmim$^+$], is mainly due to the larger hydrogen bond donor ability of this acid group. Analyzing the results of computational screening in Fig. 4, we were able to find six commercially available task-specific ILs with predicted values of Henry's constants of NH_3 significantly lower than those corresponding to the conventional ILs reported in bibliography, presenting a considerably higher exothermic behavior in Fig. 5 (NH_3-conventional ILs systems: $K_H > 0.1$ MPa, $0 > H^E > -1$ kJ/mol; NH_3-commercial ILs proposed in this study: $K_H < 0.1$ MPa, $-5 > H^E > -25$ kJ/mol). Therefore, we select the following commercially available task-specific ILs, [choline][NTf_2], [EtOHmim][BF_4], [EtOHmim][Cl], [N-EtOH][CHOO], [N-Me][NO_3] and [N-1,2-Me][NO_3], as potential solvents with promising characteristics to be experimentally studied in the development of NH_3 absorption systems based on ILs.

3.2. Experimental evaluation of selected task-specific ILs for NH_3 absorption

3.2.1. Previous available data

Table 2 summarizes the experimental ammonia solubilities reported in the literature at nearly atmospheric pressures and near

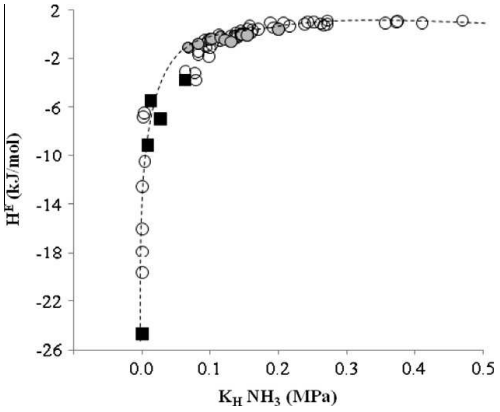

Fig. 5. Henry's law constants related to the excess molar enthalpies of NH_3 in ILs [○ simulated ILs, ◍ previously experimentally studied ILs [31,32,34], ■ commercial ILs included in this study] at T = 298.15 K computed by COSMO-RS.

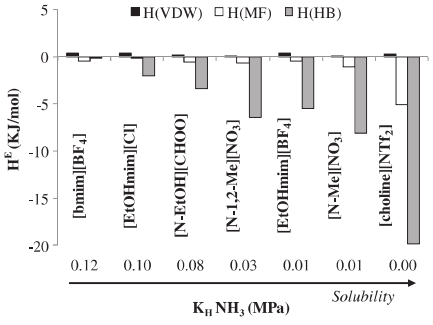

Fig. 6. Description of Henry's law constants of NH_3 in selected conventional and task-specific ILs at $T = 298.15$ K by using the interaction energies contributions [electrostatic, H(MF); Van der Waals H(VDW); and hydrogen-bonding, H(HB)] to excess molar enthalpies computed by COSMO-RS.

room temperature [31–34], together with the Henry's law constants calculated by COSMO-RS at such conditions. So far, most of the studies have been performed at ammonia pressures higher than atmospheric (up to 5 MPa). However, for practical purposes, the ammonia solubilities at near atmospheric pressures are much more interesting in cases such as air scrubbers or recovering operations from purge gas. Therefore, in this work we have obtained the ammonia absorption equilibrium curves at 0.1 MPa and two different temperatures (293 and 313.1 K). For the sake of comparison with literature data, we also report the values of NH_3 solubility in the selected ILs at these conditions. Li et al. [34] concluded that ammonia solubilities increase with increasing the length of alkyl chain of the cation of the IL, which is also observed in K_H predictions by COSMO-RS model. In addition, considering the data of IL series based on the same cation, the selection of anion with high fluorine content also allows increasing the NH_3 solubility. As can be seen, Table 2 shows some discrepancies in the results reported by the different authors. In this sense, the ammonia solubilities on [bmim][BF_4] (used in current study as conventional IL of reference) reported by Yokozeki et al. [31] (0.17 molar fraction at 298 K and 0.13 MPa) are in relatively good agreement with the later results by Li et al. [34] (0.26 at 293 K and 0.13 MPa), in contrast to the much higher solubility reported by Huang et al. [33] (0.50 at 293 K and 0.10 MPa).

3.2.2. Thermal stability

Thermogravimetric analysis experiments were conducted to determine the thermal stabilities of the six selected task-specific ILs and the conventional ILs previously studied [31,32] for NH_3 absorption. Fig. 7(A) shows the TGA weight–loss curves from room temperature up to 673 K obtained for these ILs. Fairly different behaviors were observed. [EtOHmim][BF_4], [choline][NTf_2] and

Table 2
Experimental available data of ammonia solubilities in different IL compared to Henry's law constants calculated by COSMO-RS.

Ionic liquid	T (K)	P (MPa)	Experimental solubility x_{NH_3}	Predicted K_H (MPa)	Ref.
[bmim][PF_6]	298	0.17	0.35	0.04	[31]
[bmim][BF_4]	298	0.13	0.17	0.07	
[emim][NTf_2]	298	0.14	0.13	0.04	
[hmim][Cl]	298	0.13	0.23	0.13	
[bmim][PF_6]	323	0.27	0.29	0.13	
[bmim][BF_4]	323	0.20	0.12	0.19	
[emim][NTf_2]	323	0.17	0.09	0.11	
[hmim][Cl]	323	0.10	0.06	0.32	
[emim][BF_4]	293	0.14	0.22	0.06	[34]
[bmim][BF_4]	293	0.13	0.26	0.06	
[hmim][BF_4]	293	0.17	0.38	0.05	
[omim][BF_4]	293	0.13	0.42	0.05	
[emim][BF_4]	298	0.11	0.15	0.08	
[bmim][BF_4]	298	0.22	0.31	0.07	
[hmim][BF_4]	298	0.22	0.36	0.06	
[omim][BF_4]	298	0.12	0.28	0.06	
[emim][BF_4]	313	0.14	0.13	0.15	
[bmim][BF_4]	313	0.08	0.10	0.13	
[hmim][BF_4]	313	0.23	0.27	0.12	
[omim][BF_4]	313	0.18	0.28	0.12	
[emim][CH_3CO_2]	298	0.47	0.59	0.14	[32]
[emim][$C_2H_5SO_4$]	298	0.42	0.52	0.09	
[emim][SCN]	298	0.31	0.44	0.13	
[dmea][CH_3CO_2]	298	0.16	0.47	0.08	
[emim][CH_3CO_2]	323	0.79	0.54	0.33	
[emim][$C_2H_5SO_4$]	323	0.71	0.48	0.23	
[emim][SCN]	323	0.53	0.42	0.34	
[dmea][CH_3CO_2]	323	0.28	0.47	0.23	
[bmim][BF_4]	293	0.10	0.50	0.06	[33]
[tmgh][BF_4]	293	0.10	0.52	–	
[fmghPO$_2$][BF_4]	293	0.10	0.42	–	
[tmgh][NTf_2]	293	0.10	0.54	–	
[bmim][BF_4]	293	0.10	0.31	0.06	[This work]
[EtOHmim][BF_4]	293	0.10	0.63	0.01	
[choline][NTf_2]	293	0.10	0.65	$5 \cdot 10^{-5}$	
[bmim][BF_4]	313	0.10	0.28	0.13	
[EtOHmim][BF_4]	313	0.10	0.47	0.03	
[choline][NTf_2]	313	0.10	0.59	$1 \cdot 10^{-4}$	

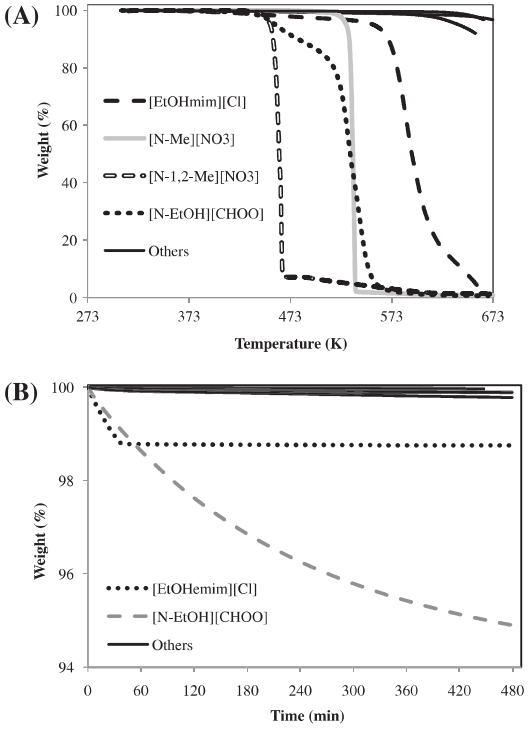

Fig. 7. Thermal decomposition of selected task-specific ILs and conventional ILs by (A) dynamic and (B) isothermal (323 K) TGA.

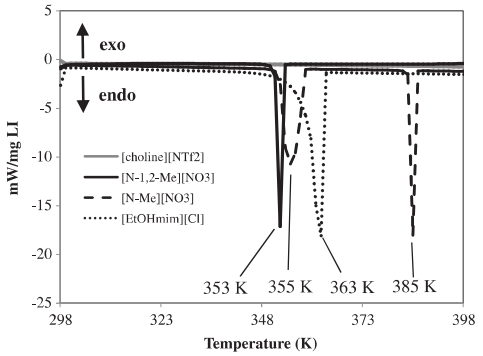

Fig. 8. DSC profiles of [EtOHmim][Cl], [N-Me][NO_3], [N-1,2-Me][NO_3] and [choline][NTf_2] ILs.

[bmim][BF_4] are stable up to more than 623 K. The thermal decomposition temperature of the rest of ILs is significantly lower and follows the order [EtOHmim][Cl] > [N-Me][NO_3] > [N-EtOH][CHOO] > [N-1,2-Me][NO_3]. In all the cases, the decomposition temperatures are far higher than the most commonly used temperatures for ammonia absorption (⩽348 K). However, it has been demonstrated that the decomposition temperatures of ILs depend on the heating rate and they cannot be accurately obtained by dynamic TGA [58]. For this reason, we also studied the stability of the ILs from the weight loss in isothermal TGA experiments performed at 323 K [Fig. 7(B)]. Most of the ILs show negligible weight loss at this temperature. However, [EtOHmim][Cl] shows an initial weight loss, although for longer times the mass is stabilized with a total weight loss lower than 1.2%. Only [N-EtOH][CHOO] shows a continuous weight loss which reaches a 5% after 8 h of analysis. This latter IL was discarded for the experimental ammonia solubility studies due to its poor thermal stability.

On the other hand, some of the ILs selected using COSMOS-RS screening are solids at room temperature, such as [EtOHmim][Cl], [N-Me][NO_3] and [N-1,2-Me][NO_3]. The melting temperatures of these compounds were obtained by differential scanning calorimetry (DSC) measurements recorded in the temperature range 298–423 K at a heating rate of 1 K/min. DSC profiles of [EtOHmim][Cl], [N-Me][NO_3] and [N-1,2-Me][NO_3] are illustrated in Fig. 8. In general, high symmetry, strong ion interactions (such as hydrogen bonding) and localized charge distribution over the cation and/or anion tend to increase the crystal lattice energy, thus resulting in IL with higher melting points [59]. From the Fig. 8, it can be seen that the melting points of [N-1,2-Me][NO_3], [EtOHmim][Cl] and [N-Me][NO_3] are 353, 363 and 385 K, respectively. The melting point of [N-Me][NO_3] corresponds to the second peak (385 K) of thermogram whereas the first peak (355 K) is due to a solid-state transition according to the behavior described in the literature [60], being both values relatively close to those (377 and 346 K) determined by Belieres et al. [60]. Therefore, the melting temperatures of [EtOHmim][Cl], [N-Me][NO_3], [N-1,2-Me][NO_3] are higher than the most commonly used temperatures for ammonia absorption (⩽348 K) and, thus, these ILs have been also discarded for the experimental ammonia solubility studies. Therefore, after TGA and DSC analyses, only two task-specific ILs, [choline][NTf_2], and [EtOHmim][BF_4], among the six solvents initially selected from COSMO-RS screening, are suitable candidates for NH_3 absorption at near ambient conditions.

3.2.3. Absorption of NH_3 in task-specific ILs

A series of gas–liquid equilibrium experiments were performed at total pressure of 0.1 MPa and temperatures of 293 and 313 K for NH_3/N_2 gas mixtures in selected ILs. Fig. 9 presents the equilibrium partial pressure of ammonia in gas phase *vs* the mole fraction of ammonia in the task-specific ILs [EtOHmim][BF_4] and [choline][NTf_2]. In addition, the gas–liquid equilibrium measurements were carried out for the conventional IL [bmim][BF_4] used as reference, in order to validate the results of our technique by comparison with available literature data. Experimental measurements show that the selected ILs absorb an amazingly high amount of ammonia. Thus, the solubilities of ammonia in [EtOHmim][BF_4] at 313 and 293 K are, respectively, 0.47 and 0.63 in molar fraction (Table 2). COSMO-RS analysis provided even higher NH_3 absorption capacity of [choline][NTf_2] respect to [EtOHmim][BF_4], what is verified by isothermal experiments at 313 K (Table 2). We measured a solubility of ammonia in [choline][NTf_2] at 0.1 MPa and 313 K of 0.59 in molar fraction, significantly higher than the corresponding solubility (0.47) in [EtOHmim][BF_4]. The fact of finding very close NH_3 uptake by [choline][NTf_2] at the two different temperatures tested (313 and 293 K) may be ascribed to its state, which depends on the temperature tested. It was shown by Nockemann et al. [53], using differential scanning calorimetry (DSC) and polarizing optical microscopy (POM), that this compound melts at 303 K, and that solid state polymorphism is present. Thus, between 276 K and the melting point, a plastic crystalline state could be detected [53]. In our work, we visually checked that the [choline][NTf_2] is gelled below 299 K. To the best of our knowledge, the solubilities obtained with the selected task-specific ILs are

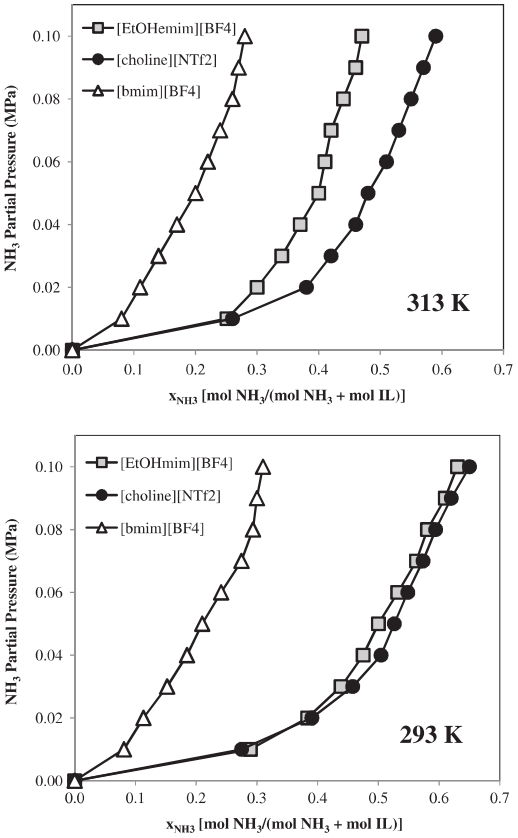

Fig. 9. Ammonia absorption curves in selected task-specific ILs at 313 and 293 K.

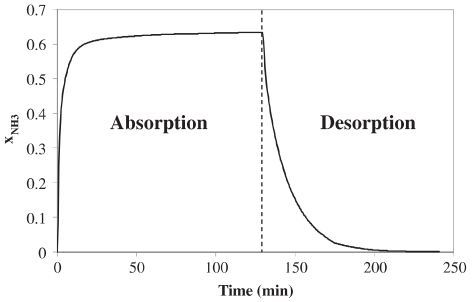

Fig. 10. Ammonia absorption and desorption curves in [EtOHmim][BF_4] at 293 K and 0.1 MPa.

much higher, at low ammonia pressures, that the previously reported in the literature for other ILs. For the sake of comparison, Table 2 collects the available NH_3 solubility data in the range of 293–323 K and 0.1–0.7 MPa. The ammonia solubility in the IL used as reference ([bmim][BF_4]) obtained in this work at 0.1 MPa and 293 K was 0.31 (molar fraction), very close to the values reported at similar conditions by Guihua et al. [34] (0.26 at 293 K and 0.13 MPa) and by Yokozeki et al. [31] (0.17 at 298 K and 0.13 MPa). On the contrary, the ammonia solubility in [bmim][BF_4] at 0.1 MPa and 293 K reported by Huang et al. [33], with a value of 0.5, seems to be significantly overestimated (see Table 2). Fig. 9 shows that, as expected, ammonia solubilities generally decreased with increasing temperature and increased with NH_3 partial pressure.

Desorption of the absorbed ammonia from the IL is a key issue for potential applications. Fig. 10 depicts the ammonia absorption–desorption curves on [EtOHmim][BF_4] at 293 K and 0.1 MPa. As can be seen, both absorption and desorption of NH_3 proceed frankly fast, thus precluding the need of heating or vacuum for desorption, which has been reported with other ILs [33]. Furthermore, the amount of NH_3 absorbed is completely desorbed at the absorption temperature. Thus, the ILs tested have demonstrated a high ammonia absorption capacity, which can be completely regenerated. Computational COSMO-RS analysis supported by experimental results allowed selecting task-specific ILs with a high ammonia absorption capacity and easy regeneration, with promising potential application in fast absorption–desorption cycles.

4. Conclusions

A computational-experimental strategy research was developed to propose new ILs with favorable properties for NH_3 absorption. First, COSMO-RS method was used to analyze the solute–solvent intermolecular interactions and to perform a rational screening among 272 conventional and task-specific ILs, for selecting a set of optimum cation–anion combinations for NH_3 absorption. The results obtained confirm the general suitability of COSMOS-RS method to predict gas–liquid equilibrium data in IL systems, such as, the solubilities and Henry's law constants. Computational and experimental evidences probe that ammonia forms efficient intermolecular interactions with hydrogen bond donor groups present in the IL structure. As a results, we propose two new commercially available task-specific ILs, [EtOHmim][BF_4] and [choline][NTf_2], whose characteristics would allow future implementation of novel ammonia absorption systems. High thermal stability, adequate liquid-phase window, high ammonia solubility at near room temperature and atmospheric pressure, together with rapid absorption and desorption allowing complete regeneration, make of these ILs quite promising solvents for ammonia capture and recovery in absorption–desorption cycles.

Acknowledgements

The authors are grateful to the Spanish "Ministerio de Ciencia e Innovación (MICINN)" and "Comunidad de Madrid" for financial support (projects CTQ2008-01591, CTQ2008-05641 and S2009/PPQ-1545). J. Bedia acknowledges the Spanish MICINN for financing his research through the "Juan de la Cierva" post-doctoral program. We are very grateful to "Centro de Computación Científica de la Universidad Autónoma de Madrid" for computational facilities.

Appendix A. Supplementary material

Supplementary data associated with this article can be found, in the online version, at doi:10.1016/j.seppur.2011.08.014.

References

[1] M.A. Sutton, D. Fowler, Introduction: fluxes and impacts of atmospheric ammonia on national, landscape and farm scales, Environ. Pollut. 119 (2002) 7–8.
[2] J.W. Erisman, A. Bleeker, J. Galloway, M.A. Sutton, Reduced nitrogen in ecology and the environment, Environ. Pollut. 150 (2007) 140–149.

[3] M.A. Sutton, J.W. Erisman, F. Dentener, D. Möller, Ammonia in the environment: from ancient times to the present, Environ. Pollut. 156 (2008) 583–604.
[4] W.B. Faulkner, B.W. Shaw, Review of ammonia emission factors for United States animal agriculture, Atmos. Environ. 42 (2008) 6567–6574.
[5] P.M. Ndegwa, A.N. Hristov, J. Arogo, R.E. Sheffield, A review of ammonia emission mitigation techniques for concentrated animal feeding operations, Biosyst. Eng. 100 (2008) 453–469.
[6] S.M. Roe, M.D. Spivey, H.C. Lindquist, K.B. Thesing, R.P. Strait, Estimating ammonia emissions from anthropogenic nonagricultural sources – Draft final report, Emission Inventory Improvement Program, 2004.
[7] R.W. Melse, N.W.M. Ogink, W.H. Rulkens, Overview of European and Netherlands' regulations on airborne emissions from intensive livestock production with a focus on the application of air scrubbers, Biosyst. Eng. 104 (2009) 289–298.
[8] J. Koornneef, A. Ramirez, T. van Harmelen, A. van Horssen, W. Turkenburg, A. Faaij, The impact of CO_2 capture in the power and heat sector on the emission of SO_2, NO_x, particulate matter, volatile organic compounds and NH_3 in the European Union, Atmos. Environ. 44 (2010) 1369–1385.
[9] EC, 2001.Directive 2001/81/EC of the European Parliament and of the Council of 23 October 2001 on National Emission Ceilings for Certain Atmospheric Pollutants European Parliament and Council.
[10] O. Brettschneider, R. Thiele, R. Faber, H. Thielert, G. Woznya, Experimental investigation and simulation of the chemical absorption in a packed column for the system NH_3–CO_2–H_2S–NaOH–H_2O, Sep. Purif. Technol. 39 (2004) 139–159.
[11] S.Y. Junga, S.J. Leea, J.J. Parka, S.C. Leea, H.K. Junb, T.J. Leec, C.K. Ryud, J.C. Kim, The simultaneous removal of hydrogen sulfide and ammonia over zinc-based dry sorbent supported on alumina, Sep. Purif. Technol. 63 (2008) 297–302.
[12] C.W. Parka, J.H. Byeonb, K.Y. Yoonc, J.H. Parka, J. Hwanga, Simultaneous removal of odors, airborne particles, and bioaerosols in a municipal composting facility by dielectric barrier discharge, Sep. Purif. Technol. 77 (2011) 87–93.
[13] P. Wasserscheid, T. Welton, Ionic Liquids in Synthesis, Wiley-VCH Verlag GmbH & Co., KGaA, Weinheim, 2008.
[14] E.D. Bates, R.D. Mayton, I. Ntai, J.H. Davis, CO_2 capture by a task-specific ionic liquid, J. Am. Chem. Soc. 124 (6) (2002) 926–927.
[15] R. Giernoth, Task-specific ionic liquids, Angew. Chem., Int. Ed. 49 (2010) 2834–2839.
[16] D. Han, K.H. Row, Recent applications of ionic liquids in separation technology, Molecules 15 (2010) 2405–2426.
[17] J.L. Anthony, S. Aki, E.J. Maggin, J.F. Brennecke, Feasibility of using ionic liquids for carbon dioxide capture, IJETM 4 (12) (2004) 105–115.
[18] J.D. Figueroa, T. Fout, S. Plasynsky, H. McIlvried, R.D. Srivastava, Advances in CO_2 capture technology – The U.S. Department of Energy's Carbon Sequestration Program, IJGGC 2 (2008) 9–20.
[19] J.E. Bara, T.K. Carliste, C.J. Gabriel, D. Camper, A. Finotello, D.L. Gin, R.D. Noble, Guide to CO_2 separations in imidazolium-based room-temperature ionic liquids, Ind. Eng. Chem. Res. 48 (2009) 2739–2751.
[20] P.J. Carvalho, V.H. Alvarez, J.J.B. Machado, J. Pauly, J.L. Daridon, I.M. Marrucho, M. Aznar, J.A.P. Coutinho, High pressure phase behavior of carbon dioxide in 1-alkyl-3-methylimidazolium bis(trifluoromethylsulfonyl)imide ionic liquids, J. Supercrit. Fluids 48 (2009) 99–107.
[21] R. Hart, P. Pollet, D.J. Hahne, E. John, V. Llopis-Mestre, V. Blasucci, H. Huttenhower, W. Leitner, C.A. Eckert, C.L. Liotta, Benign coupling of reactions and separations with reversible ionic liquids, Tetrahedron 66 (2010) 1082–1090.
[22] M.B. Shiflett, A. Yokozeki, Chemical absorption of sulfur dioxide in room-temperature ionic liquids, Ind. Eng. Chem. Res. 49 (3) (2010) 1370–1377.
[23] S.H. Ren, Y. C Hou, W.Z. Wu, Q.Y. Liu, Y.F. Xiao, X.T. Chen, Properties of ionic liquids absorbing SO_2 and the mechanism of the absorption, J. Phys. Chem. B 114 (6) (2010) 2175–2179.
[24] M.B. Shiflett, M.A. Harmer, C.P. Junk, A. Yokozeki, Solubility and diffusivity of difluoromethane in room-temperature ionic liquids, J. Chem. Eng. Data 51 (2006) 483–495.
[25] M.B. Shiflett, A. Yokozeki, Solubility and diffusivity of hydrofluorocarbons in room-temperature ionic liquids, AIChE J. 52 (3) (2006) 1205–1219.
[26] M.B. Shiflett, A. Yokozeki, Vapor–liquid–liquid equilibria of hydrofluorocarbons + 1-butyl-3-methylimidazolium hexafluorophosphate, J. Chem. Eng. Data 51 (5) (2006) 1931–1939.
[27] M.B. Shiflett, A.D. Shiflett, A. Yokozekic, Separation of tetrafluoroethylene and carbon dioxide using ionic liquids. Sep. Purif. Technol., in press. doi:10.1016/j.seppur.2011.03.023.
[28] A. Ortiz, A. Ruiz, D. Gorri, I. Ortiz, Room temperature ionic liquid with silver salt as efficient reaction media for propylene/propane separation: Absorption equilibrium, Sep. Purif. Technol. 63 (2008) 311–318.
[29] A. Ortiz, L.M. Galan, D. Gorri, A.B. de Haan, I. Ortiz, Kinetics of reactive absorption of propylene in RTIL-Ag^+ media, Sep. Purif. Technol. 73 (2010) 106–113.
[30] A. Ortiz, L.M. Galan, D. Gorri, A.B. de Haan, I. Ortiz, Reactive ionic liquid media for the separation of propylene/propane gaseous mixtures, Ind. Eng. Chem. Res. 49 (2010) 7227–7233.
[31] A. Yokozeki, M.B. Shiffler, Ammonia solubilities in room-temperature ionic liquids, Ind. Eng. Chem. Res. 46 (2007) 1605–1610.
[32] A. Yokozeki, M.B. Shiffler, Vapor–liquid equilibria of ammonia + ionic liquid mixtures, Appl. Energy 84 (2007) 1258–1273.
[33] J. Huang, A. Riisager, R.W. Berg, R. Fehrmann, Tuning ionic liquids for high gas solubility and reversible gas sorption, J. Mol. Catal. A 279 (2008) 170–176.
[34] G. Li, Q. Zhou, X. Zhang, L. Wang, S. Zhang, J. Li, Solubilities of ammonia in basic imidazolium ionic liquids, Fluid Phase Equilib. 297 (2010) 34–39.
[35] D. Schäfer, M.S. Vogt, J. Xia, A. Perez-Salado, G. Maurer, Experimental investigation of the solubility of ammonia in methanol, J. Chem. Eng. Data 52 (2007) 1653–1659.
[36] L. Huang, W. Xue, Z. Zeng, The solubility of ammonia in ethanol between 277.35 K and 328.15 K, Fluid Phase Equilib. 303 (2011) 80–84.
[37] P.J. Carvalho, J.A.P. Coutinho, Non-ideality of solutions of NH_3, SO_2, and H_2S in ionic liquids and the prediction of their solubilities using the Flory–Huggins model, Energy Fuels 24 (2010) 6662–6666.
[38] A. Yokozekia, M.B. Shiflett, Gas solubilities in ionic liquids using a generic van der Waals equation of state, J. Supercrit. Fluids 55 (2010) 846–851.
[39] A. Klamt, F. Eckert, W. Arlt, COSMO-RS: an alternative to simulation for calculating thermodynamic properties of liquid mixtures, Annu. Rev. Chem. Biomed. Eng. 1 (2010) 101–122.
[40] M. Diedenhofen, A. Klamt, COSMO-RS as a tool for property prediction of IL mixtures – a review, Fluid Phase Equilib. 294 (2010) 31–38.
[41] J. Palomar, J.S. Torrecilla, V.R. Ferro, F. Rodríguez, Development of an a priori ionic liquid design tool 1: integration of a Novel COSMO-RS molecular descriptor on neural networks, Ind. Eng. Chem. Res. 47 (2008) 4523–4532.
[42] J. Palomar, J.S. Torrecilla, V.R. Ferro, F. Rodríguez, Development of an a priori ionic liquid design tool 2: ionic liquid selection through the prediction of COSMO-RS molecular descriptor by inverse neural network, Ind. Eng. Chem. Res. 48 (2009) 2257–2265.
[43] X. Zhang, Z. Liu, W. Wang, Screening of ionic liquids to capture CO_2 by COSMO-RS and experiments, AIChE J. 54 (10) (2008) 2717–2728.
[44] N.A. Manan, C. Hardacre, J. Jacquemin, D.W. Rooney, T.G. Youngs, Evaluation of gas solubility prediction in ionic liquids using COSMOthermX, J. Chem. Eng. Data 54 (2009) 2005–2022.
[45] J. Palomar, M. González-Miquel, A. Polo, F. Rodríguez, Understanding the physical absorption of CO_2 in ionic liquids using the COSMO-RS method, Ind. Eng. Chem. Res. 50 (2011) 3452–3463.
[46] M. González-Miquel, J. Palomar, S. Omar, F. Rodríguez, CO_2/N_2 selectivity prediction in supported ionic liquid membranes (SILMs) by COSMO-RS, Ind. Eng. Chem. Res. 50 (2011) 5739–5748.
[47] A. Navas, J. Ortega, R. Vreekamp, E. Marrero, J. Palomar, Experimental thermodynamic properties of 1-butyl-2-methylpyridinium tetrafluoroborate [b2mpy][BF4] with water and with alkan-1-ol and their interpretation with the COSMO-RS methodology, Ind. Eng. Chem. Res. 48 (5) (2009) 2678–2690.
[48] M.J. Frisch, G.W. Trucks, H.B. Schlegel, G. E. Scuseria, M.A. Robb, J.R. Cheeseman, J. A. Montgomery, T. Vreven, K.N. Kudin, J.C. Burant, J.M. Millam, S.S. Iyengar, J. Tomasi, V. Barone, B. Mennucci, M. Cossi, G. Scalmani, N. Rega, G. A. Petersson, H. Nakatsuji, M. Hada, M. Ehara, K. Toyota, R. Fukuda, J. Hasegawa, M. Ishida, T. Nakajima, Y. Honda, O. Kitao, H. Nakai, M. Klene, X. Li, J.E. Knox, H.P. Hratchian, J.B. Cross, V. Bakken, C. Adamo, J. Jaramillo, R. Gomperts, R.E. Stratmann, O. Yazyev, A.J. Austin, R. Cammi, C. Pomelli, J.W. Ochterski, P.Y. Ayala, K. Morokuma, G.A. Voth, P. Salvador, J.J. Dannenberg, V.G. Zakrzewski, S. Dapprich, A.D. Daniels, M.C. Strain, O. Farkas, D.K. Malick, A.D. Rabuck, K. Raghavachari, J.B. Foresman, J.V. Ortiz, Q. Cui, A.G. Baboul, S. Clifford, J. Cioslowski, B.B. Stefanov, G. Liu, A. Liashenko, P. Piskorz, I. Komaromi, R.L. Martin, D.J. Fox, T. Keith, M.A. Al-Laham, C.Y. Peng, A. Nanayakkara, M. Challacombe, P.M. Gill, B. Johnson, W. Chen, M.W. Wong, C. González, J.A. Pople, Gaussian03, revision B.05, Gaussian, Inc., Wallingford, CT, 2004.
[49] J. Palomar, V.R. Ferro, J.S. Torrecilla, F. Rodriguez, Density and molar volume predictions using COSMO-RS for ionic liquids: an approach to solvent design, Ind. Eng. Chem. Res. 46 (2007) 6041–6048.
[50] GmbH&CoKG, *COSMOtherm* C2.1 Release 01.08; Leverkusen, Germany, 2006. <http://www.cosmologic.de>.
[51] J. Restolho, A.P. Serro, J.L. Mata, B. Saramago, Viscosity and surface tension 1-ethanol-3-methylimidazolium tetrafluoroborate and 1-methyl-3-octylimidazolium tetrafluoroborate over a wide temperature range, J. Chem. Eng. Data 54 (2009) 950–955.
[52] Q. Zhou, L.-S. Wang, H.-P. Chen, Densities and viscosities of 1-butyl-3-methylimidazolium tetrafluoroborate + H_2O binary mixtures from (303.15 to 353.15) K, J. Chem. Eng. Data 51 (2006) 905–908.
[53] P. Nockemann, K. Binnemans, B. Thijs, T.N. Parac-Vogt, K. Merz, A.-V. Mudring, P.C. Menon, R.N. Rajesh, G. Cordoyiannis, J. Thoen, J. Leys, C. Glorieux, Temperature-driven mixing-demixing behavior of binary mixtures of the ionic liquid choline, bis(trifluoromethylsulfonyl)imide and water, J. Phys. Chem. B 113 (2009) 1429–1437.
[54] T.K. Carlisle, J.E. Bara, C.J. Gabriel, R.D. Noble, D.L. Gin, Interpretation of CO_2 solubility and selectivity in nitrile-functionalized room-temperature ionic liquids using a group contribution approach, Ind. Eng. Chem. Res. 47 (2008) 7005–7012.
[55] Q. Shi, P. Davidovits, J.T. Jayne, D.R. Worsnop, C.E. Kolb, Uptake of gas-phase ammonia. 1. Uptake by aqueous surfaces as a function of pH, J. Phys. Chem. A 103 (1999) 8812–8823.
[56] R.E. Ramirez, C. Garcia-Martinez, F. Mendez, Influence of fluorine atoms and aromatic rings on the acidity of ethanol, J. Phys. Chem. A 113 (2009) 10753–10758.

[57] W. Shi, E.J. Maginn, Molecular simulation of ammonia absorption in the ionic liquid 1-ethyl-3-methylimidazolium bis(trifluoromethylsulfonyl)imide ([emim][Tf_2N]), AIChE 55 (2009) 2414–2421.
[58] A. Fernandez, J.S. Torrecilla, J. Garcia, F. Rodriguez, Thermophysical properties of 1-ethyl-3-methylimidazolium ethylsulfate and 1-butyl-3-methylimidazolium methylsulfate ionic liquids, J. Chem. Eng. Data 52 (2007) 1979–1983.
[59] Z.B. Zhou, H. Matsumoto, K. Tatsumi, Low-melting, low-viscous, hydrophobic ionic liquids: 1-alkyl (alkyl ether)-3-methylimidazolium perfluoroalkyltrifluoroborate, Chem. Eng. J. 10 (2004) 6581–6591.
[60] J.-P. Belieres, A. Angell, Protic. Ionic, Liquids: preparation, characterization, and proton free energy level representation, J. Phys. Chem. B 111 (2007) 4926–4937.

Publicación 7:

Bedia, J.; Palomar, J.; Gonzalez-Miquel, M.; Rodriguez, F.; Rodriguez, J.J. **Screening ionic liquids as suitable ammonia absorbents on the basis of thermodynamic and kinetic analysis.** *Separation and Purification Technology*, **2012**, *95*, 188-195.

Separation and Purification Technology 95 (2012) 188–195

Contents lists available at SciVerse ScienceDirect

Separation and Purification Technology

journal homepage: www.elsevier.com/locate/seppur

Screening ionic liquids as suitable ammonia absorbents on the basis of thermodynamic and kinetic analysis

Jorge Bedia [a], Jose Palomar [a,*], Maria Gonzalez-Miquel [b], Francisco Rodriguez [b], Juan J. Rodriguez [a]

[a] Sección de Ingeniería Química, Departamento de Química Física Aplicada, Universidad Autónoma de Madrid, Cantoblanco, 28049 Madrid, Spain
[b] Departamento de Ingeniería Química, Universidad Complutense de Madrid, 28040 Madrid, Spain

ARTICLE INFO

Article history:
Received 5 March 2012
Received in revised form 23 April 2012
Accepted 6 May 2012
Available online 15 May 2012

Keywords:
Ionic liquid
Absorption
Ammonia
Gas solubility
Diffusivity
Efficiency

ABSTRACT

Different ionic liquids (ILs) have been checked as potential ammonia absorbents at near-ambient temperatures and atmospheric pressure. In a first stage, the task-specific ILs 1-2(-hydroxyethyl)-3-methylimidazolium tetrafluoroborate [EtOHmim][BF4], choline bis(trifluoromethylsulfonyl)imide [choline][NTf_2], tris(2-hydroxyethyl)methyl-ammonium methylsulfate [MTEOA][$MeOSO_3$] and 1-(2-hydroxyethyl)-3-methylimidazolium dicyanamide [EtOHmim][DCA] were selected as potential high-capacity ammonia solvents by quantum-chemical COSMO-RS analysis. Then, they were experimentally tested considering both thermodynamic and kinetic aspects. Absorption kinetics was described by a phenomenological diffusion model. The desorption curves were also obtained. Finally, an efficiency criterion based on absorption–desorption cycles was established to simultaneously consider the kinetics and thermodynamics of the phenomena for the solvent selection. As a result, we propose a set of ILs with adequate properties to be used as absorbents for ammonia separation.

1. Introduction

Ammonia (NH_3) emissions lead to a wide range of environmental problems including the formation of fine particulate matter, eutrophication of ecosystems, acidification of soils and alteration of the global greenhouse balance [1–3]. The agricultural sector has been identified as a primary contributor to atmospheric ammonia emissions [4,5]. However, increased attention is being paid to ammonia releases from anthropogenic nonagricultural sources (i.e. losses due to the volatilization of ammonia refrigeration systems) for contributing to atmospheric reactive nitrogen [6,7]. Eventually large-scale implementation of post-combustion technology for CO_2 capture in power plants may also result in higher NH_3 emissions, due to the oxidative degradation of the amine-based solvents [8]. Consequently, air quality policies, such as The National Emission Ceiling Directive of the European Commission [9], are being formulated to set national emission levels for key air pollutants including NH_3. Therefore, the development of techniques capable of capturing nitrogen reactive pollutants or reducing the volatility of ammonia-containing systems is of great interest, including separation by novel absorbents [10] and adsorbents [11] or elimination by dielectric barrier discharge reactors [12].

Room-temperature ionic liquids (ILs) are a novel type of solvents entirely composed by ions, which exhibit distinctive properties, most notably their negligible vapor pressure [13]. Moreover, an important feature is the possibility of designing ILs with the required properties for a particular application by tuning the structure of the ions, hence the term "designer solvents" [14,15]. Owing to their unique properties, ILs have generated significant interest across a wide variety of engineering applications, including their use as absorbents in gas separation processes [16], such as CO_2 capture [17–20], absorption of SO_2 [21–24] and hydrofluorocarbons [25–28] and reactive absorption of propylene [29–31].

The solubilities of ammonia in imidazolium- and guanidinium-based ionic liquids, paired with different anions, have been studied at temperatures ranging from 283 to 353 K and pressures up to 5 MPa [32–35]. The high solubility observed for NH_3 in conventional ILs compared with other organic solvents [36,37] suggests a great potential of these liquids to be used in ammonia absorption systems. We recently published a computational and experimental study for selecting ILs with optimized properties for NH_3 capture [38]. Based on thermodynamic considerations, that work proposed [EtOHmim][BF_4] and [choline][NTf_2] solvents as suitable task-specific ILs for effective ammonia absorption at near room temperature and atmospheric pressure. In this work, the thermodynamic analysis based on COSMO-RS calculations [39] and absorption experiments is extended to other commercial task-specific ILs.

On the other hand, the technical literature reports some studies on the kinetics of CO_2 absorption by ILs [40,41], but to the best of

* Corresponding author. Tel.: +34 91 4976938; fax: +34 91 4973516.
E-mail address: pepe.palomar@uam.es (J. Palomar).

1383-5866/$ - see front matter © 2012 Elsevier B.V. All rights reserved.
http://dx.doi.org/10.1016/j.seppur.2012.05.006

our knowledge there is a lack of information in that respect with regard to NH_3. In this study we analyze the kinetics of NH_3 absorption for the sake of achieving a quantitative description of the absorption rates with the different ILs tested, in terms of diffusivity. The desorption curves are also analyzed, in order to learn on the feasibility of regeneration of the proposed absorbents. In sum, the aim of this work is to consider both thermodynamic and kinetic criteria for optimizing the selection of ILs for operations based on ammonia absorption. With this purpose, an efficiency criteria is established and evaluated for analyzing the behavior of the different ILs in NH_3 absorption–desorption cycles.

2. Procedure

2.1. Computational details

The molecular geometry of all compounds (NH_3 and the ILs counterions) were optimized at the B3LYP/6-31++G** computational level in the ideal gas phase using the quantum chemical Gaussian03 package [42]. A molecular model of independent counterions was applied in COSMO-RS calculations, where the ILs are considered as equimolar mixtures of cation and anion [43]. Vibrational frequency calculations were performed in each case to confirm the presence of an energy minimum. Once molecular models were optimized, Gaussian03 was used to compute the COSMO files. The ideal screening charges on the molecular surface for each species were calculated by the continuum solvation COSMO model using BVP86/TZVP/DGA1 level of theory. Subsequently, COSMO files were used as an input in COSMOthermX [44] code to calculate the thermodynamic properties (Henry's constant of NH_3 in each IL and detailed excess enthalpies contributions of NH_3–IL mixtures). According to our selected quantum method, the functional and the basis set, we used the corresponding parameterization (BP_TZVP_C21_0108) for COSMO-RS calculations in COSMOtherm code.

2.2. Materials

High-purity gas anhydrous ammonia (purity >99.999%) was purchased from Praxair Technology Inc. and was used without further purification. The ILs tested in this study as absorbents were the following: 1-butyl-3-methylimadazolium tetrafluoroborate [bmim][BF_4], 1-2(-hydroxyethyl)-3-methylimadazolium tetrafluoroborate [EtOHmim][BF_4] and choline bis(trifluoromethylsulfonyl)imide [choline][NTf_2] supplied by Io-Li-Tec (Ionic Liquid Technologies) and tris(2-hydroxyethyl)methylammonium methylsulfate [MTEOA][$MeOSO_3$] and 1-(2-hydroxyethyl)-3-methylimidazolium dicyanamide [EtOHmim][DCA] provided by Sigma–Aldrich. All the ILs were purchased at the highest available purity (purity >97–98%). Table 1 summarizes the molecular structure as well as the molecular weight (MW) and abbreviations of the ILs. It is noteworthy the presence of hydroxyl groups in the cation of all the task-specific ILs tested. [MTEOA][$MeOSO_3$] IL bears three hydroxyl groups in its cation. The presence of hydroxyl functionalized cations increases significantly the NH_3 solubility due to the larger hydrogen bond donor ability of this acid group [38].

2.3. Physical properties measurements

Density measurements of the ILs were performed using an Anton Paar DMA-5000 oscillating U-tube density meter. The effect of the viscosity on density determination was automatically corrected by a factor depending on the viscosity of the sample. The repeatability and the uncertainty of the measurements were estimated to be less than $\pm 1 \times 10^{-6}$ g cm^{-3} and $\pm 1 \times 10^{-5}$ g cm^{-3}, respectively. Dynamic viscosities of the ILs were determined using an Anton Paar Automated Micro Viscometer (AMVn) based on the falling ball principle. The temperature was controlled by a Pt100 temperature sensor with a resolution of ±0.01 K. The estimated experimental uncertainty was less than ±0.5% and the repeatability was less than ±0.1%. The water content of ILs used in absorption experiments (after drying them under vacuum of 10^{-3} Torr at 298 K over 24 h) was checked with a Mettler Toledo DL31 Karl Fischer titrator using the one component technique. The polarizing current for the potentiometric end-point determination was 20 A and the stop voltage 100 mV. The end-point criterion was the drift stabilization (3 μg H_2O min^{-1}) or maximum titration time (10 min). The measurement was corrected for the baseline drift, defined as the residual or penetrating water that the apparatus removes per minute. The uncertainty of the measurements was estimated less than 7%. Table 2 collects the measured density and dynamic viscosity of the ILs. Density and viscosity measurements of [bmim][BF_4] have been previously reported in the literature [45–48]. The values obtained experimentally in this work for this IL are in the range of those previously reported in the literature which validates the experimental methods used for their determination. The presence of water undoubtedly affects the viscosity of ILs and could affect to their absorption capacities and other properties. However, the water content of the different ILs was always very low (<200 ppm) as previously reported [38]. Therefore, within the temperature range tested, water should not have a significant effect.

Table 1
Molecular structure, molecular weight (MW) and abbreviation of the selected ILs.

Abbreviation	Structure	MW
[bmim][BF_4]		226.02
[EtOHmim][BF_4]	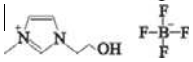	213.97
[choline][NTf_2]	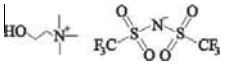	368.32
[MTEOA][$MeOSO_3$]	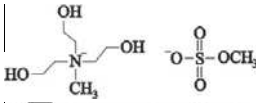	275.32
[EtOHmim][DCA]	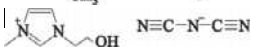	193.21

Table 2
Density and viscosity of the ILs.

IL	Temperature (K)	Viscosity (mPa s)	Density (g/cm^3)
[bmim][BF_4]	293	123.41	1.203
	313	48.25	1.189
[EtOHmim][BF_4]	293	149.34	1.365
	313	54.09	1.350
[choline][NTf_2]	303	94.54	1.522
	313	61.76	1.512
[MTEOA][$MeOSO_3$]	293	1492.12	1.344[a] [49]
	303	777.26	–
	313	440.01	–
[EtOHmim][DCA]	293	104.11	1.179 [50]
	303	60.57	–
	313	38.83	–

[a] At 298 K.

2.4. Absorption and desorption experiments

The detailed scheme of the setup used for the ammonia absorption experiments can be found elsewhere [38]. Briefly, the equilibrium and kinetic experiments were carried out in a TGA system (TGA/SDTA851e Mettler Toledo International Inc.) at atmospheric pressure and temperatures in the range of 293–313 K using around 20 mg of IL. Before each experiment, the ILs were dried under vacuum (10^{-3} Torr) at 298 K over at least 24 h. The temperature of the sample was maintained constant with a regulated external thermostatic bath (Huber minisat 125). Gas–liquid equilibrium data of ammonia in ILs were obtained by setting the partial pressure of ammonia in the NH_3/N_2 gas feed (100 N cm^3/min) and monitoring the weight increase of the sample. Blank experiments were carried out with bare N_2 gas and no weight increases of the IL samples were detected, consistently with the reported low solubility of N_2 in imidazolium-based ILs (<10^{-3} molar fraction at 1 atm and 40 °C) [51]. The equilibrium was assumed when at each constant pressure no further weight change was observed upon time (weight change rate <0.001 mg h^{-1}). The equilibration time depended on the IL.

The absorption and desorption rate curves were also obtained in the same thermogravimetric system at 293, 303 and 313 K. Ammonia absorption was performed under continuous NH_3/N_2 gas flow (100 N cm^3/min) at an ammonia partial pressure of 0.08 MPa. These conditions allow a constant gas density in the absorption chamber. The weight increase was continuously monitored and once the IL and the gas reached equilibrium (weight change rate <0.001 mg h^{-1}), desorption was carried out at the absorption temperature under dry nitrogen flow (100 N cm^3/min).

^{1}H NMR analysis of fresh and recovered IL were carried out with a Varian Unity 500 spectrometer, using a solution of [choline][NTf_2] and acetone-d_6 over 10 mmol.

3. Results and discussion

3.1. Preliminary selection of ILs for NH_3 absorption by COSMO-RS methodology

COSMO-RS (Conductor-like Screening Model for Real Solvents), developed by Klamt and co-workers [39], has demonstrated to be a valuable method for predicting the thermodynamic properties of ILs mixtures on the basis of unimolecular quantum chemical calculations for the individual molecules [52], providing a unique a priori computational tool for designing ILs with specific properties [53,54]. In addition, COSMO-RS can be successfully applied to analyze the solubility of gaseous solutes (NH_3, CO_2, N_2, hydrocarbons, etc.) in ILs in terms of the contributions of the different solute–solvents intermolecular interactions to the excess enthalpy of the liquid phase [55–57]. In a previous work [38], COSMO-RS analysis helped to elucidate the structural characteristics enhancing the solubility of NH_3 in ILs. Thus, it was found that attractive hydrogen-bond interactions determine the increasing gas solubility of NH_3 in the solvents (decreasing Henry's constant values), in good agreement with previous computational analyses by molecular dynamics [58]. Conventional ILs, such us [bmim][BF_4], behave mostly as hydrogen-bond acceptors [59] and do not possess the ability to form effective hydrogen bonds with the NH_3 solute, hence do not seem optimum solvents for ammonia absorption. However, COSMO-RS analysis allows concluding that inclusion of hydrogen-bond donor groups, as hydroxyl group, in the ILs significantly increases the absorption of ammonia, which was experimentally confirmed in a previous work [38]. In that work, we proposed two commercially available task-specific ILs, [EtOHmim][BF_4] and [choline][NTf_2], whose characteristics would allow future implementation of novel ammonia absorption systems. In this study, we have extended COSMO-RS analysis to two new commercially available ILs, namely [MTEOA][$MeOSO_3$] and [EtOHmim][DCA], being the K_H values calculated by COSMO-RS summarized in Table 3. As a general trend, higher solubilities (decreasing K_H values) of NH_3 in ILs have been associated with higher exothermicity (decreasing values of excess enthalpy) of the NH_3–IL mixture [38]. As can be seen, the four selected task-specific ILs show NH_3 Henry's constant values significantly lower than that corresponding to the conventional IL [bmim][BF_4] used as reference, being NH_3 absorption in those task-specific ILs considerably more exothermic. Therefore, the use of hydroxyl-functionalized cations significantly increases the solubility of NH_3 in ILs, mainly due to the larger hydrogen-bond donor ability of this acid group. Thus, we selected the four above mentioned ILs for further experimental study of NH_3 absorption.

3.2. Absorption of NH_3 in task-specific ILs

A series of gas–liquid absorption equilibrium experiments was performed at total pressure of 0.1 MPa and temperatures of 293 and 313 K using NH_3/N_2 gas mixtures and the selected ILs. Fig. 1 depicts the results obtained which for the sake of comparison include also those relative to the conventional IL [bmim][BF_4]. As can be seen, the results confirm the COSMO-RS prediction on the superior NH_3 absorption of the selected ILs. A good agreement is found between the trend predicted from COSMO-RS calculations and the experimental NH_3 solubilities at 313 K and 0.1 MPa, which follows the order [choline][NTf_2] (X_{NH3} = 0.59) > [MTEOA][$MeOSO_3$] (X_{NH3} = 0.57) > [EtOHmim][BF_4] (X_{NH3} = 0.47) > [EtOHmim][DCA] (X_{NH3} = 0.40) > [bmim][BF_4] (X_{NH3} = 0.28). At 313 K [choline][NTf_2] shows the highest X_{NH3} values within the whole range of ammonia partial pressure tested. However, at 293 K, higher ammonia solubilities are obtained for [MTEOA][$MeOSO_3$] and [EtOHmim][DCA] at NH_3 partial pressures higher than 0.08 and 0.02 MPa, respectively. As can be seen, [choline][NTf_2] shows fairly small differences in NH_3 uptake at the two temperatures tested. This unexpected result was ascribed to [choline][NTf_2] state [38] since this IL melts at 303 K and a solid state polymorphism occurs in the temperature range studied [60]. We visually checked that the [choline][NTf_2] is gelled below 299 K. For the rest of ILs, Fig. 1 confirms that, as expected, ammonia solubilities increased with decreasing temperature and increasing NH_3 partial pressure.

3.3. Absorption kinetics

Fig. 2 shows the rate curves of ammonia absorption and desorption obtained for the ILs at 293 K (and 0.08 MPa NH_3 partial pressure for the adsorption stage). Similar curves were obtained at temperatures of 303 and 313 K (reported as Supplementary data). As can be observed (see detail in Fig. 2), ammonia absorption proceeds relatively fast, although a significant dependence on the particular IL can be appreciated. [choline][NTf_2] seems to present the fastest absorption while [MTEOA][$MeOSO_3$] exhibits the slowest, probably due in part to its high viscosity (Table 2).

Table 3
Henry's constants (K_H) and excess molar enthalpies (H^E) of NH_3 in the ionic liquids at T = 298 K computed by COSMO-RS.

IL	K_H (MPa)	H^E (kJ/mol)
[bmim][BF_4]	0.116	−0.2
[EtOHmim][BF_4]	0.013	−5.5
[choline][NTf_2]	<10^{-4}	−24.7
[MTEOA][$MeOSO_3$]	0.011	−8.0
[EtOHmim][DCA]	0.030	−3.4

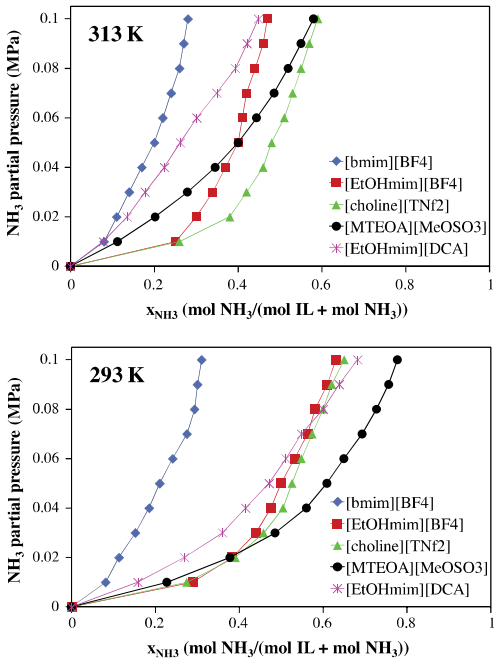

Fig. 1. Equilibrium curves of ammonia absorption in the selected task-specific ILs at 313 and 293 K.

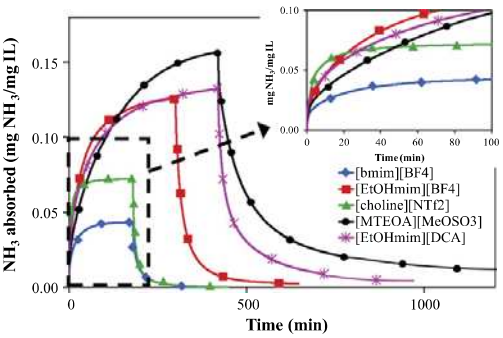

Fig. 2. Ammonia absorption and desorption curves in the ILs at 293 K (and 0.08 MPa NH_3 partial pressure for absorption).

Desorption of the absorbed ammonia from the IL is also a key issue for potential applications. The desorption curves, obtained using identical operation conditions than for absorption but in absence of NH_3 in the gas stream (bare N_2), are also showed in Fig. 2. As can be seen, the desorption of NH_3 proceeds also fast and depending on the IL. Furthermore, the NH_3 can be almost completely desorbed at the absorption temperature for most of the ILs studied. These results suggest an easy regeneration step of IL absorbent by desorption, which may be facilitated by heating or vacuum as it was reported for other ILs [34]. In addition, current results also seem to indicate that the ammonia absorption on these ILs is of physical nature. This conclusion was confirmed by ^{1}H NMR measurements which yielded identical spectra for fresh and regenerated [choline][NTf_2]. Consequently, the ILs tested can be completely regenerated by simple desorption with a nitrogen flow, except perhaps in the case of [MTEOA][$MeOSO_3$], where its high viscosity may be related to the lower desorption rate.

In order to quantify the kinetics of NH_3 absorption in the different ILs, diffusion coefficients were estimated by applying a simplified mass-diffusion model previously used for CO_2 absorption with ILs by Shiflett et al. [40,61,62]. This simplified model assumes that (i) gas dissolves through a one-dimensional diffusion process, (ii) a thin boundary layer between the gas and liquid phases exists, where the thermodynamic equilibrium is instantly established with the saturation concentration (C_s) and where the concentration is constant upon time at a given temperature and pressure, and (iii) temperature and pressure are kept constant. Fig. 3 represents a flat-bottom sample container like the one used in the TG experiments filled with IL at a certain liquid level height (L).

The process may be described by one-dimensional mass diffusion due to the local concentration difference. The NH_3 mass balance can be written as:

$$\frac{\partial C}{\partial t} = D \cdot \frac{\partial^2 C}{\partial z^2} \tag{1}$$

Initial condition:

$$C = 0 \quad \text{when } t = 0 \text{ and } z < 0 < L$$

Boundary conditions:

$$C = C_s \quad \text{when } t > 0 \text{ and } z = 0$$

$$\frac{\partial C}{\partial z} = 0 \quad \text{at } z = L$$

where C is the concentration of NH_3 dissolving in the IL as a function of time, t, and vertical location, z, L is the depth of IL in the container and $z = 0$ corresponds to the gas–liquid boundary (Fig. 3). L values (assumed to be constant and typically between 0.7 and 1.0 mm) were calculated from the IL mass used in each experiment using the IL density values (Table 2) and the dimensions of the sample container. D is the diffusion coefficient that is assumed constant and in this case must be taken as an "effective diffusion coefficient". The NH_3–IL mixtures cannot be considered diluted solutions given the high absorption capacities of the ILs tested, which would lead to some changes in density and viscosity upon the absorption process. Nevertheless, the values of D can be used for the sake of comparison between the different IL tested. The simplification of assuming diluted solutions has been previously used by other authors working with CO_2–ILs systems reaching even higher solute concentration than ours [40].

Eq. (1) can be solved analytically for the initial and boundary conditions yielding:

$$C = C_s\left[1 - 2\sum_{n=0}^{\infty}\frac{\exp(-\lambda_n^2 Dt)\sin\lambda_n z}{L\lambda_n}\right] \tag{2}$$

where $\lambda_n = (n + 1/2)\pi/L$.

The experimentally measured quantity at a specified time is the total concentration (mass per unit volume) of dissolved gas in IL. This space-averaged concentration at a given time, $\overline{C}$, can be calculated from the equation:

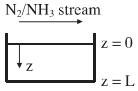

Fig. 3. Scheme of the flat-bottom sample container filled with IL used for the absorption experiments.

$$\overline{C} = \frac{1}{L}\int_0^L C dz$$

$$\overline{C} = C_s\left[1 - 2\sum_{n=0}^{\infty}\frac{\exp(-\lambda_n^2 Dt)}{L^2\lambda_n^2}\right]$$

Although this equation contains an infinite summation, only the first few terms, except for initial small time periods, are sufficient in practical applications. Shiflett and Yokozeki [40] determined that the summation was terminated after 10 terms when the numerical contribution to the summation in $\overline{C}$ became less than 10^{-12}. However, in our case, only three terms of the summation contribute significantly to $\overline{C}$. Fitting the experimental data to this equation, we obtained the saturation concentration (C_s) and the diffusion coefficient (D) at given T and P. The fitting was performed by nonlinear regression using MATLAB software.

Table 4 summarizes the values of the effective diffusion coefficients of NH_3 at the three absorption temperatures in the different ILs. The correlation coefficients (R^2) are also included, which showed fairly good values in most of the cases. Fig. 4 shows the fitting of the experimental data to the predicted $\overline{C}$ vs t curves for two of the ILs selected as representative examples of high (>0.99) and lower (0.96–0.97) values of the correlation coefficient. This effective diffusivity, D, increases with the absorption temperature, consistently with the reduction of the viscosity of the ILs with increasing temperature. The value of D in the different ILs follows the order [choline][NTf_2] > [EtOHmim][DCA] > [bmim][BF_4] > [EtOHmim][BF_4] > [MTEOA][$MeOSO_3$], in reasonable concordance with IL viscosity trends (Table 1). It should be remarked that the D values obtained in this work for the absorption of ammonia on [bmim][BF_4] are around one order of magnitude higher than those previously reported for CO_2 with this IL [40].

To learn on the ammonia desorption from the saturated IL is crucial for the sake of potential applications. Two main issues need to be analyzed (i) whether desorption is complete or not at the absorption temperature and (ii) the rate of desorption. The desorption curves of Fig. 2 show that in the case of [bmim][BF_4], [choline][NTf_2] and [EtOHmim][BF_4] complete ammonia desorption can be achieved at the absorption temperature, thus precluding the need of heating or vacuum for desorption, which has been reported with other ILs [38]. On the other hand, Fig. 5a and b shows the evolution of absorbed ammonia during the successive absorption (390 min)–desorption (480 min) cycles at 293 K (and 0.08 MPa of NH_3 partial pressure for absorption) on [EtOHmim][BF_4] and [MTEOA][$MeOSO_3$] ILs, respectively. As can be seen, the amount of ammonia absorbed at equilibrium does not change significantly through the different absorption cycles. On the other hand, the amount that remains absorbed after the desorption process neither change in the successive cycles. In the case of [MTEOA][$MeOSO_3$] not all the ammonia was desorbed in the desorption stage because longer times would be needed. However, the amount of ammonia absorbed does not change from the second to successive cycles. This behavior is observed for all the task-specific ILs, indicating their suitability for gas separation processes involving NH_3 absorption and subsequent IL regeneration by desorption.

Table 4
Effective diffusion coefficients of NH_3 in ILs at different temperatures.

IL	T (K)	$D \times 10^{-10}$ (m^2/s)	R^2
[bmim][BF_4]	293	2.10	0.991
	303	7.51	0.948
	313	12.5	0.932
[choline][NTf_2]	293	3.84	0.971
	303	10.5	0.967
	313	14.1	0.961
[EtOHmim][BF_4]	293	1.44	0.996
	303	2.76	0.998
	313	4.03	0.996
[MTEOA][$MeOSO_3$]	293	0.37	0.999
	303	0.39	0.991
	313	0.86	0.994
[EtOHmim][DCA]	293	1.18	0.991
	303	1.10	0.976
	313	2.20	0.962

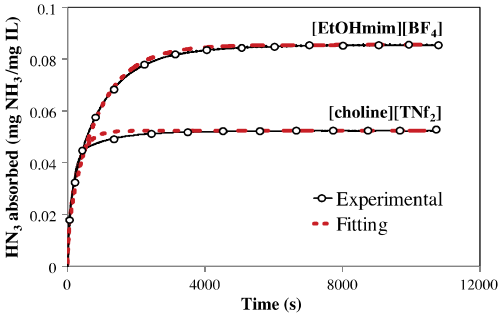

Fig. 4. Fitting of the experimental data (303 K) to the predicted $\overline{C}$ vs t curves for two of the ILs selected as representative examples of high (>0.99) and lower (0.96–0.97) values of the correlation coefficient.

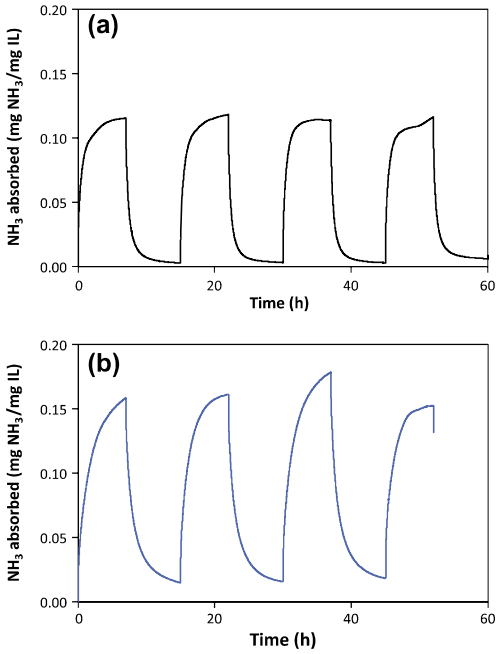

Fig. 5. Successive NH_3 absorption–desorption cycles at 293 K (and 0.08 MPa of NH_3 partial pressure for adsorption) with (a) [EtOHmim][BF_4] and (b) [MTEOA][$MeOSO_3$].

3.4. Screening of the ILs

Screening of the ILs as potential NH_3 absorbents requires considering both thermodynamic and kinetic aspects. Fig. 6 depicts

the molar fractions of NH_3 in IL at equilibrium and the corresponding diffusion coefficients at 313 K. As can be seen, in most cases the absorption capacity trend differs from that of absorption rate, with the exception of the IL [choline][NTf_2], where favorable thermodynamics and kinetics are observed.

On the other hand, the analysis of the results indicates that the absorption temperature is crucial since decreasing temperature increases the amount absorbed (Fig. 1) but decreases diffusion rates (Table 4). In sum, both the IL structure and the operating temperature play a main role in ammonia absorption. We propose an efficiency parameter for the sake of characterizing the behavior of ILs in the successive absorption–desorption cycles (see Fig. 5) under different operating conditions. This efficiency parameter is defined as the effective mass of ammonia absorbed per unit mass of IL and per unit time.

$$\text{Efficiency} = \frac{C_{ef}}{t_{op}} = \frac{C_{0.9} - C_{0.1}}{t_a + t_d}$$

where C_{ef} is the effective absorption capacity of the IL between successive absorption–desorption cycles, conventionally defined as the difference between the 90% and the 10% of the maximum absorption capacity (C_s), and t_{op} is the operating time defined as the sum of the absorption and desorption times. The significance of these terms is highlighted in Fig. 7, which depicts the absorption–desorption rate curves at 303 K (and 0.08 MPa ammonia partial pressure for absorption) on [EtOHmim][BF_4]. In spite of its conventional character, this parameter can be used for the purpose of comparing between different IL absorbents, taking into account both thermodynamic and kinetic aspects.

Fig. 8 shows the values of that efficiency parameter for the task-specific ILs tested, expressed in mmol NH_3 min^{-1} mol IL^{-1}. As can be seen, [choline][NTf_2] shows much higher values than the rest of the ILs analyzed at all the temperatures tested. Therefore, combining thermodynamic and kinetic considerations, [choline][NTf_2] appears as the most suitable IL for ammonia absorption, at least at the conditions used in this work. It should be noticed that the highest values of the efficiency do not corresponds to the lowest absorption temperatures tested for none of the ILs. All the ILs show the highest efficiency at 303 K, with the exception of [choline][NTf_2], where the temperature was 313 K. At the lowest temperature (293 K) within the range tested, the slower kinetic dominates over the favorable thermodynamics for all the ILs considered; whereas at the highest temperature (313 K), despite the higher diffusivities due to the lower viscosity, the loss of absorption capacity results in a decrease of efficiency.

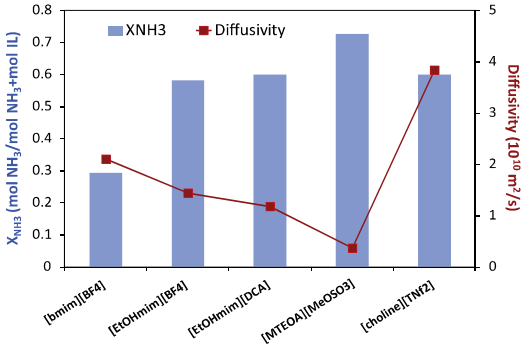

Fig. 6. Ammonia absorption capacities expressed in molar fraction vs apparent diffusion coefficients obtained experimentally at 293 K and atmospheric pressure for the task-specific ILs studied.

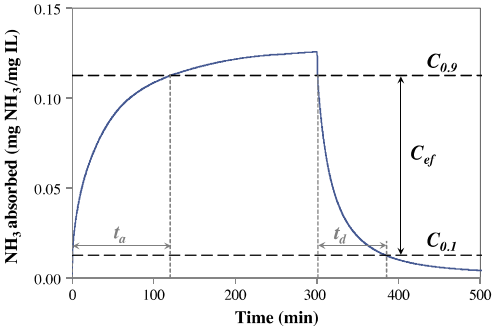

Fig. 7. Scheme for the calculation of the conventional efficiency parameter.

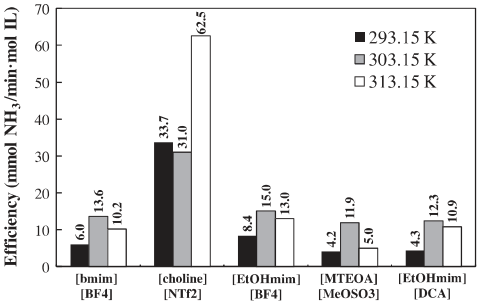

Fig. 8. Efficiency of task-specific ILs for NH_3 absorption–desorption cycles at different temperatures (and 0.08 MPa NH_3 partial pressure for absorption).

These counterbalance effects allow selecting an intermediate temperature for the absorption process. The exception case of [choline][NTf_2], where the maximum efficiency is displace to the highest temperature tested (313 K), is most probably due to the aforementioned solid state polymorphism occurring within the 293–303 K temperature range [60].

It is also worth mentioning that the IL used as reference, [bmim][BF_4], shows efficiency values similar or even higher than those corresponding to the task-specific ILs except for [choline][NTf_2]. The reference IL shows the lowest equilibrium ammonia absorption (Fig. 1), but a relatively high effective diffusivity (Table 4); thus requiring short desorption times, giving rise to efficiency values quite similar to that of [EtOHmim][BF_4] and higher than [MTEOA][$MeOSO_3$] and [EtOHmim][DCA].

The rate at which the equilibrium is reached could depend very much on the contact between gas and liquid phases. Therefore, the values of the efficiency factor obtained in the thermogravimetric system could not be comparable to those obtained in different G–L contactors. However, this parameter may be very useful to compare the absorption properties of different ILs, allowing to take into account both thermodynamics and kinetics in the selection of the IL absorbent.

4. Conclusions

This work evaluates different task-specific ILs (ILs) [EtOHmim][BF_4], [choline][NTf_2], [MTEOA][$MeOSO_3$] and [EtOHmim][DCA] as potential ammonia absorbents at near-ambient temperatures and atmospheric pressure. These ILs were previously

selected from quantum-chemical COSMO-RS analysis. Both thermodynamic and kinetic aspects have been analyzed. The absorption rate curves have been described by a phenomenological diffusion model, which allows quantitative comparison between the different ILs in terms of effective diffusivity of NH_3. Desorption curves have also been obtained, in order to learn on the feasibility and the rate of regeneration of the ILs after absorption. Finally, combining both kinetic and thermodynamic aspects in absorption–desorption cycles, we propose [choline][NTf_2] as the most suitable solvent among the selected ILs for NH_3 absorption, since it shows much higher values of conventionally defined efficiency within the range of temperatures tested.

Acknowledgements

The authors are grateful to the Spanish "Ministerio de Ciencia e Innovación (MICINN)" and "Comunidad de Madrid" for financial support (Projects CTQ2011-26758 and S2009/PPQ-1545). J. Bedia acknowledges the Spanish MICINN for financing his research through the "Juan de la Cierva" post-doctoral program. We are very grateful to "Centro de Computación Científica de la Universidad Autónoma de Madrid" for computational facilities.

Appendix A. Supplementary material

Supplementary data associated with this article can be found, in the online version, at http://dx.doi.org/10.1016/j.seppur.2012.05.006.

References

[1] M.A. Sutton, D. Fowler, Introduction: fluxes and impacts of atmospheric ammonia on national, landscape and farm scales, Environ. Pollut. 119 (2002) 7–8.
[2] J.W. Erisman, A. Bleeker, J. Galloway, M.A. Sutton, Reduced nitrogen in ecology and the environment, Environ. Pollut. 150 (2007) 140–149.
[3] M.A. Sutton, J.W. Erisman, F. Dentener, D. Möller, Ammonia in the environment: from ancient times to the present, Environ. Pollut. 156 (2008) 583–604.
[4] W.B. Faulkner, B.W. Shaw, Review of ammonia emission factors for United States animal agriculture, Atmos. Environ. 42 (2008) 6567–6574.
[5] P.M. Ndegwa, A.N. Hristov, J. Arogo, R.E. Sheffield, A review of ammonia emission mitigation techniques for concentrated animal feeding operations, Biosyst. Eng. 100 (2008) 453–469.
[6] S.M. Roe, M.D. Spivey, H.C. Lindquist, K.B. Thesing, R.P. Strait, Estimating Ammonia Emissions from Anthropogenic Nonagricultural Sources – Draft Final Report, Emission Inventory Improvement, Program, 2004.
[7] R.W. Melse, N.W.M. Ogink, W.H. Rulkens, Overview of European and Netherlands' regulations on airborne emissions from intensive livestock production with a focus on the application of air scrubbers, Biosyst. Eng. 104 (2009) 289–298.
[8] J. Koornneef, A. Ramirez, T. van Harmelen, A. van Horssen, W. Turkenburg, A. Faaij, The impact of CO_2 capture in the power and heat sector on the emission of SO_2, NO_x, particulate matter, volatile organic compounds and NH_3 in the European Union, Atmos. Environ. 44 (2010) 1369–1385.
[9] EC, 2001. Directive 2001/81/EC of the European Parliament and of the Council of 23 October 2001 on National Emission Ceilings for Certain Atmospheric Pollutants European Parliament and Council.
[10] O. Brettschneider, R. Thiele, R. Faber, H. Thielert, G. Woznya, Experimental investigation and simulation of the chemical absorption in a packed column for the system NH_3–CO_2–H_2S–NaOH–H_2O, Sep. Purif. Technol. 39 (2004) 139–159.
[11] S.Y. Junga, S.J. Leea, J.J. Parka, S.C. Leea, H.K. Junb, T.J. Leec, C.K. Ryud, J.C. Kim, The simultaneous removal of hydrogen sulfide and ammonia over zinc-based dry sorbent supported on alumina, Sep. Purif. Technol. 63 (2008) 297–302.
[12] C.W. Park, J.H. Byeon, K.Y. Yoon, J.H. Park, J. Hwang, Simultaneous removal of odors, airborne particles, and bioaerosols in a municipal composting facility by dielectric barrier discharge, Sep. Purif. Technol. 77 (2011) 87–93.
[13] P. Wasserscheid, T. Welton, Ionic Liquids in Synthesis, Wiley-VCH Verlag GmbH & Co. KGaA, Weinheim, 2008.
[14] E.D. Bates, R.D. Mayton, I. Ntai, J.H. Davis, CO_2 capture by a task-specific ionic liquid, J. Am. Chem. Soc. 124 (6) (2002) 926–927.
[15] R. Giernoth, Task-specific ionic liquids, Angew. Chem. Int. Ed. 49 (2010) 2834–2839.
[16] D. Han, K.H. Row, Recent applications of ionic liquids in separation technology, Molecules 15 (2010) 2405–2426.
[17] D. Figueroa, T. Fout, S. Plasynsky, H. McIlvried, R.D. Srivastava, Advances in CO_2 capture technology – The U.S. Department of Energýs Carbon Sequestration Program, IJGGC 2 (2008) 9–20.
[18] J.E. Bara, T.K. Carliste, C.J. Gabriel, D. Camper, A. Finotello, D.L. Gin, R.D. Noble, Guide to CO_2 separations in imidazolium-based room-temperature ionic liquids, Ind. Eng. Chem. Res. 48 (2009) 2739–2751.
[19] P.J. Carvalho, V.H. Alvarez, J.J.B. Machado, J. Pauly, J.L. Daridon, I.M. Marrucho, M. Aznar, J.A.P. Coutinho, High pressure phase behavior of carbon dioxide in 1-alkyl-3-methylimidazolium bis(trifluoromethylsulfonyl)imide ionic liquids, J. Sup. Fluids 48 (2009) 99–107.
[20] F. Karadas, M. Atilhan, S. Aparicio, Review on the use of ionic liquids (ILs) as alternative fluids for CO_2 capture and natural gas sweetening, Energy Fuels 24 (2010) 5817–5828.
[21] R. Hart, P. Pollet, D.J. Hahne, E. John, V. Llopis-Mestre, V. Blasucci, H. Huttenhower, W. Leitner, C.A. Eckert, C.L. Liotta, Benign coupling of reactions and separations with reversible ionic liquids, Tetrahedron 66 (2010) 1082–1090.
[22] M.B. Shiflett, A. Yokozeki, Chemical absorption of sulfur dioxide in room-temperature ionic liquids, Ind. Eng. Chem. Res. 49 (2010) 1370–1377.
[23] S.H. Ren, Y.C. Hou, W.Z. Wu, Q.Y. Liu, Y.F. Xiao, X.T. Chen, Properties of ionic liquids absorbing SO_2 and the mechanism of the absorption, J. Phys. Chem. B 114 (6) (2010) 2175–2179.
[24] M. Jin, Y.C. Hou, W.Z. Wu, S.H. Ren, S.D. Tian, L. Xiao, Z.G. Lei, Solubilities and thermodynamic properties of SO_2 in ionic liquids, J. Phys. Chem. B 115 (2011) 6585–6591.
[25] M.B. Shiflett, M.A. Harmer, C.P. Junk, A. Yokozeki, Solubility and diffusivity of difluoromethane in room-temperature ionic liquids, J. Chem. Eng. Data 51 (2006) 483–495.
[26] M.B. Shiflett, A. Yokozeki, Solubility and diffusivity of hydrofluorocarbons in room-temperature ionic liquids, AIChE J. 52 (2006) 1205–1219.
[27] M.B. Shiflett, A. Yokozeki, Vapor-liquid-liquid equilibria of hydrofluorocarbons +1-butyl-3-methylimidazolium hexafluorophosphate, J. Chem. Eng. Data 51 (2006) 1931–1939.
[28] M.B. Shiflett, A.D. Shiflett, A. Yokozeki, Separation of tetrafluoroethylene and carbon dioxide using ionic liquids, Sep. Purif. Technol. 79 (2011) 357–364.
[29] A. Ortiz, A. Ruiz, D. Gorri, I. Ortiz, Room temperature ionic liquid with silver salt as efficient reaction media for propylene/propane separation: absorption equilibrium, Sep. Purif. Technol. 63 (2008) 311–318.
[30] A. Ortiz, L.M. Galan, D. Gorri, A.B. de Haan, I. Ortiz, Kinetics of reactive absorption of propylene in RTIL-Ag+ media, Sep. Purif. Technol. 73 (2010) 106–113.
[31] A. Ortiz, L.M. Galan, D. Gorri, A.B. de Haan, I. Ortiz, Reactive ionic liquid media for the separation of propylene/propane gaseous mixtures, Ind. Eng. Chem. Res. 49 (2010) 7227–7233.
[32] A. Yokozeki, M.B. Shifflet, Ammonia solubilities in room-temperature ionic liquids, Ind. Eng. Chem. Res. 46 (2007) 1605–1610.
[33] A. Yokozeki, M.B. Shifflet, Vapor–liquid equilibria of ammonia + ionic liquid mixtures, Appl. Energy 84 (2007) 1258–1273.
[34] J. Huang, A. Riisager, R.W. Berg, R. Fehrmann, Tuning ionic liquids for high gas solubility and reversible gas sorption, J. Mol. Catal. A 279 (2008) 170–176.
[35] G. Li, Q. Zhou, X. Zhang, L. Wang, S. Zhang, J. Li, Solubilities of ammonia in basic imidazolium ionic liquids, Fluid Phase Equilib. 297 (2010) 34–39.
[36] D. Schäfer, M.S. Vogt, J. Xia, A. Perez-Salado, G. Maurer, Experimental investigation of the solubility of ammonia in methanol, J. Chem. Eng. Data 52 (2007) 1653–1659.
[37] L. Huang, W. Xue, Z. Zeng, The solubility of ammonia in ethanol between 277.35 K and 328.15 K, Fluid Phase Equilib. 303 (2011) 80–84.
[38] J. Palomar, M. Gonzalez-Miquel, J. Bedia, F. Rodríguez, J.J. Rodríguez, Task-specific ionic liquids for ammonia efficient absorption, Sep. Purif. Technol. 82 (2011) 43–52.
[39] A. Klamt, F. Eckert, W. Arlt, COSMO-RS: an alternative to simulation for calculating thermodynamic properties of liquid mixtures, Annu. Rev. Chem. Biomed. Eng. 1 (2010) 101–122.
[40] M.B. Shiflett, A. Yokozeki, Solubilities and diffusivities of carbon dioxide in ionic liquids [bmim][PF6] and [bmim][BF4], Ind. Eng. Chem. Res. 44 (2005) 4453–4464.
[41] L.M. Galán Sánchez, G.W. Meindersma, A.B. de Haan, Kinetics of absorption of CO_2 in amino-functionalized ionic liquids, Chem. Eng. J. 166 (2011) 1104–1115.
[42] M.J. Frisch, G.W. Trucks, H.B. Schlegel, G.E. Scuseria, M.A. Robb, J.R. Cheeseman, J.A. Montgomery, T. Vreven, K.N. Kudin, J.C. Burant, J.M. Millam, S.S. Iyengar, J. Tomasi, V. Barone, B. Mennucci, M. Cossi, G. Scalmani, N. Rega, G.A. Petersson, H. Nakatsuji, M. Hada, M. Ehara, K. Toyota, R. Fukuda, J. Hasegawa, M. Ishida, T. Nakajima, Y. Honda, O. Kitao, H. Nakai, M. Klene, X. Li, J.E. Knox, H.P. Hratchian, J.B. Cross, V. Bakken, C. Adamo, J. Jaramillo, R. Gomperts, R.E. Stratmann, O. Yazyev, A.J. Austin, R. Cammi, C. Pomelli, J.W. Ochterski, P.Y. Ayala, K. Morokuma, G.A. Voth, P. Salvador, J.J. Dannenberg, V.G. Zakrzewski, S. Dapprich, A.D. Daniels, M.C. Strain, O. Farkas, D.K. Malick, A.D. Rabuck, K. Raghavachari, J.B. Foresman, J.V. Ortiz, Q. Cui, A.G. Baboul, S. Clifford, J. Cioslowski, B.B. Stefanov, G. Liu, A. Liashenko, P. Piskorz, I. Komaromi, R.L. Martin, D.J. Fox, T. Keith, M.A. Al-Laham, C.Y. Peng, A. Nanayakkara, M. Challacombe, P.M. Gill, B. Johnson, W. Chen, M.W. Wong, C. González, J.A. Pople, Gaussian03, revision B.05, Gaussian, Inc., Wallingford, CT, 2004.
[43] J. Palomar, V.R. Ferro, J.S. Torrecilla, F. Rodriguez, Density and molar volume predictions using COSMO-RS for ionic liquids: an approach to solvent design, Ind. Eng. Chem. Res. 46 (2007) 6041–6048.

[44] GmbH&CoKG, COSMOtherm C2.1 Release 01.08, Leverkusen, Germany, 2006. <http://www.cosmologic.de>.
[45] S. Zhang, X. Lu, Q. Zhou, X. Li, X. Zhang, S. Li, Ionic Liquids – Physicochemical Properties, Elsevier, Amsterdam, The Netherlands, 2009. pp. 72.
[46] C. Schreiner, S. Zugmann, R. Hartl, H.J.J. Gores, Fractional Walden rule for ionic liquids: examples from recent measurements and a critique of the so-called ideal KCl Line for the Walden plot chem, Eng. Data 55 (2010) 1784–1788.
[47] K.R. Seddon, A. Stark, M.-J. Torres, Viscosity and density of 1-alkyl-3-methylimidazolium ionic liquids, ACS Symp. Ser. 819 (2002) 34–49.
[48] H. Tokuda, S. Tsuzuki, M.A.B.H. Susan, K. Hayamizu, M. Watanabe, How ionic are room-temperature ionic liquids? An indicator of the physicochemical properties, J. Phys. Chem. B 110 (2006) 19593–19600.
[49] A. Arce, A. Soto, J. Ortega, G. Sabater, Viscosities and volumetric properties of binary and ternary mixtures of Tris(2-hydroxyethyl) methylammonium methylsulfate + water + ethanol at 298.15 K, J. Chem. Eng. Data 53 (2008) 770–775.
[50] G.V.S.M. Carrera, C.A.M. Alfonso, L.C. Branco, Interfacial properties, densities, and contact angles of task specific ionic liquids, J. Chem. Eng. Data 55 (2010) 609–615.
[51] T.K. Carlisle, J.E. Bara, C.J. Gabriel, R.D. Noble, D.L. Gin, Interpretation of CO_2 solubility and selectivity in nitrile-functionalized room-temperature ionic liquids using a group contribution approach, Ind. Eng. Chem. Res. 47 (2008) 7005–7012.
[52] M. Diedenhofen, A. Klamt, COSMO-RS as a tool for property prediction of IL mixtures – a review, Fluid Phase Equilib. 294 (2010) 31–38.
[53] J. Palomar, J.S. Torrecilla, V.R. Ferro, F. Rodríguez, Development of an a priori ionic liquid design tool 1: integration of a Novel COSMO-RS molecular descriptor on neural networks, Ind. Eng. Chem. Res. 47 (2008) 4523–4532.
[54] J. Palomar, J.S. Torrecilla, V.R. Ferro, F. Rodríguez, Development of an a priori ionic liquid design tool 2: ionic liquid selection through the prediction of COSMO-RS molecular descriptor by inverse neural network, Ind. Eng. Chem. Res. 48 (2009) 2257–2265.
[55] A. Klamt, Prediction of the mutual solubilities of hydrocarbons and water with COSMO-RS, Fluid Phase Equilib. 206 (2003) 223–235.
[56] J. Palomar, M. González-Miquel, A. Polo, F. Rodríguez, Understanding the physical absorption of CO_2 in ionic liquids using the COSMO-RS method, Ind. Eng. Chem. Res. 50 (2011) 3452–3463.
[57] M. González-Miquel, J. Palomar, S. Omar, F. Rodríguez, CO_2/N_2 selectivity prediction in supported ionic liquid membranes (SILMs) by COSMO-RS, Ind. Eng. Chem. Res. 50 (2011) 5739–5748.
[58] W. Shi, E.J. Maginn, Molecular simulation of ammonia absorption in the ionic liquid 1-ethyl-3-methylimidazolium bis(trifluoromethylsulfonyl)imide ([emim][Tf2N]), AIChE 55 (2009) 2414–2421.
[59] A. Navas, J. Ortega, R. Vreekamp, E. Marrero, J. Palomar, Experimental thermodynamic properties of 1-butyl-2-methylpyridinium tetrafluoroborate [b2mpy][BF4] with water and with alkan-1-ol and their interpretation with the COSMO-RS methodology, Ind. Eng. Chem. Res. 48–5 (2009) 2678–2690.
[60] P. Nockemann, K. Binnemans, B. Thijs, T.N. Parac-Vogt, K. Merz, A.-V. Mudring, P.C. Menon, R.N. Rajesh, G. Cordoyiannis, J. Thoen, J. Leys, C. Glorieux, Temperature-driven mixing-demixing behavior of binary mixtures of the ionic liquid choline, bis(trifluoromethylsulfonyl)imide and water, J. Phys. Chem. B 113 (2009) 1429–1437.
[61] J. Crank, The Mathematics of Diffusion, second ed., Oxford University Press, London, 1975.
[62] Y. Hou, R.E. Baltus, Experimental measurements of the solubility and diffusivity of CO_2 in room-temperature ionic liquids using a transient thin-liquid-film method, Ind. Eng. Chem. Res. 46 (2007) 8166–8175.

Publicación 8:

Gonzalez-Miquel, M.; Palomar, J.; Rodriguez, F. **Selection of ionic liquids for enhancing the gas solubility of volatile organic compounds.** *The Journal of Physical Chemistry B*, **2013**, *117*, 296−306.

THE JOURNAL OF PHYSICAL CHEMISTRY B

Article

pubs.acs.org/JPCB

Selection of Ionic Liquids for Enhancing the Gas Solubility of Volatile Organic Compounds

Maria Gonzalez-Miquel,[†] Jose Palomar,*[,‡] and Francisco Rodriguez[†]

[†]Departamento de Ingeniería Química, Universidad Complutense de Madrid, 28040 Madrid, Spain

[‡]Sección de Ingeniería Química (Departamento de Química Física Aplicada), Universidad Autónoma de Madrid, Cantoblanco, 28049 Madrid, Spain

Supporting Information

ABSTRACT: A systematic thermodynamic analysis has been carried out for selecting cations and anions to enhance the absorption of volatile organic compounds (VOCs) at low concentration in gaseous streams by ionic liquids (ILs), using COSMO-RS methodology. The predictability of computational procedure was validated by comparing experimental and COSMO-RS calculated Henry's law constant data over a sample of 125 gaseous solute−IL systems. For more than 2400 solute−IL mixtures evaluated, including 9 solutes and 270 ILs, it was found that the lower the activity coefficient at infinite dilution (γ^{∞}) of solutes in the ILs, the more the exothermic excess enthalpy (H^{E}) of the equimolar IL−solute mixtures. Then, the solubility of a representative sample of VOC solutes, with very different chemical nature, was screened in a wide number of ILs using COSMO-RS methodology by means of γ^{∞} and H^{E} parameters, establishing criteria to select the IL structures that promote favorable solute−solvent intermolecular interactions. As a result of this analysis, an attempt of classification of VOCs respect to their potential solubility in ILs was proposed, providing insights to rationally select the cationic and anionic species for a possible development of absorption treatments of VOC pollutants based on IL systems.

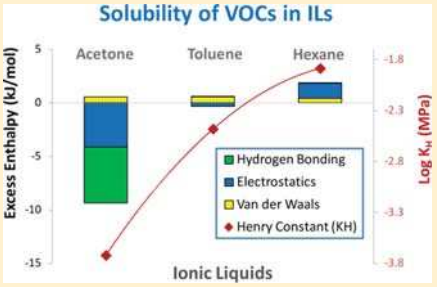

1. INTRODUCTION

Room-temperature ionic liquids (ILs) are a broad category of organic salts which have being receiving growing attention in both academia and industry during the past decade.[1−3] The unique properties of these novel solvents, such as their low vapor pressures and tailorability (i.e., the possibility of selecting/designing the adequate cations and anions to obtain a solvent with specific properties), have made them attractive for a wide variety of engineering applications.[4−7] In particular, the use of ILs as media in gas separation processes appears specially promising, to the effect that they are being broadly investigated as absorbents for a variety of gaseous compounds including CO_2,[8−16] H_2S,[17] H_2,[14,15,18−21] inert gases,[19,20,22,23] N_2,[10,11,19,20] O_2,[8,11,20] SO_2,[8,24] NH_3,[25,26] and VOCs such as alkanes,[8−12,19,20,23,27,28] alkenes,[8,9,11,12,27,28] hydrofluorocarbons,[29−31] dimethyl sulfide, dimethyl disulfide and toluene.[32,33]

Considering the huge variety of cation and anion combinations for possible ILs, computational methods to estimate thermodynamic properties have been demonstrated of great utility for preselecting the best cation−anion combinations for a specific IL application. At this point, COSMO-RS (Conductor-like Screening Model for Real Solvents) developed by Klamt and co-workers is regarded as a valuable method to predict the thermodynamic properties of ILs mixtures on the basis of unimolecular quantum chemical calculations for the individual molecules,[34,35] providing an a priori computational tool for designing ILs with the required properties.[36,37] In fact, several publications have shown the general suitability of COSMO-RS method to predict properties of IL systems, including the solubilities and Henry's law constants of several gases in ILs.[25,26,33,38−43] Moreover, an important feature is that the different intermolecular interactions (electrostatic forces, hydrogen bonding and van der Waals forces) between the mixture components can be quantified by COSMO-RS, contributing to the interpretation of gas solubility in ILs from a molecular point of view.[44] In our previous works, COSMO-RS was successfully used as a guide for driving a rational selection of ILs with upgraded features for several gas absorption applications.[25,26,33,40,41] An appreciable input for understanding the physical absorption of CO_2 and the CO_2/N_2 selectivity in ILs was reported on the basis of an energetic analysis performed for the excess enthalpies and the intermolecular interactions of the solute−IL mixtures, with results leading to propose novel brominated-based ILs with optimized characteristics for CO_2 capture[40] and $[SCN^-]$-based ILs to be applied as solvents in supported ionic liquid membranes (SILMS) for CO_2/N_2 separation processes.[41] In addition, an innovative computational−experimental research

Received: October 23, 2012
Revised: December 13, 2012
Published: December 13, 2012

strategy was developed to propose optimized ILs for gas absorption, including novel task-specific ILs such as [EtOHmim][BF_4] and [choline][NTf_2] for ammonia absorption,[25,26] and commercially available imidazolium-[NTf_2] ILs for toluene absorption,[33] with experimental evidences supporting the favorable thermodynamic and kinetic performance of the selected solvents.

Volatile organic compounds (VOCs) are well-known as common air pollutants characterized by their high vapor pressures and low boiling points.[45] Recovery of VOCs from industrial atmospheric emissions has become a great challenge in the last decades, prompted by specific international legislations[46,47] which limit the concentration for VOCs emissions into atmosphere. In this regard, the development of novel absorption techniques based on ILs is being considered as a potential alternative to efficiently recover VOCs, overcoming the disadvantages (i.e., high volatily, toxicity and flammability) of the organic solvents used in conventional absorption processes.

Under this scenario, the aim of this paper is to serve as a guide for selecting cations and anions to form IL structures with optimized properties to enhance the gas solubility of VOCs at low concentrations. For this purpose, a systematic theoretical analysis of the solute−ILs thermodynamics and energetic interactions was carried out by applying COSMO-RS methodology, which involved the following steps:

(i) Evaluating the capability of COSMO-RS to predict the solubility behavior of different solutes in ILs: the experimental versus the computed values of the Henry's law constants of more than 125 solute−IL systems were compared.

(ii) Analyzing the relationship between the activity coefficient at infinite dilution (γ^{∞}) of solutes in ILs and the excess enthalpy (H^E) of the equimolar IL−solute mixtures: the activity coefficients (γ^{∞}) of more than 2400 solute−IL mixtures, including 9 solutes (acetone, benzene, chloroform, ethane, ethene, phenol, H_2S, H_2 and trifluoroethane) and 270 ILs (considering 15 anions of diverse nature and 18 cations from different families, see Table 1) were computed by COSMO-RS and related with the excess enthalpy (H^E) of the liquid mixtures, in order to compare the affinity of ILs for solutes with very different vapor pressure.

(iii) Classification of the gaseous compounds attending to both the volatility of the solutes and their activity coefficients in ILs: from the analysis of the computed and reported experimental data, different cases regarding gaseous compounds were detected, ranging from aliphatic compounds, which showed high positive deviations from Raoult's law (low solubility in ILs) to polar organic solutes, which presented remarkably negative deviations from ideality (high solubility in ILs).

(iv) Systematic gas solubility and energetic COSMO-RS analysis of the solute−IL systems focused on three common indoor VOC solutes,[48] i.e. acetone, phenol, and chloroform: first, the chemical nature of the gases and the IL solvents was analyzed by means of the polarized charge distributions on the molecular surfaces provided by COSMO-RS. Then, COSMO-RS screenings of the Henry's law constants of the selected solutes in 270 representative ILs were carried out to obtain an overall picture of the gas solubility behavior of the systems. Afterward, the contributions of the intermolecular interactions (misfit-electrostatic, hydrogen bonding, and van der Waals) to the excess enthalpy of the IL−solute mixture were analyzed to determine their effects on the physical solubility of these VOCs in the ILs.

(v) Providing a general evaluation of the influence of the IL structure on the solubility of a representative sample of VOCs: the COSMO-RS screening was extended to analyze the activity coefficients and intermolecular interactions of 14 VOC solutes with different chemical nature in ILs, selecting those cations and anions that provided, respectively, the highest negative and positive deviations from the ideality and, consequently, the potentially most favorable and unfavorable properties to absorb VOCs.

Table 1. List of Ionic Liquids

abbreviation	name
	Cations
eim^+	1-ethylimidazolium
$emim^+$	1-ethyl-3-methylimidazolium
$emmim^+$	1-ethyl-2,3-dimethylimidazolium
OH-$emim^+$	1-(2-hydroxyethyl)-3-methylimidazolium
meO-$emim^+$	1-(2-methoxypropyl)-3-methylimidazolium
ph-$emim^+$	1-(phenylethyl)-3-methylimidazolium
$bmim^+$	1-butyl-3-methylimidazolium
$hxmim^+$	1-hexyl-3-methylimidazolium
$omim^+$	1-octyl-3-methylimidazolium
$dcmim^+$	1-decyl-3- methylimidazolium
bpy^+	1-butylpyridinium
1b3mpy^+	1-butyl-1-methylpyridinium
$bmpyr^+$	1-butyl-1-methylpyrrolidinium
$bpyr^+$	1-butylpyrrolidinium
1b4DMApy^+	1-butyl-4-(dimethylamino)pyridinium
b-M^+	1-butylmorpholinium
b-Q^+	1-butylquinolinium
bbbb-P^+	tetrabutylphosphonium
bbbb-N^+	tetrabutylammonium
$choline^+$	(2-hydroxyethyl)trimethylammonium
	Anions
BF_4^-	tetrafluoroborate
$FeCl_4^-$	tetrachloroferrate
$CF_3CO_2^-$	trifluoroacetate
$CF_3SO_3^-$	trifluorosulfonate
$CH_3CO_2^-$	acetate
SCN^-	methanesulfonate
$C_4H_{10}PO_4^-$	diethylphosphate
$formate^-$	formate
DCN^-	dicyanamide
FEP^-	tris(pentafluoroethyl)trifluorophosphate
NO_3^-	nitrate
$BC_4N_4^-$	tetracyanoborate
PF_6^-	hexafluorophosphate
$C(CN)_3^-$	methanetricarbonitrile
NTf_2^-	bis(trifluoromethylsulfonyl)imide

2. COMPUTATIONAL METHODOLOGY

The molecular geometry of all compounds (solutes and ILs counterions) was optimized at the B3LYP/6-31++G** computational level in the ideal gas phase using the quantum chemical Gaussian 03 package.[49] A molecular model of independent counterions was applied in COSMO-RS calculation, where ILs are treated as equimolar mixture of cation and anion.[40] Vibrational frequency calculations were performed in each case to confirm the presence of an energy minimum. Once molecular models were optimized, Gaussian03 was used to

dx.doi.org/10.1021/jp310499p | J. Phys. Chem. B 2013, 117, 296−306

compute the COSMO files. The ideal screening charges on the molecular surface for each species were calculated by the continuum solvation COSMO model using BVP86/TZVP/DGA1 level of theory. Subsequently, COSMO files were used as an input in COSMOthermX[50] code to calculate the thermodynamic properties (Henry's law constants and activity coefficients of solutes in ILs, and detailed excess enthalpies contributions of solute–IL mixtures) and to compute the σ-profiles of the compounds. According to our chosen quantum method, the functional and the basis set, we used the corresponding parametrization (BP_TZVP_ C21_0111) that is required for the calculation of physicochemical data and that contains intrinsic parameters of COSMOtherm, as well as specific parameters.

Alternatively, Henry's law constants can be determined from the COSMO-RS calculations using the semiempirical Antoine equation to estimate the vapor pressure in the expression:

$$K_H = \gamma_i^{\infty} p_0^{vap} \quad (1)$$

where K_H is the Henry's law constant, γ_i^{∞} is the activity coefficient of the solute at infinite dilution in the IL calculated by COSMOthermX, and p_0^{vap} is the vapor pressure of the pure gas, estimated by either COSMOthermX or the Antoine equation (obtained from NIST database).

3. RESULTS

3.1. Gas Solubilities in ILs from COSMO-RS Analysis.

The capability of COSMO-RS to predict the solubility behavior of different solutes in ILs was evaluated by comparing the experimentally available Henry constants ($K_{H,experimental}$) to the computed Henry constants ($K_{H,COSMO\text{-}RS}$) of more than 125 solute–IL systems,[8–33] including 27 solutes and 24 ILs, with a wide variety of cations and anions. The comparisons include compounds of very different nature such as inert gases, aromatics, alkanes, and alkenes, or gases like CO_2, SO_2, or H_2S, which present a wide range of Henry constant values (i.e., from 0.005 MPa for toluene in [dcmim][NTf_2] to 602.6 MPa for H_2 in [bmim][CH_3SO_4]) at near room temperature and atmospheric pressure. Based on results of Figure 1, it is concluded that a priori COSMO-RS method provides reasonably predictions of the solubility behaviors of gas solutes in ILs for the whole range of K_H values reported in the literature, as indicated by the goodness-of-fit between the experimental and the computed data in Figure 1A (slope = 1.09, square correlation coefficient R^2 = 0.88, and standard deviation σ = 0.88). Note that the vapor pressures used to perform the Henry constant calculations in Figure 1A were those estimated by COSMO-RS methodology. Meanwhile, Figure 1B shows the comparison between the experimental and the computed K_H values of the systems when implementing the empirical Antoine equation to calculate the vapor pressure of the solutes. The statistical parameters (slope = 0.93, R^2 = 0.89, and σ = 0.85) show a slightly enhanced agreement between the predicted and the experimental values of the Henry constants of the solutes in the ILs. In general, implementing empirical equations to determine the vapor pressure of the solutes instead of using the vapor pressure estimated by COSMO-RS methodology in Version C2.1 Release 01.11 of COSMO*therm* does not lead to significant changes in the overall data predictions. However, it might be appropriate to consider the empirical vapor pressure of specific solutes such as CO_2 or H_2S, whose values are not well estimated by the used version of

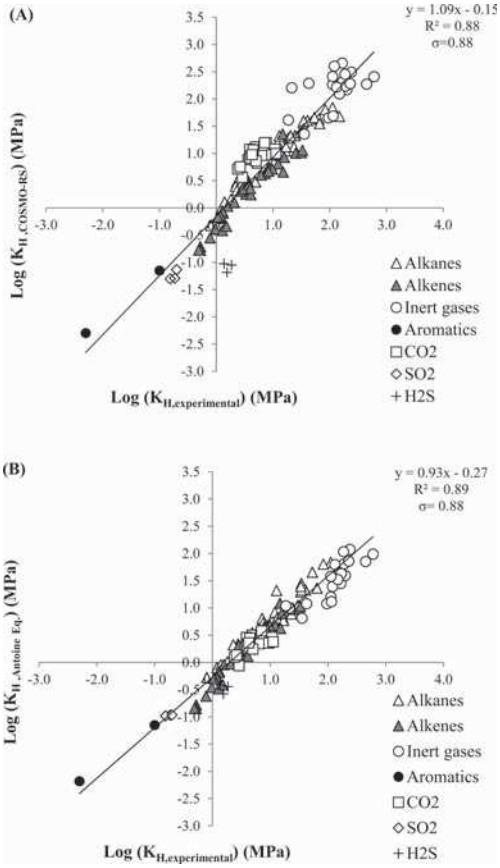

Figure 1. Experimental vs COSMO-RS Henry constants of solutes in ILs at near-ambient temperature and atmospheric pressure using vapor pressures of pure compounds (A) predicted by COSMO-RS and (B) estimated by empirical Antoine equation.

COSMO-RS method, hence providing some discrepancies between the experimental and the estimated solubility behavior of the solutes. For instance, an overestimation of the CO_2 vapor pressure ($P_{vap,COSMO\text{-}RS}$ = 29 794.3 kPa versus $P_{vap,empirical}$ = 7186.5 KPa) leads to estimated Henry constant values 2-fold higher than the experimentals (i.e., $K_{H,COSMO\text{-}RS}$ = 15.9 MPa versus $K_{H,exptl}$ = 7.6 MPa for CO_2 in [bmim][BF_4]); on the contrary, the underestimation of the H_2S vapor pressure ($P_{vap,COSMO\text{-}RS}$ = 501.14 kPa versus $P_{vap,empirical}$ = 7186.5 KPa) leads to lowering the estimated Henry constant values (i.e., $K_{H,COSMO\text{-}RS}$ = 1.55 MPa versus $K_{H,exptl}$ = 0.07 MPa for H_2S in [bmim][BF_4]).

Previous studies by our group evidenced relationships between the Henry constants of the gas solutes in the ILs and the excess enthalpy (H^E) of the IL–solute liquid mixture for the cases of CO_2, N_2, NH_3, and toluene compounds,[25,26,33,40,41] with results illustrating that the higher the exothermicity of the mixture (or the stronger intermolecular interactions between the solute and the solvent), the higher the

dx.doi.org/10.1021/jp310499p | J. Phys. Chem. B 2013, 117, 296–306

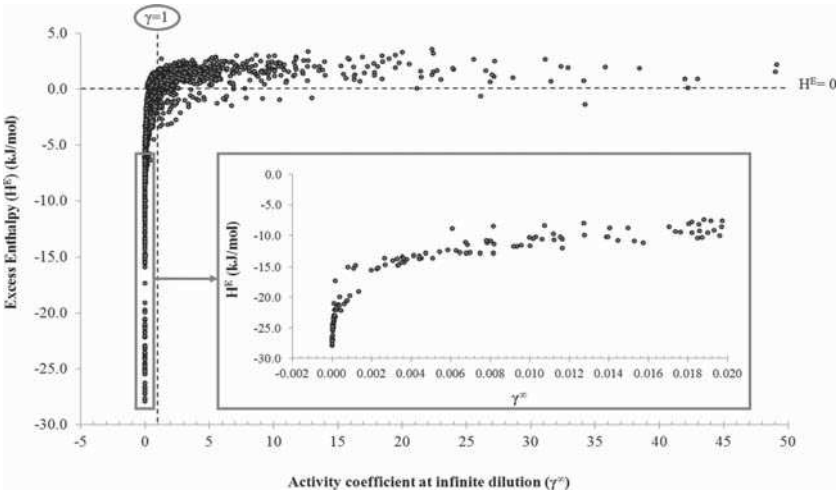

Figure 2. Relationship between the excess enthalpies (H^E) of IL–solute equimolar mixtures and the activity coefficients at infinite dilution (γ^∞) of solutes in ILs (T = 298 K, P = 1 bar).

Table 2. Classification of Gaseous Solutes in Terms of Their Solubilities in ILs

	phase at 298 K and 1 atm			
	condensed		gaseous	
favorable interactions [AM(γ^∞) < 1]	1	acetone, phenol, chloroform	2	alkanes (C < 2), alkenes (C < 2) fluoroalkanes, fluoroalkenes (C < 2) CO_2, SO_2, NH_3, H_2S, H_2
unfavorable interactions [AM(γ^∞) > 1]	3	toluene, benzene	4	alkanes (4 > C > 2), alkenes (4 > C > 2) Ar, N_2, Xe, O_2

solubility of the solute in the IL (this is the lower Henry constant values). In this work, the activity coefficient at infinite dilution (γ^∞) of more than 2400 solute–IL mixtures, including 9 solutes (acetone, benzene, chloroform, ethane, ethane, phenol, H_2S, H_2, and trifluoroethane) and 270 ILs, were related to the excess enthalpy of the IL–solute mixtures, both computed by COSMO-RS (Figure 2). Considering the activity coefficients instead of the Henry constants allows leaving aside the effect of the very different vapor pressure of the 9 pure solute compounds studied. The screening included ILs based on different cation families (imidazolium, pyridinium, pyrrolidinium, phosphonium, ammonium, quinolinium, and morpholinium) and a wide variety of anions ([FEP$^-$], [NTf_2^-], [$FeCl_4^-$], [$CF_3SO_3^-$], [$CF_3CO_2^-$], [$B(CN)_4^-$], [NO_3^-], [$CH_3CO_2^-$],[$CH_3PO_4^-$], [$C(CN)_3^-$], [DCN$^-$], [BF_4^-], [SCN^-], [PF_6^-], and [$CHOO^-$], see Table 1). In Figure 2, two different areas can be distinguished based on the activity coefficient values: the one corresponding to negative deviation from Raoult's law (γ^∞ < 1) and the other corresponding to positive deviation from Raoult's law (γ^∞ > 1). It can be seen that the solutes–IL systems presenting activity coefficients γ^∞ < 1 are related to an exothermic behavior of the liquid mixture, where the attractive forces between molecules of solute and IL are greater than the solute–solute or IL–IL cohesive forces. In these cases, the partial vapor pressure of the solute component in the mixture is lower than that expected from Raoult's law, implying an enhanced solubility of the gas solute in the IL solvent because of their mutual chemical affinity. In fact, it can be appreciated in the enlarged area of Figure 2 that the higher the exothermicity of the liquid mixture, the lower the activity coefficient of the solute in the solvent, related to the more favorable intermolecular interactions between IL and solute respect to the pure compounds. These results suggest that the systems showing negative deviations from Raoult's law involve solutes which can be better absorbed by ILs. On the contrary, those solute–IL systems setting along the area corresponding to γ^∞ > 1 present an excess enthalpy of the mixture around zero value, which implies no particular affinity between the molecules of the solute and the IL solvent; these systems present a partial vapor pressure of the solute higher than that of the pure compound and, consequently, a lower absorption capacity of the solutes in the ILs.

The trends explained above suggest the possibility of classifying the different solubility behaviors of the gases in the ILs attending to the volatility of the solutes and their activity coefficients in ILs. An attempt at classifying the solutes included in Figure 1 (whose gas solubility behavior has been experimentally measured in bibliography) is presented in Table 2, attending to both the γ^∞ values of each one of the solutes in ILs (either those reported in bibliography or those calculated by COSMO-RS in 270 ILs) and the phase state of the compounds at 298 K and 1 atm. These criteria lead to differentiate four groups of solutes. (i) Group 1, those with low volatility (which are in condensed phase at 298 K and 1 atm) showing attractive interactions with ILs [i.e., AM (γ^∞) < 1, where AM stands for the arithmetic mean]. The solutes of this group correspond to VOCs functionalized with strong polar compounds, as acetone, chloroform, and phenol. They present

dx.doi.org/10.1021/jp310499p | J. Phys. Chem. B 2013, 117, 296–306

Table 3. VOCs–ILs Systems Exhibiting (A) Minimum and (B) Maximum Values of Activity Coefficients at Infinite Dilution (γ^{∞}) and Henry Constants (K_H) Provided by COSMO-RS Screening over 135 Imidazolium-Based ILs at 298 K[a]

		(A) Potential Highest Gas Solubility			
VOC		best absorbent	γ^{∞} (min)	K_H (MPa)	main VOC–IL interactions[b]
favorable absorption	phenol	[emmim][acetate]	2.3×10^{-5}	4.3×10^{-9}	HB (f)
	acetone	[eim][FEP]	0.01	1.9×10^{-4}	HB (f) > MF (f)
	ethyl acetate	[eim][FEP]	0.02	1.4×10^{-4}	HB (f) > MF (f)
	chloroform	[emmim][acetate]	0.02	5.0×10^{-4}	HB (f) > MF (f)
	CH_2Cl_2	[emmim][acetate]	0.04	1.7×10^{-3}	MF (f) > HB (f)
moderate absorption	tetrafluoroethane	[omim][acetate]	0.27	1.6×10^{-1}	HB (f) > MF (f) > VDW (u)
	ethene	[omim][FEP]	0.48	2.9	VDW (u) ≫ MF (f)
	ethane	[omim][FEP]	0.73	6.0	MF (u) ≫ VDW (u)
	toluene	[omim][FEP]	0.77	3.3×10^{-3}	VDW (u) ≫ MF (f)
	benzene	[omim][FEP]	0.77	1.3×10^{-2}	VDW (u) ≫ MF (f)
unfavorable absorption	hexafluoroethane	[omim][FEP]	1.49	2.2	MF (u) ≫ VDW (u)
	CCl_4	[omim][FEP]	1.59	6.0	MF (u) > VDW (u)
	hexane	[omim][FEP]	1.83	1.0×10^{-1}	MF (u) ≫ VDW (u)
	octane	[omim][FEP]	2.69	1.3×10^{-2}	MF (u) ≫ VDW (u)
		(B) Potential Lowest Gas Solubility			
VOC		worst absorbent	γ^{∞} (max)	K_H (MPa)	main VOC–IL interactions[b]
favorable absorption	phenol	[eim][FEP]	0.98	1.9 × 10−4	HB (u) > MF (f) ≈ VDW (u)
	acetone	[eim][Acetate]	2.05	3.7 × 10−2	HB (u) > MF (f)
	ethyl acetate	[eim][Acetate]	3.88	3.0 × 10−2	HB (u) > MF (f)
	chloroform	[eim][FEP]	1.29	2.8 × 10−2	VDW (u) ≫ MF (u)
	CH_2Cl_2	[eim][FEP]	0.72	3.4 × 10−2	VDW (u)
moderate absorption	tetrafluoroethane	[eim][FEP]	0.53	0.31	MF(u) > HB(u) ≈ VDW(u)
	ethene	[emim][DCN]	2.07	12.6	MF (u) > HB (u)
	ethane	[emim][DCN]	5.71	46.7	MF (u) > HB (u)
	toluene	[emim][DCN]	8.59	3.6 × 10−2	MF (u) > HB (u)
	benzene	[emim][DCN]	4.96	8.3 × 10−2	MF (u) > HB (u)
unfavorable absorption	hexafluoroethane	[emim][DCN]	263.04	395.0	MF (u) ≫ VDW (u)
	CCl_4	[emim][DCN]	34.31	0.4	MF (u) ≫ VDW (u)
	hexane	[emim][DCN]	109.29	6.1	MF (u) ≫ VDW (u)
	octane	[emim][DCN]	436.26	2.2	MF (u) ≫ VDW (u)

[a]Description of main VOC–IL intermolecular contributions obtained from the excess enthalpy of equimolar mixtures. [b]HB: Hydrogen bond; MF: polar-misfit; VDW: van der Waals. (f): favorable interactions; and (u): unfavorable interactions.

the lowest range of Henry constants in the ILs (always less than 0.1 MPa for all of the 270 ILs). (ii) Group 2: gaseous solutes at 298 K and 1 atm showing effective interactions with ILs [i.e., AM (γ^{∞}) < 1] such as short-chain alkanes and alkenes, or some gases like CO_2, SO_2, H_2, H_2S, and NH_3, which in general present Henry constants not higher than 50 MPa. (iii) Group 3: liquid solutes at 298 K and 1 atm showing unfavorable interactions with ILs [i.e., AM (γ^{∞}) > 1], such as the aromatic compounds benzene or toluene, which present Henry constants lower than 1 MPa. And (iv) Group 4: gaseous solutes which show unfavorable interactions with ILs [i.e., AM (γ^{∞}) > 1], such as inert gases (Ar, Xe, N_2) or other gaseous compounds such as O_2, which generally present Henry constants higher than 50 MPa. In summary, Table 2 exposes a wide range of gas solubility behaviors for VOCs in ILs, mainly depending on the chemical nature of the organic compounds and their structural features. In view of this, a deeper understanding of the IL–solute systems would be of great help for propounding effective industrial applications based on ILs to separate VOCs from gas streams. For this purpose, in this work the COSMO-RS computational analysis was first focused on three common indoor VOCs classified as group 1 in Table 2: acetone, phenol, and chloroform, which potentially present a favorable absorption in ILs. Later, the COSMO-RS analysis was extended to a representative sample of 14 organic compounds (see Table 3) from different nature in order to evaluate the overall trends of the solubility of VOCs in ILs.

3.2. Gas Solubility of Acetone in ILs. The COSMO-RS screening of the Henry constants of acetone in 270 ILs, including 18 cations based on different families and 15 different anions, is presented in Figure 3. The overall K_H values of acetone in the ILs are lower than 0.02 MPa, which indicates a general high gas solubility of this solute in ILs. Moreover, this screening shows that the solubility of acetone in ILs is mainly influenced by both the cation and the anion, with the value of the Henry constant of the solute differing by more than 1 order of magnitude depending on the ions of the solvents. Thus, cations that present functional groups with acidic character as hydroxyl (i.e., [OH-emim$^+$] or [choline$^+$]) and big anions with disperse charge (i.e., [FEP$^-$] or [NTf$_2^-$]) seem capable to provide much higher solubilities (lower Henry constants) of acetone in the IL solvent.

COSMO-RS method calculates the thermodynamic properties of fluid mixtures by using the polarized charge distribution of their individual compounds visualized as histogram σ-profiles.[14] Therefore, based on COSMO-RS methodology, the σ-profile of one compound includes the main chemical information necessary to predict its possible interaction in a fluid phase. The COSMO-RS histogram can be qualitatively divided into three main regions upon the following cutoff

dx.doi.org/10.1021/jp310499p | J. Phys. Chem. B 2013, 117, 296–306

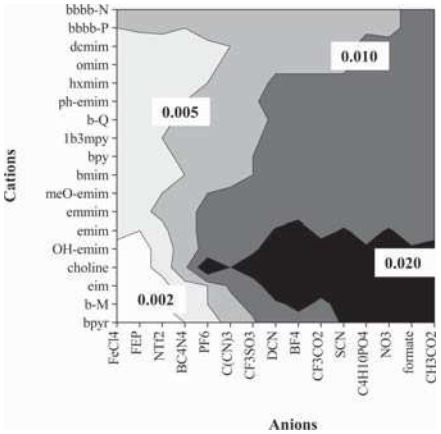

Figure 3. Screening of the Henry constants (MPa) of acetone in ILs at T = 298 K computed by COSMO-RS.

values: the hydrogen bond (HB) donor region ($\sigma < -0.0082$ e/Å^2), the HB acceptor region ($\sigma > +0.0082$ e/Å^2) and the nonpolar region ($-0.0082 < \sigma < +0.0082$ e/Å^2). An overview over the properties and usage of σ-profile can be found in refs 51 and 52. Figure 4A shows the σ-profile of the acetone solute, which presents a peak at +0.012 e/Å^2 resulting from the carbonyl oxygen that indicates HB acceptor capacity of the compound. On the contrary, the absence of a prominent peak in the region $\sigma < -0.0082$ e/Å^2 of the σ-profile of the acetone indicates that the solute does not show HB donor capacity. In addition, the broad distribution of charge on the σ polarity scale of Figure 4A represents the remarkably polar character of the acetone molecule. Therefore, from the analysis of the σ-profile of the acetone, it can be foreseen that ILs with HB donor groups (acidic character) might enhance its solubility. This premise leads to think about [eim$^+$] cation as an appropriate structure for enhancing the solubility of acetone because of the acidic character of N−H group, which is represented in the σ-profile of the cation in Figure 4B by a noticeable concentration of charge at the strong HB donor region (−0.21 e/Å^2). In fact, the acidic character of the imidazolium cations decreases with the increasing number of alkyl substituents attached to the imidazolium ring in the following order: [eim$^+$] > [emim$^+$] > [emmim$^+$], as clearly shown by their σ-profiles in Figure 4B. An alternative to confer acidic character to an imidazolium cation is its functionalization with hydroxyl group (see the case of [OH-emim$^+$] in Figure 4B). On other hand, anions are generally not able to establish hydrogen-bonding interactions with HB acceptor groups as acetone. However, Figure 4C shows that anions such as [$CH_3CO_2^-$] can present groups with located charge at positive σ region and, therein, basic character. Therefore, HB acceptor anions may promote anion−cation hydrogen bonding which would compete with acetone−cation interactions. On the contrary, big anions with disperse charge such as [FEP$^-$] are not strong HB acceptor species, which may allow enhancing the acetone solubility in the ILs based on this kind of anions. Once we analyzed the chemical nature of individual species in acetone−IL mixtures, the next step of COSMO-RS analysis was to relate the acetone solubility in ILs to the different intermolecular interactions contributing to the

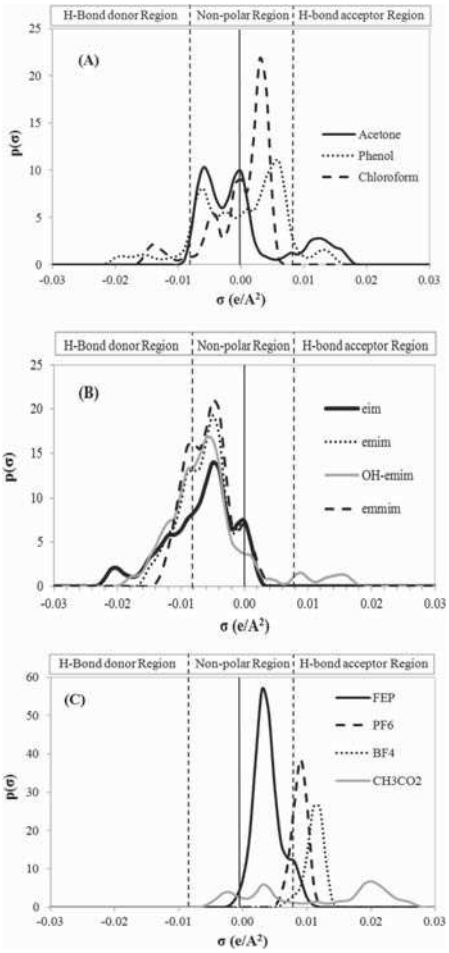

Figure 4. σ-Profiles of (A) VOC solutes, (B) IL cations, and (C) IL anions.

excess enthalpy of the acetone−IL equimolar mixtures. Figure 5 presents the relationship between K_H and H_E values for representative IL−acetone mixtures, showing the effect of the anion and the cation by the analysis, respectively, of IL common anion (Figure 5A) and cation (Figure 5B) series. Results indicated that the attractive hydrogen-bonding interactions (exothermic mixing process; i.e. negative values of H_E) between acetone and IL determine the increasing solubility of acetone in these solvents (decreasing K_H values). Meanwhile, the attractive electrostatic interactions (Misfit) between the polar solute and the polar solvents play a secondary role, and the van der Waals interactions make almost negligible contributions to the excess enthalpies of these systems. These results support that ions capable of increasing the solubility of acetone in ILs are those able to establish attractive hydrogen bonds in the mixture with acetone. Indeed, a further glance at the effect of the cation in Figure 5A

dx.doi.org/10.1021/jp310499p | J. Phys. Chem. B 2013, 117, 296−306

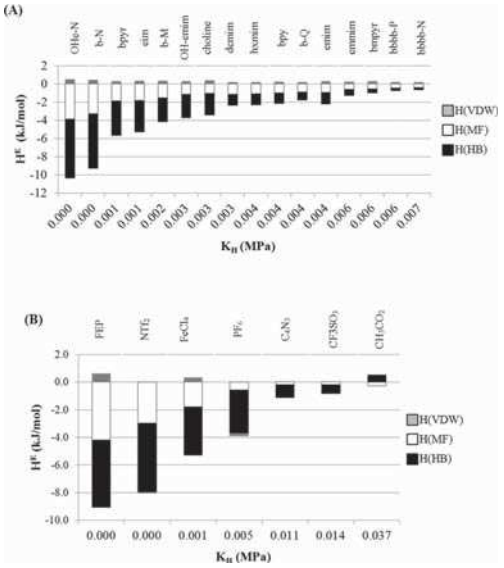

Figure 5. Relationship between the Henry constants (K_H) and the different intermolecular interaction contributions to the excess enthalpy [H(VDW), H(HB), and H(MF)] of acetone–IL systems at T = 298 K computed by COSMO-RS. (A) Effect of the cation considering NTf_2 as the common anion. (B) Effect of the anion considering eim as the common cation.

illustrates that for IL with common anion [NTf_2^-] the more the acidic groups in the cation ([eim^+] > [$emim^+$] > [$emmim^+$]), the higher the solubility of this solute in ILs. In addition, those cations functionalized with acidic groups, such as OH^- or NH^-, significantly enhance the acetone solubility in ILs in relation to their nonfunctionalized analogues. It can be seen that cationic family does not have a significant impact on the solubility of the acetone in the ILs. On the other hand, if one considers a series of ILs with common cation ([eim^+] in Figure 5B) it is clear that big anions with disperse charge, such as [FEP^-] and [NTf_2^-], allow for better HB interaction between the solute and the cation, resulting in higher solubilities of acetone in ILs; this is the opposite of what happens with anions that present located charge and strong basic groups, such as [$CH_3CO_2^-$] or [$CF_3SO_3^-$], which tend to interact with the cation, hence hindering the effective interaction between the acetone and the ILs.

3.3. Gas Solubility of Phenol in ILs. Figure 6 shows the screening of the Henry constants of phenol in ILs computed by COSMO-RS. The extremely low K_H values of phenol in the ILs suggest the high capacity of this kind of solvents to absorb the phenol solute. As it is represented in Figure 6, the solubility of phenol in ILs is clearly controlled by the anions, whose adequate selection allows decreasing 2 orders of magnitude the K_H values. The solubility of phenol is enhanced by those anions presenting basic character, such as [$CH_3CO_2^-$], formate, or [$CF_3CO_2^-$] anions, and only slightly improved by cations without acidic hydrogen atoms like [bbbb-N^+] or [$emmim^+$]. This behavior can be attributed to the HB donor character of the solute molecule, as supported by the σ-profile of phenol in Figure 4A which presents a peak at −0.016 e/Å^2, assignable to

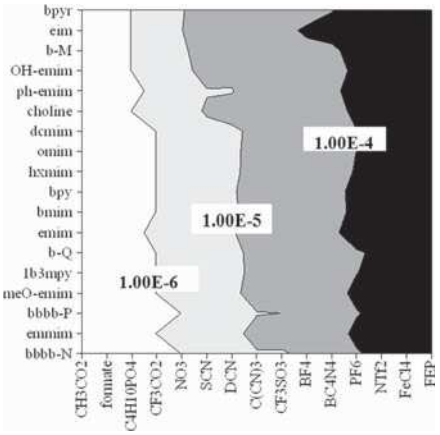

Figure 6. Screening of the Henry constants (MPa) of phenol in ILs at T = 298 K computed by COSMO-RS.

the strong acidic hydrogen atom of the hydroxyl group of phenol. The relationship between the solubility of phenol in ILs (in terms of Henry constant) and the intermolecular interaction contributions to the excess enthalpy of the liquid mixture is depicted in Figure 7. This figure shows that exothermic HB contributions to the H_E of phenol–IL mixing process are related to decreasing Henry constants of this solute in the IL solvents. It indicates that the affinity between the acidic OH group of the solute and the HB acceptor groups of anions is controlling the solubility of the phenol in the ILs. This is the case of the acetate and formate anions, whose basic carboxyl groups are capable to effectively interact by HB formation with the hydroxyl group of the phenol. Note that the head family does not have a significant impact on the phenol solubility, although cations without acidic hydrogen atoms (like [bbbb-N^+] or [$emmim^+$]), and cation families with less HB donor character (i.e., imidazolium, ammonium, or posphonium rather than pyrrolidinim or morpholinium), slightly enhance the solubility of phenol in ILs. In sum, the selection of the anion is critical to boost the phenol absorption in ILs, since the anion plays the main role in establishing effective hydrogen-bonding interactions with this solute.

3.4. Gas Solubility of Chloroform in ILs. The COSMO-RS screening of the Henry constants of chloroform in ILs is presented in Figure 8. The K_H values of this solute in the sample of 270 ILs cover the range from 0.00 to 1.20 MPa (depending on the selection of the cation and anion), indicating the remarkable solubility of chloroform in the IL solvents. As for the case of the acetone, the solubility of chloroform in ILs is determined by both the cation and the anion. The σ-profile of chloroform (Figure 4A) shows three peaks in the nonpolar region corresponding to the carbon and chlorine atoms. However, the small peak located at the HB donor region (−0.014 e/Å^2) of the σ-profile, which is associated to the hydrogen atom, indicates a slightly acidic character and polarity of this solute. As shown in the screening (Figure 8), the solubility of chloroform is enhanced by ILs with the highest HB acceptor character, like those containing anions such as [$CH_3CO_2^-$], whereas a big anion with disperse charge as [FEP^-] or [NTf_2^-] does not promote favorable solute–IL

dx.doi.org/10.1021/jp310499p | J. Phys. Chem. B 2013, 117, 296–306

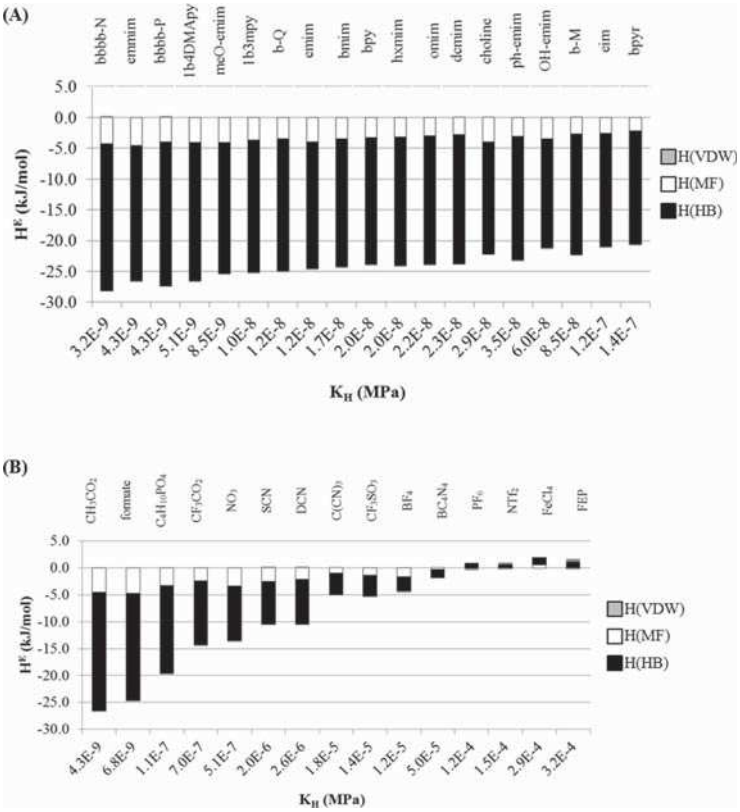

Figure 7. Relationship between the Henry constants (K_H) and the different intermolecular interaction contributions to the excess enthalpy [H(VDW), H(HB), and H(MF)] of phenol−IL systems at T = 298 K computed by COSMO-RS. (A) Effect of the cation considering CH_3CO_2 as the common anion. (B) Effect of the anion considering emmim as the common cation.

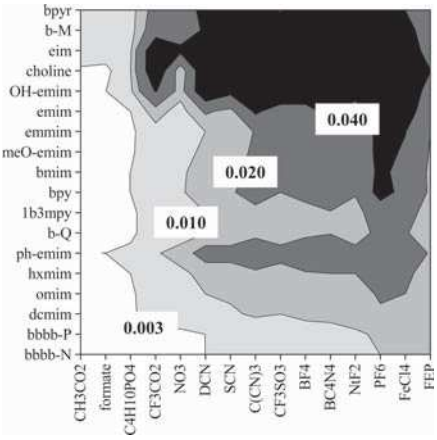

Figure 8. Screening of the Henry constants (MPa) of chloroform in ILs at T = 298 K computed by COSMO-RS.

intermolecular interactions. The selection of cations in the absence of strong HB donor groups, i.e., [emmim$^+$], [bbbb-P$^+$], or [bbbb-N$^+$], also increases the absorption, mainly for the case of anions with intermediate HB acceptor character, such [$CF_3SO_3^-$]. Figure 9 shows the relationship between the Henry constants and the different contributions to the excess enthalpy of the chloroform−ILs mixtures. As for the case of the acetone, the results indicate that the attractive hydrogen-bonding interactions determine the solubility between the solute and the solvent, while the electrostatic interactions play a secondary role, and the van der Waals interactions almost do not contribute to the excess enthalpy of the liquid mixture. However, in the case of the chloroform solute, the attractive hydrogen-bonding interactions which control the solubility are those between the acidic hydrogen atom of chloroform and the basic groups of the ions of the IL solvents. Figure 9A illustrates the higher affinity of the solute for the least acidic cations, as in the case of [emmim$^+$] > [emim$^+$] > [eim$^+$]; the length of the alkyl chain does not cause noticeable change of the hydrogen-bonding attraction as exemplified by the imidazolium series from [emim$^+$] to [dcmim$^+$]; as for the head family, results suggest that imidazolium, ammonium, and phophonium work better than pyridinium-, pyrrolidinium-, or morpholinium-

dx.doi.org/10.1021/jp310499p | J. Phys. Chem. B 2013, 117, 296−306

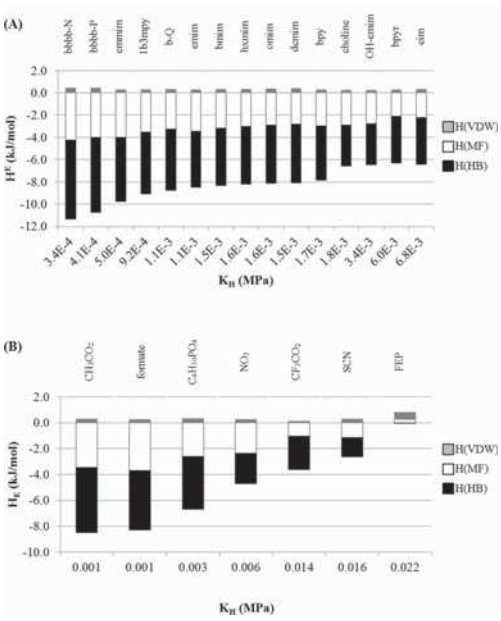

Figure 9. Relationship between the Henry constants (K_H) and the different intermolecular interaction contributions to the excess enthalpy [H(VDW), H(HB), and H(MF)] of chloroform–IL systems at T = 298 K computed by COSMO-RS. (A) Effect of the cation considering CH_3CO_2 as the common anion. (B) Effect of the anion considering emim as the common cation.

based cations. This is most likely because the latter tends to present more acidic character than the former, hence promoting hydrogen bonding between the cation and the anion in detriment of chloroform–anion interactions (see Table 3). As for the effect of the anion, Figure 9B shows the significantly higher affinity of the chloroform for the most basic ions, such as [$CH_3CO_2^-$] or formate rather than [FEP^-].

3.5. Evaluation of the Overall Trends of VOCs Solubility in ILs. In order to provide a general evaluation of the influence of the structure of ILs on the solubility of VOCs, we have selected a representative sample of 14 organic compounds, including alkanes, alkenes, halogenated, aromatics, esters, and ketones. The COSMO-RS screening was performed for each one of the selected solutes over 135 imidazolium-based ILs, with the aim to provide an overview of the gas solubility behavior of VOCs in ILs. For this purpose, the extreme cases corresponding to the solute–IL systems with the lowest [γ^∞(min)] and the highest [γ^∞(max)] activity coefficient values were identified, and the results are collected in Table 3, A and B, respectively. The minimum activity coefficient, γ^∞(min), is associated to the most favorable IL structure to absorb the VOC solute, whereas the maximum activity coefficient, γ^∞(max), is associated to the worst IL structure to absorb the VOC solute. In order to show more clearly the data reported in the mentioned table (Table 3A,B), the values obtained for the γ^∞(min) and γ^∞(max) for each one of the VOCs solutes in the ILs are illustrated in Figure 10. Moreover, throughout this document the effect that the chemical structure of both VOC

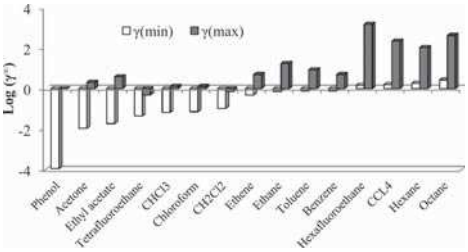

Figure 10. Minimum (γ_{min}) and maximum (γ_{max}) values of activity coefficients at infinite dilution (γ^∞) of VOCs in ILs obtained from COSMO-RS screening at 298 K over 135 imidazolium-based ILs.

and IL has on the solute–solvent interactions which determine the absorption capability has been discussed. For that reason, the energetic contributions to the excess enthalpy of the VOC-IL systems that present γ^∞(min) is collected in Table S23 in the Supporting Information. Figure 11 shows a plot of those

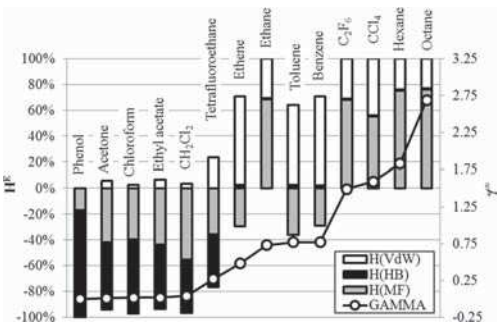

Figure 11. Relationship between the minimum values of activity coefficients at infinite dilution, γ^∞(min), and the percentages of the different intermolecular interaction contributions to the excess enthalpy [H(VDW), H(HB), and H(MF)] for VOCs in ILs reported in Table 3, computed by COSMO-RS at T = 298 K.

different energetic contributions expressed as percentages, in order to visually represent the data more clearly. On the basis of these results, we propose the following classification of VOC compounds respect to their solubilities on ILs, considering the effect of rationally selecting the cationic and anionic species for a potential absorption process:

(i) VOCs with favorable absorption in ILs: solutes containing strong polar functional groups with remarkable HB donor/acceptor character, such as phenol, acetone, ethyl acetate, and chloroform. Considering the noticeably low values of γ^∞(min) < 0.1, these solutes exhibit a strong negative deviation from ideality. These solutes are classified as group 1 in Table 2, and present very low values of Henry's constant (Table 3A) and an overall high solubility in ILs. The gas solubility behavior of this kind of VOCS in ILs is mainly determined by HB interactions (Table 3, Figure 11). Hence, the affinity of the IL solvent for these VOC solutes can be greatly enhanced selecting an adequate anion–cation combination that promote attractive hydrogen bonding between the solute and the IL.

(ii) VOCs with moderate absorption in ILs: solutes containing short alkyl chains or aromatic character (i.e., ethane,

dx.doi.org/10.1021/jp310499p | J. Phys. Chem. B 2013, 117, 296–306

ethene, benzene) which exhibit activity coefficients in ILs with a moderate negative deviation from ideality ($0.1 < \gamma^{\infty}(\min) \leq 1$). The solubility behavior of these solute−solvent systems, i.e., VOCs whose absorption can be moderately enhanced by selecting adequate ILs, is generally determined by van der Waals interactions (which are weaker in the mixture than in the pure fluid, providing endothermic contributions) and favorable polar-misfit interactions between the VOC solute and the IL solvent (Table 3A, Figure 11). The most appropriate ILs to enhance the solubility of most of these VOCS are those composed of cations with long alkyl chains and large anions with disperse charge like [FEP$^-$]. It is should be noted that the moderate IL capacity to absorb these VOCs (classified as groups 2 and 3 in Table 2) depends on both the relatively low activity coefficients and the vapor pressure of pure solute compound. This is evident for the tetrafluoethane/ethane/toluene series, which presents increasing $\gamma^{\infty}(\min)$ trend (0.27/0.73/0.77) but a variety of gas solubilities in terms of K_H values (1.6×10^{-1}/6.0/3.3×10^{-3}), due to the different volatility of the solutes.

(iii) VOCs with unfavorable absorption in ILs: aliphatic solutes such as hexane or octane and perhalogenated compounds such as CCl_4 which present high values of $\gamma^{\infty}(\min) > 1$; this indicates a positive deviation from ideality (Table 3A, Figure 11), and hence a higher volatility of the solute in the IL than that of the pure compound. All these solutes exhibit unfavorable solute−solvent interactions, with their solubilities in ILs ranging from very low (VOCs classified as group 4 in Table 2, with high vapor pressure of pure compound) to intermediate (VOCs with high molar weight and relatively low vapor pressure). Figure 11 shows that the unfavorable solubility behavior of these VOCs in ILs is related to the repulsive electrostatic interactions. Moreover, Table 3B and Figure 10 show that the solubility of these solutes in ILs can be strongly diminished by selecting small imidazolium cations and polar anions such as [SCN$^-$] that promote repulsive electrostatic interactions with the nonpolar compounds included in this type of VOCs. These [SCN$^-$]-based ILs can be applied in aliphatic/aromatic separation (i.e., heptane/benzene[53]) or in oil desulfurization processes,[54] including extractive membrane technologies to separate organosulfur compounds from refinery products.[55]

4. CONCLUSIONS

A systematic COSMO-RS analysis of the thermodynamics and energetic interactions of a wide sample of VOC−IL systems was performed. COSMO-RS shows a general predictability of the gas solubility behavior of different solutes in ILs. A clear relationship between the activity coefficient at infinite dilution (γ^{∞}) of solutes in the ILs and the excess enthalpy (H^E) of the equimolar IL−solute mixtures was reported, observing a remarkably negative deviation from Raoult's law for strong exothermic VOC−IL mixtures. A comprehensive gas solubility screening and detailed energetic analysis of three representative polar VOCs (acetone, phenol, and chloroform) in ILs systems indicated that favorable solute−solvent interactions can be conveniently tuned by cation and anion selection, enhancing the gas solubility of these VOCs in ILs. Finally, the COSMO-RS study was extended to a sample of 14 representative VOCs with strong structural differences, with results leading to propose a classification of VOCs respect to their solubilities in ILs. This classification gave an insight into the rational selection of the cationic and anionic species that provided, respectively, the highest negative and positive deviations from the ideality and, consequently, the most favorable and unfavorable properties to absorb VOCs in ILs.

■ ASSOCIATED CONTENT

Supporting Information

Table S1: Experimental and COSMO-RS Henry constants of solutes in ILs at near-ambient temperature and atmospheric pressure using vapor pressures of pure compounds predicted by COSMO-RS and estimated by empirical Antoine equation. Tables S2−S4: Screening of the Henry constants of acetone, phenol, and chloroform in ILs at T = 298 K computed by COSMO-RS. Table S5−S22: Screening of the activity coefficients and excess enthalpy of acetone, benzene, chloroform, ethane, ethane, phenol, H_2S, H_2, and trifluoroethane in ILs at T = 298 K computed with COSMO-RS. Table S23: Activity coefficients, excess enthalpies, and intermolecular interaction contributions of VOCs in ILs at T = 298 K computed by COSMO-RS. This material is available free of charge via the Internet at http://pubs.acs.org.

■ AUTHOR INFORMATION

Corresponding Author

*Tel.: 34 91 4976938. Fax: 34 91 4973516. E-mail: pepe.palomar@uam.es.

Notes

The authors declare no competing financial interest.

■ ACKNOWLEDGMENTS

The authors are grateful to the Ministerio de Economía y Competitividad and Comunidad de Madrid for financial support (projects CTQ2011-26758 and S2009/PPQ-1545, respectively).

■ REFERENCES

(1) Huddleston, J. G.; Willauer, H. D.; Swatloski, R. P.; Visser, A. E.; Rogers, R. D. *Chem. Commun.* **1998**, 1765−1766.
(2) Tokuda, H.; Hayamizu, K.; Ishii, K.; Abu Bin Hasan Susan, M.; Watanabe, M. *J. Phys. Chem. B* **2004**, *108*, 16593−16600.
(3) Tokuda, H.; Hayamizu, K.; Ishii, K.; Abu Bin Hasan, M.; Susan, M. Watanabe. *J. Phys. Chem. B* **2004**, *109*, 6103−6110.
(4) Wasserscheid, P.; Welton, T. *Ionic Liquids in Synthesis*; Wiley-VCH: Weinheim, Germany, 2008.
(5) Huang, J.; Reuther, T. *Aust. J. Chem.* **2009**, *62*, 298−308.
(6) Bara, J. E.; Carlisle, T. K.; Gabriel, C. J.; Camper, D.; Finotello, A.; Gin, I.; Gin, D. L.; Noble, R. D. *Ind. Eng. Chem. Res.* **2009**, *48*, 2739−2751.
(7) Lu, X. Y.; Burrel, G.; Separovic, F.; Zhao, C. *J. Phys. Chem. B* **2012**, *116*, 9160−9170.
(8) Anderson, J. L.; Dixon, J. K.; Brennecke, J. F. *Acc. Chem. Res.* **2007**, *40*, 1208−1216.
(9) Camper, D.; Becker, C.; Koval, C.; Noble, R. *Ind. Eng. Chem. Res.* **2005**, *44*, 1928−1933.
(10) Carlisle, T. K.; Bara, J. E.; Gabriel, C. J.; Noble, R. D.; Gin, D. L. *Ind. Eng. Chem. Res.* **2006**, *45*, 6279−6283.
(11) Condemarin, R. A.; Scovazzo, P. *Chem. Eng. J.* **2009**, *147*, 51−57.
(12) Kilaru, P. K.; Scovazzo, P. *Ind. Eng. Chem. Res.* **2008**, *47*, 910−919.
(13) Kumelan, J.; Perez-Salado Kamps, A.; Tuma, D.; Maurer, G. *J. Chem. Eng. Data* **2006**, *51*, 1802−1807.
(14) Jacquemin, J.; Husson, P.; Majer, V.; Padua, A. H.; Costa-Gomes, M. F. *Green Chem.* **2008**, *10*, 944−950.
(15) Raeissi, S.; Peters, C. J. *Green Chem.* **2009**, *11*, 185−192.

(16) Almantariotis, D.; Gefflaut, T.; Padua, A. A. H.; Coxam, J. Y.; Costa-Gomes, M. F. *J. Phys. Chem. B* **2010**, *114*, 3608−3617.
(17) Jalili, A. H.; Rahmati-Rostami, M.; Ghotb, C.; Hosseini-Jenab, M.; Ahmadi, A. Naser *J. Chem. Eng. Data* **2009**, *54*, 1844−1849.
(18) Costa-Gomes, M. F. *J. Chem. Eng. Data* **2007**, *52*, 472−475.
(19) Jacquemin, J.; Husson, P.; Majer, V.; Costa-Gomes, M. F. *Fluid Phase Equilib.* **2006**, *240*, 87−95.
(20) Jacquemin, J.; Costa-Gomes, M. F.; Husson, P.; Majer, V. *J. Chem. Thermodyn.* **2006**, *38*, 490−502.
(21) Kumełan, J.; Perez-Salado Kamps, A.; Tuma, D.; Maurer, G. *Fluid Phase Equilib.* **2007**, *260*, 3−8.
(22) Kumean, J.; Perez-Salado Kamps, A.; Tuma, D.; Maurer, G. *Ind. Eng. Chem. Res.* **2007**, *46*, 8236−8240.
(23) Kumean, J.; Perez-Salado Kamps, A.; Tuma, D.; Maurer, G. *J. Chem. Eng. Data* **2007**, *52*, 2319−2324.
(24) Anderson, J. L.; Dixon, J. K.; Maginn, E. J.; Brennecke, J. F. *J. Phys. Chem. B* **2006**, *110*, 15059−15062.
(25) Palomar, J.; Gonzalez-Miquel, M.; Bedia, J.; Rodríguez, F.; Rodríguez, J. J. *Sep. Purif. Technol.* **2011**, *82*, 43−52.
(26) Bedia, J.; Palomar, J.; Gonzalez-Miquel, M.; Rodriguez, F.; Rodriguez, J. J. *Sep. Purif. Technol* **2012**, *95*, 188−195.
(27) Camper, D.; Becker, C.; Koval, C.; Noble, R. *Ind. Eng. Chem. Res.* **2006**, *45*, 445−450.
(28) Lee, B. C.; Outcalt, S. L. *J. Chem. Eng. Data* **2006**, *51*, 892−897.
(29) Shiflett, M. B.; Yokozeki, A. *Ind. Eng. Chem. Res.* **2006**, *45*, 6375−6382.
(30) Kumełan, J.; Perez-Salado Kamps, A.; Tuma, D.; Yokozeki, A.; Shiflett, M. B.; Maurer, G. *J. Phys. Chem. B* **2008**, *112*, 3040−3047.
(31) IUPAC Ionic Liquids Database (IL Thermo), www.ilthermo.boulder.nist.gov.
(32) Quijano, G.; Couvert, A.; Amrane, A.; Darracq, G.; Couriol, C.; Le Cloirec, P.; Paquin, L.; Carrié, D. *Chem . Eng. J.* **2011**, *66*, 2707−12.
(33) Bedia, J.; Ruiz, E.; de Riva, J.; Ferro, V. R.; Palomar, J.; Rodriguez, J. J. *AIChE J.* **2012**, DOI: 10.1002/aic.13926.
(34) Klamt, A.; Eckert, F.; Arlt, W. *Annu. Rev. Chem. Biom. Eng.* **2010**, *1*, 101−122.
(35) Diedenhofen, M.; Klamt, A. *Fluid Phase Equilib.* **2010**, *294*, 31−38.
(36) Palomar, J.; Torrecilla, J. S.; Ferro, V. R.; Rodríguez, F. *Ind. Eng. Chem. Res.* **2008**, *47*, 4523−4532.
(37) Palomar, J.; Torrecilla, J. S.; Ferro, V. R.; Rodríguez, F. *Ind. Eng. Chem. Res.* **2009**, *48*, 2257−2265.
(38) Zhang, X.; Liu, Z.; Wang, W. *AIChE J.* **2008**, *54* (10), 2717−2728.
(39) Manan, N. A.; Hardacre, C.; Jacquemin, J.; Rooney, D. W.; Youngs, T. G. *J. Chem. Eng. Data* **2009**, *54*, 2005−2022.
(40) Palomar, J.; Gonzalez-Miquel, M.; Polo, A.; Rodríguez, F. *Ind. Eng. Chem. Res.* **2011**, *50*, 3452−3463.
(41) Gonzalez-Miquel, M.; Palomar, J.; Omar, S.; Rodríguez, F. *Ind. Eng. Chem. Res.* **2011**, *50*, 5739−5748.
(42) Sistla, Y. S.; Khanna, A. *J. Chem. Eng. Data* **2011**, *56*, 4045−4060.
(43) Sumon, K. Z.; Henni, A. *Fluid Phase Equilib.* **2011**, *310* (1−2), 39−55.
(44) Navas, A.; Ortega, J.; Vreekamp, R.; Marrero, E.; Palomar, J. *Ind. Eng. Chem. Res.* **2009**, *48*, 2678−2690.
(45) Oyama, S. T.; Hunter, P. *Control of Volatile Organic Compounds Emissions: Conventional and Emerging Technologies*; Wiley-Interscience: New York, 2000.
(46) Clean Air Act Amendments. National Air Quality and Emissions Trends Report; EPA, USA, 1998.
(47) Directive 2001/81/EC of the European Parlament and of the Council of 23 October 2001 on national emission ceilings for certain atmospheric pollutants.
(48) Building Assessment Survey and Evaluation Study: Volatile Organic Compounds. EPA, USA, 2012. http://www.epa.gov/iaq/base/voc_master_list.html
(49) Frisch, M. J.; Trucks, G. W.; Schlegel, H. B.; Scuseria, G. E.; Robb, M. A.; Cheeseman, J. R.; Montgomery, J. A.; Vreven, T.; Kudin, K. N.; Burant, J. C.; Millam, J.M.; Iyengar, S. S.; Tomasi, J.; Barone, V.; Mennucci, B.; Cossi, M.; Scalmani, G.; Rega, N.; Petersson, G. A.; Nakatsuji, H.; Hada, M.; Ehara, M.; Toyota, K.; Fukuda, R.; Hasegawa, J.; Ishida, M.; Nakajima, T.; Honda, Y.; Kitao, O.; Nakai, H.; Klene, M.; Li, X.; Knox, J. E.; Hratchian, H. P.; Cross, J. B.; Bakken, V.; Adamo, C.; Jaramillo, J.; Gomperts, R.; Stratmann, R. E.; Yazyev, O.; Austin, A. J.; Cammi, R.; Pomelli, C.; Ochterski, J. W.; Ayala, P. Y.; Morokuma, K.; Voth, G. A.; Salvador, P.; Dannenberg, J. J.; Zakrzewski, V. G.; Dapprich, S.; Daniels, A. D.; Strain, M. C.; Farkas, O.; Malick, D. K.; Rabuck, A. D.; Raghavachari, K.; Foresman, J. B.; Ortiz, J. V.; Cui, Q.; Baboul, A. G.; Clifford, S.; Cioslowski, J.; Stefanov, B. B.; Liu, G.; Liashenko, A.; Piskorz, P.; Komaromi, I.; Martin, R. L.; Fox, D. J.; Keith, T.; Al-Laham, M. A.; Peng, C. Y.; Nanayakkara, A.; Challacombe, M.; Gill, P. M.; Johnson, B.; Chen, W.; Wong, M. W.; González, C.; Pople, J. A. *Gaussian03, revision B.05*; Gaussian, Inc.: Wallingford, CT, 2004.
(50) *COSMOtherm C2.1 Release 01.11*; COSMOlogic GmbH & Co. KG: Leverkusen, Germany, 2010; http://www.cosmologic.de.
(51) Eckert, F.; Klamt, A. *AlChE J.* **2002**, *48* (2), 369−382.
(52) Klamt, A.; Eckert, F. *Fluid Phase Equilib.* **2000**, *172*, 43−72.
(53) Domańska, U.; Królikowska, M. *J. Chem. Eng. Data* **2011**, *56*, 124−129.
(54) Kedra-Królik, K.; Fabrice, M.; Jaubert, J. N. *Ind. Eng. Chem. Res.* **2011**, *50*, 2296−2306.
(55) Petra, C.; Katalin, B. B. Application of Ionic Liquids in Membrane Separation Processes, Ionic Liquids: Applications and Perspectives; 2011. ISBN: 978-953-307-248-7. Available from: http://www.intechopen.com/books/ionic-liquids-applications-and-perspectives/application-of-ionic-liquids-in-membrane-separation-processes.

ANEXO II.
NOMENCLATURA

NOMENCLATURA

SÍMBOLOS

Latinos

AM	Arithmetic mean
C	Concentration, mg/ml
$\bar{C}$	Space average concentration, mg/ml
C_0	Initial concentration, mg/ml
Cp	Heat capacity, J/(kg · K)
C_s	Saturation concentration, mg/ml
C_{ef}	Effective absorption capacity, mmol solute/(min·mol IL)
D	Diffusion coefficient, m^2/s
D_i	Diffusion coefficient of solute i, m^2/s
Fg	Gravitational force, kg·m/s^2
g	Acceleration of gravity, m/s^2
H	Holding force, kg·m/s^2
H_i^E	Contribution of compound i to the excess enthalpy of the mixture, kJ/mol
$H_i^{E'}$	Corrected contribution of compound i to the excess enthalpy of the mixture, kJ/mol
H_m^E, H^E	Excess enthalpy of the mixture, kJ/mol
$H_m^{E\prime}$, $H^{E\prime}$	Corrected excess enthalpy of the mixture, kJ/mol
H(HB), H(H-bond)	Energetic contribution of the hydrogen bonds to the excess enthalpy of the mixture, kJ/mol

H(MF)	Energetic contribution of the misfit or the electrostatic interactions to the excess enthalpy of the mixture, kJ/mol
H(VdW)	Energetic contribution of the van der Waals forces to the excess enthalpy of the mixture, kJ/mol
K_H	Henry´s law constant, MPa
$K_{H,Antoine\ Eq.}$	Henry´s law constant estimated by using the Antoine equation to calculate the vapor pressure of the solute, MPa
$K_{H,COSMO\text{-}RS}$	Henry´s law constant estimated by using the energy file of COSMO-RS to calculate the vapor pressure of the solute, MPa
K_H^i	Henry´s law constant of solute i, MPa
K_{reac}	Constant of reaction
L	Depth of the IL in the sample container, mm
m	Mass, g or mg
m_{BAL}	Mass balance reading, mg
m_i	Mass of compound i, mg
m_s	Mass of the sample, mg
m_{sc}	Mass of the sample container, g or mg
m_{sc+s}	Mass of the sample container with sample, g or mg
M_i	Molecular weight of compound i, g/mol
N	Total number of points
p(σ)	Probability of charge distribution on the molecular surface
P	Pressure, Mpa or bar

P_i	Partial pressure of solute i, Mpa or bar
P_0^{vap}	Vapor pressure of the pure compound, MPa
$P_{vap,COSMO-RS}$	Vapor pressure of the solute estimated by COSMO-RS, Mpa
$P_{vap,empirical}$	Vapor pressure of the solute estimated by empirical correlation, MPa
R^2	Correlation coefficient
S (i/j)	Selectivity of solute i over solute j
SD	Standard deviation
t	Time, s or min or h
t_{op}	Operating time (absorption + desorption), min
T	Temperature, K or ^oC
T_{cap}	Capture temperature, ^oC
T_{rev}	Reversal temperature, ^oC
u(X)	Maximum uncertainties of parameter X
V	Volume, nm^3 or cm^3
V_i	Molal volume of solute i, cm^3/mol
V_{IL}	Molecular volume of the ionic liquid, nm^3
V_s	Volume of the sample, cm^3
V_{sc}	Volume of the sample container, cm^3
V_{sc+s}	Volume of the sample container with sample, cm^3
X^{calc}, X_{calc}	Calculated value of parameter X
$X^{COSMO-RS}$, $X_{COSMO-RS}$	Estimated value of parameter X by COSMO-RS

X^{exp}, X_{exp}, X_{exptl},$X_{experimental}$	Experimental value of parameter X
X_i	Molar fraction of compound i
z	Vertical location, mm
[C+A]	Molecular model of independent counterions structure
[CA]	Molecular model of ion-paired structure
$[i]_{COSMO}$	Quantum-chemical geometry optimization of the compound i in continuum solvation model
$[i]_{GAS}$	Quantum-chemical geometry optimization of the compound i in ideal gas phase environment
$[i]_{GAS\text{-}Energy}$	Quantum-chemical geometry optimization of the compound i in ideal gas phase environment using the energy file of COSMO-RS to calculate the vapor pressure of the compounds in order to estimate the thermodynamic properties
$[i]_{GAS\text{-}Pvap}$	Quantum-chemical geometry optimization of the compound i in ideal gas phase environment using the Antoine equation to calculate the vapor pressure of the compounds in order to estimate the thermodynamic properties
(f)	Favorable intermolecular interactions
(u)	Unfavorable intermolecular interactions

Griegos

γ^{∞}	Activity coefficient at infinite dilution
γ_i^{∞}	Activity coefficient of solute i at infinite dilution
γ^{∞}(max)	Maximum value of activity coefficients at infinite dilution
γ^{∞}(min)	Minimum value of activity coefficients at infinite dilution
ϕ	Association parameter
μ	Viscosity, Pa·s
ρ	Density, g/cm^3
σ	Charge distribution on the molecular surface, e·Å^2; standard deviation
σ-profile	Histogram of charge distribution on the molecular surface computed by COSMO-RS
$\Delta_{sol}G^{\infty}$	Excess Gibbs energy of absorption, kJ/mol
$\Delta H_{dissolution}$	Enthalpy of dissolution, kJ/mol
ΔH_{reac}	Enthalpy of reaction, kJ/mol
ΔH_{reg}	Enthalpy of regeneration, kJ/mol
$\Delta_{sol}H^{\infty}$	Excess enthalpy of absorption, kJ/mol
$\Delta_{sol}S^{\infty}$	Excess entropy of absorption, kJ/mol

ABREVIATURAS

ACM	Activity coefficient model
B	Buoyancy effect
COSMO-RS	Conductor-like screening model for real solvents
DSC	Differential scanning calorimetry
EOS	Equation of state
GCM	Group contribution method
ILs	Ionic liquids
IPCC	Intergovernmental Panel on Climate Change
IUPAC	International Union of Pure and Applied Chemistry
LLE	Liquid-liquid equilibrium
MD	Molecular dynamics
MEA	Monoethanolamine
MF	Misfit or electrostatic interactions
ML	Molecular liquid
MPE	Mean prediction error
MSB	Magnetic suspension balance
MW	Molecular weight
POM	Polarized optical microscopy
RevILs	Reversible ionic liquids
SILMs	Supported ionic liquid membranes
SLE	Solid-liquid equilibrium

SLMs	Supported liquid membranes
TGA	Thermogravimetric analyzer
UHV	Ultrahigh vacuum
VdW	Van der Waals forces
VLE	Vapor-liquid equilibrium
VOCs	Volatile Organic Compounds